An Agent-based Platform for Demand Response Implementation in Smart Buildings

Warodom Khamphanchai

Dissertation submitted to the faculty of the Virginia Polytechnic Institute and State University in partial fulfillment of the requirements for the degree of

Doctor of Philosophy
in
Electrical Engineering

Saifur Rahman

Manisa Pipattanasomporn

Alireza Haghighat

Robert P. Broadwater

Thomas C. Clancy

Ahmed Al-Durra

March 15th 2016
Arlington, Virginia

Key Words: Demand Response, Home Energy Management System, Building Energy Management System, Internet of Things, Multi-Agent Systems

An Agent-based Platform for Demand Response Implementation in Smart Buildings

Warodom Khamphanchai

Abstract

The efficiency, security and resiliency are very important factors for the operation of a distribution power system. Taking into account customer demand and energy resource constraints, electric utilities not only need to provide reliable services but also need to operate a power grid as efficiently as possible. The objective of this dissertation is to design, develop and deploy the Multi-Agent Systems (MAS) – together with control algorithms – that enable demand response (DR) implementation at the customer level, focusing on both residential and commercial customers.

For residential applications, the main objective is to propose an approach for a smart distribution transformer management. The DR objective at a distribution transformer is to ensure that the instantaneous power demand at a distribution transformer is kept below a certain demand limit while impacts of demand restrike are minimized. The DR objectives at residential homes are to secure critical loads, mitigate occupant comfort violation, and minimize appliance run-time after a DR event.

For commercial applications, the goal is to propose a MAS architecture and platform that help facilitate the implementation of a Critical Peak Pricing (CPP) program. Main objectives of the proposed DR algorithm are to minimize power demand and energy consumption during a period that a CPP event is called out, to minimize occupant comfort violation, to minimize impacts of demand restrike after a CPP event, as well as to control the device operation to avoid restrikes.

Overall, this study provides an insight into the design and implementation of MAS, together with associated control algorithms for DR implementation in smart buildings. The proposed approaches can serve as alternative solutions to the current practices of electric utilities to engage end-use customers to participate in DR programs where occupancy level, tenant comfort condition and preference, as well as controllable devices and sensors are taken into account in both simulated and real-world environments. Research findings show that the proposed DR algorithms can perform effectively and efficiently during a DR event in residential homes and during the CPP event in commercial buildings.

An Agent-based Platform for Demand Response Implementation in Smart Buildings

Warodom Khamphanchai

General Audience Abstract

Nowadays, more and more appliances are connected to the electrical power grid, both in residential and commercial buildings. Electric utilities are trying to keep up with this fast growing power demand. In addition, during stress conditions in a power system (e.g., high power demand in hot summer days or cold winter days), there is a need for utilities to reduce power demand to match with available supply, or increase electric power generation to cover the increased demand. In order to increase power generation, electric utilities have to run their expensive peaking power plants. Alternatively, reducing power demand from end-use customers through financial and other incentives, is another promising approach that is becoming popular and is being implemented by many electric utilities. This approach is called "demand response".

This dissertation proposes the approaches for demand response implementation both at a home level and a building level. At a home level, the main objective is to help an electric utility reduce power demand seen by a distribution transformer serving several homes. Given a certain demand limit as a result of an unanticipated event, the proposed approach ensures that the instantaneous power demand at a distribution transformer is kept below a certain limit while the comfort of homeowners is not compromised. At a commercial building level, the main objective is to help an electric utility reduce power demand using a Critical Peak Pricing (CPP) signal during a hot summer day. The proposed approach helps to minimize power demand and energy consumption of small- and medium-sized buildings during a given CPP event period while tenants' comfort is not compromised.

Acknowledgments

First of all, I would like to express my profound gratitude and appreciation to my advisor, Dr. Saifur Rahman, for his constructive guidance, suggestions, and recommendations throughout my entire journey pursuing a PhD degree. He exemplifies how a hard-working and disciplined individual should be rewarded. He set the bar for me to keep doing good work and never give up. I have learned a lot from him. I really appreciate his support not only for my research but also in my entire academic life at Advanced Research Institute, Virginia Tech. He gave me tons of opportunities to work and learn from various projects which are really significant to my future professional career.

I would like to pay my utmost gratitude to Dr. Manisa Pipattanasomporn for her invaluable advices, suggestions, and recommendations throughout my PhD journey. I truly appreciate her support in my research, in the projects I have participated, and my entire academic life at Advanced Research Institute, Virginia Tech. Her encouragement really helps me pull off all obstacles and difficulties not only in my research but also in my personal life.

I also would like to express my special gratitude for Dr. Robert Broadwater, DR. Alireza Haghighat, Dr. Thomas Charles Clancy, and Dr. Ahmed Al-Durra who served as members of my PhD committee. I would like to thank them for their precious time attending my exams. Their observations, questions, and remarks have helped me to refine the dissertation in both the theoretical and practical aspects in which I might have overlooked.

I present my sincere and thanks to all faculty, staff and friends at Advanced Research Institute, Virginia Tech for their help and support along my journey studying in the U.S. I never feel that I was alone working on this research as we always shared information, knowledge as well as helped each other to overcome both technical and mathematical difficulties.

Lastly, I offer my deepest gratitude to my father Pongsan Khamphanchai and mother Wiwian Khamphanchai for their motivation, encouragement and support throughout my life. They were always there to cheer me up when I was down. I wish my PhD degree is a big reward for their sacrifice and years of hard work to support me to get higher education. I would like to dedicate my dissertation to them.

Table of Content

List of Figures

List of Tables

Abbreviations

AC	Air Conditioner
ACL	Agent Communication Language
AHP	Analytical Hierarchy Process
AMS	Agent Management System
AOP	Agent Oriented Programming
AP	Agent Platform
BAS	Building Automation System
BEM	Building Energy Management
CD	Clothes Dryer
CFP	Call for Proposal
CPP	Critical Peak Pricing
DERs	Distributed Energy Resources
DF	Directory Facilitator
DL	Demand Limit
DLC	Direct Load Control
DOE	U.S. Department of Energy
DR	Demand Response
DR AGG	Demand Response Aggregator
DRK	Demand Restrike
DRKP	Demand Restrike Potential
EDRP	Emergency Demand Response Program
EDRE	Emergency Demand Response Event
EMS	Energy Management System
ESs	Expert Systems
EV	Electric Vehicle
FIPA	Foundation for Intelligent Physical Agents
GUI	Graphic User Interface
GUID	Globally Unique Name
HEM	Home Energy Management
HVAC	Heating, Ventilating, and Air Conditioning
IDE	Integrated Development Environment
IP	Interaction Protocol
iB2G	Intelligent Building-to-Grid System
ISO	Independent System Operator
JADE	JAVA Agent Development Framework
LAN	Local Area Network
MAS	Multi-Agent systems
MP	Mathematical Programming
MTS	Message Transport Service
RTP	Real Time Pricing
TOU	Time of Use
WH	Water Heater

1. INTRODUCTION

1.1 Background

Conventionally, one of the most common corrective control actions deployed as a result of deficiency of bulked power supply due to unanticipated contingencies, such as loss of generator, or loss of line, is load shedding. However, implementing load shedding imposes electricity outages to a large number of customers as this is typically performed at the transmission or sub-transmission level. In addition, as electric power utilities as well as Independent System Operators (ISO) desire to operate the power system with such high reliability (e.g., low SAIFI, low SAIDI), implementing a load shedding scheme seems to be one of their impediments. With the introduction of smart grid and advanced metering infrastructure (AMI), there is now a more effective and promising solution through implementing "demand response (DR)" at customer premises (i.e., residential homes and commercial buildings).

Technically, a DR event is defined as a period of time during which there is the need for a utility or an ISO to send a request for a demand reduction to end-use customers – especially when there is a power supply shortfall in a system (e.g., during a system stress condition or a disturbance or fluctuation in renewable energy sources). DR is a mechanism used to reduce peak demand during the critical time (DR event) and shift that demand to a subsequent non-critical period, thus leading to the more efficient use of an electrical infrastructure. Generally, a DR implementation includes utility taking actions to remotely turn off selected end-use appliances or customers taking actions to reduce and manage their power demand. This can be carried out by a control center sending demand limit (DL) requests (kW) to selected substations. These requests are subsequently transferred to reduce load at selected distribution transformers, homes, and commercial buildings. However, a stringent DR request could also negatively impact the comfort level of customers and could result in a new higher peak (also called "demand restrike") after a DR event ends.

Implementing DR in a distribution system involves local optimization processes at different levels (transformer/customer premises), without only relying on a centralized control system. In order to tackle this local optimization problem, a distributed control system such as an agent-based system is exploited. In recent years, multi-agent systems (MAS) have been in the limelight compared to other approaches in providing decentralized intelligent management and control of a power distribution network. Fundamentally, MAS consists of multiple distributed intelligent agents, which reside in physical devices scattered throughout the system. Agents work in collaboration with each other to achieve a desired goal in a specific environment. Particularly, MAS are employed to deal with complex tasks, which cannot be solved by a single agent. The overall target is broken down into smaller components, a set of which is assigned to a selected agent. The MAS concept has been applied to address emerging issues in power distribution systems, such as control of distributed energy resources, real-time microgrid management, self-healing, restoration and reconfiguration of power systems.

1.2 Statement of Problems

- **Moving toward decentralized power systems:** There is a trend that in the near future the power distribution network will be decentralized, comprising multiple smaller sub-systems with a number of intelligent entities (e.g. smart homes, smart buildings, smart meters, renewable energy resources, smart devices etc.) scattered throughout the system. These entities are likely to generate a significant amount of data that can overwhelm the current traditional power system operations. Therefore, there is the need for an intelligent and autonomous or advanced control method for future power system applications.
- **Low reliability of power distribution system:** Power system reliability is becoming a challenge for the future power system operation. Due to the fact that a typical distribution power system has a lot of branches that are exposed to external environment, they are prone to contingencies that are caused by a variety of unanticipated events such as lightning strike, storms, line to ground fault, vehicle accidents, etc. This results in low reliability of the distribution system.
- **Large outages due to the structure of conventional power systems:** Conventionally, deficiency of bulked power supply resulting from an unanticipated loss of generators or loss of transmission lines imposes an outage (or partial outage) on large blocks of utility's end-use customers depending on its affected service area. This is because today's existing corrective control actions, e.g., load shedding schemes, are mainly targeted at transmission or sub-transmission level in which large blocks of customer are taken off the grid causing financial costs and inconvenience on customers.
- **Possibility of cascading failures due to unanticipated contingencies:** In a situation of power system stress conditions caused by unanticipated contingencies or anticipated severe increases in system peak loads, an electric utility or ISO/RTO needs to ensure a stress condition is alleviated before it becomes more severe, causing a cascading failure in a system.
- **Demand response (DR) is not popular in the residential sector and small- and medium-sized commercial buildings:** In recent years, many electric utilities and Independent System Operators (ISOs) across the U.S. adopted a variety of demand response (DR) programs to curtail their electric power demand. Their reasons vary from deferring costly electrical infrastructure upgrades to mitigate power system reliability concerns. In today's environment, DR programs are already well-developed in large commercial and industrial markets. However, DR implementations in residential homes as well as small- and medium-sized commercial buildings are immature and still in its infancy. These buildings constitute significant potential for power demand reduction and can be used as an effective resource to respond to unanticipated events causing stress conditions in a power system or to respond to events to improve efficiency of power grid operation in peak hours period during the summer.
- **Comfort is often compromised when DR is performed for residential customers:** With the current DR implementation, Direct Load Control (DLC) is the most prevalent method for DR in residential homes, in which a utility sends a signal to turn off or cycling air conditioner compressors or water heaters, causing interruption and inconvenience to end-use customers. In addition, customer comfort and their choices to control their

appliances are limited. In addition, impacts of a potential increase in power demand after a DR event (so called demand rebound or demand restrike) are not properly addressed.

- **Need a low-cost solution for energy management in small- and medium-sized commercial buildings:** At a building level, with the current DR implementations, most building energy management system (BEM) or building automation system (BAS) solutions are proprietary and used in large buildings. BAS are not popular in most small- and medium-sized buildings due to lack of awareness of benefits, lack of inexpensive packaged solutions, and sometimes due to the owner not being the tenant and so finding no incentive to invest in these systems. Due to lack of building monitoring and control, especially in small- and medium-sized buildings, significant portions of energy consumption of a building is wasted. Effective and low-cost solution to make devices coordinate and communicate autonomously and seamlessly together in order to achieve the global objective of a building's owner (e.g., perform DR in response to price or reliability signals sent by a utility taking into account the level of occupancy and occupant comfort requirements) has not yet been addressed.
- **Lack of proper DR strategies:** Load reduction strategies of most automated BEM solutions need to be established in advance in order to participate in DR programs. Therefore, those strategies cannot keep up with dynamic behaviors of power demand and energy consumption of a building that is likely to change over a course of the day due to building or zone occupancy level, tenants preferences, and devices' settings etc. In addition, impacts of a potential increase in power demand after a DR event (so called demand rebound or demand restrike) are not properly addressed.

1.3 Objectives of Study

This study focuses on the development of multi-agent system (MAS) platforms and associated demand response algorithms for both residential and small-/medium-sized commercial buildings. That is, the first half of this dissertation is dedicated to MAS platform development for implementing an Emergency Demand Response Event (EDRE) in the residential sector, particularly at the transformer level and at the home level, together with the EDRE algorithm. With the knowledge of the MAS development and the DR algorithm deployment from the residential sector, the MAS platform for the building energy management application, along with the DR algorithm in response to the Critical Peak Pricing (CPP) event, is proposed, developed, and deployed in a real world environment. Overall, the objectives of this study are summarized below:

1. To design and develop MAS for DR implementation at the distribution transformer level and the home level;
2. To propose a DR algorithm at the distribution transformer level and the home level to alleviate power system stress conditions which can occur due to unanticipated contingencies or severe increase in system peak loads;
3. To demonstrate the efficiency and effectiveness of the proposed DR algorithms using the developed simulation tools;
4. To design and develop MAS for DR implementation in a commercial building;
5. To propose DR algorithm at a building level in response to a CPP event callout;

6. To validate the usability of the proposed platform with the real hardware devices in a selected commercial building.

1.4 Scope and Assumptions

The scope of this dissertation is to develop an agent-based platform and propose/implement DR algorithms to alleviate power system stress conditions at the distribution transformer level and the home level and to improve efficiency of a power grid operation at commercial building level. In addition, the impacts of DR implementation when there is a sharp increase in power demand after a DR event (so called demand restrike) are also identified and studied. The constraints taken into account in this study include limitation of controllable devices, power balance, voltage limit, assigned priorities of devices, customer comfort, etc.

In this study, assumptions with respect to implementing DR are as follows:

- Communications between a distribution transformer and houses can be facilitated by wireless communications using communication technologies such as Zigbee PRO with extended range 63 mW module where outdoor range is up to 2 miles line of sight and data exchange standards such as Zigbee API.
- All controlled devices (e.g., home appliances and building equipment) are IP enabled and capable of communicating with one another.
- There is no communication disruption during a DR event.
- A commercial building has a two-way communication with a utility or an ISO over the OpenADR architecture facilitated by the mature web technology using a standard HTTP/HTTPS communication protocol with the XMPP as a data exchange standard.

1.5 Contributions

The contributions from this work can be summarized as follows:

1. An insight into the design and development of MAS for power system applications especially at the customer level;
2. A basis for conducting simulation and practical implementation of an agent-based technology with an end-use power distribution network;
3. A simulation architecture for DR implementation at the distribution transformer level and the home level comprising both the physical layer: a distribution transformer, connected homes, and DR-enable appliances/devices, and the cyber layer: MAS, decision-making processes and control algorithms;
4. MAS and control algorithms to implement DR at the distribution transformer and the home levels aiming to:
    a. Alleviate power system stress conditions
    b. Save energy in a building during its normal operating state

5. MAS and control algorithm to implement DR in commercial buildings in response to CPP signals, comprising both the physical layer: a building, and DR-enable equipment and the cyber layer: MAS, decision-making processes and control algorithms;
6. An agent-based platform for building energy management that allows developing, integrating, and implementing demand response algorithms in a real-world environment.
7. The proposed demand response algorithm takes into account occupancy level, occupant comfort and their preferences while minimizing power and energy consumption during a CPP event.
8. Results validation in a real-world environment, which may help foster and accelerate the development of market-ready products, like embedded Building Energy Management (BEM) systems and device controllers for HVAC, lighting and plug loads, etc.

1.6 Organization of the Dissertation

This dissertation comprises 7 chapters as follows:

Chapter 1 provides a brief introduction of the dissertation including background, statement of problems, objectives of study, scope of work and assumptions. Contributions of this dissertation are also mentioned in this chapter.

Chapter 2 summarizes the literature search into two categories: the background information and the in-depth information. The background information section provides the basic information about smart grid, demand response, power distribution system, home energy management system (HEM), building energy management system (BEM), and multi-agent system (MAS). The in-depth information section discusses the research related to demand response implementation at the home and building levels. In the last section, knowledge gaps are illustrated and identified.

Chapter 3 presents the overall framework of the proposed methodology, which is broken down mainly into the following tasks:

- To develop an agent-based platform for DR implementation in residential homes;
- To develop an algorithm for DR implementation in residential homes to alleviate power system stress conditions during a callout of an emergency demand response event (EDRE);
- To develop an agent-based platform for DR implementation in commercial buildings that can enable intelligent sensing and control of existing hardware devices deployed in a building;
- To develop an algorithm for DR implementation in commercial buildings to alleviate power system stress conditions in response to a CPP event via an OpenADR architecture based upon a call from a utility.

Chapter 4 presents the case study to validate the proposed DR algorithm for residential homes to alleviate power system stress conditions due to a callout of an Emergency Demand Response Event (EDRE). Simulation results and discussion are also provided.

Chapter 5 presents the case study to validate the proposed DR algorithm for commercial buildings to improve efficiency of a power grid operation due to a callout of a CPP event. Results of the real-world case study are presented and elaborated. In addition, sensitivity analysis is conducted to analyze the impact of the occupancy level on building power demand and energy consumption during a CPP event.

Chapter 6 includes the summary, conclusions, and recommended future work

2. LITERATURE SEARCH

This chapter summarizes the literature search into two categories: the background information and the in-depth information. The background information section provides the basic information about smart grid, demand response, power distribution system, home energy management system (HEM), building energy management system (BEM), and multi-agent system (MAS). The in-depth information section discusses the research related to demand response implementations at the distribution transformer/home level and the building level in detail. In the last section, knowledge gaps are identified.

2.1 Background Information

2.1.1 Smart Grid

A. Smart Grid Concept

In the near future, the electric industry tends to transform from centralized, producer controlled network into the one that more distributed controllable network and more customer-interactive. Smart grid is the promising concept, philosophies and technologies which make this transformation possible by enabling the communication over power transmission and distribution system. By means of two-way digital communication and plug-and-play capabilities, smart grid projects begin to multiply. In addition, this interaction mostly running "in the background", thus it minimize human intervention that substantially saving on energy that would otherwise be consumed [1].

In terms of overall vision, the smart grid is:

- **Intelligent:** working autonomously faster than human response which has capability of sensing system overloads and rerouting power to protect or minimize a potential outage.
- **Efficient:** needless of adding infrastructure for meeting increased customer demand
- **Accommodating:** various type of energy sources such as wind, solar, coal and natural gas are accepted. Capability to integrate any other better ideas or technologies, for example, energy storage technologies.
- **Motivating:** real time communication between customer and utility is enabled thus customer can monitor and tailor their energy consumption based on individual preference.
- **Opportunistic:** create new opportunities and markets by means of its ability to capitalize on plug-and-play innovation wherever and whenever appropriate.
- **Quality-focuses:** capable of delivering the power quality necessary – free of sags, spikes, disturbances and interruptions – to power our increasingly digital economy and the data centers, computers and electronics necessary to make it run
- **Resilient:** increasingly resistant to attack and natural disasters as it becomes more decentralized and reinforced with Smart Grid security protocols
- **Green:** slowing the advance of global climate change and offering a genuine path toward significant environmental improvement

B. Key Characteristics of Smart Grid

According to [2], key characteristics of a smart grid include:

- Self-healing
- Consumer friendly
- Attack resistant
- Provide power quality for 21st century needs
- Able to accommodate all generation and storage options
- Enable markets and
- Optimize assets and operate efficiently

2.1.2 Demand Response (DR)

A. DR Concept

Demand Response (DR) implementation to reduce end-use electricity consumption has become a crucial element for electric utilities in today's power system operation [3]. According to FERC [4], DR is defined as changes in electricity demands from their typical patterns in response to changes in the price of electricity (time-based DR programs), or in response to demand curtailment requests from a utility (incentive-based DR programs).

In recent years, many electric utilities [5], [6], [7], [8] and Independent System Operators (ISOs)/ Regional Transmission Operator (RTOs) [9], [10], [11], [12] across the U.S. have adopted a variety of DR programs to curtail their electric power demand. Their reasons vary from deferring costly electrical infrastructure upgrades to mitigating power system reliability concerns. In a situation of power system stress conditions causing by unanticipated contingencies or anticipated severe increases in system peak loads [13], an electric utility or ISO/RTO needs to ensure a stress condition is alleviated before it becomes more severe, causing a cascading failure in a system.

B. DR Category

Typically, DR programs can be categorized as follows [14]:

1. Time-based DR programs:

- Critical Peak Pricing (CPP): a DR event which is called 5-15 times per year on weekdays during summer season
- Time of Use (TOU)

2. Incentive-based programs:

- Emergency Demand Response Program (EDRP): a DR program that provides incentive payments to customers for load reduction achieved during an emergency DR event (stress condition)
- Real Time Pricing (RTP)
- Direct Load Control (DLC)

DR programs can be also categorized by their intended objectives as follows:

1. **DR Programs with the main concern on grid reliability** (e.g., contingencies or renewable energy fluctuation):
   - Emergency Demand Response Program (EDRP)
   - Direct Load Control (DLC)
2. **DR Programs with the main concern on energy market/efficiency or grid operation:** TOU, RTP
   - Time of Use (TOU)
   - Real Time Pricing (RTP)
   - Critical Peak Pricing (CPP)

C. DR Benefits

Automate demand response at customer sites enables market participants to provide relief quickly and easily, making demand response a valuable asset for participation in ancillary services market. DR programs help utilities maintain grid reliability and enable customers to realize its significant value. DR can be used to provide synchronized reserve. Implementing DR programs increase power system operations efficiency and could lead to cost reductions of their implementations by increasing competition to provide them .It also has the potential to provide additional revenues for the services and enhances opportunities for investment in DR resources.

DR programs (i.e., EDRP) can improve reliability (e.g., reduce SAIDI, reduce SAIFI) and economy of a system and to obviate a possibility and consequences of forced outage on large blocks of end-use customers. It allows customers to proactively monitor and control their power consumption which can result in significantly reduction of a total system power demand.

In the perspective of an electric utility, DR programs can (1) prevent power shortages; (2) improve reliability (SAIFI, SAIDI) of a system; and (3) defer investment on capital-intensive infrastructure such as power plants or transmission lines.

In terms of customers' perspective, DR programs lead to a higher reliability of electrical service to customers and help them to save money by reducing energy usage. Benefits of DR to a utility and customers can be summarized as shown in Table 2-1.

Table 2-1. Benefits of DR perceived by both utility and customers

Home owner	Utility
1. Achieve higher reliability	1. Reliability (e.g., SAIFI, SAIDI) of the system is improved.
2. Less risk of comfort level violation	2. Mitigate effect of Demand Restrike
3. Reduce electricity bill	3. Defer investment on capital-intensive infrastructure (e.g., power plant)
4. Reduce household carbon footprint	4. Reduce GHG's emission

D. DR Technologies

Generally, there are two enabling technologies to implement DR [6] as follows:

1. **Automated DR (Auto-DR) technology incentive**: allows enabled customers to participate in DR programs utilizing a load control device or energy management system (EMS) that automatically initiates load reduction activities based upon settings customers establish in advance. This eliminates the need to turn off or adjust equipment manually when events occur. Incentives are based upon realized energy reductions. Depending on customers' situation and the size of electrical load, Auto-DR offers two incentive options:

Option 1: Auto-DR Express: incentive for systems that control standard technologies such as dimmable ballasts, temperature reset controls for HVAC and duty cycling of HVAC compressors and fans that automatically reduce load during DR events.

Option 2: Auto-DR Customized: incentive for the purchase and installation of remotely activated equipment that facilitates site-wide automatic load reduction such as controls for lighting, motors, pumps, fans, air compressors, process equipment, HVAC load control devices and more.

2. **Permanent load shifting incentive**: AC is accounted for a major operational expense of the overall consumption. If customer cooling load is considerable, he/she may qualify for incentives that can help shift your energy use to off-peak hours. By installing a Thermal Energy Storage system, customer will be able to produce cooling energy in the evening and deploy it during high-demand afternoon hours. Therefore, customer power demand and energy consumption can be substantially reduced during peak periods.

E. DR Implementations

Early DR Implementations: Early demand response efforts were primarily manual in nature. Requests to reduce demand were typically made a day or more in advance and communicated to the end user through fax or telephone messaging. Once received, local energy management system set points were altered to reduce consumption in accordance with the communicated request and contractual requirements. There was little automation in either the generation/distribution of the request or in effecting an appropriate response.

CPP: Critical Peak Pricing (CPP) and Time-of-Use DR programs are the most commonly used is the time-based DR programs [15], [16], [17], [18], [19], [20], [21] in which demand reduction can be achieved in response to time of the day as well as electricity prices. CPP, typically referred to as critical peak days or event days, is an electrical rate where utilities charge an increased price above normal pricing for peak hours on the CPP day. CPP times coincide with peak demand on the utility; these CPP events are generally called between 5 to 15 times per year and occur when the electrical demand is high and the supply is low especially during the summer season. With CPP DR program, customers on a flat standard rate who enroll in a peak time rebate program receive rebates for using less electricity when a utility calls for a peak time event.

EDRP: With regard to reliability of a power distribution system, incentive-based DR programs, such as Emergency Demand Response Programs (EDRP), are more desirable than time-based DR programs. Implementing EDRP, load reduction at customer premises is required when a power system is in stress conditions. Currently, EDRP has been widely used at the transmission or sub-transmission levels where industrial or commercial load reduction can be achieved [22], [23], [24]. Participating customers are notified by a program sponsor (e.g., DR AGG) in advance to respond to an Emergency Demand Response Event (EDRE).

DLC: Currently, one of the popular approaches among incentive-based DR programs is direct load control (DLC). With this approach, water heaters [25] or air conditioner compressors [26] at customers premises can be remotely shut off or cycled on and off by utilities or demand response aggregators (DR AGG). This generally leads to customer loss of comfort and inconvenience.

TOU: Customers receive monthly bill credits for reducing energy during a specified time of a day sent by a utility or a DR AGG. Demand reduction can be achieved in response to time of the day and electricity price. TOU DR event can be called 24/7, 365 days of a year. The trigger of TOU event can result from an emergency condition realized by an ISO or a utility or during a high power demand requirement period of a day.

RTP: Electricity bill can be lowered if customers reduce energy usage during hours with high temperature-driven prices and/or shift usage to lower priced hours. Customers decide when to reduce energy usage. There is no energy event in which to participate. There is no minimum requirement for energy reduction. RTP DR program is available year-round. Energy charges will increase when higher temperature is expected.

Commercial Solutions/AGG: Commercially, Siemens has released the Demand Response Management System (DRMS) called Surgical Demand Response. This system gives utilities an ability to selectively execute a demand curtailment at specific substations or feeder lines [27].

OpenADR: OpenADR [28] (Open Automated Demand Response) was developed at the Demand Response Research Center [29] (DRRC) as part of an ongoing effort to help building and facilities managers implement automated demand response within their facilities. It was designed to allow buildings to invoke pre-planned demand shedding strategies quickly and automatically when requested by utility operations by integrating automated building responses. At its core, the OpenADR architecture defines a data model for energy cost and reliability that is common among and relevant to an energy provider and its customers. By providing a common data model among these parties and defining the semantics for accessing and changing elements within this model, energy providers and consumers can efficiently exchange demand response requests based on both price and grid reliability criteria.

One particular feature that differentiates OpenADR from other automated DR architectures is that utility DR requests contain no information about specific devices or operations that should be curtailed or stopped. OpenADR only conveys the utility's request for demand reduction to the customer - either by direct request or through distribution of increased energy cost rate schedules that will, in turn, motivate load shedding and reduced demand.

In practice, OpenADR is implemented as a client/server system that highly leverages design elements found in similar successful commercial Internet designs. It is readily adapted to widely-available Internet communications infrastructures and, due to its hierarchical design can mirror the layered organizations typically found in energy distribution systems – namely utilities, aggregators, and end users. In order to effectively share model data between participating entities, OpenADR defines an extensive set of XML (eXtensible Markup Language [30]) formatted messages that describe model element identifiers and their values. These XML-formatted messages are used to communicate current and future energy pricing, time of use pricing schedules and as well as explicit demand reduction requests between the OpenADR Demand Response Automation Server (DRAS) and its clients.

Comparing to the other automated DR architectures, OpenADR provides multi-faceted benefits as follows.

- Simplify and reduce DR-related costs by use of standardized messaging formats
- Promote interoperability between utility servers and multi-vendor clients
- Increase customer participation and reduce operating cost associated with manual responses to DR requests through use of automation
- Allow energy consumers to customize local response to utility DR requests
- By promoting standardized architecture and messaging format, OpenADR encourages wide-scale integration and embedding of DR capabilities into various consumer devices

The example of implementation of OpenADR in the case where a utility must shed loads to maintain grid stability is given as follows.

First use case: a utility knows that one or more pre-registered clients are participating in a particular DR program and they have agreed to respond, within certain pre-arranged limits, to utility requests to shed load over a given time interval. The magnitude of the expected load shed and the speed at which it can be affected are fully specified by the specific DR program to which a client has subscribed. The utility issues a DR event request to participating clients to shed loads and receives verification that the request has been received. Clients then begin shedding load in keeping with pre-agreed criteria. Failure to perform as agreed, as indicated by interval-recording revenue meter data, will result in penalties at a later date when utility rate charges are reconciled. An OpenADR client may optionally indicate that it will not participate in a DR program ("opt out") for some period of time. While this typically does not override a client's obligations to comply with DR program requests, such a response may ease the complexity of utility dispatch operations.

Second use case: utilities modify energy costs in an attempt to motivate reduction in demand. The OpenADR server can issue "price events" that describe elevated energy costs over a particular time interval. Participating clients can respond to these requests by shedding load, according to the communicated schedule, and reduce their energy costs. Conversely, some clients may decide to accept the "opportunity costs" of higher energy rates because local conditions require energy consumption to continue at normal rates. Since utility back office operations are ultimately responsible for local "time of use" readout and revenue settlement, local DR behavior can remain relatively independent of utility DR requests while accurate contractual or revenue obligations can be insured.

The followings are desirable requirements for customers wishing to participate in a DR program via the OpenADR architecture.

- Specific customer-side responses to these requests are formulated by and completely under control of the end user.
- In addition, the OpenADR messaging protocol has provisions for customers to individually respond to DR requests with an "opt out" signal – further increasing flexibility permitted for customer response.
- The end result is a system that promotes automated responses to utility DR requests while maximizing the local flexibility exercised in responding to those requests.

2.1.3 Home Energy Management System (HEM)

A. Background of HEM

The growing trend that smart meters, home energy management systems, and demand response (DR)-enabled appliances will become more prevalent has paved the way for residential customers to participate in DR programs being offered by electric utilities. Time-based DR programs are commonly used to allow demand reductions in response to electricity prices. Event-based DR programs are used to allow demand reductions in response to emergency events in a system such as lightning strike, storms, line to ground fault, vehicle accidents, etc. In order to participate in a demand response programs, HEM is an integral part to provide an interface between a home and a utility or a DR aggregator (e.g., EnerNOC [31]).

B. HEM Concept

In the context of demand response, home energy management system (HEM) is one of the crucial elements in such a way that it responses to demand limit signal sent by a utility during a DR event. Typically, in a house, there are four types of energy intensive appliances: air conditioner unit, clothes dryer, water heater, as well as a nascent electric vehicle. In addition, a rooftop PV panel can also be installed on a roof of a house in order to supply power to the house when energy from solar radiation is available.

C. Current Implementation and Development of HEM

Recently, more and more commercial products for home/building automation systems have become available to tackle the mentioned problems. Some examples of these products are SmartThings [32], Staples Connect™ [33], GE Brillion™ [34], Lowe's Iris [35], Revolv [36] etc. These solutions allow homeowners or small building owners to monitor or control specific compatible devices. However, there are still certain limitations for users or developers of that particular platform including incompatibility between vendors, limited number of supported devices, standards, communication technologies or data exchange protocols. Even though advanced users or developers can sign up to develop applications or add new devices to the platform, they are limited by the need to rely on specific tools provided by the platform. This makes the development ecosystem/vendor specific for that particular platform.

2.1.4 Building Energy Management System (BEM)

A. Background of BEM

Buildings consume over 40% of the total energy in the U.S. and over 70% of the nation's total electricity today. Over 90% of these buildings are either small-sized (< 5,000 ft^2) or medium-sized (5,000-50,000 ft^2) [37][38]. The U.S. Department of Energy (DOE) targets to save $2.2 trillion in energy-related costs by reducing building energy use by 50% compared to the 2010 baseline [39]. However at the current stage, study [39] shows that due to the lack of building monitoring and control, significant portion of the energy consumed in buildings is wasted. Building Automation Systems (BAS) is a promising approach to address these concerns. For small- and medium-sized buildings, heating consumption is the dominant end use, followed by lighting, plug loads and cooling [40].

Specifically, Heating, Ventilation, and Air-Conditioning (HVAC), lighting and plug loads account for almost 90% of all consumption in buildings. Existing BAS solutions are still cost-prohibitive and being used mostly in large buildings. BAS are not popular in most small- and medium-sized buildings due to lack of awareness of benefits, lack of inexpensive packaged solutions, and sometimes due to the owner not being the tenant and so finding no incentive to invest in these systems [41]. Small- and medium-sized buildings signify a huge market for BAS deployment as they represent over 90% of all commercial buildings in the United States according to U.S. Energy Information Administration (EIA) [41].

B. BEM Concept

A Building Energy Management System (BEM) or A Building Automation System (BAS) is a computer-based control system used to control and monitor building electrical and mechanical equipment such as Heating, Ventilating, and Air Conditioning system (HVAC), lighting loads controllers, plug loads controllers, fire systems, as well as security systems [42].BEM systems are most commonly implemented in large buildings with extensive electrical and mechanical equipment where power demand and energy consumption are high.

Benefits of BEM system that are realized to building tenant/occupants are as follows:

- Good control of internal comfort conditions
- Possibility of individual room control
- Increase staff productivity
- Effective monitoring and targeting of energy consumption
- Improved equipment reliability and life
- Effective response to HVAC-related complaints
- Save time and money during the maintenance

Benefits of BEM system that are realized to building owner are as follows:

- Higher rental value
- Flexibility on change of building use
- Individual tenant billing for services facilities manager

- Central or remote control and monitoring of a building
- Increased level of comfort and time saving
- Remote monitoring and control of equipment (e.g., AHU, Fire pumps, plumbing pumps, electrical supply etc.)

Benefits of BEM system that are realized to maintenance companies are as follows:

- Ease of information availability problem
- Computerized maintenance scheduling
- Effective use of maintenance staff
- Early detection of problems
- More satisfied occupants

C. Current Implementation and Development of BEM

Yet while new buildings offer opportunities to builders and operators to take advantage of state-of-the-art energy efficient technologies and know-how, the existing buildings would require comprehensive, "deep" retrofits to achieve similar savings. A new building diagnostic and controls revolution is underway within the buildings sector, primarily in the commercial buildings sector. In it, application-based systems are presenting an opportunity to implement strategies in which highly "optimized" control capable of constantly increasing efficiency levels while improving resource allocation (both local and global) is an inherent attribute of the strategy rather than an explicitly programmed feature.

Introduction of sensors and controls, as well as information technology and communication protocols between the buildings and the electric grid, has led to digitized sensing, metering, communication and controls. Using these technological advances and careful coordination, buildings could provide valuable comfort and productivity services to building owners and occupants, such as automatically and continuously improving building operations and maintenance, while at the same time reducing energy costs.

Buildings can act as dispatchable assets, providing services in order to respond to contingencies in a power system such as fluctuations of intermittent renewable energy sources. Transaction-based building controls are one part of the transactional energy framework. While these controls realize benefits by enabling automatic, market-based intra-building efficiency optimizations, the transactional energy framework provides similar benefits using the same market-based structure, yet on a larger scale and beyond just buildings, to the electricity market and the society at large. The premise of transaction-based control is that interactions between various components in a complex energy system can be controlled by negotiating immediate and contingent contracts on a regular basis in lieu of or in addition to the conventional command and control pattern.

Transaction-based control of BEM should provide: 1. Insight into current and projected energy use, 2. Comfort preferences of tenants or owners, 3. Generation capacity from distributed energy resources. The realized benefits of transaction-based controls are as follows:

- Provide building-specific advice to owners
- Outline return on investment and timescales for efficiency upgrades

- Calculate and point to amount of energy wasted per year
- Provide specific advice for occupants willing to trade their comfort and convenient levels against monetary gain
- Allow equipment to respond to market financial incentives
- Provide substantial energy savings and new cash flow opportunities to buildings
- Effectively turn currently disparate and passive assets into coordinated engines of efficiency and productivity
- Offer opportunity to extract services out of loads and assets that previously did not exist
- Deliver targeted benefits to building owners while enabling ancillary benefits such as reduced energy costs, energy use and related emissions to society as a whole

Driven by building codes, prescriptive measures, energy audits, advanced in efficient lighting, HVAC and energy management systems, the residential and commercial building sectors have lowered their energy intensity by over 30%. Existing building codes apply only to new construction and major renovations of existing buildings in the U.S. and can lead to additional savings of between 10 and 20% compared to previous standard levels. Burdened by badly performing equipment, appliances, walls and windows, the existing buildings faces cost barriers and several other obstacles to increased energy efficiency. Even buildings are made more energy efficient through codes, standards and beyond-code design processes, over $30 billion worth of consumed energy is wasted by the lack of controls or the inability to use existing building automation systems (BAS) properly. The preferences, desires and flexibility of building occupants are also hardly ever considered in energy efficiency decision making.

While building occupants could offer a large and tradable resource of exchanging comfort levels for energy savings (in exchange for some monetary gain, for example), the current state is leaving them out of the equation. The large expense of deep retrofits (and with it long payback times), the lack of broad access to sensing and measuring technologies, and the current disregard for occupants willingness to trade some comfort for savings are a few reasons why the outlook for greater gains in energy saving and energy efficiency for the existing buildings is substantially less positive than in new buildings.

Many HVAC systems are controlled by thermostats. Typically, a building administrator or a building engineer selects a desired temperature set point. Thermostat uses current space temperature sensor information to control the damper position that controls the air flow (or turns the compressor on or off), thereby satisfying the heating and cooling needs of the zone. In a conventional control system, indoor temperature and indoor set point temperature are the only information required to control the amount of heating and cooling to the zone. However, regarding a transactive-based control system, thermostats use price information to make control decisions. Although much of the discussion so far has been for thermostatically controlled HVAC systems, transactive-based controls can be applied to non-thermostatically controlled systems as well (such as distributed generation, or other load resources). With appropriate technology and coordination, buildings could provide valuable services to owners and occupants, such as automatically and continuously improving building operations.

On a larger scale, groups of buildings could transact with each other in a cap-and-trade type of arrangement, where one building could reduce energy or increase efficiency measures more easily than another, and then trade energy savings or efficiency gains for some compensation. Smarter

building: residential buildings, expanded penetration of smart controls scheduling appliances, automatically adjusting thermostat set points, dimming lights, and delaying water heater electric heating, are some of the technological changes needed. Transaction-based control will be accepted better if it can be flexibly tailored to the needs and capabilities of each building, the building owner, and the building's occupants. Enabling demonstrations of the transaction-based controls in individual buildings and then in a cluster of buildings to be flexible and portable across various BAS protocols and systems, should significantly reduce the cost of implementation compared to conventional approaches.

Many new Internet-protocol-based controls provide a rudimentary ability to integrate individual appliances and assets within the building to allow the building to automatically and continuously raise its efficiency. The requirements to make the building smarter are new and better use of existing communication, control and sensing technologies that:

- Make buildings capable of automatically receiving and acting upon signals from internal and external sensors and monitors
- Characterize the magnitude of change in demand as a result of responding to DR signals
- Function reliably with the means of verifying operation through low-cost and non-intrusive technologies
- Capable of delivering continuous and automated operational improvements
- Provide smart grid related services
- Cost-effective and economical to implement
- Non-disruptive during operation and minimally disruptive during installation to make buildings capable of automatically receiving and acting upon signals from internal and external sensors and monitors

The framework that enables these services will provide the market structure to facilitate the different transactions to occur. It will also require the development and deployment of new networks, devices and controls to support real-time, two-way communications between the participating players/actors. It will further require new and intelligent applications at numerous nodes throughout the network to facilitate and automate the wide variety of transactions, and to manage and activate control and monitoring systems that are involved in the delivery of transactional energy services.

Some open source building automation solutions are available such as Freedomotic [43], OpenRemote [44], and openHAB [45] etc. These platforms provide open, flexible architectures, and hardware/protocol agnostic tools for developing residential or commercial automation. The intelligence of buildings can be enhanced to implement automated rules, scripts, or event triggering for a specific device(s). However, the solution to make devices coordinate and communicate autonomously and seamlessly together in order to achieve the global objective of a building's owner (e.g., perform DR when the price of electricity is high) has not yet been addressed.

There are some available open source platforms that allow developers to develop BEM from scratch as follows. One platform is JADE (Java Agent Development Framework), software framework fully implemented in Java [46]. The advantage is that developers can easily build a FIPA-compliant multi-agent system with their set of Java classes. The disadvantage is limited support on hardware and software resource management, which is a prime important requirement

for a BEM system that needs to run on a small-form-factor computers or an embedded system. Another platform is Spade [47], which is a platform based on the XMPP/Jabber technology and written in the Python programming language. There is also AgentScape [48], a distributed agent middleware. Its design philosophy is "less is more", meaning AgentScape provides a minimal but sufficient support for agent applications.

2.1.5 Multi-Agent System (MAS)

In recent years, multi-agent systems (MAS) have been in the limelight compared to other approaches in providing decentralized intelligent management and control of a power distribution network. Fundamentally, MAS consists of multiple distributed intelligent agents, which reside in physical devices scattered throughout the system. Agents are working in collaboration with each other to achieve a desired goal in a specific environment. Particularly, MAS are employed to deal with complex tasks, which cannot be solved by a single agent. The overall goal is broken down into smaller targets, a selection of which is assigned to a selected agent.

A. Agent Oriented Programming (AOP)

An Agent Oriented Programming (AOP) is a relatively new software paradigm that brings the concepts and merits from the theories of artificial intelligence into the mainstream realm of distribution system [49].

The followings are AOP characteristics:
- Autonomy: AOP can independently carry out complex, and often long-term, tasks. Moreover, it can be operated without human intervention.
- Proactivity: AOP can take initiative to perform a given task even without an explicit stimulus from a user.
- Ability to communicate: AOP can interact with other entities (cyber elements) in order to achieve the system goal or an individual goal.

Agents can be distributed on distinct physical devices. In addition, Agents could be mobile so that their execution would be transferability to different processors (multi-threading processing).

According to [50], a software program can be declared as an agent if it exhibits the following characteristics:
1. Sociality: an agent can interact with its environment
2. Autonomy: an agent can learn from its environment
3. Reactivity and Pro-activity: an agent reacts to its environment in a timely manner
4. Autonomy and Pro-activity: an agent takes initiatives to achieve its goals
5. Sociality and Reactivity: an agent accomplishes tasks on behalf of its user

B. What is Multi-Agent Systems (MAS)?

Multi-Agent Systems (MAS) are the systems consisting of multiple agents working and communicating together to achieve the system target or their own targets. However, an agent might work alone as a single entity or work with other agents by communication, collaboration

and negotiation processes in system environment. The MAS consist of distributed agents that achieve an objective cooperatively. They can execute their tasks synchronously or asynchronously, and access decentralized database as needed. The MAS are employed to deal with complex tasks, which cannot be solved by a single agent, by dividing system goal into smaller targets and giving them to each agent. Therefore the objective and goal are achieved by interoperating of agents. In the MAS, there are two ways which agents can interact to each other; direct and indirect interaction. For directly interaction, agents can communicate and negotiate to near-by agents or agent which is specified to be a receiver of a sending message from sender agent. For indirect interaction, in an arbitrary system, agents need to react to their environment. By doing so, other agents are affected as well because agents' environment has already changed.

C. Why MAS?

In addition, multi-agent systems offer following advantages:

- Multi-agent systems propose inherent benefits of flexibility and extensibility.
- The philosophy behind multi-agent systems is that a huge and complex task be divided into several smaller tasks assigned to several entities. This reduces the need for maintenance and processing of large data.

D. Agent Architecture

Agent architectures are the fundamental mechanisms underlying the autonomous software components that support effective behavior in dynamic, real-world and open environments. Agent architectures can be separated into four main categories as followings Logic based, Reactive, BDI, and Layered architectures [50].

E. MAS Communication and Coordination

Communication and coordination between agents are essential components of MAS. In fact, agents should capable of communicating with users, system resources and each other in order to collaborate, negotiate and cooperate to achieve their goals. Hence, comparing to human, agents need to have communication languages as well. Basically, there are two existing and well-known communication languages of agents which are KQML and FIPA ACL. KQML is the first agent communication language while FIPA ACL is currently the prevalent studied and used. The prime features of FIPA ACL which make it different from KQML are the feasibility of using different content languages and predefined interaction protocols which help to manage agents' conversations. Coordination of agents is the process in which the agents, when act together in agent's community, need to be coherent. There are multiple reasons why agents need to be coordinated. First, conflict among agents can occur due to agents' goal either global or individual. Second, individual agents' goal may be dependent to other agents. Third, agents' characteristics which normally agents might have different capabilities and knowledge. Forth, agents' goals can be achieved rapidly due to smaller tasks are allocated to each agent.

FIPA is the international non-profit foundation which established in order to develop software agent technology standards collection [51]. The most important FIPA standards are agent communication, agent management and agent architecture. The followings are the brief

discussions of these topics mentioned. FIPA-ACL is the language, which is used and studied in this research due to its benefits over KQML language. Typically, the most important component of FIPA-ACL is message speech act or called performative. For example, 'My name is Henry' message is the message which inform sender's name to recipient. In this example, inform is a speech act or performative of the message. The most commonly used performatives are inform, query, request, agree, refuse and not understood.

In fact, the FIPA standards stated that for any agent, which need to be fully compliant with each other and the system, is required to be able to receive any FIPA-ACL performative message at a very least respond. In case of agent receive any message which cannot be processed, a not understood message will be sent back to the sender. However, sending a message to the recipient has something more than just a communication act or performative. In this topic, the FIPA-ACL message structure has not been discussed. The next topic will introduce the concept of how to manage the agents.

The FIPA request interaction protocol (IP) allows an initiator agent to request a participant agent to process and perform action. Whether to accept or refuse the request the participant agent after receive and process the request will make decision and reply back to the initiator.

Another example of FIPA interaction protocol is the "Call for Proposal" (CFP), the initiator sends CFP message to the participant. Then, the participant will decide whether to send "Refuse" or "Propose" message back to the initiator. In case of "Refuse" message is sent by the participant, the initiator agent will do nothing. If "Propose" message in sent instead, then the initiator need to make decision whether to send "Reject Proposal" or "Accept Proposal" message return to the participant. The participant will not continue this negotiation process if it receives "Reject Proposal" message. In contrary, if an "Accept Proposal" message is sent to it, the participant will send "Failure" or "Inform" message to the initiator. The initiator will process that message and take action. If the initiator receives "Failure" message, it means that the action which the participant proposed to the initiator has been attempted but the attempt failed. If the initiator receives "Inform" message, it means that this negotiation process is complete and the participant agent will perform action which the initiator requested.

F. Agent Management

As agents need to be compliant with each other and the system, agent management is required for collaborating them together. Agent management is a framework within FIPA that will determine the status of existing, operable or manageable for the compliant agents. The logical reference model for agents' registration, migration, creation, location, communication and operation is established by agent management. The important elements of agent management are described as follows:

Agent Platform (AP): AP is the physical layer of MAS consisting of physical devices such as machines, operating systems, agents, FIPA agent management components and (if available) additional support software. In the real system, agents do not need to reside in the same host or AP.

Agent: Agent is a high-level software abstraction which has autonomous attribute working to achieve its own target. Agent can be characterized by its behavior and ontology. Any agent must have its own identity which can be assigned by using FIPA Agent Identifier (AID). Therefore, agents are identified and distinguished by their different AIDs. Basically, agent description and agent service description are two important components of any agent which will help to describe agent name and declare its services.

Agent Management System (AMS): AP is mandated to have AMS. AMS is responsible for providing the management system which is able to operate an AP. Typically, AMS manages the creation, deletion or migration of agents. To acquire an AID, agent need to register itself with AMS and then agent is stored in a directory within an AP.

Directory Facilitator (DF): DF can be employed as an optional component of an AP. DF provides yellow pages services to other agents. Any single agent might have its own services which needed to publicize then agent may send request to DF to register those services.

Message Transport Service (MTS): FIPA-ACL message can be transported by deployment of MTS service provided by an AP. ACL message can be passed between agents on the same AP or between agents reside on different APs. FIPA-ACL message structure consists of transport information, encoded message, message parameters and message content.

By creating MAS in JADE building toolkit, JADE remote agent management will be automatically created as depicted in Fig. 2-1.

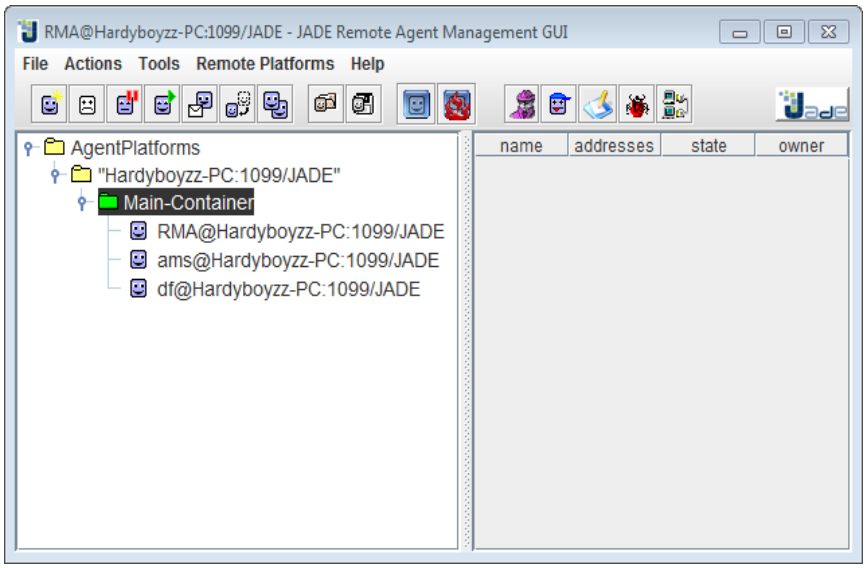

Fig. 2-1. JADE Remote Agent Management GUI

G. MAS Applications

Nowadays, Multi-agent systems are being used in many systems. Basically, the MAS applications can be divided into the following two categories:

Single-agent systems: These applications include situations where a human may require assistance while using a computer software e.g., meeting scheduler software, information retrieval and filtering software, mail management engine, news filtering engine, search engine, etc.

Multi-agent systems: Agents work together to achieve a particular goal. The applications of MAS can be applied either in physical systems or simulations of physical systems. Examples include traffic monitoring, decision support systems, manufacturing systems, telecommunications and network management, aircraft maintenance, military logistics planning, real world simulation, power systems etc. [52], [53]. In addition, MAS applications in distribution power systems may include power system restoration [54], protection [55], distributed generation control [56] and islanded operation [57]. MAS applications have also been extended for transformer's condition monitoring [58], [59]. However, there are limited a number of studies that use MAS for DR applications at a distribution transformer. The working group of the IEEE Power & Energy Society (PES) also investigates the use of MAS for power engineering applications [60].

H. JAVA Agent Development Framework (JADE) for MAS Development

JADE, which stands for Java Agent Development Framework, is selected as a study tool to facilitate the implementation of multi-agent system with simulated circuit. JADE, basically, is an open source platform for development of peer-to-peer agent based applications. JADE, probably, claims as the most widespread agent-oriented middleware in use today. JADE is a completely distributed middleware system with a flexible infrastructure allowing easy extension with add-on modules. The framework facilitates the development of complete agent-based applications by means of a run-time environment implementing the life-cycle support features required by agent, the core of logic of agents themselves, and a rich suite of graphical tools. In addition, as JADE is written completely in Java, it benefits from the huge set of languages features and third-party libraries on offer, and thus offering a rich set of programming abstractions allowing developers to construct JADE multi-agent systems with relatively minimal expertise in agent theory.

There are four steps associated with the process of developing MAS with JADE.

Step1: Creating agents

In this step, a setup() method is created in order to initialize an agents and declare agents' parameters. Normally, the operations which will perform in setup() method are opening a connection to a database (MATLAB/Simulink), registering services that agent provides to yellow pages service (DF agent), registering agents' name or agents' AID to AMS agent, showing a GUI and starting initial agent behaviors.

Regarding to agent creation, any agents in the system need to be identified by an 'agent identifier'. Basically, each agent instance must have a globally unique name (GUID) and a number of addresses shown in the form <local-name>@<platform-name>.

In Fig. 2-2, an agentCoordinator agent is automatically created corresponding to the MACSimJX middleware running under MATLAB/Simulink environment. This agent acts as a link between JADE and MACSimJX. During running the simulation circuit, system environment data in MATLAB/Simulink environment such as bus voltage, bus current or required power by

loads are the input signals to agentCoordinator. Then, the agentCoordinator will pass that received data to agents that interested in them. Typically, agentCoordinator receives all data sending from MATLAB/Simulink environment. However, there is not mandated that an agent need to take all data. Any single agent can choose data which it interested in. After all agents are named, then every single agent is needed to define its own interest data received from agentCoordinator agent.

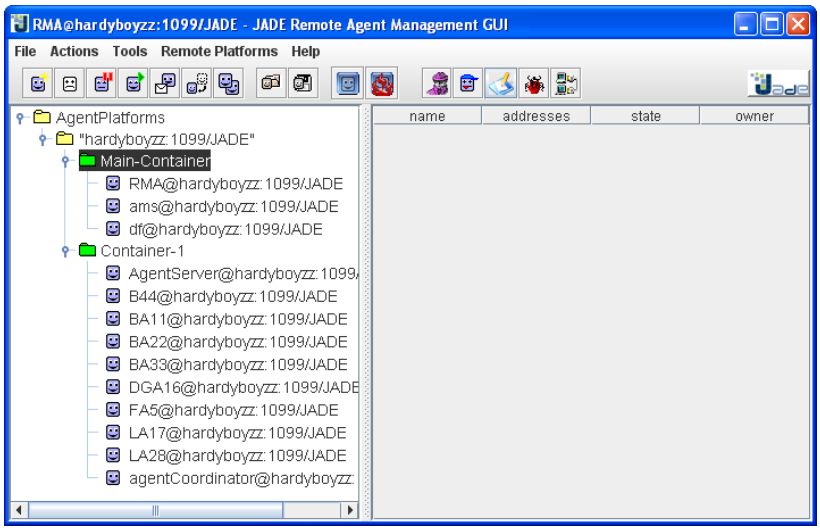

Fig. 2-2. Agents Creation

Step2: Agent tasks

The actual job, or jobs, that an agent will perform, depends on its behaviors. A behavior of any agent represents a task that agent can carry out. Basically, behavior can be added anytime to agent at setup() method or another behavior. Due to the merit of java which can handle multi-threading processing, several behaviors of an agent can be run simultaneously. However, agents' behaviors are also needed to be scheduled for cooperative actions. Normally, a single JAVA thread is used per single agent.

Step3: Agent communications

The most fundamental feature of JADE which is implemented in accordance with FIPA standards is agent communication. Asynchronous message passing is used for agent communication.

An agent has its own mailbox or called message queue. Whenever a receiving agent receive message from a sending agent via distributed JADE run-time, message will be passed and queued in the mailbox message queue. However, the algorithm for agent to pick up the message from message queue and how agent processes that message depends on the agent programmer.

According to FIPA-ACL message structure, the specific format of message in JADE needs to have the following fields.

1. The message sender
2. The receivers

3. The communication act (also called ‘performative’)
4. The content is the fact the sender intend to send to the receiver
5. The content language is the syntax used to express the content
6. The ontology used for expressing the symbols or vocabulary in the content
7. Additional fields used to control the simultaneous conversation

Step4: Agent discovery: the yellow pages service

DF agent provides the yellow pages service, which basically is an optional service in AP, allowing agents to publish their services to other agents. Therefore, the published services are readily and easily for other agents to discover and exploit. Basically, any agent is capable of publishing its services or discovering other agents’ services. It should be noted that an agent may or may not publish it services corresponding to its architecture. Moreover, it is not a mandated number for agent services.

2.2 In-Depth Information

2.2.1 Research on DR at Residential Homes

There is a number of previous work that proposes different methodologies for DR implementation at a distribution network level. Authors in [61], [62], [63] propose DR strategies to implement residential DR based on time-based DR programs e.g., real time pricing (RTP). Authors in [64] propose an EDRP that enables the use of residential load resources in response to contingencies in a distribution system. However, loads are modeled as lumped loads and characteristics of household appliances are not taken into account. The Analytic Hierarchy Process (AHP)-based DR strategy to alleviate power system stress conditions is presented in [65].

In this paper, to reduce the power demand at the distribution transformer level, the demand limit (DL) of all homes during a DR event is identical regardless of different homes’ characteristics. There is a chance that unexpected impacts of an overly increased power demand following a DR event (i.e., demand restrike or DRK) can be experienced. Authors in [66] and [67] suggest the approaches to tackle and mitigate impacts of DRK and reduce power demand during a DR event using dynamic pricing techniques. However, as the amount of load reduction cannot be guaranteed and depends heavily on customer preferences, these approaches are undesirable.

Topics related to Electric Vehicles (EVs) have gained popularity as they have lower environmental impacts, and becoming economically viable [68]. The topic of integrating EVs into a power distribution network is of great interest as improper EV charging can pose serious overloading challenges to a distribution network especially in the case of high EV penetration. Some of the foreseeable impacts include distribution transformer overload, line overload, voltage sags, increased line losses and sharp peak demand increases [69], [70], [71], [72]. Several approaches are proposed to overcome these negative impacts by controlling EV charging profiles at customer premises. Some approaches focus on centralized control where EVs are controlled from a central control center to maximize system load factor [70] or minimize system losses [73]. The others exploit decentralized control approaches where EV charging is controlled locally to minimize the requirement of communication infrastructure. These approaches mainly focus solely

on controlling EV loads [74], [75], [76], while characteristics of other potentially controllable appliances are not considered.

The agent-based DR implementation in a distribution network considering economic and reliability of the system is proposed in [77], [78], [79]. Other DR work in distribution networks include mitigation strategies of an overly increase in electricity power demand (i.e., rebound peak) during low electricity price period [80]. Nevertheless, the mitigation strategies of an overly increase of power demand following a DR event (i.e., demand restrike) introduced by [80] due to a DR implementation during a power system stress condition have not yet been widely studied.

2.2.2 Research on DR at Commercial Buildings

There is number of previous work that proposes different methodologies for DR implementation at a building level. Authors in [81] discuss how EnerNOC [32] works with commercial and industrial customers to provide reliable reductions in power and energy demand in these markets. Regarding this paper, EnerNOC's Network Operation Center can fully automate DR at customer sites. Such automation enables market participants to provide relief quickly and easily demand reduction during a DR event, making DR a valuable asset for participation in the ancillary services market. This is a landmark development that will increase building's energy efficiency and could lead to cost reductions for these services by increasing competition to provide them. The potential additional revenue for the services also enhances opportunities for investment in DR resources. Examples of end-use devices that are curtailable are chillers and air handlers, external lighting and signage, HVAC systems, internal lightings, office equipment, etc.

A typical commercial building might have several chillers that supply a number of air-handling units (AHU) or air handlers with chilled water on demand. If several air handlers require the full output of one chiller, and another air handler suddenly also requires cooling, traditional building control algorithms simply start up a second chiller to meet the demand and the building's electrical load ratchets upward accordingly. Authors in [82] presents a transaction–based building control system that behaves differently. Instead of honoring an absolute demand for more chilled water, the air handler requests such service in the form of a bid (expressed in dollars), increasing its bid in proportion to its "need" (divergence of the zone or supply air temperature from its set point). The chiller controls, with knowledge of the electric rate structure, can easily express the cost of service as the cost of the kWh to run the additional chiller plus the incremental kW demand charge (if it applies). If the zone served by this air handler just began to require cooling, its "need" is not very great at first, so it places a low value on its bid for service and the additional chiller stays off until the level of need increases. Meanwhile, if another air handler satisfies its need for cooling, the cost of chilled water immediately drops below the bid price because a second chiller is no longer required, and the air handler awaiting service receives chilled water. Alternatively, a peer-to-peer transaction can take place in which an air handler with a greater need for service displaces (literally outbids) another whose thermostat setting is nearly satisfied. Benefits offered by this approach are (1) the ability to limit demand by providing the most "cost-effective" service that is to prioritize the most important needs before serving lass important ones, and (2) the decrease in energy demand and consumption by preventing operations of entire chiller to meet a small load. The main contribution of this paper is the use of common denominator for control that makes expression of this multi-level optimization much simpler than an engineered

solution would be. It allows controls to be expressed in local, modular terms while accounting for their global impact on the entire system. Automated Lighting control system: simple scheduling or sensor-based systems can actuate electric lights according to occupancy or ambient light levels. RTUs are more grid-responsive, so they can interact with the grid and provide demand response and ancillary services benefiting both the building owner/customer and the utility. Use of advanced controls and automated fault detection and diagnostics on existing RTUs will result in significant energy and cost savings and also enhanced maintenance by introducing condition-based maintenance practices and targeting maintenance when needed.

Authors in [83] propose an intelligent Multi-Agent control system for energy and comfort management in a smart building. There are three main factors to measure comfort and indoor air quality of a building: indoor temperature, illumination, and carbon dioxide concentration. Fuzzy logic controllers are used to optimize energy consumption as well as to maintain comfort inside a building. A Graphic User Interface (GUI) is developed using MATLAB GUIDE tool to provide an interface to a user to give priority to building loads as well as access a setting menu. Authors in [84] presents a Multi-Agent System with the main objective to save energy consumption and maintain comfort of a building. HVAC and lighting loads are monitored and controlled to reach the desired objectives. This paper also considers the integration of renewable energy resources such as solar PV, wind, and battery energy storage with a building. The fuzzy control logic is designed as a controller. The objective functions of the proposed methodology are formulated as non-linear multi-objective optimization problems and solved by using Genetic Algorithm (GA). Authors in [85] employs a Multi-Agent System to minimize heating energy, cooling energy, and lighting loads power consumption of a building. In order to simulate a case study, a building is modeled using EnergyPlus [86]: a whole building energy simulation program that engineers, architectures, and researchers use to model energy and water use in buildings. These objectives functions are mathematically formulated as non-linear optimization problems in which are solve using AMPL [87] optimization tool that use CPLEX [88] as a solver. Authors in [89] proposes a Multi-Agent System to manage plug loads and integrate renewable energy resources with a building with the main objective to minimize electricity cost as well as maintain a comfort of a building. This objective is formulated a multi-objective optimization problem having objective as a quadratic function. The problem is then solved by using quadratic programming, 0-1 integer linear programming or the heuristic algorithm.

2.3 Conclusions and Knowledge Gaps

2.3.1 Demand Response Strategy at Residential Homes

Based on the literature search with respect to current approaches to handle demand response at residential homes, it can be concluded that load reduction cannot be guaranteed and depends heavily on customers' preferences. This is because most of the proposed algorithms do not take into account customer preference, nor have two-way communication in place to ensure that a targeted load reduction can be achieved. Another knowledge gap is that homeowner's choices to control their appliances are limited with current technologies. Therefore, customer's comfort and convenient are not taken into account when designing DR strategies.

Regarding most literature to impose DR at residential homes, it can be seen that fairness of allocation of limited supply resources is also an overlooked factor. All houses are treated the same in those studies. In addition, DR impacts on an end-use distribution network are not fully studied and understood. This is because end-use distribution network is modeled as lump load in many studies. Hence, the true DR potentials at an end-use distribution network are not fully evaluated.

Another factor that is needed to consider is the demand restrike (DRK) after a DR event in which has not been rigorously studied. This is the power demand that will restrike if all appliances are turned back on right after a DR event.

In addition, there is also lack of extensive studies on load reshape assurance at a distribution transformer level that gives end-use customers flexibility to control their appliances. This is essential part because local intelligent at a distribution transformer allows houses to be treated differently based on their power demand requirement. There is also a need to study adverse impacts of a DR event, e.g., transformer overload causing by a DRK, has not been addressed.

Regarding the literature search, there are only few publications that discuss EDRP implementation at a distribution level and at a home level especially at an end-use distribution network (a secondary side of a distribution transformer). In most studies, end-use loads are modeled as lumped loads and characteristics of household appliances are not taken into account for this type of DR implementation.

Lastly, literature search shows that characteristics of other potentially controllable appliances (e.g., air conditioner, water heater, or clothes dryer etc.) rather than electric vehicles are not considered in most recent literature.

2.3.2 Demand Response Strategy at Commercial Buildings

At present, most building automation system (BAS) and building energy management system (BEM) solutions are proprietary and used in large buildings. BAS and BEM are not popular in most small- and medium-sized buildings due to lack of awareness of benefits, lack of inexpensive packaged solutions, and sometimes due to the owner not being the tenant and so finding no incentive to invest in these systems.

Due to lack of building monitoring and control especially small- and medium-sized buildings, significant portion of energy consumption of a building is wasted. Effective and low-cost solution to make devices coordinate and communicate autonomously and seamlessly together in order to achieve the global objective of a building's owner (e.g., perform DR when the price of electricity is high) has not yet been addressed.

While some buildings have embedded controls and some computing power, seemingly such most of the existing solutions are inefficient to maintain acceptable comfort and productivity to satisfy the building occupants.

Load reduction strategies of most automated BEM solutions are established in advance in order to participate in DR programs. Therefore, those strategies cannot keep up with dynamic

behaviors of power demand and energy consumption of a building that is likely to change over a course of the day. This is because the factors that will affect a power demand and an energy consumption of a building such as occupancy level, building thermal characteristics, tenant preferences, and devices' settings and their ability to be react to this dynamic behaviors are not fully studied.

In addition, regarding the literature search it has been found that many buildings fail to perform as their designers intended to provide comfort and convenience to tenants. This is due to building administrators or building engineers cannot properly operate buildings and tenants behave differently than the designers expected. Therefore, this will significantly impede the participation and implementation of small- and medium-sized commercial buildings in a demand response programs, such as Critical Peak Pricing (CPP), Real Time Pricing (RTU), Emergency Demand Response Program (EDRP), or Time of Use (TOU), etc.

3. METHODOLOGY

This chapter presents the overall framework of the study, and describes the approaches used to accomplish the proposed research.

3.1 Overall Study Framework

The overall framework of this dissertation, shown in Fig. 3-1, is driven by three main problems. First, electric utilities have limited choices to mitigate stress conditions in a power grid, with the current practice of load shedding and direct load control, participation in demand response (DR) event is not favorable by end-use customers. Second, during the hot summer peak period, electric utilities have to start their costly stand-by generators to serve peak loads. Third, comfort is often compromised when DR actions are performed at end-use customers leading to dissatisfaction of home residents and building occupants. ***Thus, the main question is how utilities can engage customers in DR events such that their comfort is not compromised***.

Therefore, clearly it can be seen that there are needs to respond to power grid stress conditions, to reduce peak power demand for more efficient operations of a power grid, and to have better integration and participation of controllable loads at customer premises.

In order to address this question, the focus of this dissertation is to develop an agent-based platform and associated control algorithms to enable demand response implementation at both the transformer/home levels and the building level. The devised algorithms takes into account occupancy level, customer comfort and preference, and load priority.

In this dissertation, four tasks to be accomplished include:

- **Task 1:** develop an agent-based platform to facilitate DR implementation at the distribution transformer and home levels
- **Task 2:** devise a DR algorithm to alleviate stress conditions given a callout of an emergency DR event (EDRE)
- **Task 3:** develop an agent-based platform to facilitate DR implementation at a building level
- **Task 4:** devise a DR algorithm in response to a critical peak pricing (CPP) at a building level as a resource to help improve efficiency of power grid operations

The proposed agent-based platforms, together with corresponding algorithms, are validated as presented in the case studies discussed in Chapters 4 and 5 for DR implementation at the transformer/home levels and the building level, respectively.

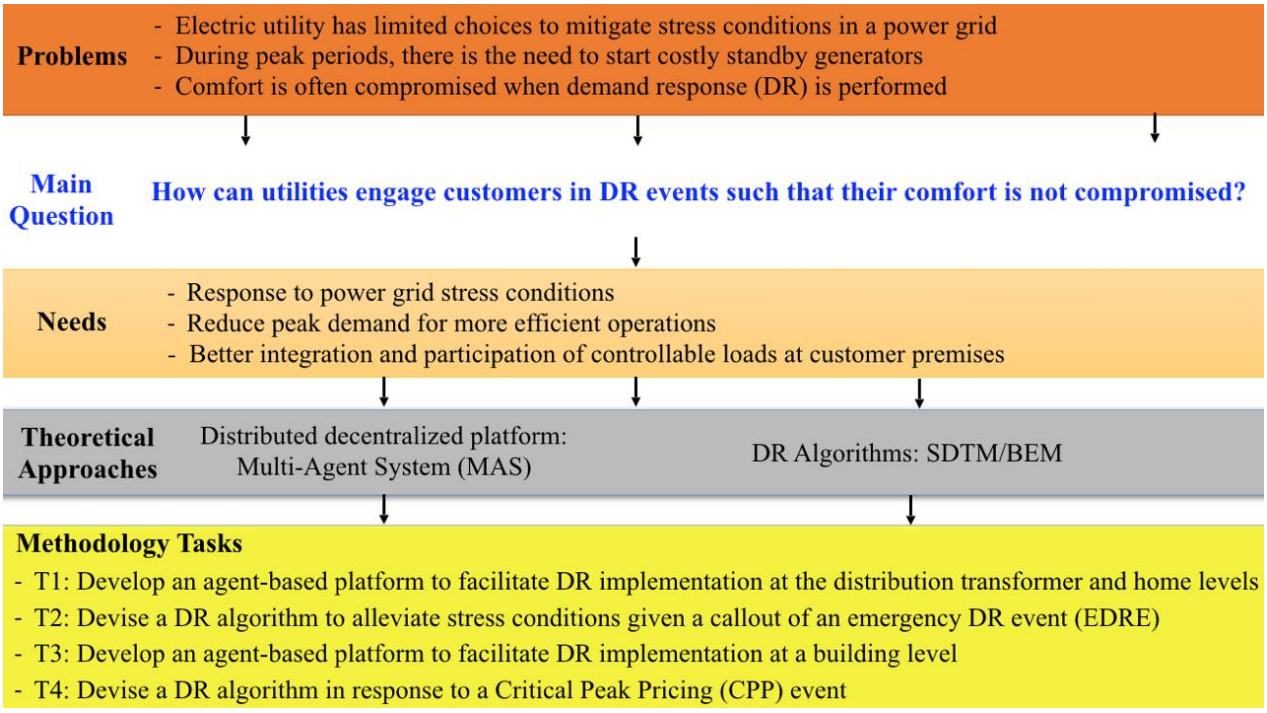

Fig. 3-1. Overall study framework

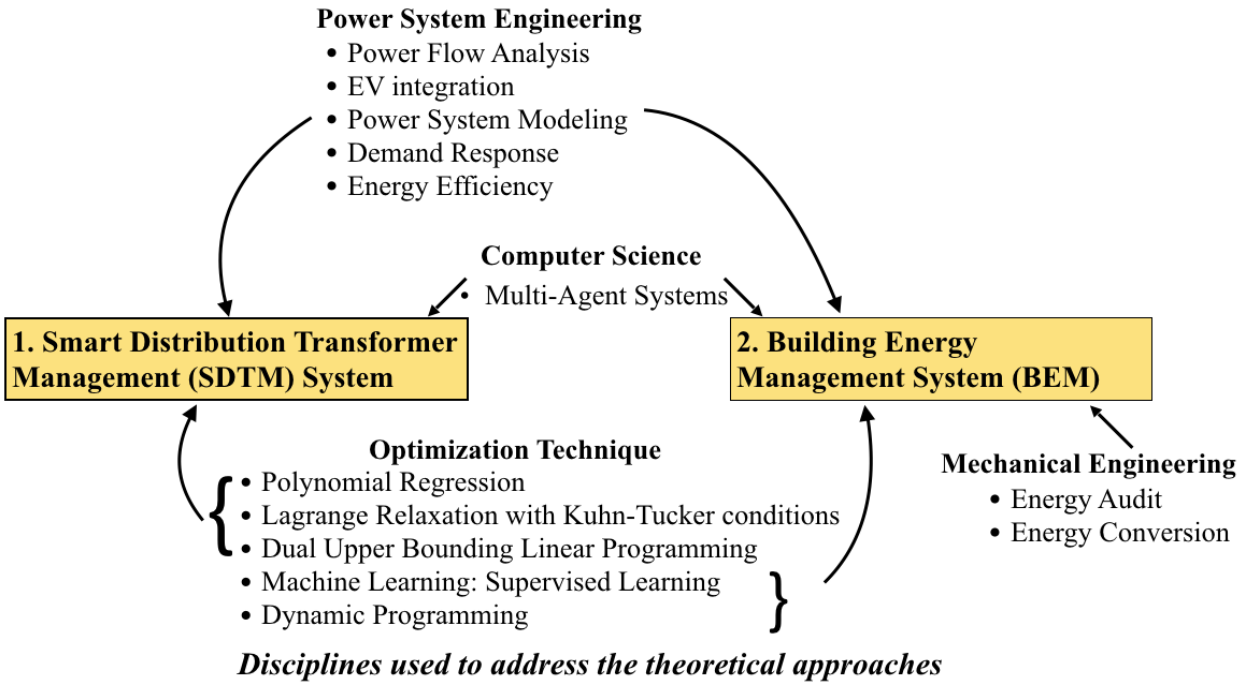

Fig. 3-2. Disciplines used in this dissertation

Three related disciplines for **the Smart Distribution Transformer Management (SDTM) system** are: (1) power system engineering: power system analysis, electric vehicle (EV) integration, power system modeling, demand response, and distributed energy resources integration; (2) optimization technique: polynomial regression, Lagrange relaxation with Kuhn-Tucker conditions, dual upper bounding linear programming; and (3) multi-agent systems: resource allocation.

For **the building energy management system (BEM)**, there are four related disciplines used, which are: (1) power system engineering; (2) optimization technique: machine learning techniques and dynamic programming; (3) multi-agent systems; and (4) mechanical engineering: energy audit, and energy conversion.

3.2 An Agent-based Platform for DR Implementation at the Transformer and the Home Levels

This section presents an agent-based platform for DR implementation at the transformer and at the home levels. Taking into account the point of connection to a utility's power distribution network, a single-phase transformer (e.g., 25 kVA rating) serves several homes in the same neighborhood is of particularly interest. The proposed agent-based platform has been designed in the context of the Smart Distribution Transformer Management (SDTM) system, which consists two layers: physical layer and cyber layer shown in Fig. 3-3.

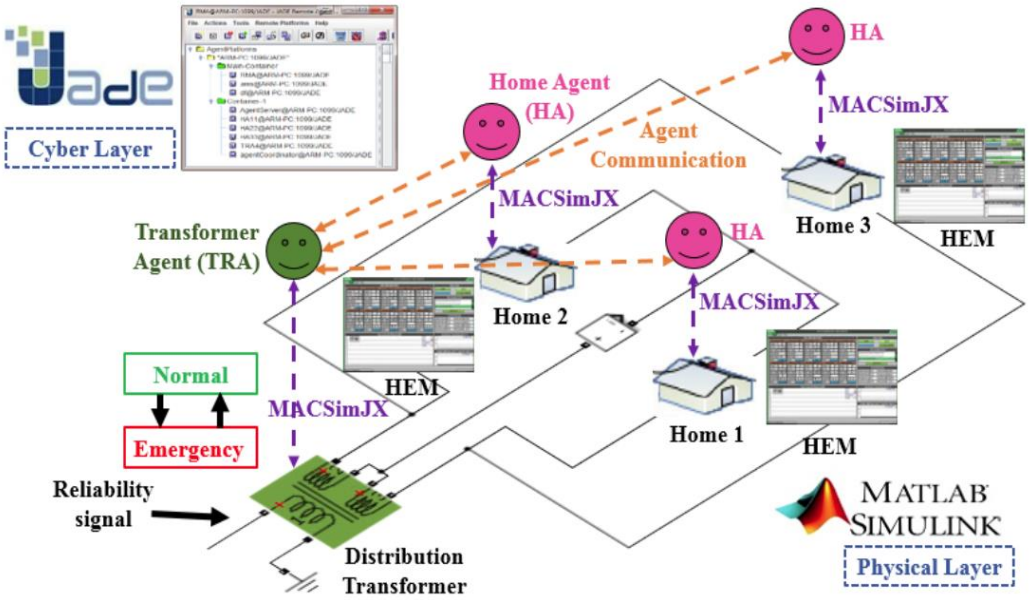

Fig. 3-3. Integrated system of the physical (a transformer, several homes, and DR-enabled appliances); and cyber layer (MAS: multi-agent system and HEM- home energy management).

Since the proposed agent-based platform needs to work in collaboration with devices in the physical layer, the development of simulation models for the physical layer, including a

distribution transformer serving several homes, must be discussed. This is presented in Section 3.2.1, and followed by its corresponding agent-based platform discussed in Section 3.2.2.

3.2.1 SDTM Physical Layer

The physical layer is where real physical devices are located. This layer comprises a distribution network with a single-phase distribution transformer serving several houses and DR-enabled household appliances.

A. Power Distribution Network Modeling

An emerging power distribution network (i.e., <69 kV) is illustrated in Fig. 3-4. The proposed SDTM system focuses on implementing DR at a home level through a distribution transformer, as circled, where a single-phase transformer (e.g., 25 kVA, 37.5 kVA, or 50 kVA) serves several houses in the same neighborhood.

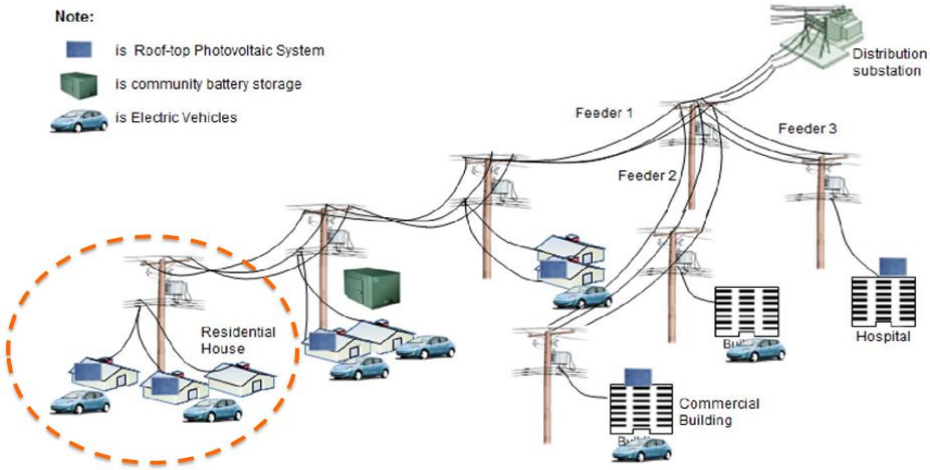

Fig. 3-4 An emerging power distribution network architecture

In the simulated environment shown in Fig. 3-3, a distribution network with a single-phase distribution transformer serving three houses is modeled in MATLAB/Simulink.

B. Home Energy Management System (HEM) Modeling

A house typically has power-intensive appliances (i.e., air conditioner (AC), water heater (WH), clothes dryer (CD), and electric vehicle (EV)), as well as a home energy management system (HEM), and a smart meter to provide two-way communication with an electric utility.

In the context of demand response, HEM is one of the crucial elements as it responses to demand limit or price signals sent by a utility during a DR event. The HEM system and its control algorithm – previously developed at Advanced Research Institute, Virginia Tech [90] as a stand-alone software package using C++ language is responsible for monitoring and scheduling the

operation of in-home appliances according to a specified set of requirements. An HEM system is designed to be able to intelligently manage and control four types of energy intensive appliances: an air conditioner (AC) unit, a water heater (WH), a clothes dryer (CD), and an electric vehicle (EV) according to their pre-defined priority when a demand limit is imposed on a home's energy consumption. This system enables utility to shape their load profiles.

During a DR event, an HEM receives an external demand limit level (kW) and duration (hours) signals via an advanced metering infrastructure (AMI) meter. An HEM system is required to make sure that the total household power demand during a DR event does not exceed that limit. The HEM algorithm developed in [91] is capable of controlling the operation of power-intensive appliances (i.e., AC, WH, CD, and EV) according to their priorities and demand limit, and make sure that critical loads, such as refrigerator and computer loads are served.

In order to model multiple homes in a distribution network, random characteristics of appliances and different usage patterns can be achieved by using the Monte Carlo methods to sample parameters required for modeling AC, CD, WH, and EV based on their corresponding random functions. It should be noted that these power-intensive appliances are modeled in [91]. One of the contribution of this dissertation is the Monte Carlo methods to sample different parameters of appliances based on their random characteristics and inherited probability density functions which have not been discussed in [92].

The sample parameters of each type of appliances can be obtained using various sampling techniques such as analytical inversion, numerical inversion, probability mixing method, rejection technique, as well as numerical evaluation depending upon complexities of density functions. The procedure of performing each appliance parameters generation is discussed in the following sections.

B.1 Model an air conditioner (AC)

Base on the AC unit model developed in [92], in order to simulate an AC unit, there are three main categories of the built-in parameters: temperature profile, building structure, and space cooling characteristic that need to be sampled. In this work, these parameters are randomized for different houses in the same distribution circuit and the aggregated load profile of a number of houses developed in [91] is generated.

1. Temperature profile: outdoor temperature (acquired from the National Climatic Data Center (NCDC) [92]) should be the same for all house in the same neighborhood. For the indoor temperature set points (data from ASHRAE [93]), normally during winter the temperature set point is approximately 72~76°F ± (1~2) °F; during summer the temperature set point is approximately 76~80°F ± (1~2) °F. A normal random function is used to determine the variation in temperature set points among different houses as described below.

Given: a temperature set point as a discrete random variable T (e.g., T∈[70,71,72,73,74,75,76,77,78]), the population distribution of T is known to be normal with mean μ and variance σ^2 that is $T \sim N(\mu, \sigma)$. Thus $p(T, \mu, \sigma) = \frac{1}{\sigma\sqrt{2\pi}} e^{-\frac{(T-\mu)^2}{2\sigma^2}}$. The fundamental

formulation of Monte Carlo (FFMC) of this discrete random variable is given as $Min\{P(n)|P(n) \geq \eta\}$, where $P(n) = \sum_{i=1}^{n} p_i$, $P(n)$ is a cumulative distribution function (cdf) of an outcome n of a random variable T, p_i is a probability density function (pdf) i of a random variable T, η is a random number. Therefore, by generating a random variable η, the n outcome of its corresponding random variable T can be obtained by selecting a minimum $P(n)$ that is greater than or equal to η.

2. Building structure: a density function (Fig. 3-5) derived from the data obtained from the American Housing Survey [94] is used to determine the variation in floor plan, areas of walls, areas of ceilings, areas of windows, and R-values among different houses in the same distribution circuit. A home's floor plan area can be obtained according to the density function using the rejection technique as shown in Fig. 3-6.

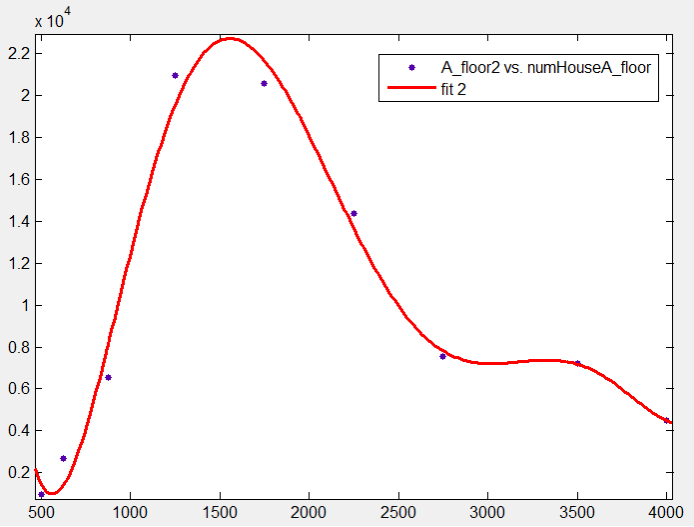

Fig. 3-5. Floor plan area of American house

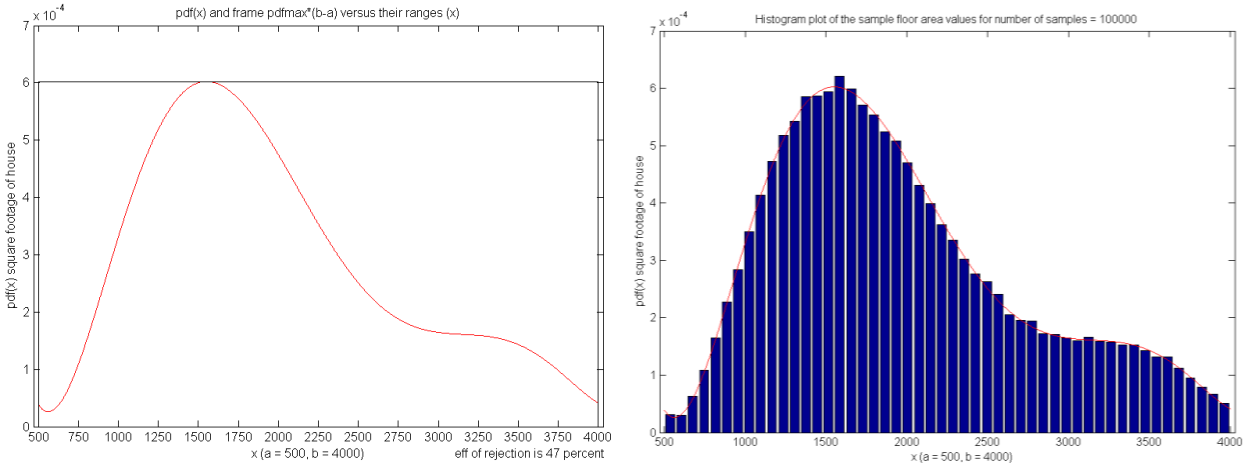

Fig. 3-6. Sample floor plan area of houses using rejection technique (efficiency = 47%)

Given: a floor area (in ft^2) as a continuous random variable x (e.g., x ∈ [500, 4000]), the probability density function of x is given in Fig. 3-5 and derived using the MATLAB curve fitting tool. In this case the analytical inversion is impractical because a mathematical inverse formulation [$x = P^{-1}(\eta)$] of x cannot be obtained. Instead, the rejection techniques is used as explained in the steps below.

Step1: Enclose $p(x)$ by a frame $P_{max}(b-a)$ shown in Fig. 3-6.

Step2: Generate two random numbers η_1 and η_2

Step3: Sample random variable x using $x = a + \eta_1(b-a)$

Step4: Accept x if $\eta_2 p_{max} \leq p(x)$

Note: this is the technique that all pairs $(x, y = \eta_2 p_{max})$ are accepted if they are bounded by $p(x)$, otherwise they are rejected. A histogram of the 100,000 samples of x is plot to ensure the validity of the results. Essentially, this techniques sample form the area under the pdf (i.e., cdf). The efficiency of using this technique can be calculated as.

$$efficiency = \frac{\int_a^b p(x)dx}{p_{max}(b-a)} \qquad \text{(Eq. 3-1)}$$

After a floor area (x) is sampled, other related parameters of a house structure can be calculated as follows:

- Type of house: small ($x \leq 1{,}500\ ft^2$), medium ($1{,}500 < x \leq 3{,}000\ ft^2$), large ($x > 3{,}000\ ft^2$)
- Ceiling area (ca) = x
- Windows area (wia) = $0.1 \cdot x$
- Wall area (waa) is calculated from floor area (x) and window area (wia) as follow:
- If $x \leq 1{,}700\ ft^2$: waa = $40\sqrt{x} - wia$, else waa = $40\sqrt{2x} - wia$
- Resistant of wall (rwa) ∈ [13, 15]) is determined using a uniform random function
- Resistant of ceiling (rca) ∈ [38, 60]) is determined using a uniform random function
- Resistant of windows (rwa) ∈ [1/1.2, 1/0.2]) is determined using a uniform random function
- Wall height (wh) = 10 feet

3. Space cooling characteristic: usually, the sizing is based on the building floor plan, activities, occupants and environment. The unit sizing is calculated according to ASHRAE [94] as follows:

- Refrigeration capacity (C_{cool}) required in BTU/h of a house is given as:

$$C_{cool} = x \cdot 10$$

- Rated power of an air conditioner in kW is given as:

$$P_{AC} = C_{cool}/10{,}000$$

B.2 Model a water heater (WH)

Base on the WH unit model developed in [92], there are three primary categories of the built-in parameters: temperature profile, water heater characteristic, and hot water usage profile that are sampled. These parameters are randomized for different houses in the same distribution circuit.

1. Temperature profile: a uniform random function is used to determine the variation in hot water temperature set points (typical residential hot water temperature set points are between 110°F and 130°F). Tank ambient temperature is assumed to be the same as the room temperature which can be acquired from the AC units setting section. Inlet water temperature is assumed to be the same as the ground temperature which can be obtained from Soil Climate Analysis Network (SCAN) [95].

Given: a hot water temperature set point as a discrete random variable T (i.e., T ∈ [110,111,…,129,130]), the population distribution of T is known to be a uniform distribution with min: a, max: b, mean: $\frac{a+b}{2}$, and range: n. Thus a probability density function $p(T) = \frac{1}{n}$. The fundamental formulation of Monte Carlo (FFMC) of this discrete random variable is given as $Min\{P(n)|P(n) \geq \eta\}$, where $P(n) = \sum_{i=1}^{n} p_i$, $P(n)$ is a cumulative distribution function (cdf) of an outcome n of a random variable T, p_i is a probability density function (pdf) i of a random variable T, η is a random number. Therefore, by generating a random variable η, the n outcome of its corresponding random variable T can be obtained by selecting a minimum $P(n)$ that is greater than or equal to η.

2. Water heater characteristics: a uniform random function is used to determine the variation in the R-values (R12-R25), tank sizes (40-80 gallons), and rated power (4.5, 5.5 kW) of water heater units. The steps of randomly selecting these values are the same as explained in the steps to obtain the hot water temperature set point above.

3. Hot water usage profiles: there are three steps for sampling hot water usage: first, find when hot water is consumed based on the hot water hourly usage fraction (Fig. 3-7) which can be sampled based on the probability density function using the rejection technique depicted in Fig. 3-8; Second, find what is the flow rate in gallon/minute (for simplicity, in this study assume flow rate is fixed at 1.50 gallon/minute); Finally, find how long (minutes) hot water has been drawn (Fig. 3-9).

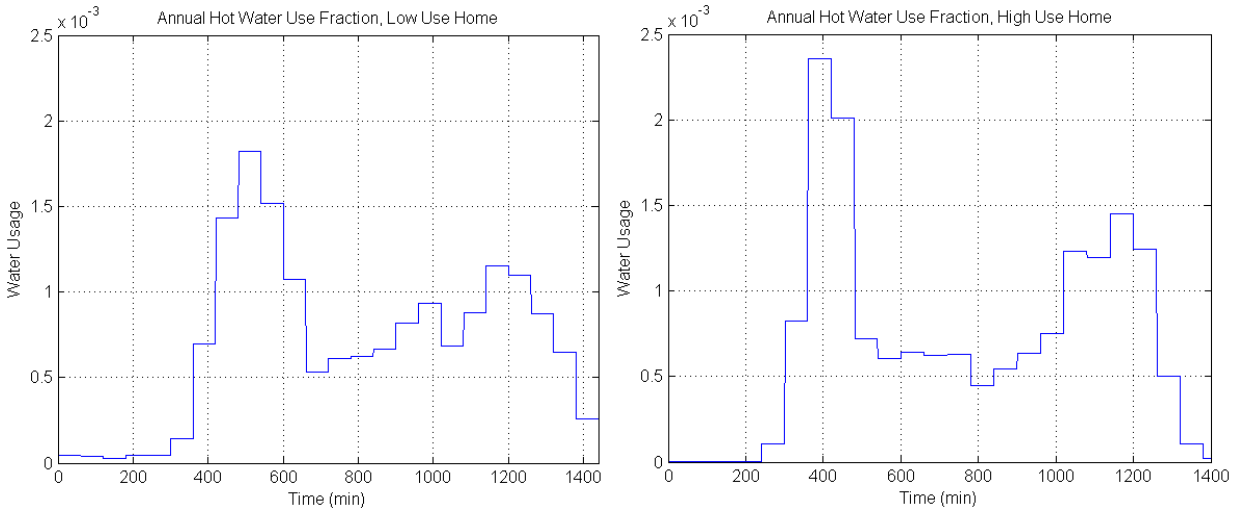

Fig. 3-7. Annual hot water use fraction for low use home and high use home

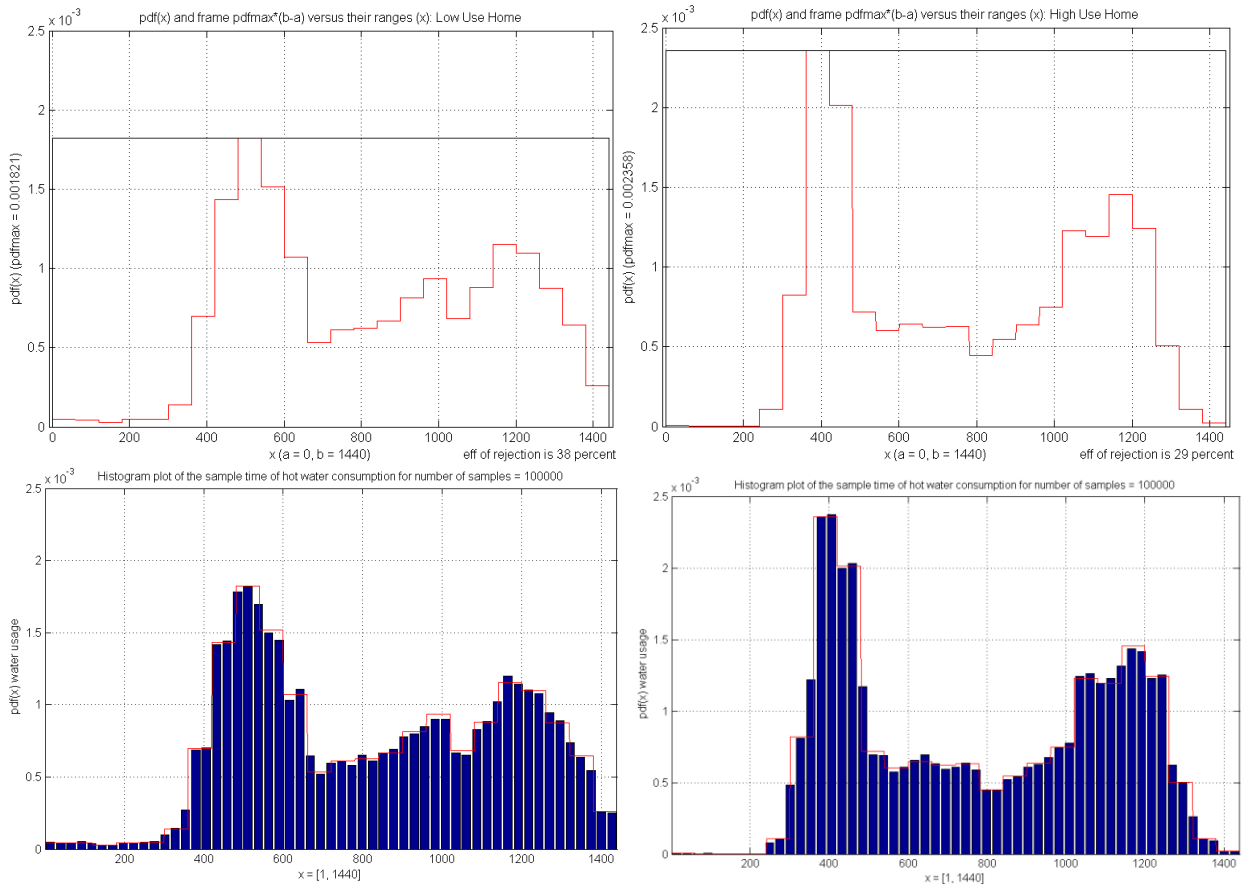

Fig. 3-8. Sample when water is consumed in low use house and high use house using rejection technique with the efficiencies of 38% and 29% respectively

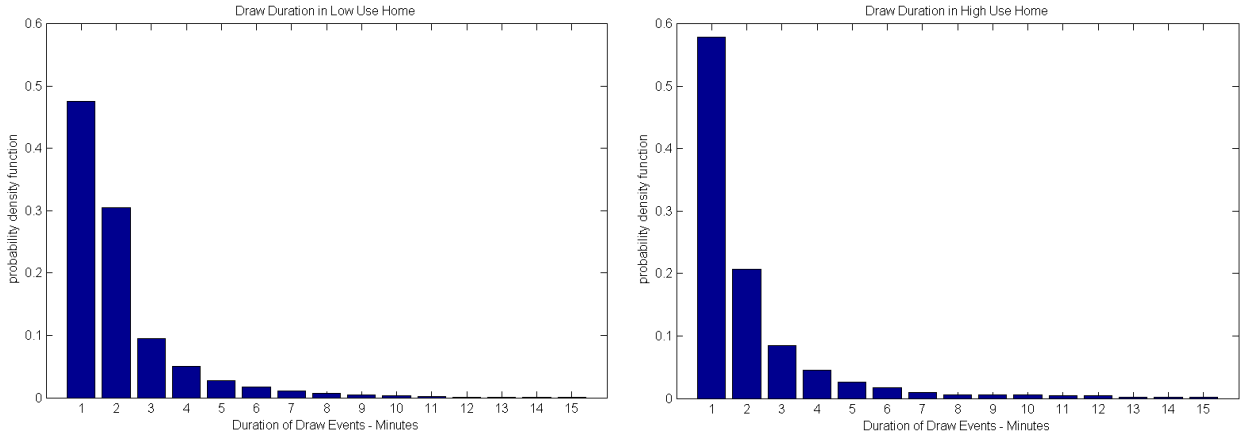

Fig. 3-9. Hot water drawn duration in low use home and high use home

Given: a hot water hourly usage fraction (in minute) as a continuous random variable x, the probability density function of x is given in Fig. 3-7 and derived using the MATLAB curve fitting tool. The rejection techniques is used to sample variable x as explained in the steps below.

Step1: Enclose $p(x)$ by a frame $P_{max}(b-a)$ shown in Fig. 3-8.
Step2: Generate two random numbers $\eta_1$and η_2
Step3: Sample random variable x using $x = a + \eta_1(b-a)$
Step4: Accept x if $\eta_2 p_{max} \leq p(x)$

Note: this is the technique that all the pairs $(x, y = \eta_2 p_{max})$ are accepted if they are bounded by $p(x)$, otherwise they are rejected. A histogram of the 100,000 samples of x is plot to ensure the validity of the results. Essentially, this techniques sample form the area under the pdf (i.e., cdf). The efficiency of using this technique can be calculated as.

$$efficiency = \frac{\int_a^b p(x)dx}{p_{max}(b-a)} \qquad \text{(Eq. 3-2)}$$

Given: a hot water drawn duration D as a discrete random variable (i.e., D ∈ [1, 2, …, 14, 15]), the probability density function $p(n)$ is shown in Fig. 3-9. The fundamental formulation of Monte Carlo (FFMC) of this discrete random variable is given as $Min\{P(n)|P(n) \geq \eta\}$, where $P(n) = \sum_{i=1}^{n} p_i$, $P(n)$ is a cumulative distribution function (cdf) of an outcome n of a random variable D, p_i is a probability density function (pdf) i of a random variable D, η is a random number. Therefore, by generating a random variable η, the n outcome of its corresponding random variable D can be obtained by selecting a minimum $P(n)$ that is greater than or equal to η.

B.3 Model a clothes dryer (CD)

Base on the CD unit model developed in [92], there are three built-in parameters of the clothes dryer unit consisting of motor rated power, heating coil rated power, and numbers of drying level (assume the same). To simplify the CD model, in this study assume that those three parameters are the same for all houses. However, clothes dryer starting times are sampled based on a normal distribution with mean and variance are 4 pm and 1 hour respectively.

Given: a CD starting time as a discrete random variable T, the population distribution of T is known to be normal with mean μ and variance σ^2 that is $T \sim N(\mu, \sigma)$. Thus $p(T, \mu, \sigma) = \frac{1}{\sigma\sqrt{2\pi}} e^{-\frac{(T-\mu)^2}{2\sigma^2}}$. The fundamental formulation of Monte Carlo (FFMC) of this discrete random variable is given as $Min\{P(n)|P(n) \geq \eta\}$, where $P(n) = \sum_{i=1}^{n} p_i$, $P(n)$ is a cumulative distribution function (cdf) of an outcome n of a random variable T, p_i is a probability density function (pdf) i of a random variable T, η is a random number. Therefore, by generating a random variable η, the n outcome of its corresponding random variable T can be obtained by selecting a minimum $P(n)$ that is greater than or equal to η.

B.4 Model an electric vehicle (EV)

Base on the EV unit model developed in [92], there are three categories of the built-in parameters of an electric vehicle: rated charging power, plug-in time, and battery state of charge (SOC) that are needed to be sampled. These parameters are randomized for different houses in the same distribution circuit.

1. **Rated charging power:** three popular EV models in the US market are focused in this study: GM Chevy Volt, Nissan Leaf, and Tesla Roadster. The battery size, energy available, all electric range, charging power, and the assumed percent share of those models based on their popularity are presented in the Table 3-1, and depicted in Fig. 3-10.

Given: a popular EV model in the U.S. as a discrete random variable M (i.e., M ∈ [1, 2, 3]), the probability density function $p(n)$ is shown in Fig. 3-10. The fundamental formulation of Monte Carlo (FFMC) of this discrete random variable is given as $Min\{P(n)|P(n) \geq \eta\}$, where $P(n) = \sum_{i=1}^{n} p_i$, $P(n)$ is a cumulative distribution function (cdf) of an outcome n of a random variable M, p_i is a probability density function (pdf) i of a random variable M, η is a random number. Therefore, by generating a random variable η, the n outcome of its corresponding random variable M can be obtained by selecting a minimum $P(n)$ that is greater than or equal to η.

Table 3-1. Popular EV models in the U.S. market

Model	Battery Size	Energy Available	All Electric Range	Charging Power	% share
GM Chevy Volt	16 kWh	8 kWh	40 miles	3.3 kW (recommended)	70
Nissan Leaf	24 kWh	19.2 kWh	100 miles	3.3 kW (recommended)	20
Tesla Roadster	53 kWh	37.1 kWh	244 miles	9.6 kW (recommended)	10

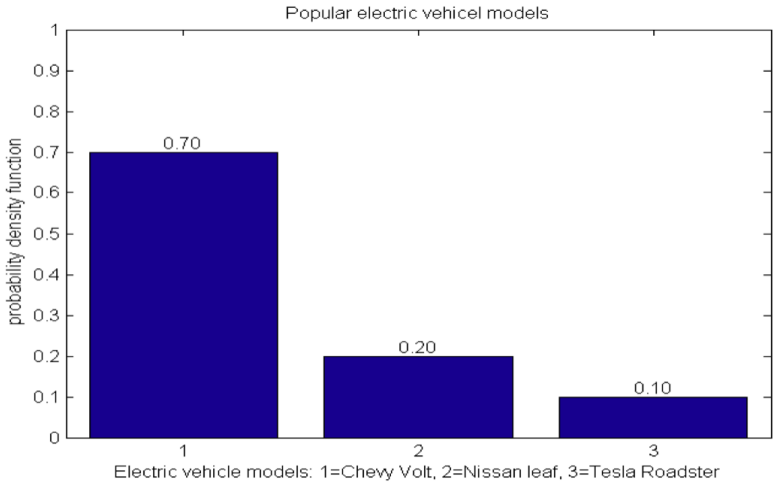

Fig. 3-10. Probability density function of the popular EV models in the U.S. market

2. Plug-in Time: a normal random function is used to determine the variation of EV plug-in time with mean and variance of 6 pm and 1 hour respectively.

Given: an EV starting time as a discrete random variable T, the population distribution of T is known to be normal with mean μ and variance σ^2 that is $T \sim N(\mu, \sigma)$. Thus $p(T, \mu, \sigma) = \frac{1}{\sigma\sqrt{2\pi}} e^{-\frac{(T-\mu)^2}{2\sigma^2}}$. The fundamental formulation of Monte Carlo (FFMC) of this discrete random

variable is given as $Min\{P(n)|P(n) \geq \eta\}$, where $P(n) = \sum_{i=1}^{n} p_i$, $P(n)$ is a cumulative distribution function (cdf) of an outcome n of a random variable T, p_i is a probability density function (pdf) i of a random variable T, η is a random number. Therefore, by generating a random variable η, the n outcome of its corresponding random variable T can be obtained by selecting a minimum $P(n)$ that is greater than or equal to η.

3. Battery State of Charge (SOC): the daily driving distances data or American driving pattern curve, shown in Fig. 3-11, is used to determine the battery SOC of an EV.

Given: a daily driving distance (in mile) as a discrete random variable D. The probability density function $p(n)$ is shown in Fig. 3-11. The fundamental formulation of Monte Carlo (FFMC) of this discrete random variable is given as $Min\{P(n)|P(n) \geq \eta\}$, where $P(n) = \sum_{i=1}^{n} p_i$, $P(n)$ is a cumulative distribution function (cdf) of an outcome n of a random variable D, p_i is a probability density function (pdf) i of a random variable D, η is a random number. Therefore, by generating a random variable η, the n outcome of its corresponding random variable D can be obtained by selecting a minimum $P(n)$ that is greater than or equal to η.

After a daily driving distance (D) is obtained, a SOC of an EV's battery can be calculated as follows.

$$SOC = \left(\frac{Range_{electric} - D}{Range_{electric}}\right) \cdot 100\% \qquad \text{(Eq. 3-3)}$$

Where,

SOC : state of charge of an EV (%)
$Range_{electric}$: all electric range of an EV (mile)
D : daily driving distance (mile)

Therefore time to fully charge an EV (in minute) from the previous calculated SOC is calculated as:

$$T_{100\%SOC} = (1 - SOC) \cdot \left(\frac{EV_{batt\_size}}{P_{charging}}\right) \cdot 60 \qquad \text{(Eq. 3-4)}$$

Where,

$T_{100\%SOC}$: time to fully charge an EV to 100% SOC (minute)
EV_{batt_size} : battery size of an EV in (kWh)
$P_{charging}$: charging power of an EV in (kW)

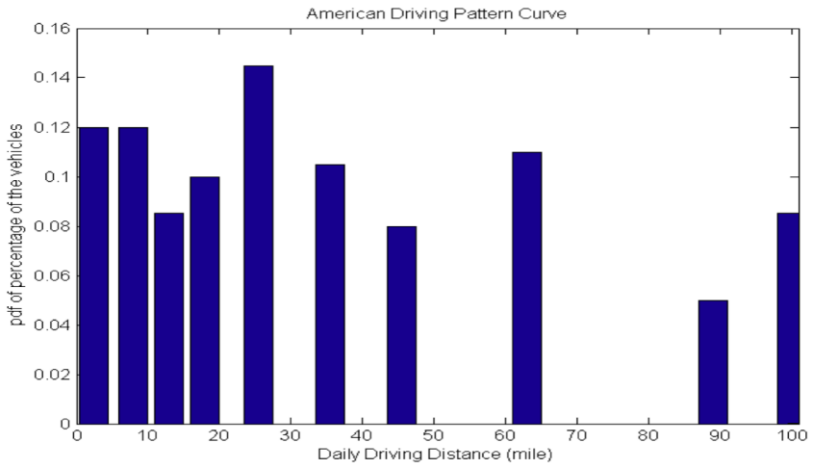

Fig. 3-11. American driving pattern curve

B.5 Model critical loads

Critical loads data are acquired from the RELOAD database [96].

B.6 Sample parameters obtaining from the previously described sampling techniques

Table 3-2 illustrates sampled parameters of homes characteristics and their corresponding parameters of power-intensive appliances obtained from the sampling techniques discussed in Section A.2.1 to A.2.5. In addition, homeowners can also set their preferences as shown below.

Table 3-2. House attributes and home owners' preference setting

	Home 1 (HA1,HEM1)	Home 2 (HA2,HEM2)	Home 3 (HA3,HEM3)
Home parameters:			
- ID	950009001	950009002	950009003
- size	small (1,500 ft^2)	medium (2,500 ft^2)	small (1,500 ft^2)
- Elec. panel size	125 A	225 A	125 A
- Voltage rating	120/240 V	120/240 V	120/240 V
- Status	true	True	true
- season	summer	summer	summer
- weather	sunny	Sunny	sunny
Appliances ratings and customer preference setting:			
1. WH	3.8 kW, p=2, 120 .810 F°	4.5 kW, p=2, 120 .510 F°	off
2. AC	1.92 kW, p=1, 76 692 F°	2.6 kW, p=1, 76 662 F°	1.92 kW, p=1, 80 092 F°
3. CD	2.88 kW, p=3, start 17:00	4.9 kW, p=3, start 16:50	off
4. EV	-	3.3 kW, p=4 start 16:30	-
Assumptions:			
Residents (N)	4 people	3 people	2 people

C. Data Flow Diagram of the Proposed SDTM

Fig. 3-12 illustrates interactions between relevant actors, systems and technologies required to achieve the specific goal of the proposed SDTM application.

The objective, actors and scenarios are described in more detail below, which manifest how the proposed MAS performs during a DR event:

1) Objective: The objective of the proposed SDTM application is to reduce instantaneous power demand (kW) at a distribution transformer during a system stress condition or when a distribution transformer is overloaded.

2) Actors: Relevant actors include DR aggregator (DR AGG), distribution transformer, home, and DR-enabled appliances, such as air conditioner (AC), water heater (WH), clothes dryer (CD), and electric vehicle (EV).

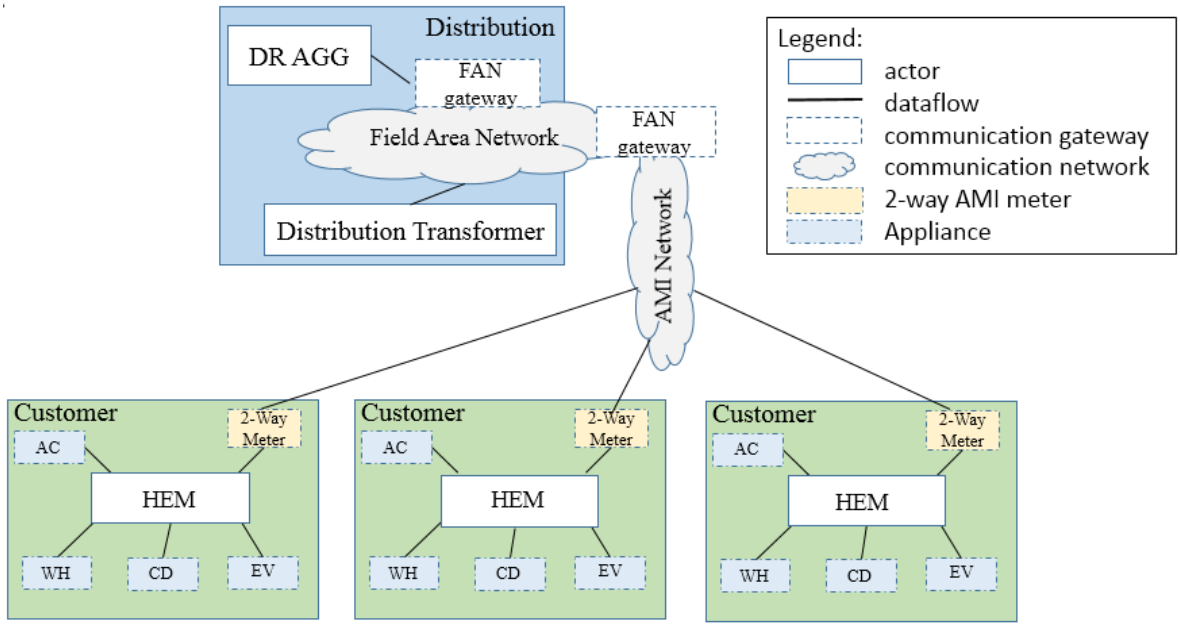

Fig. 3-12. Data flow diagram of the proposed SDTM

3) Scenarios: These include chronological order of steps to implement SDTM during a DR event. A DR event may occur (a) during a system stress condition (e.g. loss of generators or transmission lines, weather-related severe increase in system peak loads, highly fluctuated power generation from intermittent sources like solar or wind), or (b) because of distribution transformer overloading (e.g., coincident charging of multiple EVs).

3.1 In case of a DR event happens due to a system stress condition, a distribution transformer receives a reliability signal from a DR AGG over a field area network (FAN) via a FAN gateway requesting to keep its power demand below a certain level during a DR event. In case of a DR event happens due to an overloading condition of a distribution transformer, the transformer assesses its loading capability and tries to keep a power demand below that capability to minimize

the impact to a transformer's life.

3.2 A distribution transformer informs all of its connected homes over an AMI network via a FAN gateway about a DR event and asks participating homes (via HEMs) to reduce their power demand accordingly.

3.3 After receiving a request through a two-way AMI meter, participating homes reduce their electricity usage through an automated DR (via HEM) that manages energy consumption of selected DR-enabled appliances.

Related assumptions for the proposed SDTM system are as follows: (1) all controlled devices (e.g., transformer, HEM, appliances) are IP enabled and capable of communicating with one another. This can be facilitated by wireless communications using TCP/IP protocol [97]; and (2) it is assumed that there is no communication disruption during a DR event.

Although the SDTM architecture presented focuses mainly on the 3-wire split-phase distribution system being widely used in the United States, the proposed algorithm can be adopted for use with any network configurations. In terms of scalability, the proposed SDTM can be easily expanded to manage power demand at a distribution feeder level or at a distribution substation level. The power demand management goals during a DR event can be archived by the similar approach accounting for cable/line constraint, distribution transformer constraints as well as voltage level constraint, etc.

3.2.2 SDTM Cyber Layer: MAS development

MAS, developed using the Java Agent Development Framework (JADE) [99] platform, is developed as the cyber layer of the proposed SDTM. MAS consists of multiple distributed intelligent agents residing at their corresponding physical devices. The detailed explanation on MAS architecture and design is given in this section, including the proposed agent architecture, agent behavior design, agent knowledge representation, agent ontology, as well as communication and negotiation processes among agents during a DR event. This agent-based platform serves as a host to implement the proposed DR algorithm discussed in Section 3.3.

A. Agent Architecture

The proposed MAS architecture comprises two types of agents: a transformer agent (TRA) and a home agent (HA). A TRA resides at a distribution transformer and a HA resides at each home. The detail description of each type of agents is given as follows.

***A.1 Transformer agent (TRA*)**: A TRA is designed to be able to monitor and assess the operating state of a distribution transformer (i.e., normal or emergency). This can be accomplished by acquiring knowledge from a DR AGG and its associated HAs, as well as sensing its voltage and current information. When detecting a change in the transformer's operating state to an emergency condition, the TRA will make an attempt to reduce its total power demand. This is carried out by working and collaborating with its associated HAs. Fig. 3-13 depicts the TRA architecture as a state-based agent.

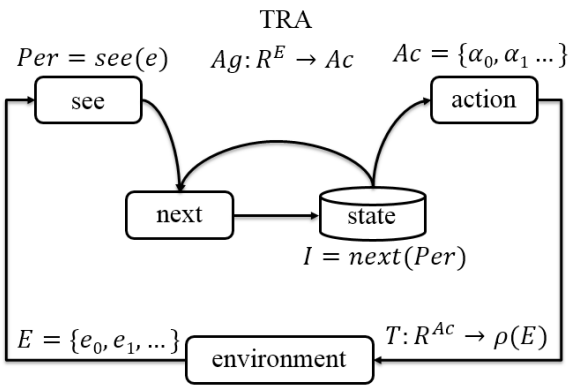

Fig. 3-13. TRA architecture

The explanation of a TRA architecture is given as follows.

Environment **(*Env*):** a continuous environment of a TRA is modeled as a finite set of discrete environment states $E = \{e_0, e_1, \dots, e_u\}$. The formal form of a TRA environment is given as $Env = < E, e_0, T >$. The environment E changes dynamically according to a state transformer T that maps a run of agent action R^{Ac} to next possible environment state $\rho(E)$. $e_0 \in E$ is an initial state of TRA environment.

The construction of any TRA environment state i denoted by e_i is defined as:

$$e_i = [t, DRe, Agm, Elec], where\ e_i \in E$$

Where $t, DRe, Agm, and\ Elec$ are agent-interaction and non-agent-interaction parameters as given in Table 3-3.

Table 3-3. TRA environment identification parameters

Agent-interaction parameters	Non-agent-interaction parameters
1. DR event (DRe) = {DL (kW), DR event period (min)}	1. Time {t (min)}
2. Agent message (Agm) = {Sender, Performative, Ontology, Content}	2. Electrical parameters (Elec) = {instantaneous power demand (P_D, kW), accumulated energy consumption (E, kWh)}

Perception **(*Per*):** after a TRA sees an environment $e_i \in E$, it maps e_i to a perception $P_j \in Per$ based on its knowledge on environments $(see(e_i) \rightarrow P_j)$, where Per is a set of TRA perceptions $Per = \{P_0, P_1, \dots, P_u\}$. The main criteria to differentiate perceptions is by considering a situation whether or not a DR event happens in a system. The construction of any TRA perception P_j is defined as:

TRA's criteria to identify its perception

1: If $e_i = [t, DRe = null, Agm, Elec]$
2: $see(e_i) \rightarrow P_j = P_0$, where P_0 is a default perception such that there is no DR
3: event in the system.
4: Else
$see(e_i) \rightarrow P_j = \{t, DRe, Agm, Elec\}, where\ P_j \in Per$

For instance,

If e_0 = [0, {*null,null*}, {*null,null,null,null*}, {15.3,0}], $see(e_0) \rightarrow P_0$. This implies that at the initial environment (e_0), the TRA sees the default perception, i.e., no DR event.

If e_3 = [10.00, {16,120}, {*DR Aggregator, REQUEST, DROntology, DR event*}, {20.7, 3.57}], $see(e_3) \rightarrow P_1$. This implies that a TRA receives a *REQUEST* message from a DR AGG, a TRA then perceives that a DR event has occurred.

If e_5 = [10.12,{16,120},{HA, *AGREE*, DROntology, DR participation}, {19.67,3.72}], $see(e_5) \rightarrow P_2$. This implies that a TRA receives an *AGREE* message from an HA, a TRA then perceives that the HA is willing to participate in a DR event.

Next state function (next): a TRA internal state i denoted by $i_i \in I$ is changed regarding its previous state i_{i-1} and its current perception P_j, thus $i_{i-1} \times P_j \rightarrow i_i$, where I is a set of feasible internal states of a TRA. The construction of any TRA internal state i_i is defined as:

$$i_i = \{Op\_States_{TR}, DRe, Agm\}, where\ i_i \in I$$

Where Op_States_{TR} is an operating state either "normal" or "emergency" of a distribution transformer. The TRA internal state is changed by using the next state function which has the following formal form:

$$next(i_{i-1}, P_j = see(e_j)) \rightarrow i_i, \text{ where } i_i, i_{i-1} \in I$$

For instance, let $i_o = \{normal, null, null\}$ and $i_1 = \{Emergency, DRe, Agm\}$, given e_0, e_3 and e_5:

$next(i_0, P_0 = see(e_0)) \rightarrow i_0$
$next(i_0, P_1 = see(e_3)) \rightarrow i_1$
$next(i_1, P_2 = see(e_5)) \rightarrow i_1$

Agent action (***Ac***)***:*** An agent action is a set of available agent actions $Ac = \{\alpha_0, \alpha_1, c\alpha_u\}$. It defines the capability of an agent that reacts to an external environment or other agents in pursuit of its own goal(s). For a multi-agent system, an agent environment can change even without an agent interaction. Hence, let α_0 denotes an action that an agent does nothing. In this paper, the set of available TRA actions for a DR application is $Ac = \{\alpha_0, \alpha_1, \alpha_2\}$.
Where,

α_0: do nothing

α_1: acknowledge a DR event notified by a DR AGG

α_2: allocate demand limit (DL) to an HA based on the proposed DR algorithm discussed in the next part.

Theoretically, these available actions determine TRA behaviors (to be described in Section IV.B). Working in its environment, a TRA chooses an action to perform based on its current state i_i and available actions *Ac*. The action function of a TRA is given as:

$$action(i_i) = action(next(i_{i-1}, P_j = see(e_j))) \rightarrow \alpha_l,$$

where $\alpha_l \in Ac$.
For instance (given e_0, e_3 and e_5 from 1.2),

$action(next(i_0, see(e_0))) \rightarrow \alpha_0$
$action(next(i_0, see(e_3))) \rightarrow \alpha_1$
$action(next(i_1, see(e_5))) \rightarrow \alpha_2$

Agent control loop: manifest steps in which an agent responds and reacts to an external environment and other agents during a DR event. The control loop of a state-based TRA is shown as follows:

TRA control loop
1: TRA initializes to an initial internal state i_0.
Repeat Steps 2 to 5 until a DR event ends.
2: TRA observes environment state e_i, then generates a perception P_j from $see(e_i) \rightarrow P_j$.
3: TRA updates internal state i_i via $next(i_{i-1}, see(e_j)) \rightarrow i_i$.
4: TRA selects action to perform via $action(next(i_{i-1}, see(e_j))) \rightarrow \alpha_l$.
5: TRA performs the selected action.

A.2 Home Agent (HA): An HA resides at a home providing an interface with a TRA via a gateway (e.g., a dedicated electronics device or a smart meter) and coordinates with an HEM using TCP/IP communications. Specifically, an HA is designed to respond to a DR event notified by a TRA. An HA acts to ensure that the instantaneous power demand of the associated home does not exceed a given DL during a DR event period. As an HA receives a DR event signal, it attempts to reduce the household power demand by working with its associated HEM. The proposed HA is a purely reactive agent. Its architecture is depicted in Fig. 3-14.

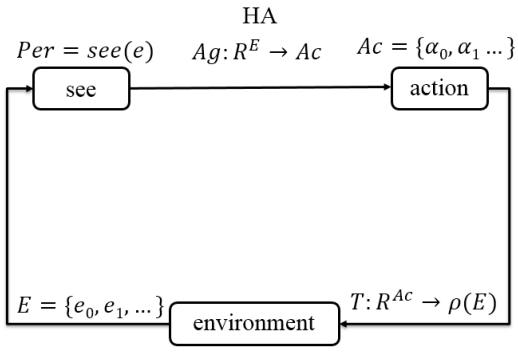

Fig. 3-14. HA architecture

Detailed description of the HA architecture is given below:

Environment (Env)***:*** a continuous environment of an HA is modeled as a finite set of discrete environment states $E = \{e_0, e_1, \dots, e_u\}$. The formal form of an HA environment is given as $Env = < E, e_0, T >$. The environment (E) changes dynamically according to a state transformer T that maps a run of agent action R^{Ac} to next possible environment state $\rho(E)$. $e_0 \in E$ is the initial state of the HA environment. The construction of any HA environment state i denoted by e_i is defined as:

$$e_i = [t, DRe, Agm, Elec], where\ e_i \in E$$

Where $t, DRe, Agm, and\ Elec$ are agent-interaction and non-agent-interaction parameters as given in Table 3-4 below.

Table 3-4. HA environment identification parameters

Agent-interaction parameters	Non-agent-interaction parameters
1. DR event (DRe) = {DL (kW), DR event period (min)}	1. Time (t, min)
2. Agent message (Agm) = {Sender, Performative, Ontology, Content}	2. Electrical parameters (Elec) = {instantaneous power demand (P_D, kW), accumulated energy consumption (E, kWh)}

Perception **(*Per*):** after an HA sees an environment $e_i \in E$, it maps e_i to a perception $P_j \in Per$ based on its knowledge on environments ($see(e_i) \rightarrow P_j$), where Per is a set of HA perceptions $Per = \{P_0, P_1, \dots, P_u\}$. The construction of any HA perception P_j is defined as:

HA's criteria to identify its perception

If $e_i = [t, DRe = null \&\& Agm.Sender.Performative! = TRA.REQUEST, Elec]$,
    $see(e_i) \rightarrow P_j = P_0$, where P_0 is a default perception such that there is no DR event in the system.
Else
    $see(e_i) \rightarrow P_j = \{t, DRe, Agm, Elec\}, where\ P_j \in E$

For instance,

If $e_0 = [0, \{null, null\}, \{null, null, null, null\}, \{5.,0\}]$, $see(e_0) \rightarrow P_0$. This implies that at the initial environment (e_0), an HA sees the default perception, i.e., no DR event.

If $e_3 = [10.00, \{null, null\}, \{TRA, REQUEST, DROntology, DR\ event\}, \{5.64,1.20\}]$, $see(e_3) \rightarrow P_1$. This implies that an HA receives a *REQUEST* message from a TRA, a HA then perceives that a DR event has occurred.

If $e_5 = [15.3, \{3.58, 120\}, \{null, null, null, null\}, \{3.40,1.35\}]$, $see(e_5) \rightarrow P_2$. This implies that an HA has received a DL with a DR event period from a TRA.

Agent action **(*Ac*):** the set of available HA actions specifically for a DR application is $Ac = \{\alpha_0, \alpha_1, \alpha_2\}$.

Where,

α_0: do nothing

α_1: respond to a DR event notified by a TRA

α_2: send control signal, DL, to an HEM

These available actions determine behaviors of an HA (to be described in detailed in Section IV(B)). Working in its environment, an HA chooses an action to perform based on its current perceptions Per and available actions Ac ($Per \rightarrow Ac$). The action function of an HA is given as:

$$action(see(e_i)) \rightarrow \alpha_l, \text{ where } \alpha_l \in Ac.$$

For instance (given e_0, e_3 and e_5 from 2.2),

$action(see(e_0)) \rightarrow \alpha_0$
$action(see(e_3)) \rightarrow \alpha_1$
$action(see(e_5)) \rightarrow \alpha_2$

Agent control loop: of a purely-reactive HA agent is shown as follows:

HA control loop
Loop Steps 1 to 3 forever: 1: HA observes environment state e_i, then generates a perception P_j from $see(e_i) \rightarrow P_j$ 2: HA selects an action via $action(see(e_i)) \rightarrow \alpha_l$ 3: HA performs the selected action

B. Agent Behavior Design

One of the most important steps of designing MAS is to design agent behaviors. Fundamentally, behaviors of an agent are its abilities to react to changes in its external environment as well as its neighboring entities in pursuit of a system goal(s) or its own goal(s). The agent class diagram showing the proposed agents and their related behaviors is depicted in Fig. 3-15 and summarized in Table 3-5.

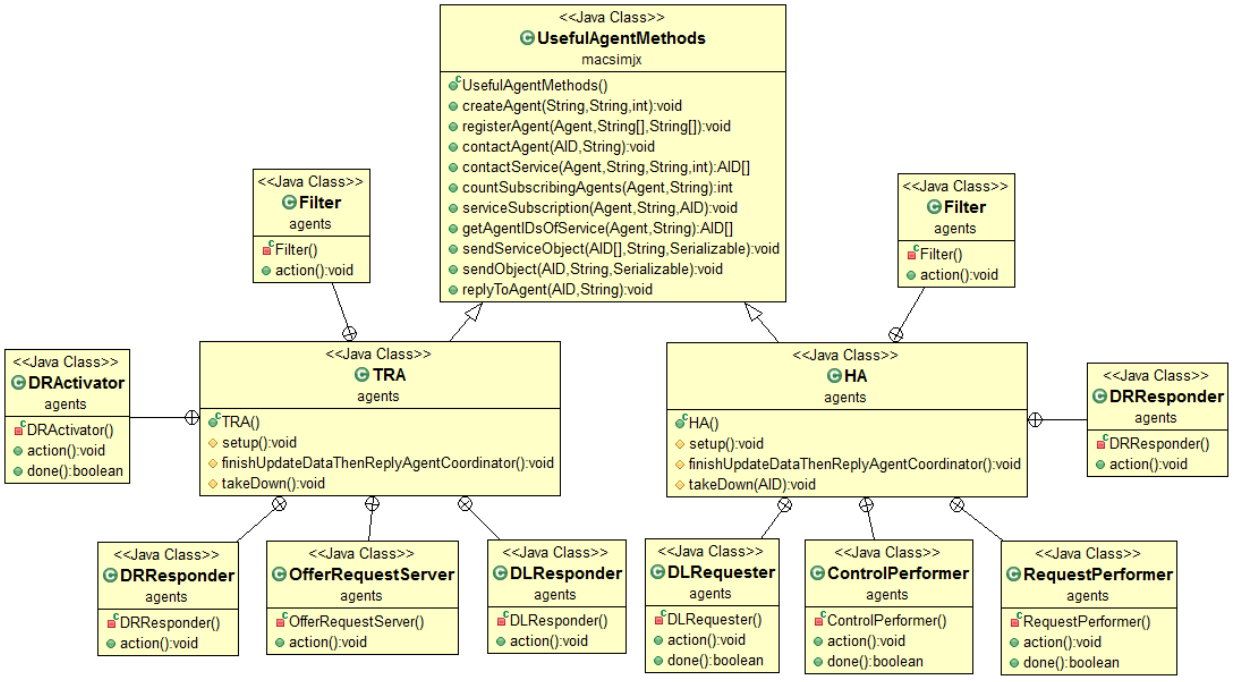

Fig. 3-15. The agent's class diagram showing agent behaviors

Table 3-5. MAS behavior description

Behaviors	Send Message	Receive Message	Description
Filter	- Receiver "AgentCoordinator" - Performative "*INFORM*"; - Conversation ID "ProcessedData/ ProcessingComplete"	- Sender "AgentCoordinator" - Performative "*INFORM*" - Conversation ID "UpdateData/ DataAmended/ Shutting Down" - Content "Agent's interests"	Agent updates its knowledge of a power distribution system through communication with the AgentCoordinator agent. Specifically,non-agent-interaction parameters of an agent environment are kept updated.
DRActivator (FIPA Request Interaction Protocol)	- Receiver "lower-layer agents" - Performative "*REQUEST*" - Ontology "DROntology" - Conversation ID "DRevent-Type: this agent-Type: lower-layer agent" - Content "RequestRespondDREvent"	- Sender "lower-layer agents" - Performative "*AGREE/REFUSE*" - Ontology "DROntology" - Conversation ID "DRevent-Type: this agent-Type: lower-layer agent"; - Content "AcknowledgeDREvent"	Agent notifies all corresponding lower-layer agents about a DR event, then requests participating agents to respond to the event accordingly. Specifically, an agent updates its corresponding lower-layer agent environment by exchanging their agent-interaction parameters.
DRResponder (FIPA Request Interaction Protocol)	- Receiver "higher-layer agent" - Performative "*AGREE/REFUSE*" - Ontology "DROntology" - Conversation ID "DRevent-Type: higher-layer agent-Type: this agent" - Content "AcknowledgeDREvent"	- Sender "higher-layer agent" - Performative "*REQUEST*" - Ontology "DROntology" - Conversation ID "DRevent-Type: higher-layer agent -Type: this agent"; - Content "RequestRespondDREvent"	Agent responds to a DR event notified by a higher-layer agent. If an agent participates in a DR program, it sends a response message with *AGREE* performative back to the higher-layer agent. Otherwise, an agent sends a response message with *REFUSE* performative. The decision making process and contents of sending and receiving messages depend on the proposed DR algorithms.
OfferRequestServer (FIPA Contract Net Interaction Protocol)	- Receiver "lower-layer agent" - Performative "*CFP*" - Ontology "DROntology" - Conversation ID "DLrequest-Type: this agent-Type: lower-layer agent" Content "CFPDLRequest" // OR - Receiver "lower-layer agent" - Performative "*ACCEPT PROPOSAL/ REJECT POROPOSAL*" - Ontology "DROntology" - Conversation ID "DLaccept/DLreject-Type: this agent-Type: lower-layer agent"; - Content "AllocateDL"	- Sender "lower-layer agent" - Performative "*PROPOSE/REFUSE*" - Ontology "DROntology" - Conversation ID "DLrequest_reply-Type: this agent-Type: lower-layer agent" - Content "ProposeDLRequest" // OR - Sender "lower-layer agent" - Performative "*INFORM-DONE/ FAILURE*" - Ontology "DROntology" - Conversation ID"DLaccept/DLreject-Type: this agent-Type: lower-layer agent" - Content "DoneDRImplementation"	Based on the FIPA Contract Net Protocol, an agent contacts and collaborates with all participating lower-layer agents who take part in a DR program. It, then, allocates DL to each lower-layer agent. The decision making process and contents of sending and receiving messages depend on the proposed DR algorithms.
RequestPerformer (FIPA Contract Net Interaction Protocol)	- Receiver "higher-layer agent" - Performative "*PROPOSE/REFUSE*" - Ontology "DROntology" - Conversation ID "DLrequest_reply-Type: this agent-Type: higher-layer agent" - Content "ProposeDLRequest"	- Sender "higher-layer agent" - Performative "*CFP*" - Ontology "DROntology" - Conversation ID "DLrequest-Type: higher-layer agent-Type: this agent" - Content "CFPDLRequest"	Agent negotiates with a higher-layer agent for an allocated DL during a DR event. The decision making process and contents of sending and receiving messages depend on the proposed DR algorithms.
ControlPerformer (FIPA Contract Net Interaction Protocol)	- Receiver "higher-layer agent" - Performative "*INFORM-DONE/ FAILURE*" - Ontology "DROntology" - Conversation ID "DLaccept/DLreject-Type: higher-layer agent-Type: this agent" - Content "ReceiveDL"	- Sender "higher-layer agent" - Performative "*ACCEPT PROPOSAL/ REJECT PROPOSAL*" - Ontology "DROntology" - Conversation ID "DLaccept/DLreject-Type: higher-layer agent-Type: this agent" - Content "AllocateDL"	Agent passes the received DL level from a higher-layer agent to its corresponding HEM. The decision making process and contents of sending and receiving messages depend on the proposed DR algorithm.
DLRequester (FIPA Request Interaction Protocol)	- Receiver "higher-layer agent" - Performative "*REQUEST*" - Ontology "DROntology" - Conversation ID "NewDLrequest-Type: higher-layer agent-Type: this agent" - Content "RequestNewDL"	- Sender "higher-layer agent" - Performative "*AGREE/REFUSE*" - Ontology "DROntology" - Conversation ID "NewDLrequest -Type: higher-layer agent -Type: this agent" - Content "AcknowledgeDLRequest"	During a DR event, based on a lower-layer agent's belief about its power demand requirement, an agent dynamically request a new DL level from a higher-layer agent. For example, an HA sends a new request for a higher demand limit when it believes that home power demand requirement is ascending.
DLResponder (FIPA Request Interaction Protocol)	- Receiver "lower-layer agent" - Performative "*AGREE/REFUSE*" - Ontology "DROntology" - Conversation ID "NewDLreques-Type: lower-layer agent-Type: this agent" - Content "AcknowledgeDLRequest"	- Sender "lower-layer agent" - Performative "*REQUEST*" Ontology "DROntology" - Conversation ID "NewDLreques-Type: lower-layer agent -Type: this agent" - Content "RequestNewDL"	Agent responds to a DL level request from a lower-layer agent during a DR event. For example, after a TRA receives a new DL request from an HA, it will try to allocate new DL levels to homes according to the proposed DR algorithms.

C. Agent Knowledge Modeling

As there are some common behaviors among agents, a knowledge base is used as a collection of agent behaviors that provides common behaviors as well as specific behaviors for each type of agent depending on available agent actions. Table 3-6 summarizes attributes that TRA and HA inherit or need to acquire by exchanging messages with one another and its external environment.

Table 3-6. Agent attributes

Attributes	Value	Attribute	Value
TRA			
- ID	String	- DL	Double (kW)
- AID	AID	- DL fair	Double (kW)
- Rating	Double(kVA)	- DL updating time	Integer (min)
- Voltage ratio	Double	- Connected homes	Integer
- Configuration	(A,B,C-N)	- HA IDs	ID*
- Priority	Integer	- HA AIDs	AID*
- Loading capability	Double (kW)	- HA status	Boolean*
- Operating state	String	- HA elec. panel size	Integer(A)*
- Service type	String	- HA priority	Integer*
- DR event	Boolean	- HA DL request	Double(kW)*
- Demand (P)	Double (kW)	- HA DRKP	Double*
- Energy (E)	Double(kWh)	- HA DL fair	Double(kW)*
HA			
- ID	String	- Max. demand ($P_{\max}$)	Double (kW)
- AID	AID	- Avg. demand (P_{avg})	Double (kW)
- Elec. panel size	Double(A)	- Max critical load ($P_{\max,\text{crit}}$)	Double
- Voltage rating	Double (V)	- DL request	Double(kW)*
- Status	Boolean	- DRKP	Double*
- Priority	Integer	- TRA IDs	ID
- DR event	Boolean	- TRA AIDs	AID
- Demand (P)	Double (kW)	- TRA status	Boolean
- Energy (E)	Double (kWh)	- DL	Double (kW)

Note: * indicates an array of that data type.

D. Agent Ontology Creation

As each agent has different knowledge about their interests and functionalities, ontology provides the way in which common understanding (semantics of knowledge) can be shared among agents. Conforming to the Foundation of Intelligent Physical Agents (FIPA) standards [98], agents communicate and update their knowledge by exchanging FIPA-ACL (Agent Communication Language) messages. These messages specify ontology that describes the structured message content expressed by FIPA-SL language. Generally, an ontology is domain-specific, i.e., it works particularly with a certain set of agents in a certain environment. In this paper, the ontology created for sharing information and common understanding among TRAs and HAs for a DR implementation is called "DROntology" (depicted in Fig. 3-16). Three essential elements of DROntology are *concepts*, *predicates*, and *agent actions*:

Concepts are expressions used to represent entities with a complex structure defined in terms of their attributes. Typically, concepts alone are not used directly as the content of an ACL

message. Instead, they are referenced inside predicates, agent actions, or other concepts. In this study, there are two concepts: the transformer concept for a TRA and the home concept for an HA. Each concept has its associated sub-concepts with respect to its attributes. The transformer concept has ID, DR Event, DL Fair, DL Allocation, and Penalty Factor as sub-concepts. The home concept has ID, Electrical Characteristics, Priority, DR Participation, DL Request, demand restrike potential (DRKP) as sub-concepts.

Predicates are expressions that indicate the current status of an agent environment and can be either true or false. The DROntology comprises four predicates as follows:

P1: AcknowledgeDREvent is used by the DRResponder behavior (Shown in Fig. 6) of a TRA or an HA as the content of an *AGREE/REFUSE* message to acknowledge a DR event notification and to provide initial information about itself to a higher-layer entity (DR AGG or TRA). The AcknowledgeDREvent predicate message is expressed as:

(*AcknowledgeDREvent* (this agent: ID) (higher-layer agent: ID) (this agent: Electrical Characteristics) (this agent: Priority) (this agent: DL Request) (this agent: DRKP))

P2: ReceiveDL is used by the HA's ControlPerformer behavior (shown in Fig. 6) as the content of an *INFORM-DONE* message to inform a TRA that an HA has already received DL. The *ReceiveDL* predicate is expressed as:

(*ReceiveDL* (this agent: ID) (higher-layer agent: ID))

P3: DoneDRImplementation is used by the DRResponder behavior as the content of an *INFORM-DONE* message to inform a higher-layer entity (DR AGG or TRA) that the DR implementation at an agent (TRA or HA) during a DR event period has completed. The DoneDRImplementation is expressed as:

(*DoneDRImplementation* (higher-layer agent: ID) (lower layer agent: ID))

P4: AcknowledgeDLRequest: is used by the TRA's DLResponder behavior as the content of an *AGREE/REFUSE* message to acknowledge a DL request sent by a HA. The *AcknowledgeDLRequest* predicate is expressed as:

(*AcknowledgeDLRequest* (this agent: ID) (lower-layer agent: ID))

Agent actions are special concepts indicating actions that can be performed by either a TRA or an HA. The DROntology consists of the following five agent actions:

A1: RequestRespondDREvent is used by the TRA's DRActivator behavior (shown in Fig. 6) as the content of a *REQUEST* message to notify a DR event and acquire initial information from its associated HAs. The *RequestRespondDREvent* agent action is expressed as:

(*RequestRespondDREvent* (this agent: ID) (lower-layer agent: ID) (this agent: DR Event))

A2: CFPDLRequest is used by the TRA's OfferRequestServer behavior as the content of a call for proposal (*CFP*) message. The *CFPDLRequest* agent action is expressed as:

(*CFPDLRequest* (this agent: ID) (lower-layer agent: ID) (this agent: DL Fair) (this agent: DL Allocation))

A3: ProposeDLRequest is used by the HA's RequestPerformer behavior as the content of a *PROPOSE* message. The *ProposeDLRequest* agent action is expressed as:

(*ProposeDLRequest* (this agent: ID) (higher-layer agent: ID) (this agent: DL Request) (this agent: DRKP))

A4: AllocateDL is used by the TRA's OfferRequestServer behavior as the content of an *ACCEPT/REJECT_PROPOSAL* message. The *AllocateDL* agent action is expressed as:

(*AllocateDL* (this agent: ID) (lower-layer agent: ID) (this agent: DL Allocation))

A5: RequestNewDL is used by the HA's DLRequester behavior as the content of a *REQUEST* message. The *RequestNewDL* agent action is expressed as:

(*RequestNewDL* (this agent: ID) (higher-layer agent: ID) (HA_i: $DL\ Request$))

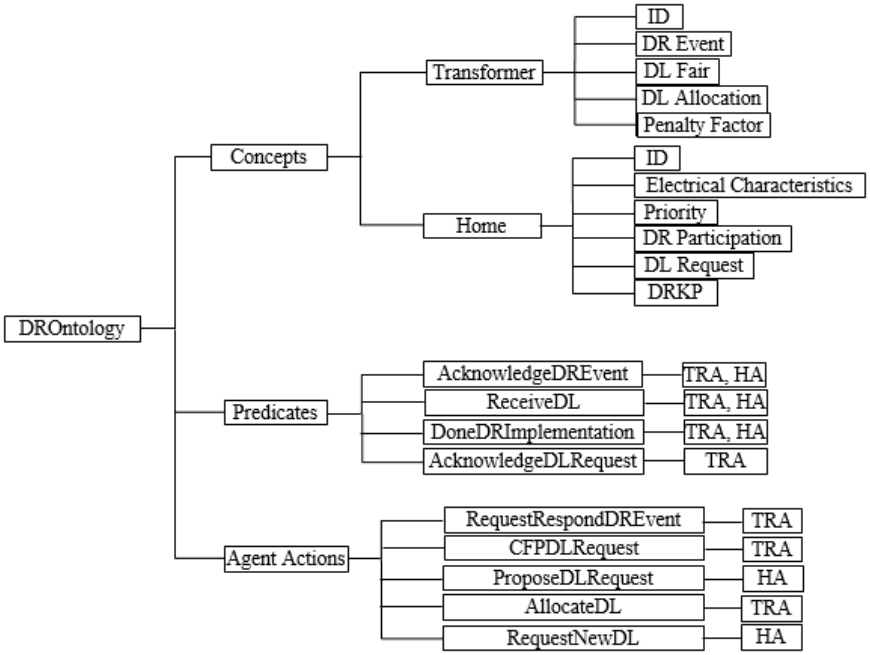

Fig. 3-16. DROntology for the proposed SDTM

E. Agent Communication and Negotiation Process

Communications between agents are required if an agent(s) cannot solve a given problem(s) solely by using its own knowledge, or if an agent need to observe its external environment via other agents. By working together, agents can accomplish the system goal. Agent

communications are essential in order to exchange knowledge among agents according to their behaviors and the designed ontology. Two FIPA interaction protocols used in communications and negotiations among a TRA and HAs are the FIPA Request Interaction Protocol and the FIPA Contract Net Interaction Protocol. During a DR event, interactions among agents of the proposed STDM system are manifested using the sequence diagrams showing in Fig. 3-17. The descriptive detail of agents interactions are given below.

Step 1: During a normal condition, a TRA and HAs update their knowledge about their external environments (power distribution system) from the AgentCoordinator (AgentCo) using the Filter behavior.

Step 2: As a DR event occurs in the system, a DRResponder of a TRA receives a DR event notification from a DR AGG. The TRA then assesses the operating state of the associated transformer. If the transformer is still in a normal operating state, the TRA will be prompt to carry out a DR implementation whenever it operating state condition changes from normal to emergency. However, if the transformer operating state is emergency, the TRA will immediately send a *REQUEST* message (RequestRespondDREvent) to all of its corresponding HAs to locate participating homes during a DR event.

Step 3: After the associated HAs receive requests from a TRA, HAs respond back by sending an *AGREE* message (AcknowledgeDREvent) performed by the DRResponder behavior.

Step 4: After a TRA receives *AGREE* messages from all HAs, it sends back *CFP* messages (CFPDLRequest) to all participating HAs.

Step 5: Each participating HA sends back a *PROPOSE* message (ProposeDLRequest).

Step 6: Based on the proposed DR algorithm (discussed in the companion paper), a TRA notifies all participating HAs of their DL during a DR event by sending an *ACCEPT PROPOSAL* message (AllocateDL).

Step 7: As soon as an HA receives a DL level, it communicates and sends a control signal specifying this DL to a HEM to control selected power-intensive appliances. The HEM then ensures that the total household power consumption does not exceed a given DL level during a DR event. Subsequently, it sends an *INFORM-DONE* message (ReceiveDL) back to a TRA.

Step 8: If an HA belief about its power demand requirement changes during a DR event, it will dynamically request a new DL level by sending a *REQUEST* message (RequestNewDL) to a TRA.

Step 9: A TRA responds to a DL level request from an HA by sending back *AGREE/REFUSE* message (AcknowledgeDL Request). Then, a TRA allocates new DL levels to participating homes by repeating steps 4 to 7.

Step 10: At the end of a DR event, all HAs send an *INFORM-DONE* message (DoneDRImplementation) back to a TRA. Likewise, a TRA sends back an *INFORM-DONE* message (DoneDRImplementation) back to a DR AGG.

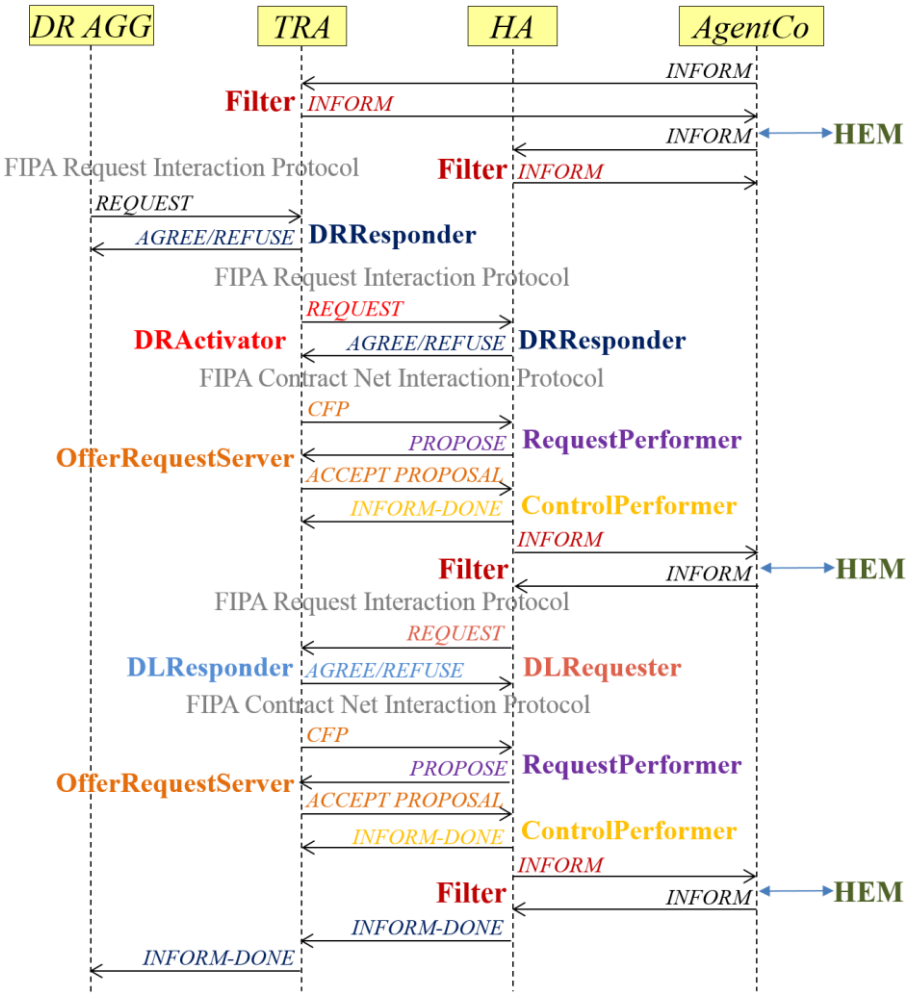

Fig. 3-17. Sequence diagram of the proposed MAS

3.3 Algorithms for DR Implementation in Residential Homes

Based on the literature search, there is still the lack of extensive studies on load reshape assurance at a distribution transformer level that gives end-use customers flexibility to control their appliances. In addition, the adverse impact of a DR event, e.g., transformer overload causing by a demand restrike (DRK) have not been addressed. To tackle these issues, the proposed algorithm has the following objectives: (1) ensures an instantaneous power demand at a distribution transformer below a certain DL level (kW); (2) minimizes the potential impact of DRK at a distribution transformer; and (3) prevents or mitigate customer comfort violations.

It is assumed that a DR event has occurred and a DR AGG assigns a DL and a DR event duration (hours) to selected distribution transformers. The proposed DR algorithm is devised and implemented at a TR level via a transformer agent (TRA), at the home level via a home agent (HA), and at the appliance level via an HEM.

3.3.1 Transformer Agent (TRA)'s Goals

A TRA located at a TR acts in pursuit of its goals by coordinating with HAs. TRA's objectives are:

1) To keep a total instantaneous power demand at a TR (P_{TR}, kW) below a certain DL level during a DR event. This paper defines two operating states of a TR as "normal" and "emergency" based on the following constraints.

$$P_{TR} = \sum_{i=1}^{N} P_{H,i} \leq Cap_{TR} \qquad \text{(Eq. 3-5)}$$

$$P_{TR} \leq DL_{AGG \rightarrow TRA} \qquad \text{(Eq. 3-6)}$$

Where, $P_{H,i}$ is an instantaneous power demand of home $i \in N$. N is a number of homes served by a TR. Cap_{TR} is a TR's loading capability. $DL_{AGG \rightarrow TRA}$ is a demand limit (kW) given to a TRA by a DR AGG.

A TR is in a normal operating state when none of the above constraints are violated; while it is in an emergency operating state when at least one constraint is violated. It should be noted that this study is based on the assumption that the voltage level at a TR varies within an acceptable limit specified by ANSI C84.1 [99].

2) To minimize the demand restrike potential – a potential rebound power demand at a TR level ($DRKP_{TR}$, kWh). This is to mitigate impact of undesired new peak demand (DRK) at a TR after a DR event ends. The $DRKP_{TR}$ is mathematically defined as:

$$DRKP_{TR} = \int_{t_{DR\_start}}^{t_{DR\_end}} (P_{TR,hist} - P_{TR})\, dt \qquad \text{(Eq. 3-7)}$$

Where, $P_{TR,hist}$ is a similar-day historical load profile of a TR during the same period as a DR event. t_{DR_start} is a DR event start time. t_{DR_end} is a DR event end time. As an actual required power demand of a TR during the same period as a DR event ($P_{TR,w/o\_DR}$) is unknown, $P_{TR,hist}$ is used with the assumption that homeowners maintain their typical behaviors for the same day type (weekday/weekend) with similar weather conditions. $DRKP_{TR}$ serves as a basis to estimate impacts of DRK as actual required power demands of homes might not be fulfilled during a DR event. Explicitly, some appliances might not be able to run as limited DL levels are imposed on homes.

3.3.2 Home Agent (HA)'s Goals

An HA acts in pursuit of homeowner's goals. If a homeowner participates in a DR program, an HA works cooperatively with its associated TRA in response to a DR event. In this study, homeowner's goals are: (1) To ensure that critical loads (e.g., lighting loads, cooking and plug loads) are served at all time; (2) To mitigate a homeowner's comfort level violation defined as deviations of room temperature and hot water temperature from their preset values; and (3) To

minimize load compensation times of selected appliances due to delay from appliances rescheduling.

3.3.3 The Overall DR Algorithm and Message Exchanges between the TRA and HAs

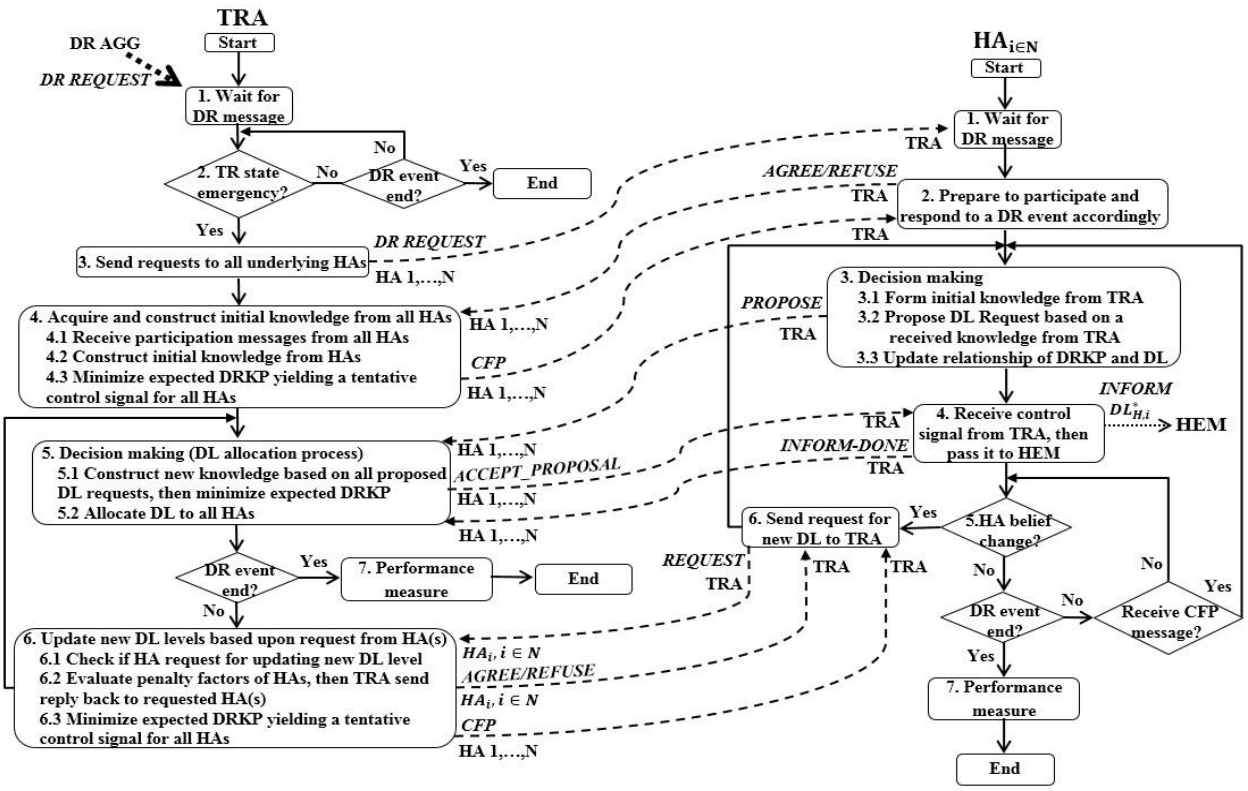

Fig. 3-18. Overall DR algorithm of a TRA residing at a distribution transformer and a HA residing at a home

The overall DR algorithm for a TRA and a HA is depicted in Fig. 3-18. Steps TRA1-TRA7 represent TRA algorithm. Steps HA1-HA7 represent HA algorithm. They work concurrently as follows.

Step TRA1: TRA waits for a DR *REQUEST* message from a DR AGG ($\boldsymbol{DL_{AGG \rightarrow TRA}}$) specifying an allocated DL and a DR event duration

Step TRA2: TRA assesses a TR operating state. If it is "normal", no action is taken. If it is "emergency", TRA works with its associated HAs as follows:

Step TRA3: TRA sends DR *REQUEST* messages to all associated HAs notifying them a DR event.

Step HA1: HA waits for a DR *REQUEST* message.

Step HA2: HA responds to the TRA with either an *AGREE* or a *REFUSE* message. The message provides the TRA an initial knowledge of this HA: (i) electrical characteristic represents an electrical meter service ampere rating of a home ($Amp\_Rating_{H,i}$); (ii) DL request ($DL_{H,req,i}$), shown in Fig. 3-19, is formed based on the objective of securing critical loads ($DL_{H,req,lower,i}$) and mitigating customer comfort level violation ($DL_{H,req,upper,i}$) given as:

$$DL_{H,req,i} \in [DL_{H,req,lower,i} = P_{H,hist,\text{crit,max,i}}, \; DL_{H,req,upper,i} = P_{H,hist,max,i}] \quad \text{(Eq. 3-8)}$$

Where, $P_{H,hist,crit,max,i}$ and $P_{H,hist,max,i}$ are a maximum power demand of critical loads and a maximum power demand of total loads of a home based on similar-day historical data respectively; and (iii) relationship $DRKP_{H,i}(DL_{H,i})$ between a demand restrike potential ($DRKP_{H,i}$) and a DL level ($DL_{H,i}$) of a home over a DR event period. This relationship is derived without the explicit knowledge from a TRA and the other neighboring HAs. The relationship is based on an average home's historical load profiles ($P_{H,hist,i}$) of the same period, climate, and day of the week (weekday/weekend). By sampling different levels of $DL_{H,i}$ ranging from its upper bound ($DL_{H,req,upper,i}$) to lower bound ($DL_{H,req,lower,i}$) and applying it to Eq. 3-9, different values of $DRKP_{H,i}$ can be obtained.

$$DRKP_{H,i} = \int_{t_{DR_{start}}}^{t_{DR_{end}}} \left(P_{H,hist,i} - DL_{H,i}\right) dt \quad \text{(Eq. 3-9)}$$
$$\text{s.t. } P_{H,hist,i} - DL_{H,i} \geq 0$$

Using polynomial regression algorithm, an approximated $DRKP_{H,i}$ as a function of a $DL_{H,i}$ is empirically represented as a quadratic function (with $a_{H,i}$, $b_{H,i}$, $c_{H,i}$ as coefficients) , depicted in Fig. 3-20, due to characteristics of the historical load profile of a home ($P_{H,hist,i}$) and a given $DL_{H,i}$ defined in Eq. 3-10 as:

$$DRKP_{H,i}(DL_{H,i}) = a_{H,i} \cdot DL_{H,i}^2 + b_{H,i} \cdot DL_{H,i} + c_{H,i} \quad \text{(Eq. 3-10)}$$

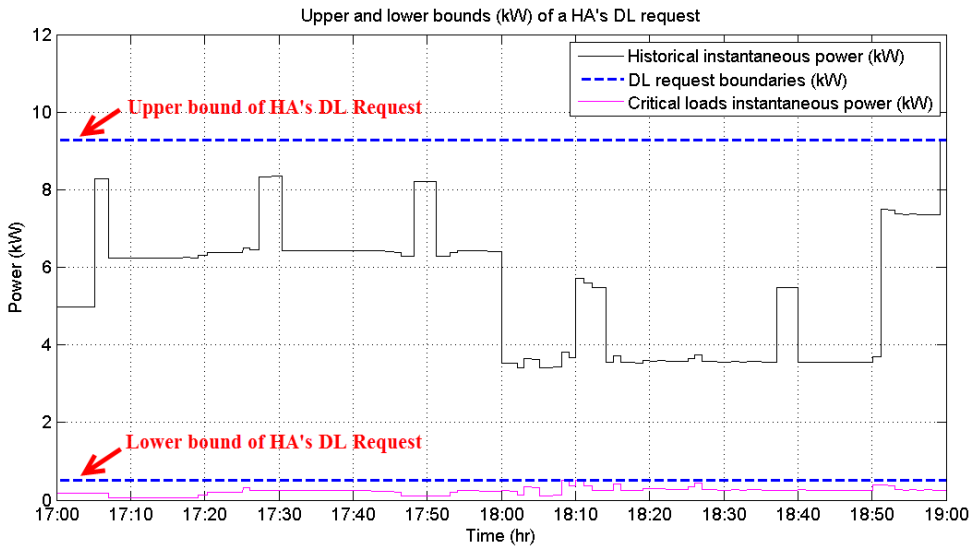

Fig. 3-19. Bounds of a HA's demand limit (DL) request

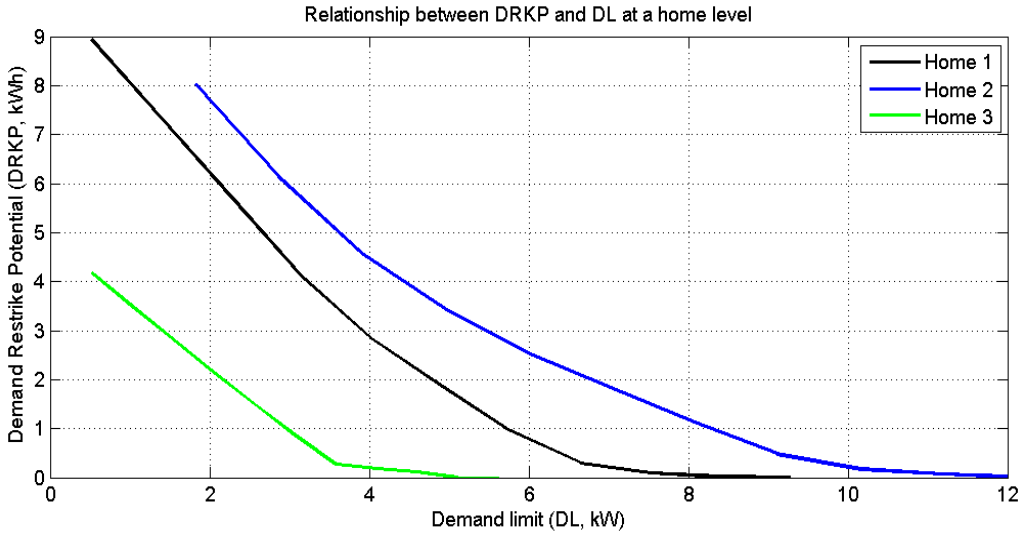

Fig. 3-20. Example of relationships between DRKP and DL at a home level

Step TRA4: TRA needs to acquire and construct initial knowledge based on information received from all HAs.

TRA4.1) The TRA receives *AGREE/REFUSE* messages from all associated HAs.

TRA4.2) TRA constructs initial knowledge about (i) fair demand limit levels of all homes ($\boldsymbol{DL_{H,\ fair}}$) defined as:

$$\boldsymbol{DL_{H,fair}} = [DL_{H,fair,1}, \ldots, DL_{H,fair,N}]^T \qquad \text{(Eq. 3-11)}$$

$$DL_{H,fair,i} = \frac{\boldsymbol{DL_{AGG \rightarrow TRA}} \times Amp\_Rating_{H,i}}{\sum_{i=1}^{N} Amp\_Rating_{H,i}}, \forall i \in N \qquad \text{(Eq. 3- 12)}$$

Where, $\boldsymbol{DL_{H,fair}}$ is defined as a vector containing fair demand limits of all homes ($DL_{H,fair,i}$, $\forall i \in N$); and (ii) an expected demand restrike potential at a TR level ($DRKP_{TR,\,exp}$) that is calculated based on the relationship $DRKP_{H,i}(DL_{H,i})$ obtained in Eq. 3-10 from all associated HAs as follows:

$$DRKP_{TR,exp} = \sum_{i=1}^{N} DRKP_{H,i}(DL_{H,i}) \qquad \text{(Eq. 3-13)}$$

<u>*TRA4.3)*</u> TRA minimizes the $DRKP_{TR,exp}$ based on its initial knowledge (from steps *TRA4.1* and *TRA4.2*) to find a tentative DL level vector ($\boldsymbol{DL_{H,ten}}$) for all HAs.
Objective function:

$$Min\ (DRKP_{TR,exp} = \sum_{i=1}^{N}\{a_{H,i} \cdot DL_{H,ten,i}^2 + b_{H,i} \cdot DL_{H,ten,i} + c_{H,i}\}) \qquad \text{(Eq. 3-14)}$$

Subject to:
Equality constraints:

(1) $\sum_{i=1}^{N} DL_{H,ten,i} = DL_{AGG \rightarrow TRA}$

Inequality constraints:

(2) $DL_{H,req,lower,i} \leq DL_{H,ten,i} \leq DL_{H,req,upper,i}, \forall i \in N$

Where, $DL_{H,ten,i}$ is a tentative DL level of a home $i \in N$. Using Lagrange relaxation technique with Kuhn-Tucker conditions, TRA solves this nonlinear optimization problem given linear and bounded constraints yielding vector $\boldsymbol{DL_{H,ten}}$.

$$\boldsymbol{DL_{H,ten}} = [DL_{H,ten,1},,,DL_{H,ten,N}]^T \qquad \text{(Eq. 3-15)}$$

Then, the TRA sends *Call for Proposal* (*CFP)* messages.

<u>Step HA3:</u> In this step, HA tries to minimize appliances' compensation time and to deploy $DL_{H,fair,i}$ and $DL_{H,ten,i}$ from a *CFP* message sent by a TRA. Pragmatically, required power demands of appliances are in discrete steps, the approximated $DRKP_{H,i}$ obtained from the initial knowledge of an HA in Eq. 3-10 does not decrease as $DL_{H,i}$ increases unless it is high enough to serve another appliance waiting to operate. Therefore, with additional knowledge from a TRA and its knowledge on current appliances' status, an HA updates the relationship $DRKP_{H,i}(DL_{H,i})$ in Eq. 3-10 as a piecewise linear function to obtain a more realistic behavior of $DRKP_{H,i}$. Intuitively, an HA will request for a suitable $DL_{H.i}$ level that it believes enough to serve its corresponding appliances. An HA also ensures that the requested $DL_{H,i}$ is not too high (with reference to its $DL_{H,fair,i}$) during that time as an HA will be panalized by a TRA. The steps to obtain the new updated $DL_{H,req,i}$ and $DRKP_{H,i}(DL_{H,i})$ are elaborated as follows:
<u>*HA3.1)*</u> HA acquires $DL_{H,fair,i}$ and $DL_{H,ten,i}$ from a *CFP* message sent by a TRA.

HA3.2) HA adjusts its $DL_{H,req,i}$ in Eq. 3-8 to a vector $\boldsymbol{DL_{H,req,i}}$ as explained in the steps *HA3.2.1* and *HA3.2.2*.

HA3.2.1) HA constructs its belief ($\boldsymbol{Belief_{H,i}}$) vector defined in Eq. 3-16. This vector represents minimum required power demands (kW) based on all possible combinations of usage status of power-intensive appliances.

$$[\boldsymbol{Belief_{H,i}}]_{\boldsymbol{Mx1}} \in \mathbb{R}^M = [\boldsymbol{Comb}]_{\boldsymbol{MxC}} \cdot [\boldsymbol{Rated}]_{\boldsymbol{Cx1}} \qquad \text{(Eq. 3-16)}$$

Where, $M = \sum_{k=1}^{C} \frac{C!}{k!(C-k)!}$ is a number of beliefs and C is a total number of appliances. $[\boldsymbol{Comb}]_{\boldsymbol{MxC}}$ is a matrix of combinations of usage status of power-intensive appliances given as:

$$[\boldsymbol{Comb}]_{\boldsymbol{MxC}} = \begin{bmatrix} s_{app,1,1} & \cdots & s_{app,1,C} \\ \vdots & \ddots & \vdots \\ s_{app,M,1} & \cdots & s_{app,M,C} \end{bmatrix} \qquad \text{(Eq. 3-17)}$$

$s_{app,j\in M,k\in C}$ is a status of an appliance $k \in C$ in a belief $j \in M$ that can be either 0 or 1. Note that, for AC, the binary status of "0" means a thermostat mode is OFF; and the binary status of "1" means a thermostat is in either COOL or HEAT mode. For WH, CD, and EV binary status of "0" means OFF; and binary status of "1" means ON. $[\boldsymbol{Rated}]_{\boldsymbol{Cx1}}$ is a vector containing rated power demands (kW) of C appliances given as:

$$[\boldsymbol{Rated}]_{\boldsymbol{Cx1}} = [Rated_{app,1}, \dots, Rated_{app,C}]^T \qquad \text{(Eq. 3-18)}$$

$Rated_{app,k\in C}$ is a rated power demand (kW) of a power-intensive appliance $k \in C$.

HA3.2.2) HA updates $DL_{H,req,i}$ as a vector $\boldsymbol{DL_{H,req,i}}$ according to the $DL_{H,fair,i}$, $DL_{H,ten,i}$, and $\boldsymbol{Belief_{H,i}}$ using the decision criteria explained below:

Step1: from the reordered $\boldsymbol{Belief_{H,i}}$ vector from min to max value, find $Belief_{H,i,j} = \max(Belief_{H,i,k} \in \boldsymbol{Belief_{H,i}})$; s.t. $Belief_{H,i,k} + P_{H,hist,crit,max,i} \leq DL_{H,ten,i}$

Step2: start from the element $Belief_{H,i,j}$ from *Step1*, a vector $\boldsymbol{DL_{H,req,i}}$ is obtained based on the following conditions:

If $Belief_{H,i,j+1} + P_{H,hist,crit,max,i} \geq DL_{H,fair,i}$, then

$$\boldsymbol{DL_{H,req,i}} = \begin{bmatrix} DL^1_{H,req} = Belief_{H,i,j} + P_{H,hist,crit,90\%,i} \\ DL^2_{H,req} = Belief_{H,i,j} + P_{H,hist,crit,max,i} \\ DL^3_{H,req} = Belief_{H,i,j+1} + P_{H,hist,crit,90\%,i} \\ DL^4_{H,req} = Belief_{H,i,j+1} + P_{H,hist,crit,max,i} \end{bmatrix} \qquad \text{(Eq. 3-19)}$$

Otherwise,

$$\boldsymbol{DL_{H,req,i}} = \begin{bmatrix} DL^1_{H,req} & DL^2_{H,req} & DL^3_{H,req} & DL^4_{H,req} \end{bmatrix}^T \qquad \text{(Eq. 3-20)}$$

$$= [1 \quad 1 \quad 1 \quad 1]^T \cdot [\, Belief_{H,i,j+1} + P_{H,hist,crit,max} \,]$$

Where, $P_{H,hist,crit,90\%,i}$ is the power demand level (kW) of a home $i \in N$ in which an hourly-average of critical loads will not exceed for 90% of the time. It can be obtained from the historical load duration of curve of critical loads of a home forming from the same period as a DR event as exemplified in Fig. 3-21. Regarding the second condition, as HA knows its own $DL_{H,fair,i}$, it will try to get a highest demand limit allowance as possible (shown in Eq. 3-20 so that impacts of DRK tend to be minimal to the homeowners.

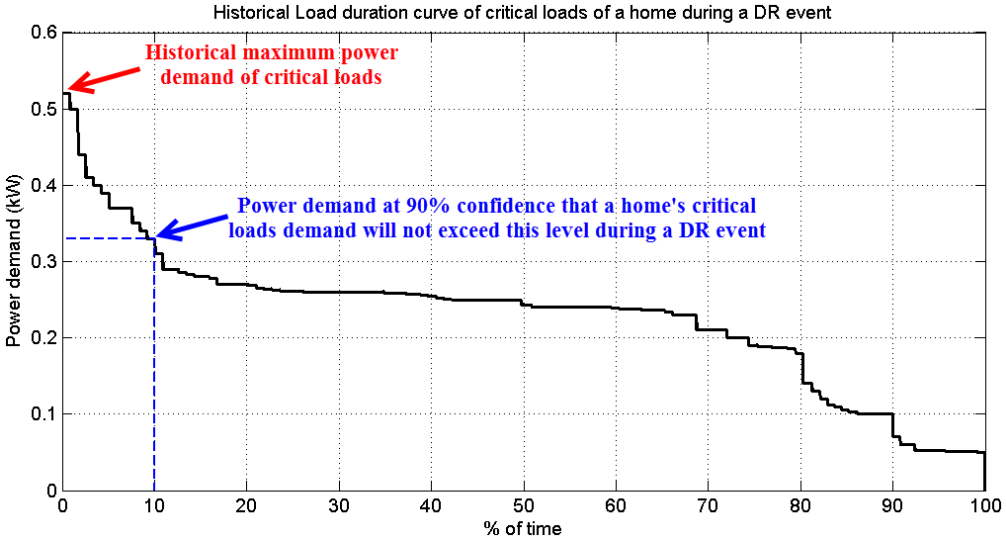

Fig. 3-21. Load duration curve of critical loads during a DR event of a home

<u>*HA3.3)*</u> After getting the $\boldsymbol{DL_{H,req,i}}$ from *HA3.2*, an HA updates the relationship $DRKP_{H,i}(DL_{H,i})$ in Eq. 3-10 as a piecewise linear function, shown in Fig. 3-22, which is mathematically defined in Eq. 3-21 - Eq. 3-26 as follows:

$$DRKP_{H,i}(DL_{H,i}) = \begin{cases} m_1 \Delta x_1 + DRKP_H^1 \; if \; DL_{H,req}^1 \le DL_{H,i} < DL_{H,req}^2 \\ DRKP_H^2 \; if \; DL_{H,req}^2 \le DL_{H,i} \le DL_{H,req}^3 \\ m_2 \Delta x_2 + DRKP_H^2 \; if \; DL_{H,req}^3 < DL_{H,i} \le DL_{H,req}^4 \end{cases} \quad \text{(Eq. 3-21)}$$

$$m_1 = \frac{DRKP_H^2 - DRKP_H^1}{DL_{H,req}^2 - DL_{H,req}^1}, \Delta x_1 = DL_{H,i} - DL_{H,req}^1 \quad \text{(Eq. 3-22)}$$

$$m_2 = \frac{DRKP_H^3 - DRKP_H^2}{DL_{H,req}^4 - DL_{H,req}^3}, \Delta x_2 = DL_{H,i} - DL_{H,req}^3 \quad \text{(Eq. 3-23)}$$

$$DRKP_H^1 = a_{H,i} \cdot (DL_{H,req}^1)^2 + b_{H,i} \cdot (DL_{H,req}^1) + c_{H,i} \quad \text{(Eq. 3-24)}$$

$$DRKP_H^2 = (\sum_{k=2}^{3} (a_{H,i} \cdot (DL_{H,req}^k)^2 + b_{H,i} \cdot (DL_{H,req}^k) + c_{H,i}))/2 \quad \text{(Eq. 3-25)}$$

$$DRKP_H^3 = a_{H,i} \cdot (DL_{H,req}^4)^2 + b_{H,i} \cdot (DL_{H,req}^4) + c_{H,i} \qquad \text{(Eq. 3-26)}$$

Where, $a_{H,i}, b_{H,i}$, and $c_{H,i}$ are obtained from Eq. 3-10 in order to estimate $DRKP_H^1$, $DRKP_H^2$, and $DRKP_H^3$ of the function $DRKP_{\boldsymbol{H,i}}(DL_{H,i})$ based on the vector $\boldsymbol{DL_{H,req,i}}$. Then an HA send a *PROPOSE* message with the updated $\boldsymbol{DL_{H,req,i}}$ and $DRKP_{H,i}(DL_{H,i})$ to a TRA.

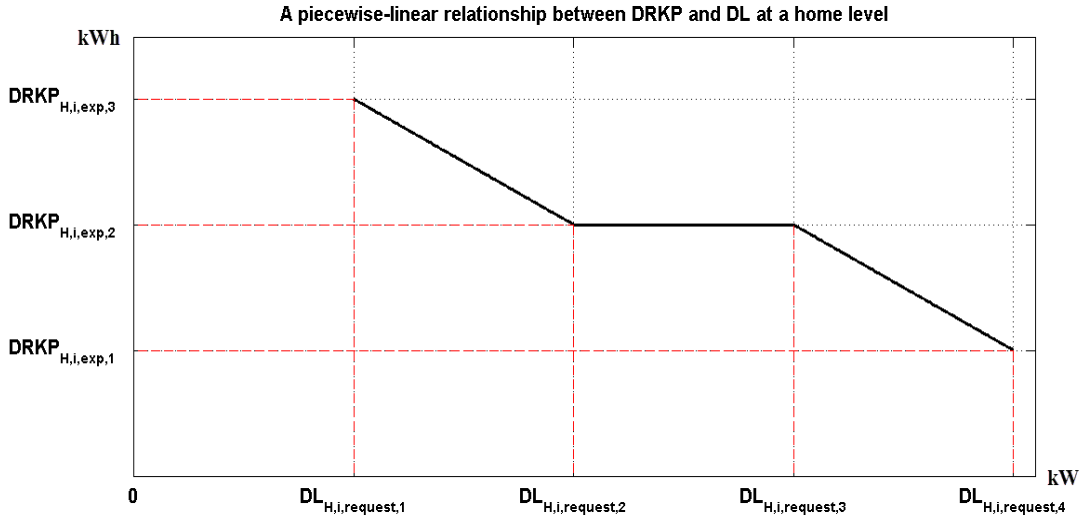

Fig. 3-22 Piecewise linear relationship between DRKP and DL of a home

Step TRA5: Once $\boldsymbol{DL_{H,req,i}}$ and $DRKP_{H,i}(DL_{H,i})$ of all participated HAs are updated, the TRA finds the optimal DL levels ($\boldsymbol{DL_H^*}$) in which the TRA and HAs mutually agree that the expected demand restrike potential at a TR level ($DRKP_{TR,exp}$) after a DR event will be minimal.

TRA5.1) After receiving all *PROPOSE* messages, the TRA constructs its new knowledge by forming a new optimization problem. The objective function of the TRA is to minimize $DRKP_{TR,exp}$ at a transformer level.

$$Min\ DRKP_{TR,exp} = Min\ (\sum_{i=1}^{N} DRKP_{H,i}(DL_{H,i}^*)) \qquad \text{(Eq. 3-27)}$$

Subject to:

Equality constraints:

(1) $\sum_{i=1}^{N} DL_{H,i}^* = DL_{AGG \to TRA}$

Inequality constraints:

(2) $DL_{H,req}^1 \leq DL_{H,i}^* \leq DL_{H,req}^4, \forall i \in N$

(3) $DL_{H,req,lower,i} \leq DL_{H,i}^* \leq DL_{H,req,upper,i}, \forall i \in N$

Where, $DL_{H,i}^*$ is an optimal DL level given to a home $i \in N$. Using Dual Upper Bounding Linear Programming, the TRA solves this linear optimization problem given piecewise linear

objective function and linear and bounded constraints. This yields a demand limit control signal vector: $\boldsymbol{DL_H^*} = [DL_{H,1}^* \ldots DL_{H,N}^*]^T$.
TRA5.2) TRA allocates $\boldsymbol{DL_H^*}$ by sending *ACCEPT_PROPOSAL* messages to all HAs. Then, the TRA receives *INFORM_DONE* messages indicating that all participating HAs have already received the $\boldsymbol{DL_H^*}$ and deployed the DL control signals at their corresponding HEMs.

Step HA4: HA receives a DL control signal ($DL_{H,i}^*$). Then, it passes the signal to an HEM. Finally, an HA sends back an *INFORM_DONE* message for successful confirmation.

Step HA5: During a DR event, an HA will periodically update its belief due to a change in run-time schedule of power-intensive appliances. These changes can result from a newly plugged-in appliance (e.g., electric vehicle is plugged in), or a condition that leads to customer comfort violations. If the HA belief ($\boldsymbol{Belief_{H,i}}$) changes during a DR event, it will request a TRA for a new DL as stipulated in ***Step HA6***, otherwise it will check whether or not a DR event has already ended. After a DR event has already ended, an HA will stop its services and evaluate its performance by carrying out the performance measure described in ***Step HA7***. If it has not, the HA will again check whether or not it receives a *CFP* message from a TRA as a result of a request to update $\boldsymbol{DL_H^*}$ sent by another HA. If the HA receives a *CFP* message, it sends a *PROPOSE* message back to the TRA as explained in ***Step HA3***.

Step HA6: HA sends a *REQUEST* message to let the TRA know that it needs to update its DL level due to a change in appliances' run-time schedule. If the HA receives an *AGREE* message, it constructs a new knowledge from the received *CFP* message. Then, the HA sends a *PROPOSE* message back to a TRA as explained in ***Step HA3***.

Step TRA6: TRA updates $\boldsymbol{DL_H^*}$ based upon the request from an HA to update its current $DL_{H,i}^*$.
TRA6.1) TRA receives a *REQUEST* message from one or more HA asking to change its DL level ($DL_{H,i}^*$).
TRA6.2) TRA makes the decision to accept/reject the request by evaluating the $\boldsymbol{PF_H}$ and the newly requested for $DL_{H,i}^*$ from an HA_i, $i \in N$ as follows:
TRA6.2.1 To ensure fairness in distributing $DL_{AGG \to TRA}$, the TRA evaluates homes' penalty factors ($\boldsymbol{PF_H}$). Each element $PF_{H,i}$ of $\boldsymbol{PF_H} = [PF_{H,1} \ldots PF_{H,N}]^T$ defined in Eq. 3-28 is a penalty factor imposed on a home $i \in N$.

$$PF_{H,i} = \begin{cases} 1 \; if \; \left(\int_{t_{DR\_start}}^{t_{eval}} DL_{H,i}^* \, dt - \int_{t_{DR\_start}}^{t_{eval}} DL_{H,fair,i} \, dt\right) < 0 \\ 0 \; if \left(\int_{t_{DR\_start}}^{t_{eval}} DL_{H,i}^* \, dt - \int_{t_{DR\_start}}^{t_{eval}} DL_{H,fair,i} \, dt\right) = 0 \quad , \forall i \in N \\ -1 \; if \left(\int_{t_{DR\_start}}^{t_{eval}} DL_{H,i}^* \, dt - \int_{t_{DR\_start}}^{t_{eval}} DL_{H,fair,i} \, dt\right) > 0 \end{cases} \quad \text{(Eq. 3-28)}$$

Where, t_{eval} is a time that a TRA evaluates $\boldsymbol{PF_H}$ as soon as it receives a request from an HA. The $PF_{H,i}$ (either -1, 0 or 1) of a home $i \in N$ is determined based on $DL_{H,i}^*$ as compared to $DL_{H,fair,i}$ in terms of energy consumption over time. This term implies an average of $DL_{H,i}^*$ that an HA receives of from t_{DR_start} to t_{eval}. $\boldsymbol{PF_H}$ is used as a decision criteria whether or not the TRA will update $\boldsymbol{DL_H^*}$ as being requested by an HA.

TRA6.2.2 TRA will send *AGREE* messages all participated HAs based on the following conditions:
(i) $PF_{H,i}$ = 1, and an HA requests a higher or lower demand limit level. This because the average of its received $DL^*_{H,i}$ is lower than its fair demand limit ($DL_{H,fair,i}$).
(ii) $PF_{H,i}$ = 0 or -1, an HA can only ask for a lower demand limit level because the average of its received $DL^*_{H,i}$ is the same ($PF_{H,i}$ = 0) or higher ($PF_{H,i}$ = -1) than its fair demand limit ($DL_{H,fair,i}$).

The TRA will sends a *REFUSE* message back to the requested HA based on the following condition. Then, the TRA stops the process of updating $DL^*_{H,i}$ of the requested HA.
iii) $PF_{H,i}$ = 0 or -1, an HA asks for a higher demand limit level because the average of its received $DL^*_{H,i}$ is the same ($PF_{H,i}$ = 0) or higher ($PF_{H,i}$ = -1) than its fair demand limit ($DL_{H,fair,i}$) at the time the $\boldsymbol{PF_H}$ is evaluated.
TRA6.3) TRA minimizes a $DRKP_{TR,exp}$ as explained in ***Step TRA4.3*** given the updated inequality constraint on the $DL_{H,i,ten}$ of the requested HA as follows:

$PF_{H,i}$	$Request$	updated constraint on $DL_{H,ten,i}$
1	higher $DL^*_{H,i}$	$DL^*_{H,i} < DL_{H,ten,i} \leq DL_{H,req,upper,i}$
1, 0, -1	lower $DL^*_{H,i}$	$DL_{H,req,lower,i} \leq DL_{H,ten,i} \leq DL^*_{H,i}$

Where, $DL^*_{H,i}$ is the currently received demand limit of an HA before it requests for a new DL level. Therefore, a new $\boldsymbol{DL_{H,ten}} = [DL_{H,ten,1} \dots DL_{H,ten,N}]^T$ for all HAs is obtained. Finally, the TRA sends *CFP* messages to all participated HAs. Then, the TRA proceeds to update a $\boldsymbol{DL^*_H}$ based upon the DL allocation process explained in ***Step TRA5***.

Step TRA7: After a DR event ends, a TRA assesses its performance as follows:
TRA7.1) TRA calculates the Power Exceed Demand Limit (PEDL) index. If PEDL is greater than zero, it means that a power demand of a distribution transformer (P_{TR}) exceeds a given $DL_{AGG \rightarrow TRA}$ during a DR event.

$$PEDL = \int_{t_{DR\_start}}^{t_{DR\_end}} (P_{TR} - DL_{AGG \rightarrow TR})\, dt \qquad \text{(Eq. 3-29)}$$

$$\text{s.t. } P_{TR} - DL_{AGG-TR} \geq 0$$

TRA7.2) The TRA assesses its performance on minimizing $DRKP_{TR}$ by evaluating an actual load profile of a distribution transformer during a DR event (P_{TR}) compared with it's historical load profile without a DR event ($P_{TR,hist}$) during the same period yieldind the index $DRKP_{TR,act}$ defined in Eq. 3-30. The smaller $DRKP_{TR,act}$, the lower impacts of DRK can be expected.

$$DRKP_{TR,act} = \int_{t_{DR\_start}}^{t_{DR\_end}} (P_{TR,hist} - P_{TR,act})\, dt \qquad \text{(Eq. 3-30)}$$

Step HA7: After a DR event ends, an HA assesses its performance as follows:

HA7.1) HA calculates the Demand Limit Below Critical Loads (DLBCL) index. If DLBCL is greater than zero the critical loads are violated during a DR event.

$$DLBCL = \int_{t_{DR_{start}}}^{t_{DR_{end}}} \left(P_{H,hist,max,i} - DL^{*}_{H,i}\right) dt \qquad \text{(Eq. 3-31)}$$

$$\text{s.t. } P_{H,hist,max,i} - DL^{*}_{H}(t) \geq 0$$

HA7.2) HA calculates Comfortable Level Violation (CLV) index defined as follows:

$$CLV = \int_{t_{DR\_start}}^{t_{DR\_end}} (\text{temp}_{\text{room}} - \text{temp}_{\text{AC,set}})\, dt + \int_{t_{DR\_start}}^{t_{DR\_end}} (\text{temp}_{\text{water}} - \text{temp}_{\text{WH,set}})\, dt \qquad \text{(Eq. 3-32)}$$

$$\text{s.t. } \left|\text{temp}_{\text{room}} - \text{temp}_{\text{AC,set}}\right| > \text{temp}_{\text{AC,deadband}}$$
$$\text{and } \left|\text{temp}_{\text{water}} - \text{temp}_{\text{WH,set}}\right| > \text{temp}_{\text{WH,deadband}}$$

Where, $\text{temp}_{\text{room}}$ is a room temperature profile during a DR event; $\text{temp}_{\text{AC,set}}$ is a room temperature set point of an air conditioner (AC); $\text{temp}_{\text{AC,deadband}}$ is an AC temperature deadband; $\text{temp}_{\text{water}}$ is a hot water temperature profile during a DR event; $\text{temp}_{\text{WH,set}}$ is a hot water temperature set point of a water heater (WH); $\text{temp}_{\text{WH,deadband}}$ is a WH temperature deadband. CLV index of a home calculated at the end of a DR event ($CLV_{DRevent}$) is compared to CLV index calculated at the same time period where there is no DR event (CLV_{w/o_DR}). If a $CLV_{DRevent}$ is not comparable with a CLV_{w/o_DR}, a customer's comfort level during a DR event is violated.

HA7.3) An HA assesses its performance on minimizing appliances' operating times by evaluating an actual demand restrike potential, $DRKP_{H,act,i}$, as follows:

$$DRKP_{H,act,i} = \int_{t_{DR\_start}}^{t_{DR\_end}} (P_{H,hist,i} - P_{H,i})\, dt \qquad \text{(Eq. 3-33)}$$

Where, $P_{H,i}$ is an actual power demand of a home $i \in N$ (kW) during a DR event.

3.3.4. Algorithm at an Appliance Level

After an HA receives a control signal $DL^{*}_{H,i}$, it passes the signal to the corresponding HEM. According to our previously proposed HEM algorithms as described in [80], the HEM works to ensure that an instantaneous power demand at home will not exceed the given demand limit $DL^{*}_{H,i}$ during a DR event. The HEM communicates and sends control signals to allow rescheduling operation of power-intensive appliances according to homeowner's preference. The delay accounts for the operating interval of the HEM is in 1-minute interval.

3.4 An Agent-Based Platform to Facilitate DR Implementation in Commercial Buildings

The knowledge gaps discussed in Section 2.3.2 prompt the development of an agent-based platform for optimizing electricity usage and implementing demand response (DR) in small- and medium- sized buildings. This main objective of the proposed agent-based platform is to enable utilities and independent system operator (ISOs) to actively leverage DR at commercial buildings as a partial substitute for generation reserve or transmission upgrade.

3.4.1. Overview of Building Energy Management System (BEMS)

Buildings consume over 40% of total energy consumption in the U.S., and majority of commercial buildings are either small- (<5,000 ft^2) or medium-sized (5,000 - 50,000 ft^2). These buildings typically do not have existing building energy management systems (BEMS) to manage their energy consumption due to unavailability of a cost-effective solution. Therefore, significant amount of energy consumptions in these building are wasted.

There are three major load types in commercial buildings. These are HVAC, lighting loads, and plug loads that are the primary focus of this study.

Various communication technologies are in used today that allow communications between the proposed agent platform and load controllers in a building. These include:

- Wired technologies, like: Power Line Communication (PLC), Ethernet and Serial (RS-485)
- Wireless technologies, like: ZigBee, Wi-Fi, Z-wave and EnOcean.

Devices communicating using the same communication technology may utilize different data exchange protocols. For a BEM system, there are many protocols that are popular or becoming popular. These are open standard protocols like: BACnet, Modbus, KNX, M-bus, Web (HTTP/HTTPS), OpenADR and Smart Energy Profile (SEP); as well as proprietary protocols like: LonWorks and DALI.

3.4.2 Physical Layer and Cyber Layer of the Proposed Agent-Based Platform

The proposed system architecture consists two layers: physical layer and cyber layer. The physical layer is where real physical devices exist. This layer comprises a building, controllers for HVAC, lighting and plug loads, as well as sensors. The cyber layer represents decision-making processes where the developed agent-based platform resides. Fig. 3-23 illustrates interactions between relevant actors, systems and technologies required to achieve a specific goal of an implementation of a DR at a building level.

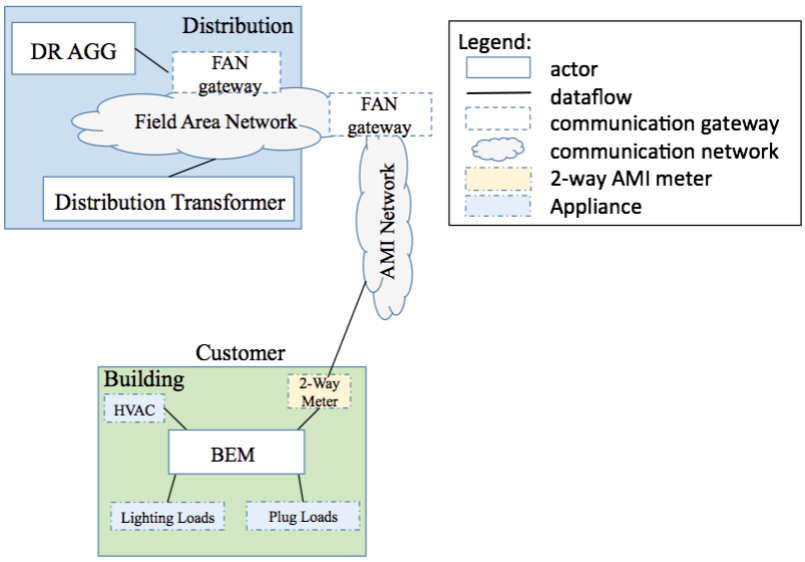

Fig. 3-23. Data flow diagram of DR implementation at a building level

The objective, actors and scenarios are described in more detail below, which manifest how the proposed Multi-Agent System (MAS) performs during a DR event:

1) Objective: The main objective is to reduce instantaneous power demand (kW) of a building during a system stress condition. The MAS acts in response to a Critical Peak Pricing (CPP) signal from a utility.

2) Actors: Relevant actors include DR aggregator (DR AGG), agents, and controllers for HVAC, lighting, and plug loads.

3) Scenarios: These include chronological order of steps to implement DR algorithm during a DR event.

3.1 In case of a DR event, MAS receives a signal from a DR AGG over a field area network (FAN) via a FAN gateway.

3.2 After receiving a request, MAS reduces electricity usage through an automated DR algorithm that manages energy consumption of selected building loads.

3.4.3 MAS Development for DR Implementation in Commercial Buildings

MAS is the fundamental core of the proposed platform. This section devotes to the discussion of agents development and its requirements.

In order to develop MAS for DR applications in commercial buildings, VOLTTRON™, a distributed agent platform developed by Pacific Northwest National Laboratory (PNNL) [100], [101], [102] is chosen as the development platform. VOLTTRON is designed to run on small-form-factor computers and is capable of interfacing with legacy devices, maintaining security and managing platform resources, and servicing for applications. VOLTTRON platform enables the deployment of intelligent sensors and controllers in residential/commercial buildings and the smart grid. Distributed agents using peer-to-peer communications in VOLTTRON cooperate to bring computation closer to data to enable distributed control decisions and data analysis.

Intelligent agents residing in VOLTTRON are designed to have most of these capabilities: reactive, pro-active, social, mobility, veracity, benevolence, rationality, and learning/adaptation.

With respect to VOLTTRON architecture and design, the platform consists of communication services (CS), resource manager (RM), authentication and authorization (AA), directory services (DS), agent instantiation and packaging (AIP) and information exchange bus (IEB) modules. For the proposed BEMOSS software architecture, VOLTTRON provides connectivity and abstraction capabilities to BEMOSS.

In terms of ***connectivity***, devices with different communication technologies and different data exchange protocols are able to integrate into the VOLTTRON platform. VOLTTRON includes drivers for interfacing with MODBUS BACnet based devices. Drivers can be written for devices which do not use those protocols based on the availability of an Application Programming Interface (API) for that device. These drivers then publish data to VOLTTRON enables a device to communicate, be monitored and controlled by an assigned intelligent agent with assistance from the Connectivity layer described in the next subsection. A device can also response to an event triggered by an associated agent or an external environment specified in the Application and Data Management layer.

In terms of ***abstraction***, VOLTTRON allows applications to communicate with devices via its message bus instead of requiring them to use the particular device protocol. Drivers can be added to the platform to increase the number of supported devices. This enables developers to develop an agent to control a device or coordinate multiple devices regardless of communication technologies or data exchange protocols used.

Fig. 3-24 shows a number of agents required to implement the proposed DR algorithm. These agents, are categorized into the following types: (1) platform agents, (2) control agents, (3) sensor agents, and (4) network agents. Each type of agents has different functionalities as described below.

(1) **Platform agents:** These agents include a device discovery agent (DDA), a platform agent (PA), and a demand response agent (DRA). The DDA is responsible for detecting the presence of devices in a building, querying their model numbers, identifying their API interfaces, and launching control agents to monitor/control discovered devices. The PA is responsible for monitoring overall platform activities. The DRA is responsible for implementing the proposed DR algorithm as explained in the Section 3.5. Its main objective is to reduce peak demand consumption during a certain period, according to the price signal or the demand reduction signal received from the OpenADR agent.

(2) **Control agents:** These agents include a thermostat agent (TA), a lighting load agent (LLA), plug load agent (PLA), and roof top unit agent (RTU). These agents are responsible for monitoring and control a thermostat, a lighting load controller, a plug load controller, and a rooftop packaged unit (RTU), respectively. Each of these agents will be automatically initiated and launched, if the device discovery agent discovers a corresponding device. It should be noted that one control agent is assigned to one hardware device.

(3) **Sensor agents:** These agents are power meter agent (PMA), multi sensor agent (MSA), motion sensor agent (MSA), and weather sensor agent (WA). These agents are responsible for monitoring and communicating with corresponding sensors and power meters to obtain their readings. Similar to control agents, sensor agents are automatically launched after the device discovery agent discovers associated devices.

(4) **Network agents:** These agents are an OpenADR agent, a multi-node agent (MNA), and a network agent (NA). The OpenADR agent is deployed as a gateway to communicate with an electricity to receive a CPP signal; it receives demand response request through a web service on the cloud. It then notifies a DRA with event information.

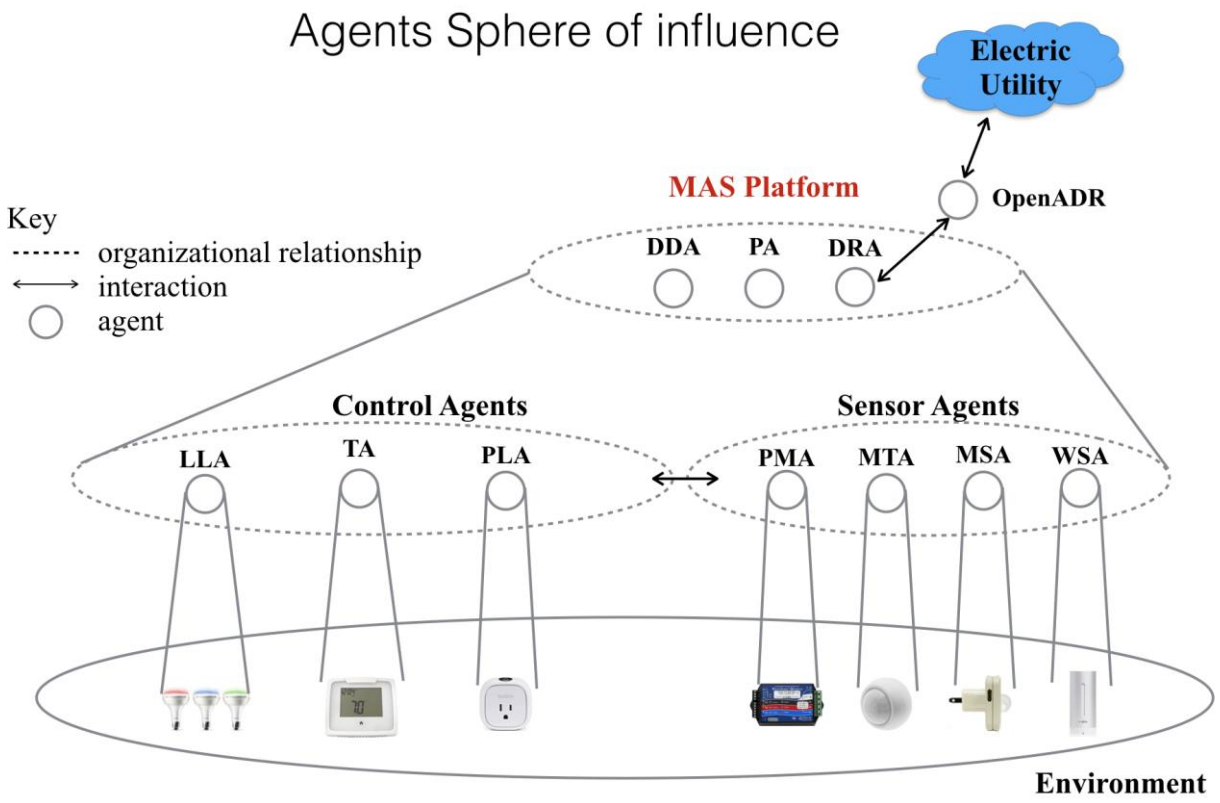

Fig. 3-24. Agents architecture to implement the proposed DR algorithm

The subsequent sections discuss MAS development to enable DR implementation in commercial buildings in detail.

A. Agent Architecture

An agent architecture is the fundamental mechanism underlying autonomous software components that support effective behavior in dynamic, real-world and open environments. Theoretically, an agent architecture can range from a purely reactive (or behavioral) architecture that reacts to an environment in a simple stimulus-response fashion to a more deliberative architecture that reasons about its action based on Belief Desire Intention (BDI) model. Any agent architecture can fall into four main categories: Logic based, Reactive, BDI, and Layered architectures depending on its required functionalities and capabilities.

Fig. 3-25 illustrates an example of a thread path of execution of a generic control agent modeled as a purely reactive agent that reacts to its environment, such as its corresponding UI, applications, or other agents.

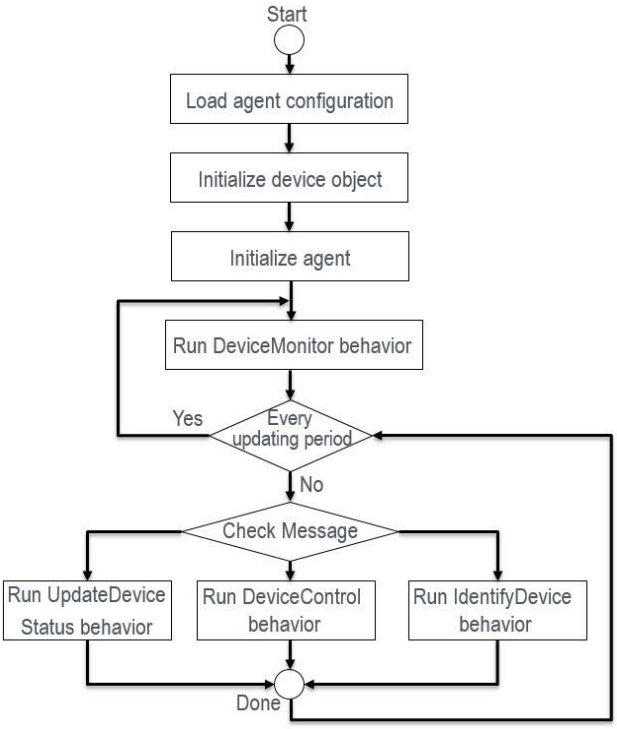

Fig. 3-25. Control agent thread path of execution

A brief discussion of the thread path of execution is given as follows:

Step 1: Agent acquires its configuration including agent's parameter setting (e.g., agent id, agent message publish/subscribe addresses), device information (e.g., IP address, API interface), database interfaces.

Step 2: Agent instantiates device object from the loaded API interface to be able to communicate, monitor, and/or control a device.

Step 3: Agent initializes itself based on settings from the previous steps by declaring necessary variables and connecting with databases and other required services.

Step 4: With the DeviceMonitor behavior (discussed in the agent behavior design section), an agent periodically gets the current status of a device by calling a method of an API interface. Then, it maps keyword and variables to agent knowledge and update both metadata database and time-series database with the recent device status.

Step 5: Receiving a message sent by its corresponding UI or an application, an agent triggers one of its reactive behaviors (UpdateDeviceStatus, DeviceControl, and IdentifyDevice) according to a message's topic and content as described in the subsequent sections.

B. Agent Behavior Design

One of the most important steps of designing MAS is to design agent behaviors. Fundamentally, behaviors of an agent are its abilities to react to changes in its external environment as well as its neighboring entities in pursuit of a system goal(s) or its own goal(s). There are three common types of agent behaviors: one-shot, cyclic, and generic behaviors explained as follows.

- 'One-shot' behavior is designed to complete in one execution phase
- 'Cyclic' behavior is designed to never complete. It executes the same operation at every poll time indefinitely unless an agent is killed.
- 'Generic' behavior is designed to embedded a status trigger and execute different operations depending on the status value. This behavior completes when a given condition is met.

For example, as shown in Fig. 3-25, generic control agent behaviors can be explained as follows:

- DeviceMonitor behavior is implemented as a cyclic behavior. A control agent will periodically update its knowledge on a device current status every a specified device monitoring time.
- UpdateDeviceStatus behavior is implemented as a generic behavior. It is called upon when other entities (e.g., UI, application, or another agent) would like to obtain a current status and setting of a device such as current temperature, thermostat temperature set point or thermostat mode, etc.
- DeviceControl behavior is implemented as generic behavior. A control agent will update device control parameters (e.g., thermostat temperature set point, change heat/cool mode and fan mode) by sending a control command using an API interface to change a current status/setting of a device.
- IdentifyDevice behavior is used in order to visually identify a device pertaining to a corresponding control agent. This behavior can be triggered by the UI sending identify device message to a control agent.

C. Agent Knowledge Representation

Meta data and time-series data are two types of knowledge that an agent needs to maintain to allow its interaction with other entities (e.g., the UI), as well as its reasoning processes. For each agent, there are two required tables to model an agent knowledge: metadata table and time-series data table.

- The metadata table is used to model agent knowledge with the data that have no timestamp, e.g., an agent identifier (AID) or an address of an agent.
- The time-series data table is used to model agent knowledge with the rest of the time-stamped data.

Table 3-7 gives example of common metadata of a control agent that is necessary for agents' knowledge modeling.

Table 3-7. Metadata of a control agent

Attributes	Data type
- AID (Agent identifier)	AID object
- Address (e.g., IP, MAC)	string
- Zone	string
- Device type	string
- MAC address	macaddr

Table 3-8 gives an example of time-series data of a thermostat agent that is necessary for agents' knowledge modeling.

Table 3-8. Time-series data of a thermostat agent

Attributes	Unit
- temperature	Fahrenheit
- thermostat mode	N/A
- fan mode	N/A
- heat setpoint	Fahrenheit
- cool setpoint	Fahrenheit
- thermostat state	N/A
- fan state	N/A

D. Agent Ontology Design

As each agent has different knowledge about their interests and functionalities, ontology provides the way in which common understanding (semantics of knowledge) can be shared among agents. Conforming to Foundation of Intelligent Physical Agents (FIPA) standards, agents communicate and update their knowledge by exchanging FIPA-ACL (Agent Communication Language) messages. These messages specify ontology that describes the structured message content expressed by FIPA-SL language. Generally, an ontology is domain-specific, i.e., it works particularly with a certain set of agents in a certain environment. Three essential elements of are concepts, predicates, and agent actions:

- Concepts are expressions used to represent entities with a complex structure defined in terms of their attributes. Typically, concepts alone are not used directly as the content of an ACL message. Instead, they are referenced inside predicates, agent actions, or other concepts.
- Predicates are expressions that indicate the current status of an agent environment and can be either true or false.
- Agent actions are special concepts indicating actions that can be performed by an agent.

E. Agent Communication

Communications between agents are required if an agent(s) cannot solve a given problem(s) solely by using its own knowledge, or if an agent needs to observe its external environment via other agents. By working together, agents can accomplish the system goal. Agent communications are essential in order to exchange knowledge among agents according to their behaviors and the designed ontology. For the current implementation, two common FIPA interaction protocols used in communications and negotiations among agents are the FIPA Request Interaction Protocol and the FIPA Contract Net Interaction Protocol. In VOLTTRON™, information exchanges between or among agents are facilitated using publish/subscribe mechanism built on the ZeroMQ Python module [103]. The current convention that is used to maintain consistency of topics exchange among agents is by hierarchically naming a topic and subtopics of an exchanged message. In short, an agent wishing to communicate with other agents requires to publish a message with the following topic format and content format on the information exchange bus (IEB).

Topic: topic/subtopic/subtopic

Message content: JavaScript Object Notation (JSON) format

F. Agent Communication with Load Controllers

An API interface allows an agent to communicate, monitor and control a device regardless of its communication technology or data exchange format (protocol-agnostic). In order to deal with heterogeneous application programming interface (API) documents offered by different hardware vendors, the mapping mechanism between agent's knowledge and an API interface is provided. This mechanism ensures that agent's knowledge obtaining from an API interface follows the agent ontology used throughout the platform for interoperability among agents and the other services. The mapping mechanism of an API interface to an agent's knowledge is shown in Fig. 3-26.

G. Agent as an Application

With its ability to communicate with other agents, web services, cloud services and database interfaces, an agent can also be developed as an application (App). The CPP algorithm as presented in Section 3.5 is an example of possible application that has been developed as an agent. The agent application development is depicted in Fig. 3-27.

There are five essential elements of the application development architecture.

1) User Interface (UI): agents accept inputs from a user via a UI, including activate application, disable application and update new application setting.

1.1 Activate application: in order to activate application a message with the following topic and content should be published on the IEB. This message is picked up by the APPLauncher agent to start the requested application.

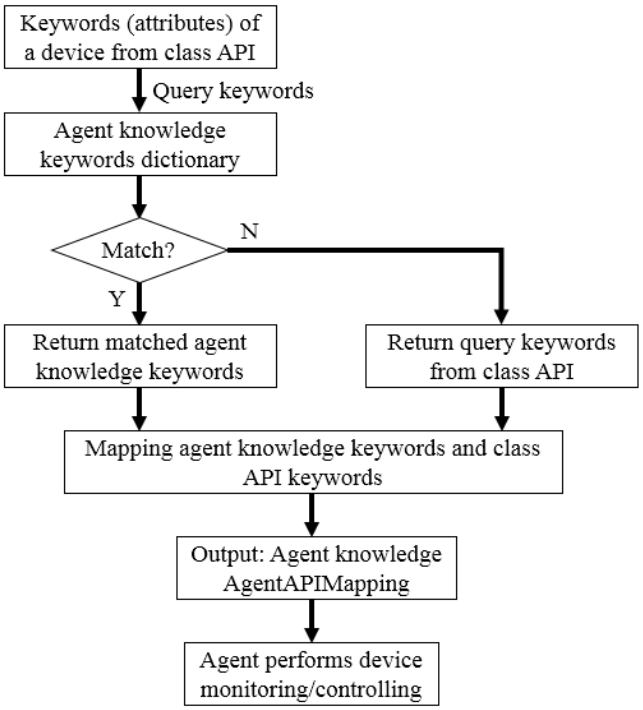

Fig. 3-26. Mapping mechanism between agent knowledge and API interface

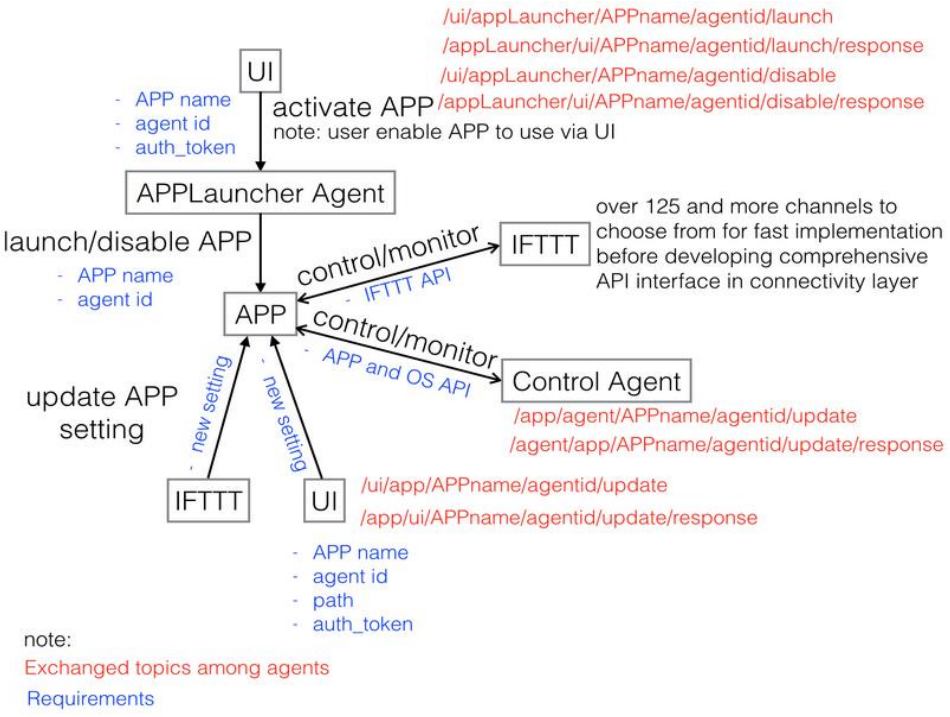

Fig. 3-27. Agent application development

Topic: /ui/appLauncher/AppName/agentid/launch

Message content: {"auth_token": "Token to grant access to App"}

Where, AppName is a name of an application, agentid is an agent identification, auth_token is a token to grant access for other agents or entities to use this application.

1.2 Disable application: in order to disable application, a message with the following topic and content should be published on the IEB. This message is picked up by the APPLauncher agent to disable the specific application.

Topic: /ui/appLauncher/AppName/agentid/disable

Message content: {"auth_token": "Token to grant access to App"}

1.3 Update application setting: in order to update application setting, for example update a schedule for brightness setting of a lighting controller, a message with the following topic and content should be published on the IEB. This message is picked up by the corresponding App to update its setting sent by the UI or other web/cloud services such as If This Then That (IFTTT) [104].

Topic: /ui/app/AppName/agentid/update

Message content: {"auth_token": "Token to grant access to App", "path": "path to the App setting file (JSON format)"}

2) APPLauncher agent: each application is required to register with the APPLauncher agent so that it can be launched once a user activates application to use. In addition, it also serves when a user would like to disable the running application.

2.1 Activate application: upon receiving a launch App message from the UI, the AppLaucher agent looks up the database whether the requested application is validated, registered, and installed. Then it looks whether the requested agent is available and running by checking with the Platform Agent. Finally, it checks whether the provided authorization token (auth_token) is valid to launch the requested application. If these conditions are satisfied, the AppLauncher agent launches the requested application providing application name (APPName) and agentid. The recently launched application will start to communicate, monitor, and/or control the control agent (e.g., thermostat agent, plugload agent, or lighting agent) using the API between the application and data management layer and the operating system and framework layer (App and OS API). Once the AppLauncher finishes launching the requested App, it replies to the UI by sending back the following message:

Topic: /appLauncher/ui/AppName/agentid/launch/response

Message content: {"result": "success/failure"}

2.2 Disable application: upon receiving a disable message from the UI, AppLauncher agent looks up whether the requested agent (agent_id) is available and running by checking with the Platform Agent. Finally, it checks whether the provided auth_token is valid to disable the requested App. If these conditions are satisfied, the AppLauncher agent disables the requested application. Once the AppLauncher finishes disabling the requested application, it replies to the UI by sending back the following message:

Topic: /appLauncher/ui/AppName/agentid/disable/response

Message content: {"result": "success/failure"}

3) Application (App): App is designed to communicate, monitor, and/or control agent(s). The steps and requirements for developing App in the platform are the same as developing an agent with additional capabilities providing APIs between layers. After an App is successfully launched by the AppLauncher agent, it starts to communicate with a control agent using App and OS API. In order to control a device, the App needs to publish a message with the following topic and content on the IEB.

Topic: /app/agent/AppName/agentid/update/

Message content: {"control parameter": "setting"}

For example, to change a mode and temperature set points of a thermostat according to a user-defined schedule, the thermostat scheduler App with an agent_id = '1TH571a4760189f" needs to publish the following message to IEB.

Topic: /app/agent/thermostat_scheduler/1TH571a4760189f/update/

Message content: {"mode": "COOL", "setpoint": "72"}

4) Control Agent: Upon receiving control message from the App, a Control agent (e.g., thermostat agent) changes the setting of a corresponding device (e.g., a thermostat) accordingly by using the API between OS layer and Connectivity layer. Once the Control agent successfully changes device setting, it replies back to the App by publishing the message with the following topic and content to IEB.

Topic: /agent/app/AppName/agentid/update/response

Message content: {"result": "success/failure"}

5) If This Then That (IFTTT): IFTTT [105] can be seamlessly integrated with any App by simply adding an interface between the IFTTT and an App agent. The term “interface” can be any channels available in IFTTT that an agent can communicate. This can be, for example, an email channel. In this case, an agent can send or receive an email from IFTTT. This can be used to send an alarm message to the building administrator to notify him/her an important circumstance in a system, e.g., device failure or malfunction, as well as to notify the building administrator for any

condition-based maintenance requirements. The crucial benefit of integrating IFTTT with agents is that it allows all possibilities to interact with third party hardware devices, web services, and cloud-based applications. As a result, this feature enables rapid test and development of agent functionalities in the case that some API interfaces for required devices or services are not available in the connectivity layer. Some of interesting IFTTT available channels, for example, are email, SMS, Pushover, SmartThings, Weather, Wemo, Nest Thermostat, etc.

3.5 Algorithm for DR Implementation in Commercial Buildings

It is assumed that a DR event occurs and an electric utility assigns a DR event signal and an event duration (minutes) to a building. The overall objective of the proposed DR algorithm at the building level is to improve efficiency of a power grid operation by participating in a Critical Peak Pricing (CPP) event. This section propose an algorithm in response to the received CPP signal as follows.

3.5.1 Objective Functions

To improve efficiency of a power grid operation in response to a CPP signal at a building level. This is a multi-objective optimization problem having objective functions as follows:

- Minimize power demand during a peak summer period when a CPP event is called out
- Minimize occupant comfort violation
- Minimize impacts of demand restrike after a CPP event
- Minimize time to control device operation to avoid demand restrike after a CPP event

3.5.2 Prerequisite Subtasks for DR Algorithm Development

In order to develop the DR algorithm based on the mentioned objective functions, there are preliminary subtasks needed to be carried out as follows.

Subtask 1: define occupant comfort conditions
Subtask 2: explore energy/power savings opportunity of HVAC loads
Subtask 3: explore energy/power savings opportunity of lighting loads
Subtask 4: explore energy/power savings opportunity of plug loads

Each subtask is discussed in detail as follows:

Subtask 1: Define occupant comfort conditions

According to American Society of Heating, Refrigerating, and Air-Conditioning Engineers (ASHRAE) [105], a conditioned air of a building with these properties: 1. cleanliness, 2. odor, 3. temperature, 4. relative humidity, 5. movement – are required to be within comfort ranges.

HVAC comfort conditions: ASHRAE established standard which outline indoor air quality (IAQ) for indoor comfort conditions that are acceptable to 80% or more of a commercial building's occupants as:

- Indoor comfort conditions (so called "comfort zone") are 68 – 75 degree F for winter, 73 – 79 degree F for summer.
- Relative humidity (RH) is approximately at 50%.
- Air velocity is at 30 feet/minute or slower.
- Air ventilation requirement is 20 cubic feet per minute of outside air for each occupant.
- Carbon dioxide (CO_2) concentration is less than 1,000 ppm.

Specifically, according to ASHRAE standard 55-2013 [106], indoor comfort condition (thermal comfort) which is a state of mind that separates from equations for heat and mass transfer and energy balances can be formulated using Fanger's comfort analysis [106]. The level of comfort is characterized using the ASHRAE thermal sensation scale (Table 3-9) as shown below. This introduces an index namely predicted mean vote (PMV) that uses the ASHRAE thermal sensation scale to find an average thermal sensation response from a large number of people.

Table 3-9. ASHRAE Thermal Sensation Scale

PMV value	Sensation
+3	Hot
+2	Warm
+1	Slightly warm
0	Neutral
-1	Slightly cool
-2	Cool
-3	Cold

The sensation of thermal comfort is significantly determined by narrow ranges of skin temperature and sweat evaporation rate depending on occupants' activity level. For example, people doing a less active activity might feel comfortable at higher skin temperatures and slower evaporation rates as compared to people doing a more active activity.

Fanger's PMV correlation is based on the identification of a skin temperature ($T_{sk,req}$) and the sweat evaporation rate ($q_{sweat,req}$) required for 'optimal' comfort conditions using data from Rohles and Nevins (1971).

$$T_{sk,req} = 96.3 - 0.156 q_{met,heat} \qquad \text{(Eq. 3-34)}$$

$$q_{sweat,req} = 0.142(q_{met,heat} - 18.43) \qquad \text{(Eq. 3-35)}$$

Where,

$T_{sk,req}$: Required skin temperature for optimal comfort conditions, °F

$q_{met,heat}$: Rate of metabolic heat generation, $Btu/h\,ft^2$

$q_{sweat,req}$: Required sweat evaporation rate for optimal comfort conditions, $Btu/h\,ft^2$

The rate metabolic heat generation ($q_{met,heat}$), the difference between the metabolic heat generation and that converted to work (e.g., working, walking, or running), is given as follows:

$$q_{met,heat} = M - \dot{w} \qquad \text{(Eq. 3-36)}$$

Where,

M : Rate of metabolic generation per unit DuBois surface area, $Btu/h\ ft^2$

$\dot{w}$: Human work per unit DuBois surface area, $Btu/h\ ft^2$

According to Fanger's comfort analysis [107], PMV is mainly defined as a function of six variables: air temperature, mean radiant temperature, air velocity, air humidity, clothing resistance, and activity level. It is the index that represents the average response of a large number of people. The correlation between PMV and thermal load is defined as follows:

$$PMV = 3.155(0.303e^{-0.114M} + 0.028)L \qquad \text{(Eq. 3-37)}$$

Where,

PMV : Predicted mean vote

L : Thermal load, $Btu/h\ ft^2$

Given the optimal comfort conditions, the thermal load, L, is defined as the difference between the rate of metabolic heat generation and the calculated heat loss from the body to the actual environmental conditions. The thermal load, L, is given as:

$$\begin{aligned} L = {} & q_{met,heat} - f_{cl}h_c\,(T_{cl} - T_a) - f_{cl}h_r\,(T_{cl} - T_r) \\ & - 156\big(W_{sk,req} - W_a\big) \\ & - 0.42\big(q_{met,heat} - 18.43\big) \\ & - 0.00077M(93.2 - T_a) - 2.78M(0.0365 \\ & - W_a) \end{aligned} \qquad \text{(Eq. 3-38)}$$

Where,

f_{cl} : Ratio of clothed surface area to DuBois surface area A_{cl}/A_D

h_c : Convection heat transfer coefficient, $Btu/h\ ft^2$°F

T_{cl} : Average surface temperature of clothed body, °F

T_a : Air temperature, °F

h_r : Radiative heat transfer coefficient, $Btu/h\ ft^2$°F

T_r : Mean radiant temperature, °F

$W_{sk,req}$: Required saturated humidity ratio at the skin temperature

W_a : Air humidity ratio

In Eq. 3-39, the clothing temperature cannot be obtained directly, however it can be calculated as follows:

$$T_{cl} = \frac{T_{sk,req} + R_{cl}f_{cl}(h_cT_a + h_rT_r)}{1 + R_{cl}f_{cl}(h_c + h_r)} \qquad \text{(Eq. 3-39)}$$

Where,

R_{cl} : Effective thermal resistance (R-value) of clothing, ft^2°F h/Btu

The other three parameters: $f_{cl}, h_c, and\ h_r$ can be approximated as:

$$f_{cl} = \begin{cases} 1.00 + 0.2I_{cl} & I_{cl} < 0.5\ clo \\ 1.05 + 0.1I_{cl} & I_{cl} > 0.5\ clo \end{cases} \quad \text{(Eq. 3-40)}$$

$$h_c = max\begin{cases} 0.361(T_{cl} - T_a)^{0.25} \\ 0.151\sqrt{V} \end{cases} \quad \text{(Eq. 3-41)}$$

$$h_r = 0.7\ Btu/h\ ft^2\text{°F} \quad \text{(Eq. 3-42)}$$

Regarding the ASHRAE standard 55-2013 "Thermal Environment Conditions for Human Occupancy" [106], the ASHRAE comfort zone, generated by [107] and shown in Fig. 3-28, is used to represent the suitable thermal comfort inside a building based on the PMV values between -0.5 and +0.5 given the metabolic rate at 1.1 met and the clothing level at 0.5 clo (typical summer indoor). This ASHRAE comfort zone representation can be used to determine a thermostat cooling temperature set point that produces thermal environment conditions acceptable to the majority of occupants in a building.

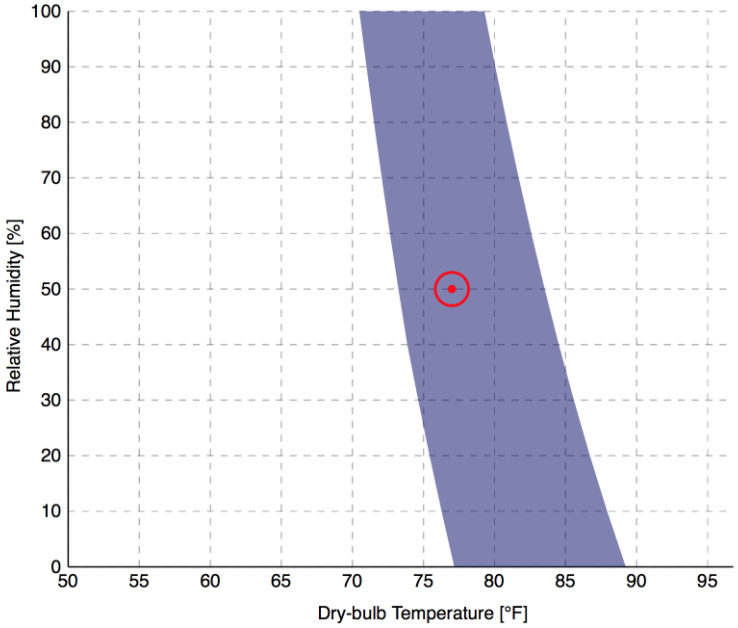

Fig. 3-28. ASHRAE 55-2013 temperature – relative humidity chart

Furthermore, as PMV is the average response of a large number of group of people, the empirical relationship between the percentage of people dissatisfied (PPD, %) with a thermal environment as a function of the PMV, shown in Fig. 3-29, is given as:

$$PPD = 100 - 95e^{-0.03353PMV^4 - 0.2179PMV^2} \quad \text{(Eq. 3-43)}$$

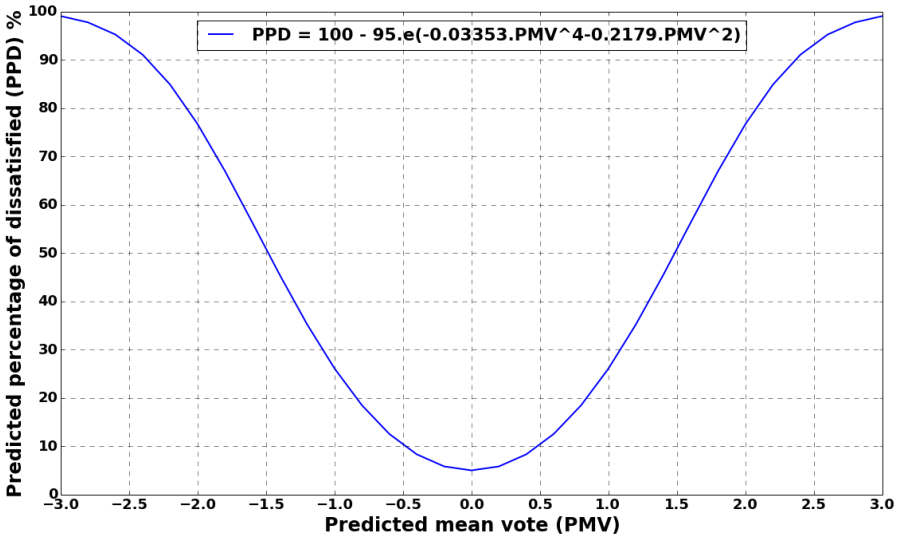

Fig. 3-29. Relationship between PPD and PMV

Lighting load comfort conditions: According to the Illuminating Engineering Society of North America (IESNA) standard 90.1-2007 [108], the illuminance recommendations (lux) for lighting levels within each building space is given in Table 3-10.

Table 3-10. IESNA recommended illumination levels for building spaces

Building Type	Space Type	Maintained Average Illuminance at working level (lux)	Measurement (working) Height (1 meter = 3.3 feet)
Educational Buildings	Play room, nursery, classroom	400	at 0.0 m
	Lecture hall	400	at 0.8 m
	Computer practice rooms	30	at 0.8 m
	Classrooms	300	at 0.8 m
Office Buildings	Single offices	300	at 0.8 m
	Open plan offices	400	at 0.8 m
	Conference rooms	300	at 0.8 m
Hospitals	General ward lighting	300	at 0.8 m
	Simple examination	500	at 0.8 m
	Examination and treatment	1000	at 0.8 m
Hotel and restaurants	Self-service restaurant, dining room	100	at 0.8 m
	Kitchen	500	at 0.8 m
	Buffet	100	at 0.8 m
Sport facilities	Sport halls	300	at 0.0 m
Wholesale and retail sales	Sales area	500	at 0.8 m
	Till area	500	at 0.8 m
Circulation areas	Corridor	50	at 0.0 m
	Stairs	50	at 0.0 m
	Restrooms	300	at 0.0 m
	Cloakrooms. washrooms, bathrooms, toilets	300	at 0.8 m

Plug load comfort conditions: Building administrator and tenant can assign priorities to their plug loads (e.g., desktop computers, printers, coffee machines, etc.) according to their need.

Subtask 2: Explore energy/power savings opportunity of an HVAC system

Fig. 3-30 illustrates essential components of a typical HVAC system, which includes a compressor, a condenser, an expansion device, and an evaporator.

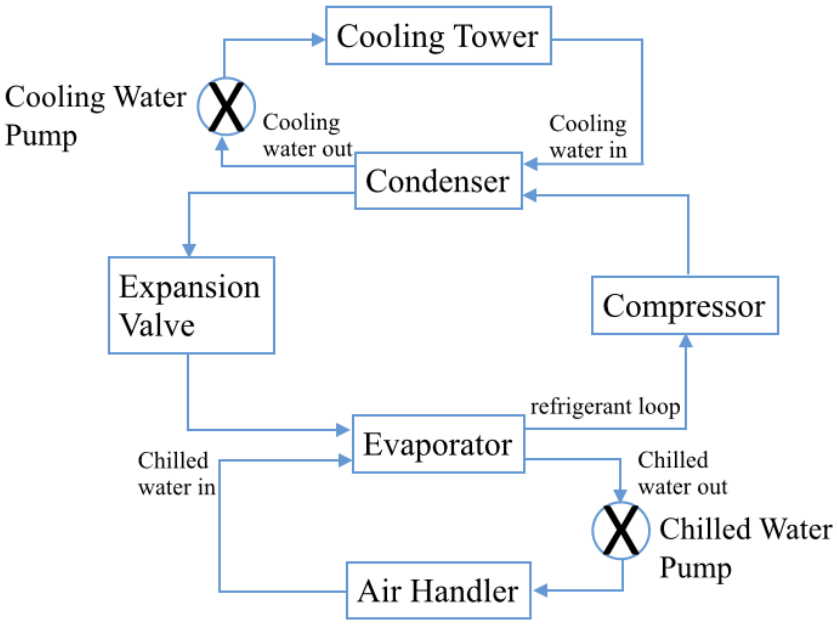

Fig. 3-30. HVAC system

Power demand of a compact HVAC system (rooftop terminal unit, RTU) is given as:

$$P_{RTU} = P_{CHWP} + P_{COMP} + P_{CWP} + P_{CTF} + P_{AHU} \quad \text{(Eq. 3-44)}$$

Where,

P_{RTU} : Instantaneous power demand of RTU (W)
P_{CHWP} : Instantaneous power demand of a chilled water pump (W)
P_{COMP} : Instantaneous power demand of a compressor (W)
P_{CHWP} : Instantaneous power demand of a cooling water pump (W)
P_{CTF} : Instantaneous power demand of a cooling tower fan (W)
P_{AHU} : Instantaneous power demand of an air-handling unit (W)

In order to reduce power demand and energy consumption of RTU, technically, there are five strategies as follows:

1. Change a cooling/heating set point
2. Control a damper position
3. Change a supply air fan speed according to ventilation requirement (e.g., CO_2 limit)
4. Use temperature sensor(s) to improve the accuracy of space temperature measurement and use occupancy/presence sensor(s) to adjust a thermostat temperature set point or mode
5. Change a thermostat fan mode

Even though power demand/energy saving opportunities for each of the proposed strategies are known and identified, the explicit calculation of power demand reduction for each action taken is difficult to obtain. This is due to heat gain and heat loss in a building or a specific zone depending on many factors, such as the heat gain from lighting equipment, building equipment, building occupants, etc., as well as heat gain and loss through building envelope. Therefore, taken into account the mentioned hurdle, in this study, the power demand reduction of each performed action can be estimated by using the parameter estimation technique to find the estimated power demand of RTU after an action (e.g., increase a thermostat cooling temperature set point) is taken.

In order to reduce the power demand of RTU, the low-hanging fruit action is to increase a thermostat cooling set point. To find the power demand reduction, the prerequisite is to find the electrical and thermal coupling characteristic of RTU to determine the steady-state power demand of RTU after the thermostat cooling set point has been increased. This study proposes the mathematical model representation of a relationship between a cooling temperature set point and a power demand of RTU as follows:

$$T\frac{dP_d(t)}{dt} + P_d(t) = P_s(\phi) + T\frac{dP_t(\phi)}{dt} \qquad \text{(Eq. 3-45)}$$

$$P_s(\phi) = P_0\left(\frac{\phi(t-t_c)}{\phi_0}\right)^{\beta_s} \qquad \text{(Eq. 3-46)}$$

$$P_t(\phi) = P_0\left(\frac{\phi(t-t_c)}{\phi_0}\right)^{\beta_t} \qquad \text{(Eq. 3-47)}$$

$$P_d(t) = P_s(\phi) + (P_t(\phi) - P_s(\phi))e^{-(t-t_c)/T} \qquad \text{(Eq. 3-48)}$$

Where,

- T : dynamic load time constant
- P_d : dynamic load function
- P_s : static load model
- P_t : transient load model
- P_0 : initial real power value
- ϕ : new thermostat cooling temperature set point
- ϕ_0 : previous thermostat cooling temperature set point
- t : time
- t_c : time delay between temperature change and response
- β_s : static load model exponential index
- β_t : transient load model exponential index

The goal of this mathematical model representation, Eq. 3-45 – Eq. 3-48, is to find a steady-state power demand of RTU (P_s) after a thermostat cooling temperature set point is changed from ϕ_0 to ϕ. Using curve fitting and parameter estimation algorithms with the objective function shown in Eq. 3-49, parameters: β_s, β_t, T, P_d, P_s, and P_t can be estimated.

$$min \sum_{i=1}^{M} (P_d(i) - P_m(i))^2 \qquad \text{(Eq. 3-49)}$$

Where,

P_d : parameter to be estimated
P_m : corresponding value of a parameter P_d based on its model
M : total number of training samples

The desired results of this step is to obtain the model that can predict:

1. The amount of power demand reduction or increment when a thermostat cooling temperature set point is raised or lowered.
2. The rate of a room temperature rises when a compressor is not working, i.e., the building thermal response when an RTU does not operate (BT_{nop})
3. The rate of a room temperature drops when a compressor is working, i.e., the building thermal response when an RTU is in operation (BT_{op})
4. The impact of occupancy level, i.e., number of people inside a room, a zone, or a building, to BT_{nop} and BT_{op}.

Eq. 3-45 - Eq. 3-49 can be simplified such that these desired results are obtained by estimating building thermal responses both when an RTU is in operation and when an RTU does not operate. The electrical and thermal coupling characteristic of RTU is then modeled based on these constants.

The thermal response of a building when an RTU does not operate (BT_{nop}) is estimated by keeping the thermostat cooling setpoint higher than the room temperature. Then, the room temperature will rise over time depending upon heat gain and heat loss through building envelope, lighting equipment, building equipment, and building occupants, etc. The amount of power demand reduction, the duration for a room temperature to increase to a new cooling setpoint, and the duration for the power demand of an RTU to descend to a new steady-state are predicted based on the estimated building thermal response.

The thermal response of a building when an RTU is in operation (BT_{op}) is estimated by keeping the cooling setpoint lower than the room temperature. Then, the room temperature will descend over time depending upon heat gain and heat loss through building envelope, lighting equipment, building equipment, and building occupants, etc. The amount of power demand increment, the duration for a room temperature to decrease to a new cooling setpoint, and the duration for the power demand of an RTU to ascend to a new steady-state are predicted based on the estimated building thermal response.

Empirically, the relationship between cooling setpoint and room temperature over time to evaluate building's thermal responses (BT: BT_{nop}, BT_{op}) as a function of an average outdoor temperature can be represented by the linear regression model as follows:

$$BT = \theta_{0bto} + \theta_{1bto} \cdot T_{outdoor,avg} \qquad \text{(Eq. 3-50)}$$

Where,

$T_{outdoor,avg}$: average outdoor temperature during 12:00 pm to 6:00 pm (°F)

BT : building thermal response (BT_{nop} or BT_{op})

$\theta_{0bto}, \theta_{1bto}$: learning parameters of the linear regression model between building thermal response and an average outdoor temperature

Hypothesis:

$$H_\theta(x) = \theta_0 + \theta_1 \cdot x \qquad \text{(Eq. 3-51)}$$

Parameters: $\theta_0,\ \theta_1$

Cost function:

$$J(\theta_0, \theta_1) = \frac{1}{2m}\sum_{i=1}^{m}(h_\theta(x^{(i)}) - y^{(i)})^2 \qquad \text{(Eq. 3-52)}$$

Goal:

$$min_{\theta_0,\theta_1}\, J(\theta_0, \theta_1) \qquad \text{(Eq. 3-53)}$$

Where,

m : a number training examples obtained from measurement of a room temperature

$J(\theta_0, \theta_1)$: cost function calculated from $\theta_0,\ \theta_1$

$h_\theta(x^{(i)})$: hypothesis of parameter x in an i-th iteration

$y^{(i)}$: actual value of parameter to be estimated in i-th iteration

Typically, the cost function $J(\theta_0,\ \theta_1)$ given in Eq. 3-52 is a convex function, therefore the optimization problem defined in Eq. 3-53 can be solved by using the gradient descent algorithm. The steps of finding $min_{\theta_0,\theta_1}\, J(\theta_0,\ \theta_1)$ are explained as follows.

Step 1: Start with initial values of $\theta_0,\ \theta_1$

Step 2: Change values of $\theta_0,\ \theta_1$ to reduce $J(\theta_0,\ \theta_1)$ by simultaneously update $\theta_0,\ \theta_1$ as:

$$\theta_j := \theta_j - \alpha\frac{\partial J(\theta_0,\theta_1)}{\partial \theta_j}, \text{ for j = 0 and j = 1} \qquad \text{(Eq. 3-54)}$$

Where,

α : learning rate

Step 3: Iteratively change $\theta_0,\ \theta_1$ until:

$$J(\theta_0,\ \theta_1)_{i-1} - J(\theta_0,\ \theta_1)_i \le \varepsilon \qquad \text{(Eq. 3-55)}$$

Where,

$J(\theta_0,\ \theta_1)_{i-1}$: cost function calculated from $\theta_0,\ \theta_1$ in the previous iteration

$J(\theta_0,\ \theta_1)_i$: cost function calculated from $\theta_0,\ \theta_1$ in this iteration

ε : gradient descent stopping criteria

The same technique can be applied to find the power demand reduction of an RTU in the case that another control action (e.g., change damper position) is taken.

Nonetheless, there is another factor that can impact the obtained building thermal response both BT_{nop}, BT_{op} which is an occupancy level of a room or a zone. Since people generally generate heat (both sensible and latent) to the environment they inhabit, if there is a variation on a number of people inside a room or a zone, it can significantly impact the values of the BT_{nop}, BT_{op} [109]. Therefore, these values have to be adjusted accordingly based on the occupancy level with the following factors to consider.

1. Zone type designation: This depends on structure, room location, and furnishing ASHRAE defines four zone types (A, B, C, and D) to quantify heat storage effect based on their heat gain and heat loss characteristics, as shown in Table 3-11.
2. Occupant activity level: sensible heat generation (SHG_p) and latent heat generation (LHG_p) of each person based on their activity inside a space are shown in Table 3-12.
3. Occupancy density: estimated number of people inside a space can be calculated as shown in Table 3-13. Cooling load factor adjustment (CLF_p): since heat storage effect can substantially reduce sensible cooling load, sensible heat gain of a space is reduced by this factor. Table 3-14 shows CLF_p taken into account a total hours that people are in a space, a total hours after people entering a space, and a zone type designation.

Thus, taking into account number of people in a space, the BT_{nop} and BT_{op} are adjusted due to sensible heat gain and latent heat gain from people, following the equations below:

$$q_{p-sen} = N \times SHG_p \times CLF_p \quad \text{(Eq. 3-56)}$$

$$q_{p-lat} = N \times LHG_p \quad \text{(Eq. 3-57)}$$

$$BT_{nop,p} = \frac{(RTU_{cooling-cap} + q_{p-sen} + q_{p-lat})}{RTU_{cooling-cap}} \cdot BT_{nop} \quad \text{(Eq. 3-58)}$$

$$BT_{op,p} = \frac{(RTU_{cooling-cap} - q_{p-sen} - q_{\square-lat})}{RTU_{cooling-cap}} \cdot BT_{op} \quad \text{(Eq. 3-59)}$$

Where,

q_{p-sen} : sensible heat gain from people (Btu/hr)
q_{p-lat} : latent heat gain from people (Btu/hr)
N : number of people
SHG_p : sensible heat generation from each person ($Btu/hr \cdot per$)
LHG_p : latent heat generation from each person ($Btu/hr \cdot per$)
CLF_p : cooling load factor adjustment
$RTU_{cooling-cap}$: cooling capacity of a RTU (Btu)

Table 3-11. Zone types – interior rooms

Zone Parameters				Zone Type
Room location	Middle Floor	Ceiling Type	Floor Covering	People and Equipment
Single story	N/A	N/A	Carpet	C
	N/A	N/A	Vinyl	D
Top floor	2.5 in. Conc.	With	Carpet	D
	2.5 in. Conc.	With	Vinyl	D
	2.5 in. Conc.	Without	*	D
	1.0 in. Wood	*	*	D
Bottom floor	2.5 in. Conc.	With	Carpet	D
	2.5 in. Conc.	*	Vinyl	D
	2.5 in. Conc.	Without	Carpet	D
	1.0 in. Wood	*	Carpet	D
	1.0 in. Wood	*	Vinyl	D
Midfloor	2.5 in. Conc.	N/A	Carpet	D
	2.5 in. Conc.	N/A	Vinyl	D
	1.0 in. Wood	N/A	*	C

* The effect of inside shade is negligible in this case

Table 3-12. Heat gain from occupants in conditioned spaces

Activity	Sensible Heat $(Btu/hr \cdot per)$	Latent Heat $(Btu/hr \cdot per)$
Seated at theater	225	105
Seated, very light work	245	155
Moderately active office work	250	200
Standing, light work (retail store)	250	200
Light bench work (factory)	275	475
Walking, 3 mph (factory)	375	625
Bowling	580	870
Heavy machine work, lifting	635	965
Athletics, gymnasium	710	1090

Table 3-13. Typical occupancy density ranges

Building type	$ft^2/Person$
Office	100 to 200
Educational	100 to 175
Medical treatment	50 to 100
Assembly	15 to 20
Restaurant	20 to 30
Retail	30 to 75
Warehouse	500 to 1000
Apartment house	300 to 500
Single-family house	500 to 1000

Table 3-14. Sensible heat cooling and load factors for people and unhooded equipment (CLF_p)

Total Hours People Are in Space	Hours after people enter space or equipment turned on									
	1	2	3	4	5	6	7	8	9	10
Zone Type A										
8	0.75	0.88	0.93	0.95	0.97	0.97	0.98	0.98	0.24	0.11
10	0.75	0.88	0.93	0.95	0.97	0.97	0.98	0.98	0.99	0.99
Zone Type B										
8	0.65	0.75	0.81	0.85	0.89	0.91	0.93	0.95	0.31	0.22
10	0.65	0.75	0.81	0.85	0.89	0.91	0.93	0.95	0.96	0.97
Zone Type C										
8	0.61	0.69	0.75	0.79	0.83	0.86	0.89	0.91	0.32	0.26
10	0.62	0.70	0.75	0.80	0.83	0.86	0.89	0.91	0.92	0.94
Zone Type D										
8	0.62	0.69	0.74	0.77	0.80	0.83	0.85	0.87	0.30	0.24
10	0.63	0.70	0.75	0.78	0.81	0.84	0.86	0.88	0.89	0.91

Subtask 3: Explore energy/power savings opportunity of lighting loads

In order to reduce power demand and energy consumption of lighting loads, a mathematical model is devised that can predict:

- The amount of power demand reduction or increment when the brightness of lighting loads decreases or increases.
- The relationship between the illuminance and the brightness level

The relationship between the power demand and the brightness level of a lighting load is given as:

$$P_{Lighting\ load} = \theta_0 + \theta_1 \cdot Bri_{\%} \qquad \text{(Eq. 3-60)}$$

Where,

$P_{Lighting\ load}$: instantaneous power demand of a lighting load (W)
θ_0, θ_1 : estimated parameters of linear regressing model of $P_{Lighting\ load}$
$Bri_{\%}$: brightness level of a fluorescent or LED lamp (range from 0% - 100%)

Empirically, the relationship between illuminance and brightness level can also be represented as a linear function given as:

$$Illumiance = \theta_0 + \theta_1 \cdot Bri_{\%} \qquad \text{(Eq. 3-61)}$$

Where,

$Illuminance$: illuminance measured at 0.8 meter from the height off the floor (lux)
θ_0, θ_1 : estimated parameters of the linear regressing model between illuminance and the brightness level
$Bri_{\%}$: brightness level of a fluorescent or LED lamp (range from 0% - 100%)

Technically, the brightness (%) of fluorescent or LED lighting load depends on the voltage applied to it. Therefore, the relationship between the power demand of a lighting load and its brightness as well as the relationship between the illuminance of a building space and a corresponding light brightness level can be empirically represented by the linear regression model, as follows.

Hypothesis:

$$H_\theta(x) = \theta_0 + \theta_1 \cdot x \qquad \text{(Eq. 3-62)}$$

Parameters: $\theta_0,\ \theta_1$

Cost function:

$$J(\theta_0, \theta_1) = \frac{1}{2m}\sum_{i=1}^{m}(h_\theta(x^{(i)}) - y^{(i)})^2 \qquad \text{(Eq. 3-63)}$$

Goal:

$$min_{\theta_0,\theta_1}\, J(\theta_0, \theta_1) \qquad \text{(Eq. 3-64)}$$

Where,

x : $Bri_{\%}$

m : number of training samples from measurements

$J(\theta_0, \theta_1)$: cost function calculated from $\theta_0,\ \theta_1$

$h_\theta(x^{(i)})$: hypothesis of parameter x in an i-th iteration

$y^{(i)}$: actual value of parameter to be estimated in i-th iteration

Typically, the cost function $J(\theta_0,\ \theta_1)$ given in Eq. 3-63 is a convex function, therefore the optimization problem defined in Eq. 3-64 can be solved using the gradient descent algorithm. The steps of finding $min_{\theta_0,\theta_1}\, J(\theta_0,\ \theta_1)$ are explained as follows.

Step 1: Start with initial values of $\theta_0,\ \theta_1$

Step 2: Change values of $\theta_0,\ \theta_1$ to reduce $J(\theta_0,\ \theta_1)$ by simultaneously update $\theta_0,\ \theta_1$ as:

$$\theta_j := \theta_j - \alpha\frac{\partial J(\theta_0,\theta_1)}{\partial \theta_j}, \text{ for j = 0 and j = 1} \qquad \text{(Eq. 3-65)}$$

Where,

α : learning rate

Step 3: Iteratively change $\theta_0,\ \theta_1$ until:

$$J(\theta_0,\ \theta_1)_{i-1} - J(\theta_0,\ \theta_1)_i \le \varepsilon \qquad \text{(Eq. 3-66)}$$

Where,

$J(\theta_0,\ \theta_1)_{i-1}$: cost function calculated from $\theta_0,\ \theta_1$ in the previous iteration

$J(\theta_0,\ \theta_1)_i$: cost function calculated from $\theta_0,\ \theta_1$ in this iteration
ε : gradient descent stopping criteria

There are four strategies used to reduce energy consumption and power demand of a lighting load as follows:

1. Dimming control: change supply voltage to dim lighting loads
2. Daylight control: use illuminance measurements from ambient light sensor(s) to measure adjust lighting loads
3. Occupancy control: use occupancy/presence sensor(s) to turn on/off or dim lighting loads
4. Time-scheduled control: schedule time to turn on/off or dim lighting loads

The power demand reduction resulting from performing these actions can be obtained from the proposed linear regression model, which can be solved using the gradient descent technique as elaborated above.

Subtask 4: Explore energy/power savings opportunity of plug loads

Power demand of a plug load is given as:

$$P_{plug\ load} = S_{plug\ load} \cdot P_{appliance} \qquad \text{(Eq. 3-67)}$$

Where,

$P_{plug\ load}$: power demand of a plug load (W)
$S_{plug\ load}$: status (on/off) of a plug load
$P_{appliance}$: power demand of a corresponding appliance (W)

A plug load controller can be used to turn on or off appliances/devices based on their assigned priority (critical or non-critical) given by a building administrator and tenants. $P_{Plug\ load}$ of specific equipment, device, or appliance can be obtained from its corresponding appliance's rating or directly from measurement.

3.5.3 The Proposed DR algorithm to help improving efficiency of a power grid operation in response to a Critical Peak Pricing (CPP) signal at a building level

In this section the DR algorithm for load control in buildings with respect to a CPP signal is devised to help improving efficiency of a power grid operation. Typically, a CPP event notification is sent one day in advance of a scheduled event. The triggers of a CPP event are, for example, day-ahead load or price forecast, forecast of extreme or unusual temperature conditions, and a system emergency of a utility of ISO. The proposed DR algorithm is devised such that the CPP event is separated into three sequential stages so that agents can perform proper optimizations in each stage. Those stages are a pre-CPP stage, a CPP event stage, and a post-CPP stage.

A. The Overall Goals for DR Implementation at a Building Level

A demand response agent (DRA) acts as a gateway between a building and an openADR server that communicates through a cloud service. After receiving a CPP signal from an

OpenADR agent, a DRA pursues the system's overall goals by coordinating with control agents: thermostat agent (TA), lighting load agent (LLA), plug load agent (PLA) to control and adjust devices' settings given knowledge on devices and building's environment from sensor agents: power meter agent (PMA), multi-sensor agent (MTA), motion sensor agent (MSA), and weather sensor agent (WSA). The overall systems goals for DR implementation of a CPP event are elaborated as follows:

1) To minimize the building's total energy consumption ($E_{total,B}$) and power demand (P_B) during a CPP event

$$\min (E_{total,B}) = \min(\int_{t_{CPP\ start}}^{t_{CPP\ end}} P_B\, dt) \quad \text{(Eq. 3-68)}$$

$$P_B = \sum_{i=1}^{N_{RTUs}} P_{RTU.i} + \sum_{i=1}^{N_{Lighting\ loads}} P_{Lighting\ load.i} + \sum_{i=1}^{N_{Plug\ loads}} P_{Plug\ load.i} \quad \text{(Eq. 3-69)}$$

Where,

P_B : total instantaneous power demand of a building (W)
$t_{CPP\ start}$: start time of a CPP event
$t_{CPP\ end}$: time that a CPP event ends
$P_{RTU.i}$: power demand of RTU unit i (W)
$P_{Lighting\ load.i}$: power demand of a lighting load unit i (W)
$P_{Plug\ load.i}$: power demand of a plug load unit i (W)
N_{RTUs} : total number of installed RTUs in a building
$N_{Lighting\ loads}$: total number of installed lighting loads in a building
$N_{Plug\ loads}$: total number of installed plug loads in a building

2) To minimize occupants' comfort violation index (CVI)

$$\begin{aligned} min\ (CVI) = min\ [& \sum_{i=1}^{N_{zones}} \Big(\int_{t_{pre-CPP,start}}^{t_{post-CPP,end}} max\Big(\big[|PMV_{i,t}| - |PMV_{PPD=10\%}|\big], 0\Big) dt \\ & + \sum_{i=1}^{N_{zones}} \int_{t_{pre-CPP,start}}^{t_{post-CPP,end}} \max\Big[\Big(\frac{\mathrm{CO_2}_{i,t} - \mathrm{CO_2}_{std-upper}}{\mathrm{CO_2}_{std-upper}}\Big), 0\Big]\, dt \\ & + \sum_{i=1}^{N_{zones}} \int_{t_{pre-CPP,start}}^{t_{post-CPP,end}} \max\Big[\Big(\frac{\mathrm{illuminance}_{\mathrm{std-lower}} - \mathrm{illuminance}_{\mathrm{i,t}}}{\mathrm{illuminance}_{\mathrm{lower}}}\Big), 0\Big] dt \\ & + \sum_{i=1}^{N_{crit-loads}} \int_{t_{pre-CPP,start}}^{t_{post-CPP,end}} \big(|status_{crit-load,norm} - status_{crit-load,i,t}|\big) dt \Big] \end{aligned} \quad \text{(Eq. 3-70)}$$

Where,

CVI : comfort violation index
N_{zones} : total number of zones in a building
$t_{pre-CPP,start}$: start time of a pre-CPP period

$t_{post-CPP,end}$: end time of a post-CPP period
$\mathrm{PMV_{i,t}}$: Predicted mean vote value of a zone i
$\mathrm{PMV_{PPD=10\%}}$: Predicted mean vote value that corresponds to 10% in PPD
PPD : Percentage of people dissatisfied (%)
$\mathrm{CO_2}_{i,t}$: level of $\mathrm{CO_2}$ concentration in a zone i (ppm)
$\mathrm{CO_2}_{std-upper}$: upper level of $\mathrm{CO_2}$ concentration in a building (ppm)
$\mathrm{illuminance_{std-lower}}$: lower limit of illuminance for lighting based on a building type and a zone type according to the IESNA standard 90.1-2007 [109] (lux)
$\mathrm{illuminance_{i,t}}$: level of illuminance in lux for lighting in a zone i (lux)
$status_{crit-load,norm}$: status of a critical-load during a normal condition ("on":1, "off":0)
$status_{crit-load,i}$: status of a critical-load i ("ON":1, "OFF":0)

3) To minimize demand restrike that will impose on the building's power demand after a CPP event ends

During a CPP event, a demand restrike of a building (DRK_B) is calculated as shown in Eq. 3-71. Technically, DRK_B estimates the rebound potential of the power demand of a buiding resulting from DR implementation during a CPP event where some devices are not able to run or partially run. After a CPP event, if all of those devices start to run at the same time, an overly increase of power demand (so called a demand restrike) can inevitably happen.

$$min(DRK_B) = min \int_{t_{CPP,end}}^{t_{post-CPP,end}} \max[\left(P_{B,t} - \max(P_{B,hist})\right), 0]dt \quad \text{(Eq. 3-71)}$$

$$P_{building} = \sum_{i=1}^{N_{RTUs}} P_{RTU.i} + \sum_{i=1}^{N_{Lighting\ loads}} P_{Lighting\ load.i} + \sum_{i=1}^{N_{Plug\ loads}} P_{Plug\ load.i} \quad \text{(Eq. 3-72)}$$

$$P_{RTU,i} = P_{RTU,op,i} \quad \text{(Eq. 3-73)}$$

$$P_{Lighting\ load,i} = \theta_0 + \theta_1 \cdot Bri_{\%,post-cpp,i} \quad \text{(Eq. 3-74)}$$

$$P_{Plug\ load,i} = (status_{plug\ load,post-CPP,i} - status_{plug\ load,CPP,i} \cdot P_{appliance,i} \quad \text{(Eq. 3-75)}$$

Where,
DRK_B : demand restrike of a building (W)
$P_{B,hist}$: historical power demand of a building in a normal condition (W)
$P_{RTU,op,i}$: power demand of an RTU unit i when it is operating (W)
$P_{appliance,i}$: rated power demand of an appliance unit i (W)

$Bri_{\%,-CPP,i}$: brightness level of a lighting load in % after a CPP event (%)

$status_{plug\ load,post-CPP,i}$: status of a plugload i after a CPP event (W)

$status_{plug\ load,CPP,i}$: status of a plugload i during a CPP event (W)

4) To minimize time to start restore ($t_{restore}$) and time taken to restore ($T_{restore}$) all settings back to a normal condition in the post-CPP stage

$$\min(t_{restore}) = \sum_{i=1}^{N_{RTUs}} t_{restore,RTU.i} + \sum_{i=1}^{N_{Lighting\ loads}} t_{restore,Lighting\ load.i} + \sum_{i=1}^{N_{Plug\ loads}} t_{restore,Plug\ load.i} \quad \text{(Eq. 3-76)}$$

$$\min(T_{restore}) = \sum_{i=1}^{N_{RTUs}} T_{restore,RTU.i} + \sum_{i=1}^{N_{Lighting\ loads}} T_{restore,Lighting\ load.i} + \sum_{i=1}^{N_{Plug\ loads}} T_{restore,Plug\ load.i} \quad \text{(Eq. 3-77)}$$

Where,

$t_{restore}$: time taken by all control agents to start to change all devices' settings back to their normal conditions

$t_{restore,RTU}$: time taken by a TA to start to restore a RTU setting back to normal condition

$t_{restore,lighting\ load}$: time taken by a LLA to start to restore a lighting load setting back to normal condition

$t_{restore,plug\ load}$: time taken by a PLA to start to restore a non-critical plug load setting back to normal condition

$T_{restore}$: time taken by all control agents to finish restoring all devices' settings and building's environment back to their normal conditions

$T_{restore,RTU}$: time taken by a TA to finish restoring a RTU setting and bring a room comfort (i.e. room temperature, CO_2 level) back to normal condition

$T_{restore,lighting\ load}$: time taken by a LLA finish restoring a lighting load setting and bring a room illuminance to normal condition

$T_{restore,plug\ load}$: time taken by a PLA to finish restoring a non-critical plug load status back to normal condition

At the end of a CPP event, after a DRK_B is evaluated, actions to mitigate the potential impact of DRK_B and minimize time taken to restore devices' settings and room comfort condition are to be taken by the DRA in coordination with control agents and sensor agents. In addition, taking comfort constraints into account, the main criteria to select an action to be performed is to give higher priority to the action that mitigates comfort violation; while giving lower priority to the action that does not lead to a reduction in comfort violation.

In order to achieve the desired objectives above, there are three sequential stages to implement the proposed DR algorithm for CPP: pre-CPP stage, CPP stage, and post-CPP stage, shown in Fig. 3-31.

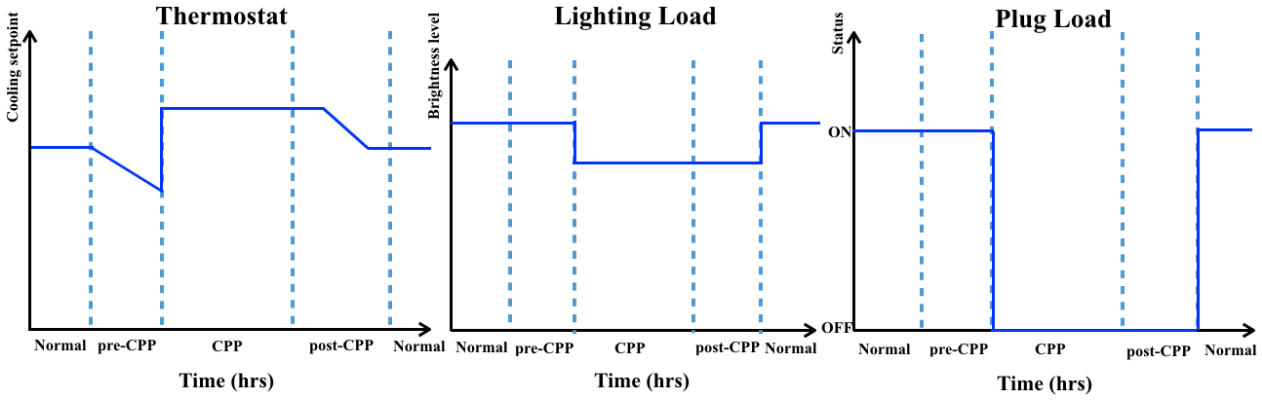

Fig. 3-31. Three sequential stages to implement the proposed DR algorithm

B. A day before a CPP event

Fig. 3-32 illustrates the sequence diagram of the proposed agents the day before a CPP event. As shown, an electric utility sends a notification given a date and time of a CPP event one day in advance to an OpenADR agent via a http webhook (push API call). An OpenADR agent, then, requests a demand response agent (DRA) to help reduce power and energy demand of a building during a CPP event using the FIPA Request-When protocol. An OpenADR agent sends a message with "request-when" performative to a DRA specifying the condition of date and time that a CPP event is true. A DRA, representing a building operator, replies back to the OpenADR whether it can participate in a CPP event by sending a message with "agree" or "refuse" performative. Subsequently, a DRA sends messages with "request-when" performative using FIPA Request-When protocol to other control agents. This is to notify and check which agents are available to participate in a CPP event. An agent wishing to participate in a CPP event sends back a message with "agree" performative. Otherwise, an agent sends back a message with "refuse" performative.

C. Normal stage before a pre-CPP stage

Fig. 3-33 shows the sequence diagram of the agents during a normal stage prior to a pre-CPP stage. In this stage, three hours before an estimated pre-CPP stage of each control agents, a DRA sends a message with "request" performative using FIPA Request Protocol to all control agents that have previously "agree" to participate in a CPP event. This is to recheck that those agents are still available to perform actions based on the proposed DR algorithm.

D. Pre-CPP stage

In this stage, as shown in Fig. 3-34, the proposed agents select optimal actions to achieve the objectives mentioned in the previous section. Actions of each agent action are elaborated below:

D.1 Demand Response Agent (DRA):

A DRA coordinates with control agents (thermostat agent: TA, lighting load agent: LLA, and plug-load agent PLA) given the knowledge on devices' status and building environment through sensor agents (power meter agent: PMA, multi-sensor agent: MTA, weather sensor agent: WSA, and motion sensor agent: MSA) as shown in Fig. 3-39. Its main goal is to shift building's electricity consumption to the period prior to the start of a CPP event. This allows the building's power demand and energy consumption during the CPP event to be minimized while the occupant comfort is not violated or less violated as possible.

D.2 Thermostat Agent (TA):

Thermal load during a CPP event can be shifted to the pre-CPP stage by performing the pre-cooling action. By lowering the cooling temperature set point, cooling capacity from the pre-CPP stage can be carried over to the CPP period. Thus, there is less need for an RTU to operate during a CPP event in order to maintain indoor air temperature within the specified comfort range as defined in [106]. In this study, there are two parameters that determine control actions of a TA: temperature set point (°F), and fan status (ON/OFF).

To help the DRA to achieve its first goal to minimize power demand (P_B) and total energy consumption ($E_{total,B}$) of a building during a CPP event, a TA will take the following action during the pre-CPP stage.

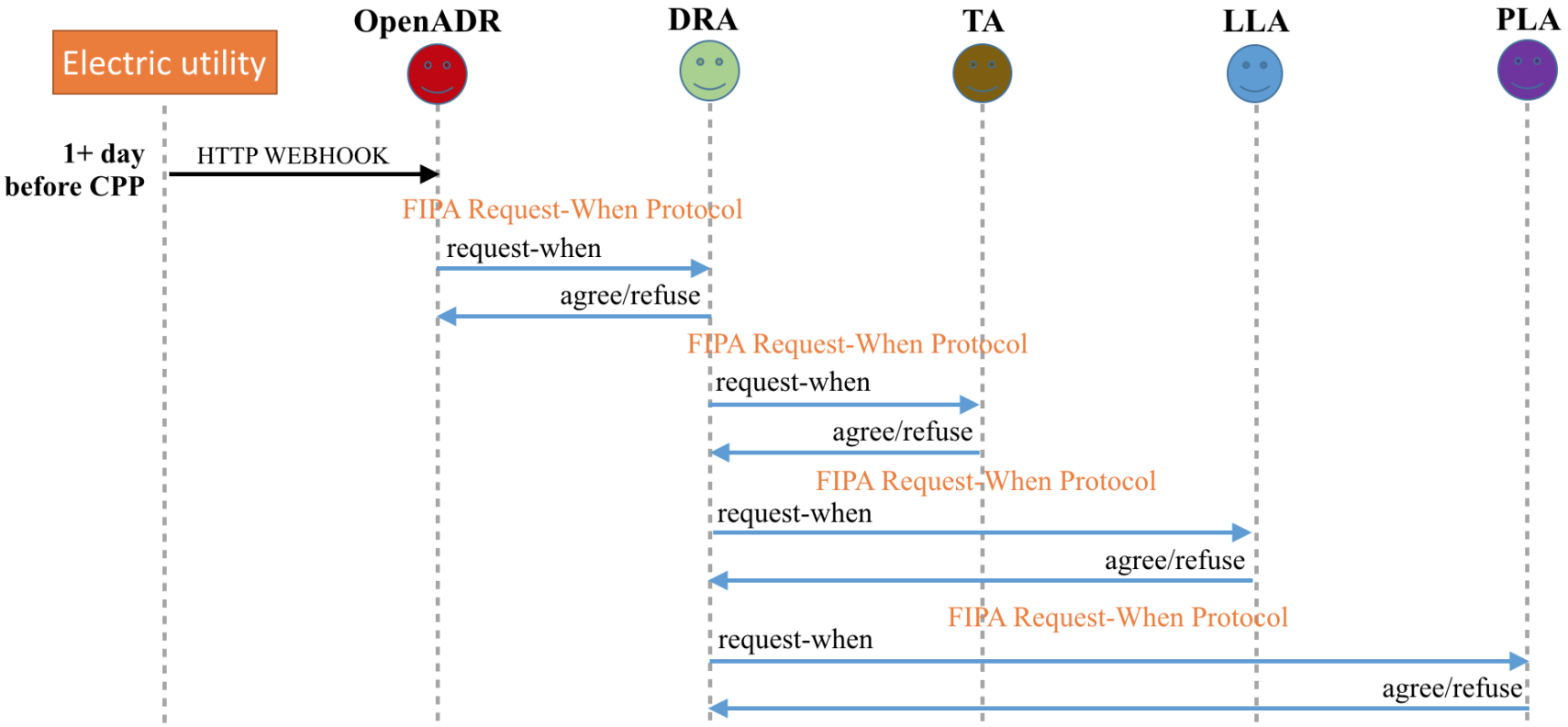

Fig. 3-32. Sequence diagram of the proposed agents the day before a CPP event

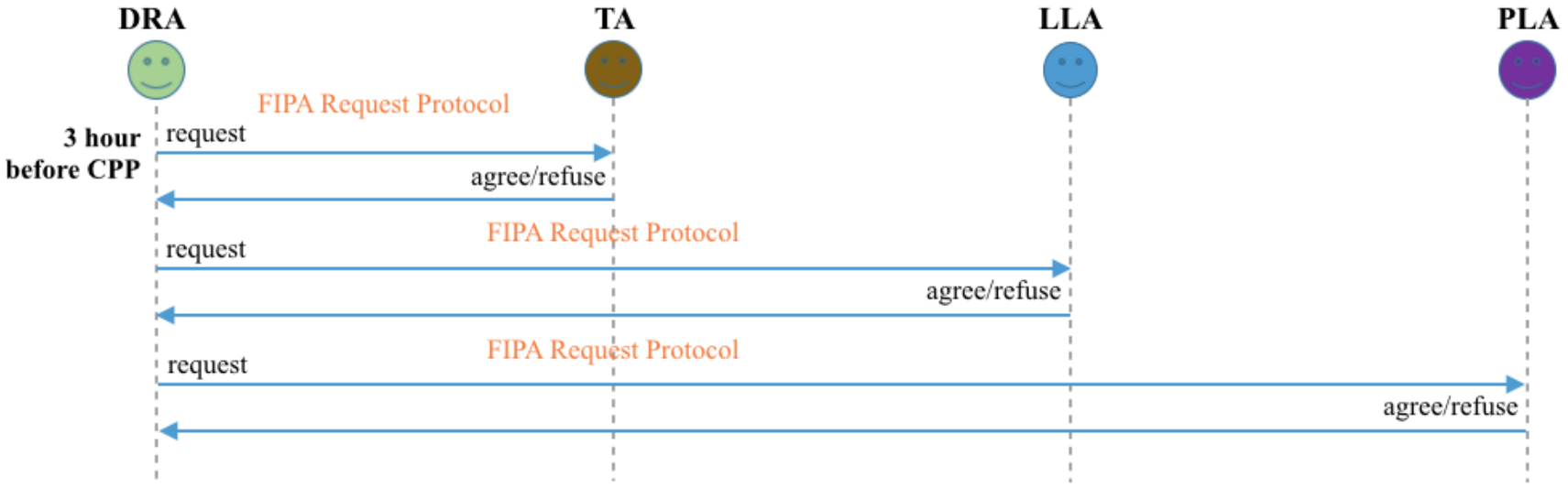

Fig. 3-33. Sequence diagram of the proposed agents during a normal stage prior to a pre-CPP stage

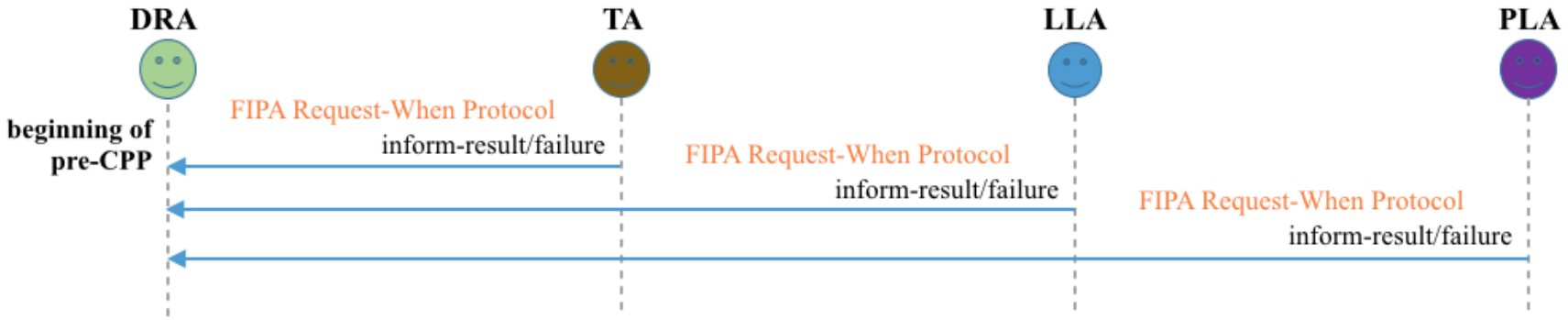

Fig. 3-34. Sequence diagram of the proposed agents during a pre-CPP stage

With the constructed believe, a TA selects an optimal thermostat cooling temperature set point before a CPP event ($T_{cooling,pre-CPP}$) so that an RTU is not likely to operate during a CPP period taken into account a building thermal response (BT_{op}, BT_{nop}) of a zone or a room inside a building. Therefore, the pre-cooling action is required to shift and minimize electricity consumption of an RTU during a CPP event. During this pre-CPP stage, a TA lowers the cooling temperature set point of its corresponding thermostat from a normal cooling temperature set point ($T_{cooling,norm}$) to a new cooling temperature set point before a CPP event ($T_{cooling,pre-CPP}$). Rather than changing a thermostat cooling set point instantaneously, a set point is gradually lowered over a period of time with multiple steps ($steps_{T_{cooling,norm} \rightarrow T_{cooling,pre-CPP}}$) at an interval of Δt_{step} (a TA control decision).

Since control actions of a TA are directly related to the PMV index and CO_2 level, a TA also helps the DRA to minimize the comfort violation index (CVI). In order to achieve its goal, the average room temperature should be as close as the room temperature that the value of PMV is equal to zero. However, CLV during a CPP event is more important therefore the weight of a CLV during the pre-CPP stage is low. A TA will try to maintain CLV during the pre-CPP stage to be within the range as specified by the ASHRAE standard 55-2013 [106].

Based on its believe, TA's choices for $T_{cooling,pre-CPP}$ and $T_{cooling,CPP}$ also affect the demand restrike of the corresponding RTU (DRK_{RTU}) and the time to restore the temperature set point back to its normal setting prior to the pre-CPP stage. A TA selects a cooling temperature set point before a CPP event ($T_{cooling,pre-CPP}$) that will minimize the difference between the thermostat cooling temperature set point during a CPP event ($T_{cooling,CPP}$) and the normal cooling temperature set point ($T_{cooling,norm}$). This action lead to minimizing both the impact of DRK_B and the time to restore thermostat temperature set point back to its normal setting after a CPP event.

Based on the above criteria, a TA performs actions during a pre-CPP stage, shown in Fig. 3-35 , by sending control signals to its corresponding thermostat with the settings calculated using Eq. 3-78 - Eq. 3-82.

$$T_{cooling,pre-CPP} = \begin{cases} T_{PMV=0} - \dfrac{BT_{nop}}{2} \cdot t_{CPP,duration}, & \mathrm{T_{PMV=-0.5}} \leq T_{pre-cooling} \\ \mathrm{T_{PMV=-0.5}}, & \mathrm{T_{PMV=-0.5}} > T_{pre-cooling} \end{cases} \quad \text{(Eq. 3-78)}$$

$$steps_{T_{cooling,norm} \rightarrow T_{cooliong,pre-CPP}} = \frac{\Delta T}{\Delta t_{step} \cdot BT_{op}} \quad \text{(Eq. 3-79)}$$

$$\Delta T = T_{cooling,norm} - T_{cooling,pre-CPP} \quad \text{(Eq. 3-80)}$$

$$\Delta T_{step} = \frac{\Delta T}{steps_{T_{cooling,norm} \rightarrow T_{cooling,pre-CPP}}} \quad \text{(Eq. 3-81)}$$

$$t_{pre-cooling,duration} = \Delta t_{step} \cdot (steps_{T_{cooling,norm} \rightarrow T_{cooling,pre-CPP}} + 1)$$ (Eq. 3-82)

Where,

$T_{cooling,pre-CPP}$: thermostat pre-cooling temperature set point (°F)

$T_{PMV=0}$: indoor air temperature that the calculated PMV is zero (°F)

$T_{PMV=-0.5}$: lower bound of an indoor air temperature that PMV = -0.5 which is still within the ASHRAE standard 55-2013 [106] limit (°F)

BT_{nop} : building thermal response when an HVAC does not operate (°F/hr)

BT_{op} : building thermal response when an HVAC operates (°F/hr)

$t_{CPP,duration}$: duration of a CPP event (hr)

$T_{cooling,norm}$: thermostat normal cooling temperature set point (°F)

$steps_{T_{cooling,norm} \rightarrow T_{cooling,pre-CPP}}$: steps to change from $T_{cooling,norm}$ to $T_{cooling,pre-CPP}$

ΔT : different between $T_{cooling,norm}$ to $T_{cooling,\square re-CPP}$ (°F)

Δt_{step} : interval to change a thermostat cooling temperature set point (control variable of a TA, hr)

ΔT_{step} : change in thermostat cooling temperature set point at every interval Δt_{step} (°F)

$t_{pre-cooling,duration}$: duration of a TA's pre-cooling action before a CPP event (hr)

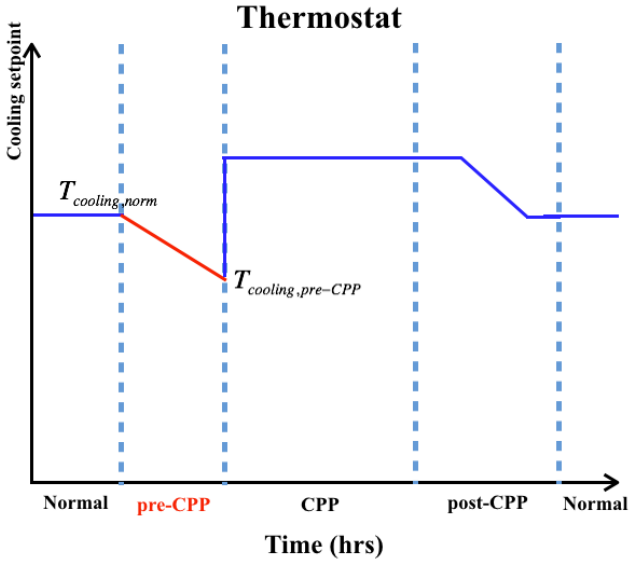

Fig. 3-35. Control actions of a thermostat agent during a pre-CPP stage

It should be noted that BT_{op} and BT_{nop} are the TA's learnable parameters obtained from Section 3.5.B subtask 2.

D.3 Lighting Load Agent (LLA), there are two parameters that determines the control action of a LLA: status ("ON","OFF") and brightness (0 – 100%).

Since increase or decrease in the brightness of a lighting load during a pre-CPP period will not contribute to a reduction in energy consumption during a CPP event, a LLA does not need to take any action during a pre-CPP stage. Furthermore, changing the brightness level during a pre-CPP stage is neither contributing to prevent the comfort violation index (CVI) from being violated, the demand restrike from lighting loads ($DRK_{Lighting\ load}$) to happen, nor reducing the time that a LLA takes to restore the operation of the lighting load back to its normal setting. Thus, a LLA does not need to take any action during the pre-CPP period as shown in Fig. 3-36. However, the current status ($status_{lighting\ load,pre-CPP}$) and its maximum power demand of a lighting load ($P_{lighting\ load,max}$) is saved by a LLA to be used later in the next event stage.

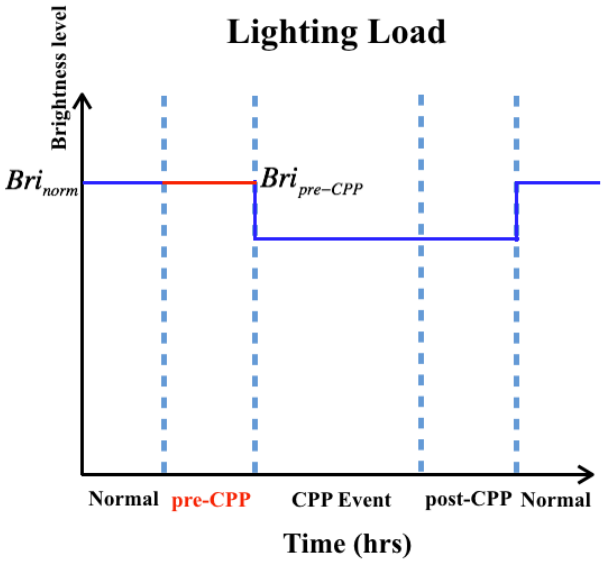

Fig. 3-36. Control action of a lighting load agent during a pre-CPP stage

D.4 Plug Load Agent (PLA): there is one parameter that determines the control action of a PLA: status (ON/OFF).

Since changing the status of a plug load during a pre-CPP stage will not contribute to the reduction in power demand and energy consumption during a CPP period, occupant comfort violation, impacts of demand restrike potential from plug loads ($DRK_{plug\ load}$), and time to restore settings after a CPP event, a PLA does not need to take any action during this time as shown in Fig. 3-37. However, the plug load current status ($status_{plug\ load,pre-CPP}$) and its maximum power demand ($P_{plug\ load,max}$) is saved by a PLA to be used later in the next event stage.

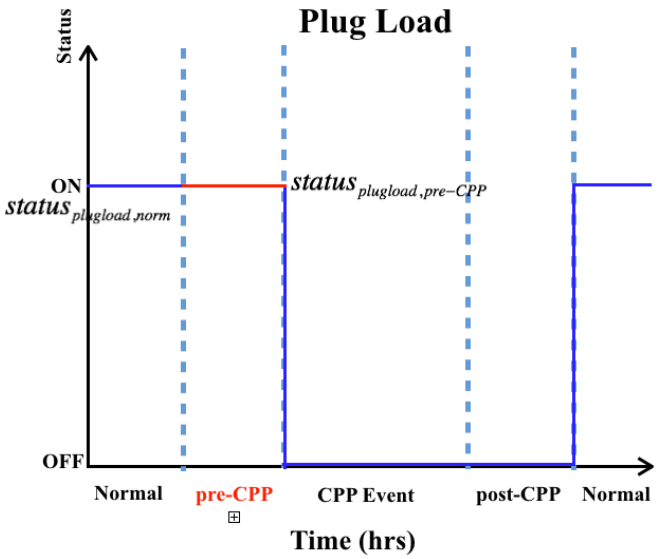

Fig. 3-37. Control action of a plug load agent during a pre-CPP stage

E. CPP event stage:

In this stage, the proposed agents will select optimal actions to achieve the objectives mentioned in the previous section. Actions of each agent are given as follows:

E.1 Demand Response Agent:

During a CPP event, a demand response agent (DRA) coordinates with control agents: thermostat agent (TA), lighting load agent (LLA), and plug-load agent (PLA) given the knowledge of sensor agents: power meter agent (PMA), weather sensor agent (WSA), multi-sensor agent (MTA), and motion sensor agent (MSA) as depicted in Fig. 3-38.

E.2 Thermostat Agent (TA): there are two parameters that determine control actions of a TA: temperature set point (°F), and fan status (ON/OFF). The DRA's overall objectives are taken into account during a CPP event to determine the course of TA's actions.

To minimize a power demand and an energy consumption of an RTU, a TA change a thermostat cooling set point ($T_{cooling,CPP}$) to the value that RTU is not likely to operate during a CPP event. This cooling set point is the value that a TA believes that an RTU is less likely to operate when room temperature increases from the value at the end of the pre-CPP stage to the end of a CPP event.

In order to minimize CLV during a CPP event, a TA will take appropriate action(s), e.g., lower a thermostat cooling set point or turn on a fan in order to maintain the PMV index within the range specified by the ASHRAE standard 55-2013 [106].

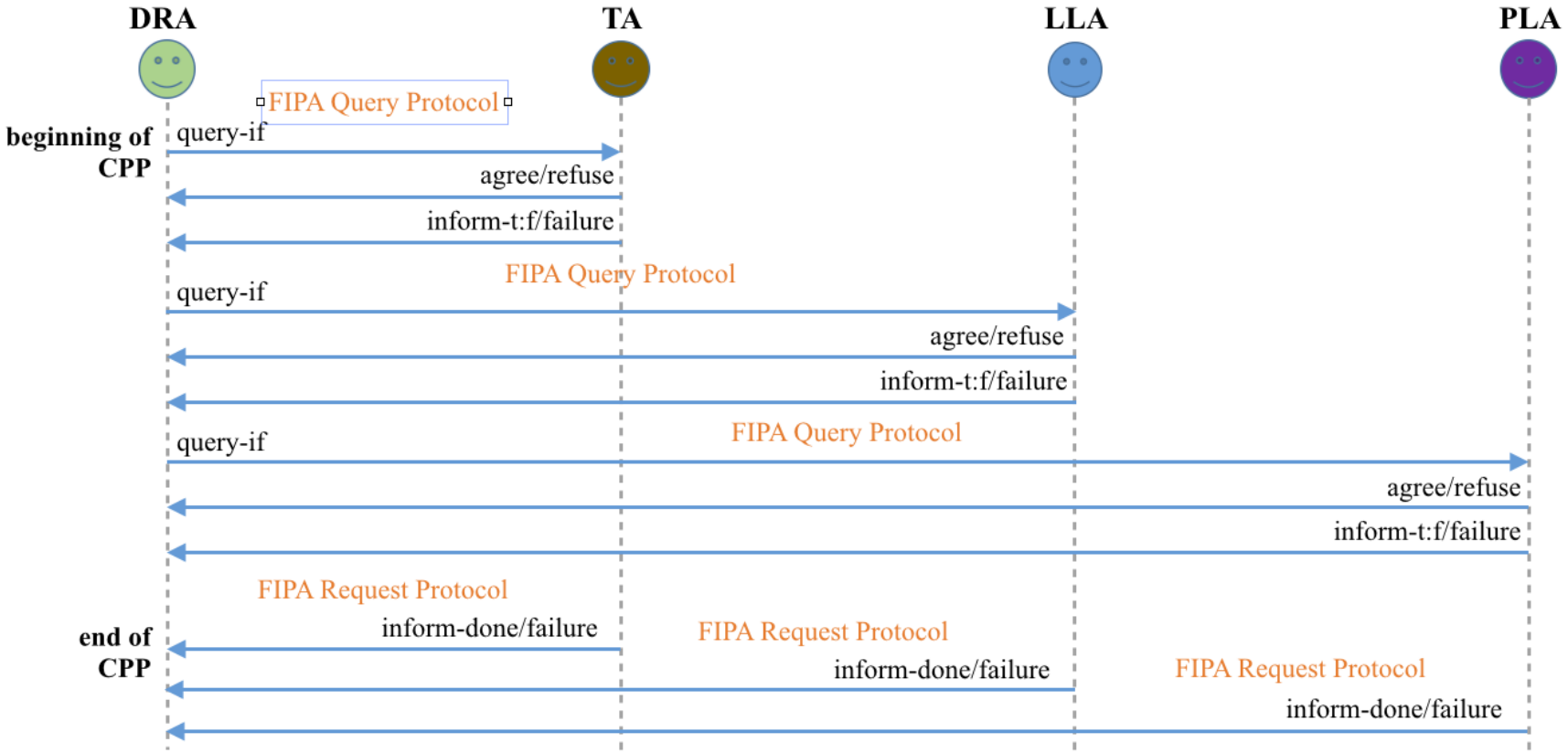

Fig. 3-38. Sequence diagram of the proposed agents during a CPP period

To minimize the impact of demand restrike potential (DRK_{RTU}), a TA ensures that the difference between the selected thermostat cooling set point during a CPP event ($T_{cooling,CPP}$) and the thermostat cooling setpoint during a normal condition ($T_{cooling,norm}$) is minimal. Therefore, the estimated time taken back from $T_{cooling,CPP}$ to $T_{cooling,norm}$ is minimal providing the building thermal response when RTU is operating (BT_{op}) .

Based on the above criteria, a TA performs actions during a CPP event stage, shown in Fig. 3-39, by sending control signals to its corresponding thermostat with the settings shown in Eq. 3-83 Eq. 3-86.

$$T_{cooling,CPP} = \begin{cases} T_{PMV=0} + \dfrac{BT_{nop}}{2} \cdot t_{CPP,duration}, & \mathrm{T_{cooling,CPP}} \leq T_{PMV=} \\ \mathrm{T_{PMV=0.5}}, & T_{cooling,CPP} > \mathrm{T_{PMV}} \end{cases} \quad \text{(Eq. 3-83)}$$

$$t_{RTU\_start,CPP} = t_{CPP,start} + \frac{\Delta T}{BT_{nop}} \quad \text{(Eq. 3-84)}$$

$$\Delta T = T_{cooling,CPP} - T_{cooling,pre-CPP} \quad \text{(Eq. 3-85)}$$

$$S_{FAN} = "ON" \quad \text{(Eq. 3-86)}$$

Where,

$T_{cooling,CPP}$	:	thermostat cooling temperature set point during a CPP event (°F)
$T_{cooling,pre-CPP}$	:	thermostat pre-cooling temperature set point (°F)
BT_{nop}	:	building thermal response when an HVAC does not operate ($°F/hr$)
t_{CPP}	:	duration of a CPP event (hr)
$\mathrm{T_{PMV=0.5}}$	:	upper bound of an indoor air temperature that PMV is 0.5 and still within the ASHRAE standard 55-2013[106] limit (°F)
$t_{RTU\_start,CPP}$	:	time that RTU is likely to start during a CPP event (hr)
$t_{CPP,start}$	:	start time of a CPP event (hrs)
ΔT	:	difference between a thermostat cooling setpoint during a CPP event and a thermostat cooling setpoint pre-cooling temperature setpoint and
S_{fan}	:	status of a fan during a CPP event

In addition, it should be noted that BT_{nop} is the TA's learnable parameters obtained from Section 3.5.B subtask 2.

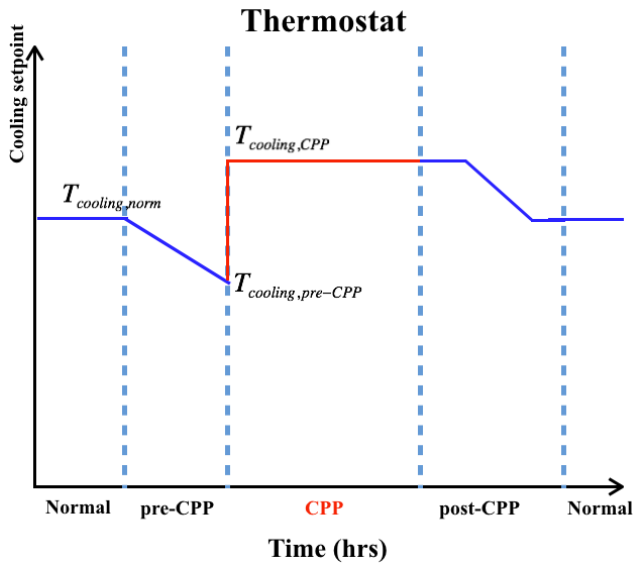

Fig. 3-39. Control action of a thermostat agent during a CPP event stage

E.3 Lighting Load Agent (LLA), there are two parameters that determines the control action of a LLA is the brightness (0 – 100%) of its associated lighting load. The DRA's overall objectives are taken into account during a CPP event to determine the course of LLA's actions.

A LLA can reduce the brightness level of a corresponding lighting load to minimize power demand and energy consumption during a CPP period. With respect to the IESNA standard 90.1-2007 [109], a LLA tries to keep an illuminance level of a room to a level that is not lower than the recommended average illuminance level based on a building type and a room type. In addition, A LLA will make sure that the reduced brightness level (Bri_{CPP}) does not create the high demand restrike of a lighting load after a CPP event ends.

Based on the above objectives, a LLA performs actions during a CPP event stage, shown in Fig. 3-40, by sending control signals to its corresponding lighting load with the settings shown in Eq. 3-89.

$$Bri_{CPP} = 1.05 \cdot [\frac{illuminance_{CPP} - \theta_{0ib}}{\theta_{1ib}}] \qquad \text{(Eq. 3-87)}$$

The difference between lighting load power demand during a normal stage and a CPP event ($\Delta P_{Lighting\ load}$) can be evaluated as in Eq. 3-88. Thus, the estimated power demand of a lighting load during a CPP event is given in Eq. 3-89.

$$\Delta P_{Lighting\ load} = \theta_{1pb}\Delta Bri = \theta_{1pb}(Bri_{CPP} - Bri_{norm}) \qquad \text{(Eq. 3-88)}$$

$$P_{Lighting\ load,CPP} = P_{Lighting\ load,norm} + \Delta P_{Lightin} \qquad \text{(Eq. 3-89)}$$

Where,

Bri_{CPP} : brightness level of light bulb(s) during a CPP event (%)

Bri_{norm} : brightness level of light bulb(s) during a normal condition (%)

$illuminance_{norm}$: illuminance level of a room during a normal stage (lux)

$illuminance_{CPP}$: minimum illuminance level of a room that is maintained during a CPP period which is recommended by the IESNA standard 90.1-2007 [109] (lux)

$\theta_{0ib}, \theta_{1ib}$: estimated parameters of linear regressing model between illuminance and brightness level

$\Delta P_{Lighting\ load}$: difference between lighting load power demand during a normal stage and a CPP event (W)

$\theta_{0pb}, \theta_{1pb}$: estimated parameter of linear regressing model between power demand of a lighting load and brightness level

ΔBri : difference between brightness level during a CPP event and a normal stage (W)

$P_{Lighting\ load,CPP}$: power demand of a lighting load during a CPP event (W)

$P_{Lighting\ load,norm}$: power demand of a lighting load during a normal stage (W)

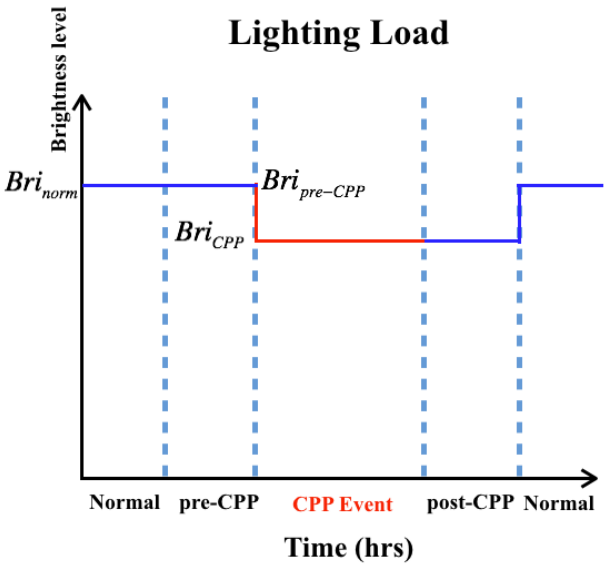

Fig. 3-40. Control action of a lighting load agent (LLA) during a CPP event stage

E.4 Plug Load Agent (PLA), one parameter that determines the control action of a PLA is the status (ON/OFF) of its associated plug load. The DRA's overall objectives are taken into account during a CPP event to determine the course of actions of a PLA.

A PLA can change the status of its corresponding plug load to "OFF" to minimize power demand and energy consumption during a CPP period. There are two kinds of loads that a PLA can be assigned to: critical load and non-critical load. To minimize comfort level violation in a building during a CPP event, a PLA will avoid turning off critical loads. A PLA will not take any

action during a CPP event to minimize the impact of demand restrike, nor to minimize time to restore settings.

Based on the above objectives, a PLA performs actions during a CPP event stage, shown in Fig. 3-41, by sending control signals to its corresponding plug load with the settings shown in Eq. 3-90. Thus, the estimated power demand of a plug load during a CPP event is given as in Eq. 3-91.

$$status_{plug\ load,CPP} = \begin{cases} 1\ (ON), & if\ \text{Plug load is critical load} \\ 0\ (OFF), & if\ \text{Plug load is non} - \text{critical load} \end{cases} \quad \text{(Eq. 3-90)}$$

$$P_{plug\ load,CPP} = s_{plug\ load,CPP} \cdot P_{appliance} \quad \text{(Eq. 3-91)}$$

Where,

$status_{plug\ load,CPP}$: status (1=ON/0=OFF) of a plug load

$P_{plug\ load,CPP}$: power demand of a plug load during a CPP event (W)

$P_{appliance}$: rated power demand of an appliance (W)

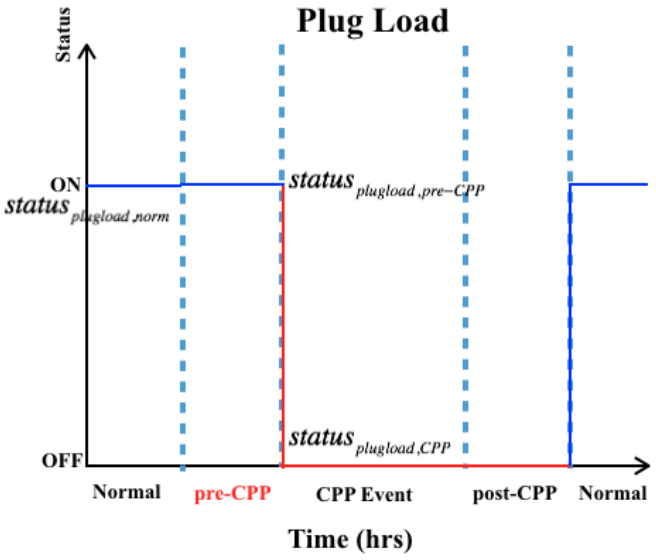

Fig. 3-41. Control action of a plug load agent (PLA) during a CPP event stage

F. Post-CPP stage:

In this stage, agents will select optimal actions to achieve the overall system objectives. Actions associated with each agent are given as follows:

F.1 Demand Response Agent (DRA):

After a CPP event, a demand response agent (DRA) minimizes the impact of demand restrike by coordinating with control agents: thermostat agent (TA), lighting load agent (LLA), and plug load agent (PLA) as shown in Fig. 3-42.

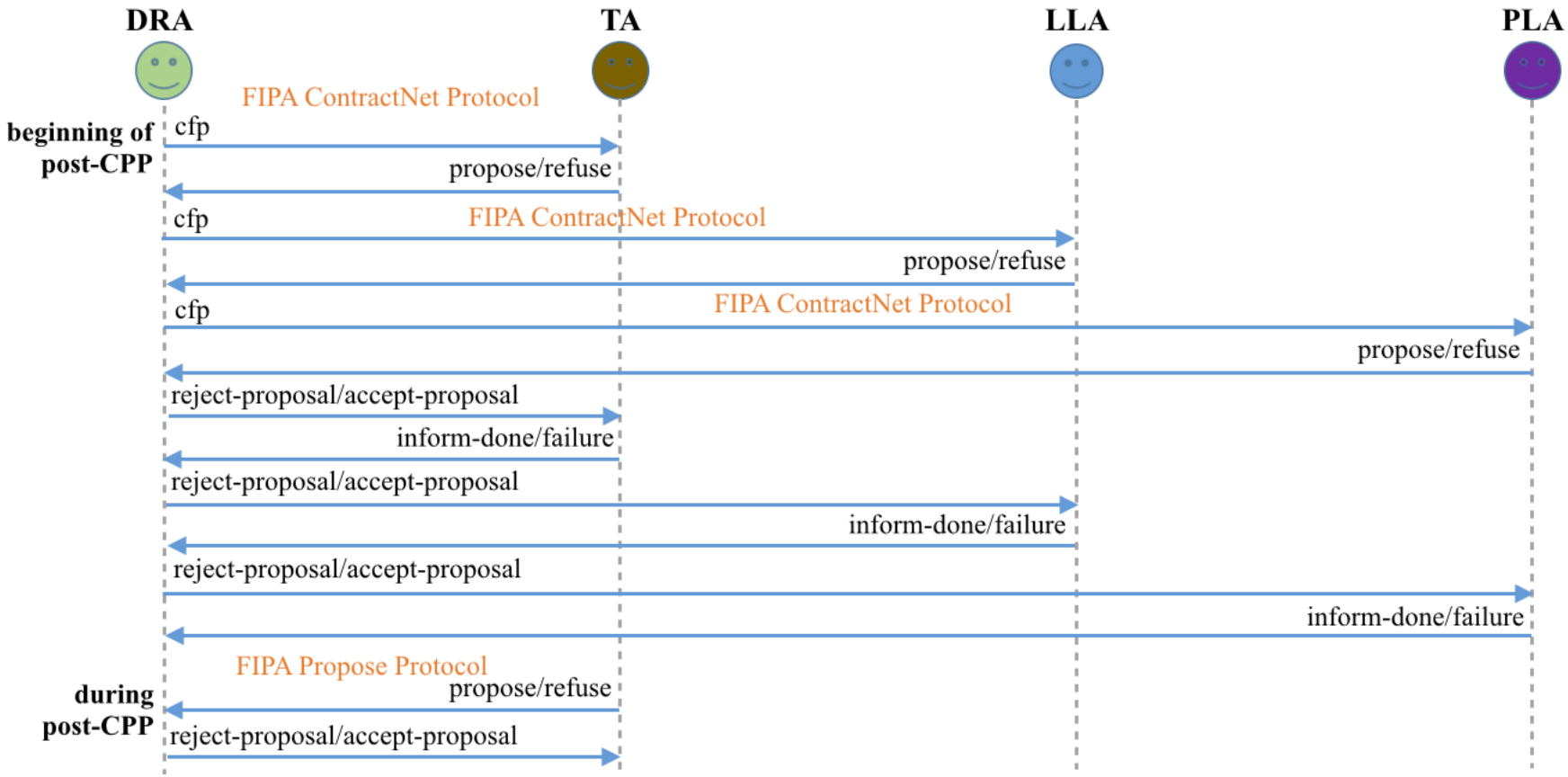

Fig. 3-42. Sequence diagram of the proposed agents during a post-CPP period

This is with the goals to minimize occupant comfort violation as well as to restore their settings as quickly as possible. In short, a DRA will try to slowly increase the total power demand of a building to avoid the rebound effect. Control agents will gradually change all set points back to normal settings.

F.2 Thermostat Agent (TA), two parameters that determine control actions of a TA include temperature set point (°F), and fan status (ON/OFF). The DRA's overall objectives are taken into account after a CPP event to determine the course of actions of a TA.

After a CPP event, the main goal of a TA is to minimize occupant comfort violation. This is accomplished by reducing the thermostat cooling setpoint from the level during a CPP event ($T_{cooling,CPP}$) to the level at the normal condition ($T_{cooling,norm}$). The TA also has the other goal, which is to minimize the impact of a DRK_{RTU}. This is accomplished by communicating with a DRA to find out when to lower the thermostat temperature set point from $T_{cooling,CPP}$ to $T_{cooling,norm}$. It also ensures that the total restored power demand of all loads will not exceed the maximum of the historical power demand of a building during the normal condition. Rather than changing the thermostat cooling temperature set point instantaneously, a TA will gradually reduce the thermostat cooling setpoint over a period of time with multiple steps $steps_{T_{cooling,CPP}\rightarrow T_{cooling,norm}}$ at every t_{step} (a TA control decision). This is to avoid the rebound of RTU power demand as well as to minimize the time taken to restore the thermostat cooling setpoint back to its normal stage.

Based on the above objectives, a TA performs actions during a CPP event stage, as shown in Fig. 3-43, by sending control signals to its corresponding thermostat with the settings given in Eq. 3-92 - Eq. 3-95.

$$steps_{T_{cooling,CPP}\rightarrow T_{cooling,norm}} = \frac{\Delta T}{t_{step} \cdot BT_{op}} \qquad \text{(Eq. 3-92)}$$

$$\Delta T = T_{cooling,CPP} - T_{cooling,norm} \qquad \text{(Eq. 3-93)}$$

$$\Delta T_{step} = \frac{\Delta T}{steps_{T_{cooling,CPP}\rightarrow T_{cooling,norm}}} \qquad \text{(Eq. 3-94)}$$

$$t_{T_{cooling,CPP}\rightarrow T_{cooling,norm}} = t_{step} \cdot (steps_{T_{cooling,CPP}\rightarrow T_{cooling,norm}} + 1) \qquad \text{(Eq. 3-95)}$$

Where,

$steps_{T_{cooling,CPP}\rightarrow T_{cooling,norm}}$: steps to change from $T_{cooling,CPP}$ to $T_{cooling,norm}$

BT_{op} : building thermal response when an RTU is operating (°F/hr)

ΔT : difference between $T_{cooling,CPP}$ and $T_{cooling,norm}$ (°F)

t_{step} : time step interval to change a thermostat cooling set point (control variable of a TA, min)

ΔT_{step} : change in thermostat cooling temperature set point at every interval t_{step} (°F)

$T_{cooling,CPP}$: thermostat cooling set point during a CPP event (°F)
$T_{cooling,norm}$: thermostat cooling set point during a normal stage (°F)
$t_{T_{cooling,CPP} \rightarrow T_{cooling,norm}}$: time taken to change cooling temperature set point from $T_{cooling,CPP}$ to $T_{cooling,norm}$ (hr)

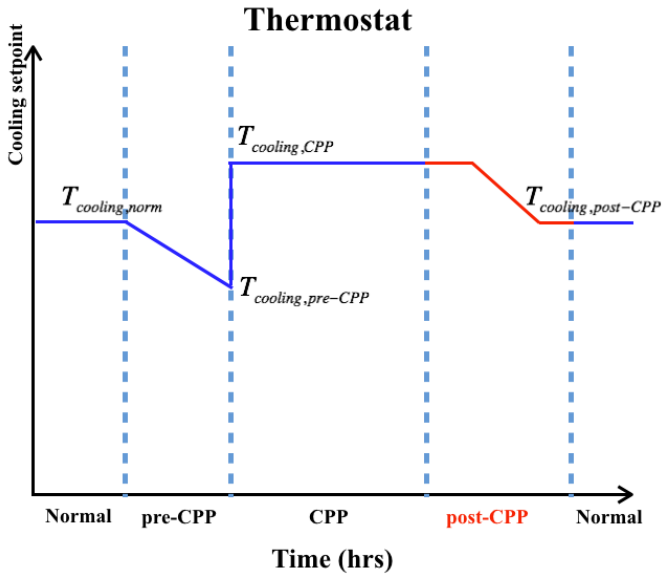

Fig. 3-43. Control action of a thermostat agent (TA) during a post-CPP stage

F.3 Lighting Load Agent (LLA), one parameter that determines the control action of a LLA is the brightness (0 – 100%) of its corresponding lighting load. The DRA's overall objectives are taken into account after a CPP event to determine the course of LLA's actions.

To minimize occupant comfort violation and impacts of a demand restrike, a LLA collaborates with a DRA to find out the optimal time to increase the brightness of associated lighting load from the level during a CPP event (Bri_{CPP}) to the normal level (Bri_{norm}). A DRA will determine whether the total restored power demand of all loads will not exceed the maximum historical power demand of a building during a normal condition. In addition, a LLA will also try to restore the brightness back to the normal level (Bri_{norm}) as quickly as possible.

Based on the above objectives, a LLA performs actions during the restore stage, shown in Fig. 3-44, by sending control signals to its corresponding lighting load with the settings shown in Eq. 3-96.

$$Bri_{post-CPP} = Bri_{norm} = Bri_{pre-CPP} \qquad \text{(Eq. 3-96)}$$

The difference between lighting load power demand during a CPP event and its normal operating condition ($\Delta P_{Lighting\ load}$) can be evaluated as in Eq. 3-97. Thus, the estimated power demand of a lighting load when it comes back to a normal stage is given in Eq. 3-98.

$$\Delta P_{Lighting\ load} = \theta_{1pb} \Delta Bri = \theta_{1pb}(Bri_{norm} - Bri_{CPP}) \qquad \text{(Eq. 3-97)}$$

$$P_{Lighting\ load,norm} = P_{Lighting\ load,CPP} + \Delta P_{Lightin} \quad \text{(Eq. 3-98)}$$

Where,

Bri_{CPP}	:	brightness level of light bulb(s) during a CPP event (%)
Bri_{norm}	:	brightness level of light bulb(s) during a normal condition (%)
$illuminance_{norm}$	:	illuminance level of a room during a normal stage (lux)
$illuminance_{min}$	:	minimum illuminance level of a room that is recommended by the IESNA standard 90.1-2007 [109] (lux)
$\theta_{0ib,}\theta_{1ib,}$	:	estimated parameter of linear regressing model between illuminance and brightness level
$\Delta P_{Lighting\ load}$	:	difference between lighting load power demand during the normal stage and a CPP event (W)
$\theta_{0pb,}\theta_{1pb}$:	:	estimated parameter of linear regressing model between power demand of a lighting load and brightness level
ΔBri	:	difference between brightness level during a CPP event and the normal stage (W)
$P_{Lighting\ load,CPP}$	:	power demand of a lighting load during a CPP event (W)
$P_{Lighting\ load,norm}$	:	power demand of a lighting load during a normal stage (W)

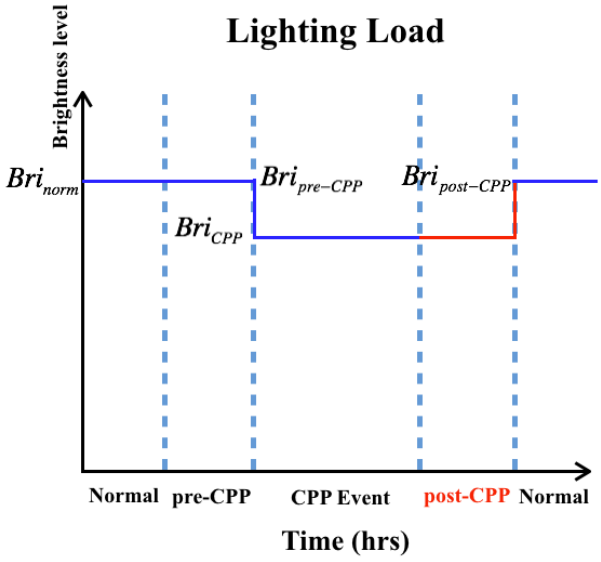

Fig. 3-44. Control action of a lighting load agent (LLA) during a post-CPP stage

F.4 Plug Load Agent (PLA), one parameter that determines the control action of a PLA is the status (ON/OFF) of its corresponding plug load. The DRA's overall objectives are taken into account after a CPP event to determine the course of PLA's actions.

There are two kinds of loads that a PLA can be assigned to: critical load and non-critical load. To minimize occupant comfort level violation during a restore event, a PLA coordinates with a DRA to return the status of a plug load to its previous status. A PLA coordinates with a DRA to find an optimal time to change the status of a non-critical plug load from "OFF" to "ON" as

quickly as possible while the goal of minimizing the impact of demand restrike is also taken into account.

Based on the above objectives, a PLA performs actions during a restore stage, shown in Fig. 3-45, by sending control signals to its corresponding non-critical plug load with the settings shown in Eq. 3-99. Thus, the estimated power demand of a plug load during a restore stage is given as shown in Eq. 3-100.

$$status_{plug\ load,restore} = \begin{cases} 1(ON), & if\ status_{plug\ load,pre-CPP} = 1 \\ 0(OFF), & if\ status_{plug\ load,pre-CPP} = 0 \end{cases} \quad \text{(Eq. 3-99)}$$

$$P_{plug\ load,restore} = s_{plug\ load,restore} \cdot P_{appliance} \quad \text{(Eq. 3-100)}$$

Where,

$status_{plug\ load,restore}$: status (1=ON/0=OFF) of a plug load during a restore stage
$status_{plug\ load,pre-CPP}$: status (1=ON/0=OFF) of a plug load during a pre-CPP stage
$P_{plug\ load,restore}$: power demand of a plug load during a restore stage (W)
$P_{appliance}$: rated power demand of an appliance (W)

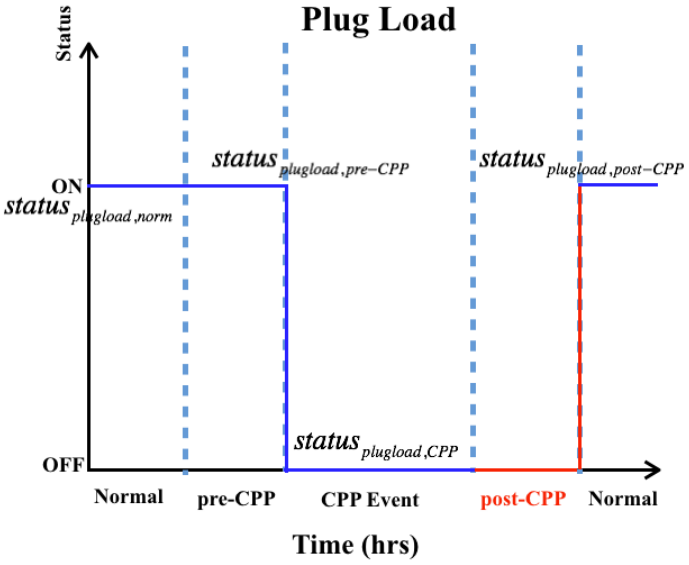

Fig. 3-45. Control action of a plug load agent (PLA) during a post-CPP stage

4. CASE STUDY 1: RESIDENTIAL HOME

This section presents a case study of the Smart Distribution Transformer Management System (SDTM) to assess the effectiveness of the proposed DR algorithm to alleviate power system stress conditions as elaborated in Section 3.3.

4.1 Description of the Case Study

The case study of the proposed Smart Distribution Transformer Management (SDTM), is shown in Fig. 4-1.

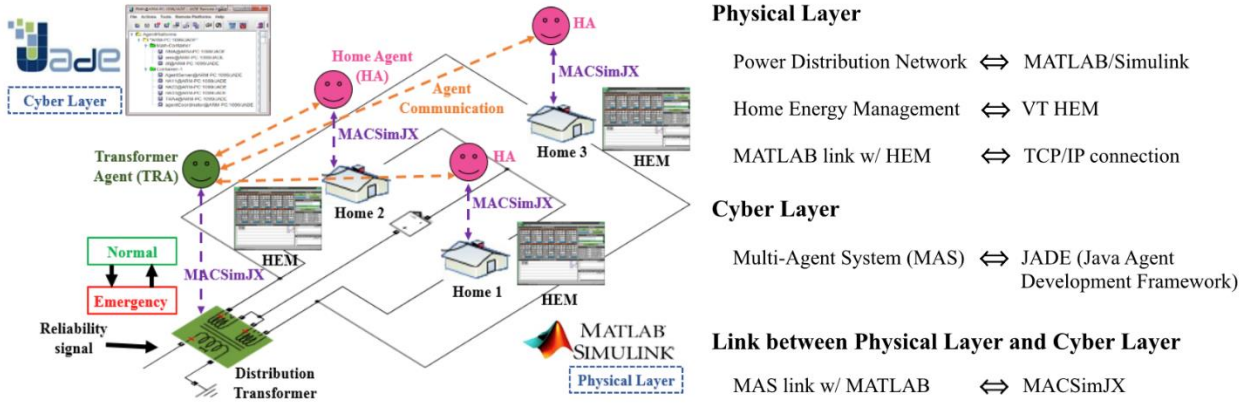

Fig. 4-1. Case study of the proposed SDTM

The physical layer comprises a distribution network with a single-phase distribution transformer serving three homes. The distribution network is modeled in MATLAB/Simulink; and the DR-enabled household appliances are modeled in the Home Energy Management (HEM) environment [110]).

The cyber layer consists of the proposed MAS (discussed in Section 3.2 and developed using the Java Agent Development Framework (JADE) [111] platform) and the HEM (stand-alone software developed in [111]). MAS comprises multiple distributed intelligent agents residing at their corresponding physical devices. The HEM is responsible for monitoring power consumption of DR-enabled household appliances and controlling appliance status during a DR event based on preset homeowner preferences. In the cyber layer, there is one *TRA* (resides at the simulated distribution transformer) and three *HAs* (resides at each simulated home).

The middleware called MACSimJX [112] is used to link the MAS with the distribution network modeled in MATLAB/Simulink. The HEM is linked with the distribution network and its corresponding agent via TCP/IP communication.

To enable real-world implementation of the proposed approach, a smart grid infrastructure that supports two-way communications between a distribution transformer and its connected homes is required; an example of which has been discussed in [113].

Table 4-1 summarizes attributes of the distribution transformer under study. Parameters, appliances ratings, and customer preference settings of three homes served by the transformer discussed above are summarized in Table 4-2.

Table 4-1. Distribution transformer (DT) attributes and DR event

Attribute	Value	Attribute	Value
DT ID	G2101CC3700	DT operating state	Normal before 17:10
DT rating	25 kVA	Home IDs (served by this transformer)	950009001 950009002 950009003
DT voltage ratio	7.2kV/120/240V	DR event	Occur at 17:10
DT configuration	BN	DL_{AGG-TR}	16 kW
DT loading capability	> 25 kW	DR event period	17:10 – 19:00

Table 4-2. Home attributes and customer preference settings

	Home 1 (HA1,HEM1)	Home 2 (HA2,HEM2)	Home 3 (HA3,HEM3)
Home parameters:			
ID	950009001	950009002	950009003
Size	1,833 ft^2	2,559 ft^2	1,310 ft^2
Elec. meter service amp	150 A	200 A	100 A
Voltage rating	120/240 V	120/240 V	120/240 V
Appliances ratings and customer preference setting:			
1. Air Conditioner (AC)	Priority #1		
1.1 Rating	1.92 kW	2.60 kW	1.92 kW
1.2 Temp set point	$76 \pm 2\ F^{\circ}$	$74 \pm 2\ F^{\circ}$	$76 \pm 2\ F^{\circ}$
1.3 Start time	Before 17:00	Before 17:00	After 17:40
2. Water Heater (WH)	Priority #2		
2.1 Rating	3.80 kW	4.50 kW	3.80 kW
2.2 Temp set point	$110 \pm 10\ F^{\circ}$	$120 \pm 10\ F^{\circ}$	$115 \pm 10\ F^{\circ}$
3. Clothes Dryer (CD)	Priority #3		
3.1 Rating (heat/motor)	2.88/0.18 kW	4.90/0.377 kW	2.88/0.18 kW
3.2 Start time	17:00	16:50	-
3.3 Required run time	60 min	60 min	-
3.4 Min ON time	20 min	20 min	20 min
3.5 Max OFF time	15 min	15 min	15 min
4. Electric Vehicle (EV)	Priority #4		
4.1 Rating	3.3 kW	3.3 kW	3.3 kW
4.2 Start time	17:05	16:30	17:45
4.3 Required run time	200 min	145 min	180 min
4.4 Model	Chevy Volt	Nissan Leaf	Chevy Volt
5. Household load	Note: CL = critical loads; HH = household loads		
5.1 Max CL during DR	0.52 kW	1.82 kW	0.52 kW
5.2 Max HH during DR	8.29 kW	11.26 kW	3.82 kW
Assumptions:			
DR event	16 kW imposed 17:10 – 19:00		
Residents (N)	2 people	4 people	2 people
N during a DR event	2 people	3 people	2 people (after 17:40)

This case study is used to demonstrate how the proposed MAS and its algorithm presented in Section 3.3 can perform a demand management at distribution transformer and a home levels during a DR event. This case study assumes that a DR event has occurred as a result of stress conditions causing by an unanticipated contingency in a transmission system (e.g., loss of generation or loss of transmission line).

4.2 Simulation Results

To assess the effectiveness of the proposed DR algorithm, this section compares the simulation result of the proposed DR algorithm with the result of the simple DR algorithm.

4.2.1 Simulation Results of the Proposed DR Algorithm

The simulation result of the proposed DR algorithm is shown in Fig. 4-2 for the distribution transformer and Fig. 4-4(a), 4-4(b), and 4-4(c) for the home 1, 2 and 3 respectively. The chronology of the events during a DR period is discussed in detail below:

At 17:10hrs, after receiving the DR event signal ($DL_{AGG \rightarrow TR}$), TRA takes no action since the transformer is in its normal operating state.

At 17:26hrs (①), the TRA is in emergency state (P_{TR} is higher than $DL_{AGG \rightarrow TR}$). The TRA, then, starts to work with participating HAs according to the proposed DR algorithm. After the DL allocation processes, the TRA allocates $\boldsymbol{DL_H^*}$ of 6.72 kW, 6.81 kW and 2.47 kW to HAs 1, 2, and 3, respectively based on the TRA belief on the $DRKP_{TR}$ and HAs' beliefs on their power demand requirements.

At 17:45hrs (②), HA3 requests the TRA for a higher DL as its belief changes due to the homeowner has just arrived home and plugged in his EV. Since the average DL that the HA3 currently received is lower than its fair DL, the TRA re-allocate $\boldsymbol{DL_H^*}$ of 5.76 kW, 6.60 kW and 3.64 kW to homes 1, 2 and 3 respectively. Noticeably, the time that the EV is charged is around 17:50hrs due to the higher-priority AC is still in operation at the time the HEM3 receives DL and is turned OFF at around 17:50hrs. Notice that the power demand of home 1 at ② and home 2 at ① decrease one minute after HEM1 and HEM2 receives the DL. This delay accounts for the operating interval of HEM, which is in 1-minute interval.

At 18:20hrs (③), HA1 requests the TRA for a lower DL as its belief changes due to the CD has finished its operation. The TRA re-allocate $\boldsymbol{DL_H^*}$ of 4.34 kW, 7.81 kW and 3.85 kW to HAs 1, 2 and 3 respectively.

At 18:29hrs (④), HA2 requests the TRA for a lower DL as its belief changes due to the CD has finished its operation. The TRA re-allocates $\boldsymbol{DL_H^*}$ of 5.76 kW, 6.39 kW and 3.85 kW to HAs 1, 2 and 3, respectively.

At 18:51hrs (⑤), HA1 requests the TRA for a higher DL as its belief changes due to the WH starts to operate as a result of hot water temperature drops below the preset value. Since the

average DL that HA1 currently received is higher than its fair DL, the TRA retains the current DL allocation. However, according to the load priority preference setting of home 1, the WH is turned on resulting in EV charging being on hold.

According to Fig. 4-3, the transformer load profile with DR (P_{TR}) is kept below the given $DL_{AGG\rightarrow TR}$ during the DR event. The TRA's PEDL index is nearly zero. The assessed demand restrike potential of the transformer ($DRKP_{TR}$) is 3.31 kWh. This can be considered as equivalent to a 3.31 kW increase in the transformer load for one hour due to load compensation of deferred appliances. In addition, the instantaneous power demand of all homes are controlled below the allocated $\boldsymbol{DL_H^*}$ (Fig. 4-4(a), 4-4(b), and 4-4(c)). According to the HAs' performance measures, all DLBCL indexes are zero as critical loads of all homes are served during the DR event. Customer comfort levels are also not violated as all homes' $CLV_{DRevent}$ are less than 1% different to their CLV_{w/o_DR}. This implies ACs and WHs operations are not affected by the DR event. Table 4-3 summarizes the actual demand restrike potential ($DRKP_{H,act,i}$) of each home and the delayed completion times of CD/EV, which represent additional time required for CD/EV to finish its operation as compared to its original schedule.

Table 4-3. Simulation results summary of the proposed DR strategy

	Home 1	Home 2	Home 3
$DRKP_{H,act,i}$	1.49 kWh	0.65 kWh	1.12 kWh
CD delayed completion time	20 minutes	39 minutes	-
EV delayed completion time	26 minutes	26 minutes	20 minutes

4.2.2 Simulation Results of the Simple DR Algorithm

The simple DR algorithm is chosen based on the fact that emergency demand response programs (EDRP) are not widely used at a distribution level, and most electric utilities have little knowledge on homes' characteristics. Accounting for this, rather than allocating the same demand limit to all homes as in [114], this paper implements the simple DR algorithm that allocates a fixed fair DL during a DR event based on homes' electrical meter service ampere ratings defined in Eq. 3-12 in Section 3.3.

The simulation results of the simple DR algorithm are shown in Fig. 4-3 for the distribution transformer and Fig. 4-5(a), 4-5(b), and 4-5(c) for the homes 1, 2 and 3, respectively. The chronology of events during a DR event is elaborated as follows:

After receiving the DR event signal ($DL_{AGG\rightarrow TR}$) with 16 kW DL from 17:10 to 19:00 hrs at ①, the TRA immediately allocates fair DLs based on the homes' electrical meter service ampere ratings. These are 5.33, 7.11, and 3.56 kW for HA1, HA2 and, HA3 respectively. These DL are retained until the DR event ends.

According to Fig. 4-3, the total instantaneous power at the transformer (P_{TR}) is kept below the given $DL_{AGG\rightarrow TR}$ during the DR period (the TRA's PEDL index is zero).

The assessed demand restrike potential of the transformer ($DRKP_{TR}$) is 7.58 kWh. This can be considered as equivalent to a 7.58 kW increase in a load of the transformer for one hour due to load compensation of appliances that have been deferred. This can cause an undesired

transformer overload condition as well as under-voltage problem as the impacts of DRK following a DR event. Nevertheless, the instantaneous power consumption of all three homes are controlled below the allocated $\boldsymbol{DL_H^*}$ (Fig. 4-5(a), 4-5(b), and 4-5(c)) without violating their critical loads levels (all DLBCL indexes are zero) and their comfort level preferences (all homes' $CLV_{DRevent}$ are less than 1% different to their CLV_{normal}).

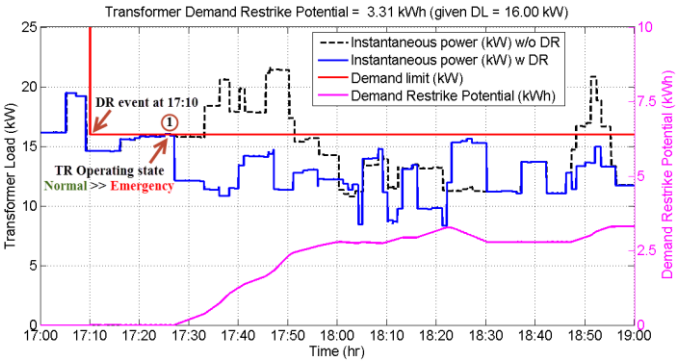

Fig. 4-2. Simulation results of the proposed DR strategy.

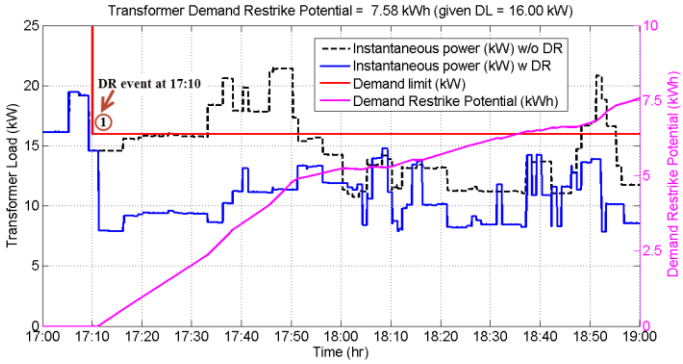

Fig. 4-3. Simulation results of the simple DR strategy.

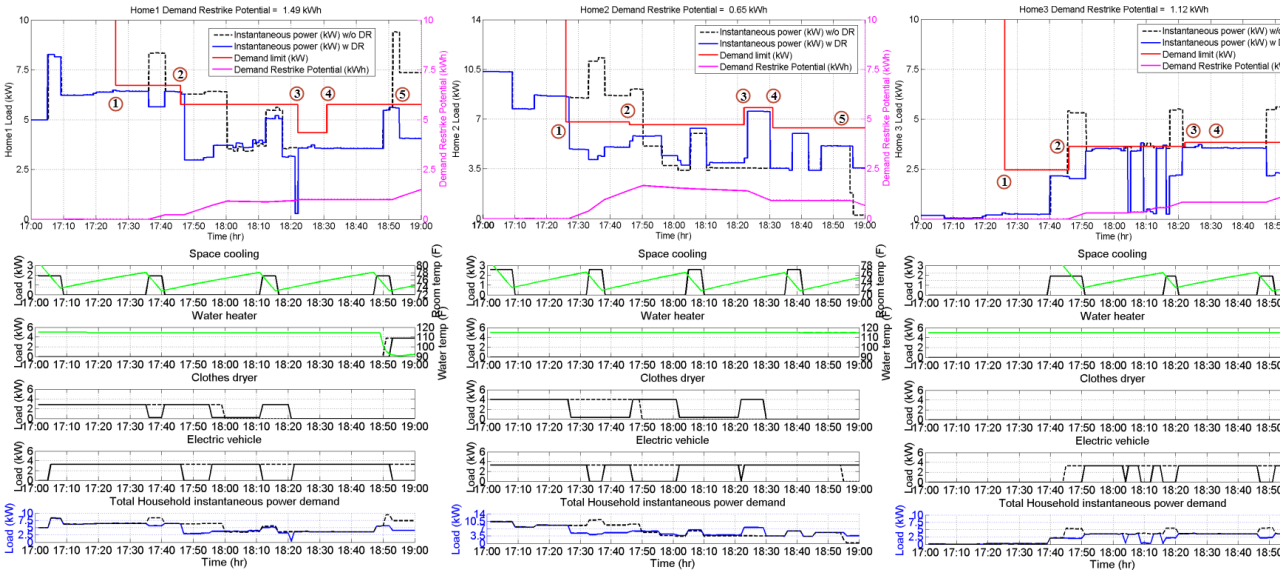

(a) (b) (c)

Fig. 4-4. Simulation results of the proposed DR strategy showing instantaneous power, demand limit, and demand restrike potential as well as the operations of energy-intensive appliances of each home without DR (dotted line) and with DR (continuous line) of: (a) home 1; (b) home 2; and (c) home 3.

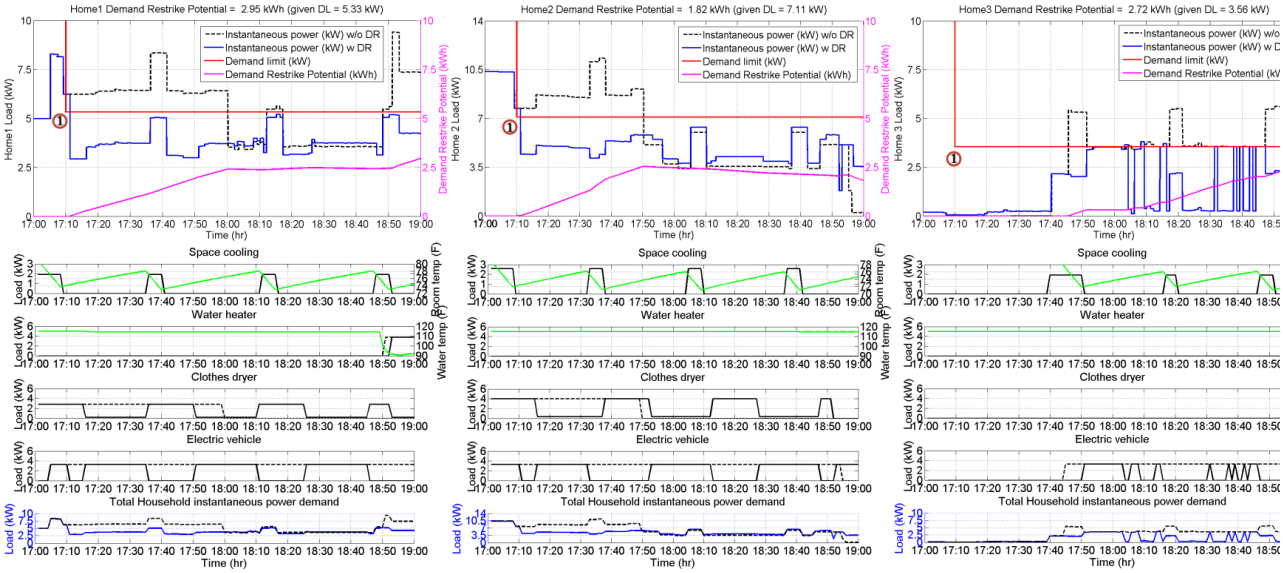

(a) (b) (c)

Fig. 4-5. Simulation results of the simple DR strategy showing instantaneous power, demand limit, and demand restrike potential as well as the operations of energy-intensive appliances of each home without DR (dotted line) and with DR (continuous line) of: (a) home 1; (b) home 2; and (c) home 3.

Table 4-4 summarizes the actual demand restrike potential ($DRKP_{H,act,i}$) of each home and the delayed completion time of CD and EV.

Table 4-4. Simulation results summary of the simple DR strategy

	Home 1	Home 2	Home 3
$DRKP_{H,act,i}$	2.95 kWh	1.82 kWh	2.72 kWh
CD delayed completion time	68 minutes	61 minutes	-
EV delayed completion time	49 minutes	45 minutes	49 minutes

4.3 Simulation Results and Discussion

Considering performance measures of the TRA and HAs, the proposed DR algorithm considerably reduce the demand restrike potential both at the transformer level ($DRKP_{TR}$) and the home level ($DRKP_{H,i}$) as compared to the simple DR algorithm. The assessed $DRKP_{TR}$ of the transformer is 3.31 kWh with the proposed DR algorithm representing 56% reduction compared to the 7.58 kWh $DRKP_{TR}$ with the simple DR algorithm. The lesser the demand restrike potential at the transformer level implies the lesser the chance that an overload condition at the transformer occurs following a DR event. At the home level, it can be seen that the delayed completion time of scheduled appliances (CDs and EVs) are substantially reduced as well as the demand restrike potential of all homes. The HEM also successfully performs load shifting and rescheduling. Hence, the proposed DR algorithm is more efficient and effective than the simple DR algorithm in mitigating the undesired impacts of the DRK.

Based on the PC with Intel® core™ i7-3820 CPU @3.60 GHz, 12 GB RAM, and Windows 7 64-bit operating system, the algorithm computation time is in order of several hundred milliseconds for the TRA to allocate $\boldsymbol{DL}_{\boldsymbol{H}}^{*}$ or re-allocate $\boldsymbol{DL}_{\boldsymbol{H}}^{*}$ to HAs according to the request from the DR AGG. This computation time is considered sufficiently fast to perform control at the distribution transformer and the home levels as appliances are typically controlled at minute intervals.

5. CASE STUDY 2: COMMERCIAL BUILDING

This section presents the case study to assess the effectiveness of the proposed DR algorithm in commercial buildings in response to a critical peak pricing (CPP) signal as elaborated in Section 3.5. The proposed DR algorithm has been tested and validated with the base case with no CPP event. The single-zone Potomac conference room at the Virginia Tech Architecture building in Alexandria, VA is selected as the test location. In addition, the impacts of space occupancy level to the load profile during a CPP event are also presented.

5.1 Description of the Case Study

In this case study, it is assumed that a CPP event is notified to a building operator one day in advance through an OpenADR web service, and the event starts at 13:04 hrs and ends at 16:04 hrs on 06/19/2015.

In order to achieve the desired objectives (minimize a building's power demand during a CPP event, minimize occupant comfort violation, minimize demand restrike after a CPP event, and minimize time to restore all settings after a CPP event), the three sequential steps described in Section 3.5 have been performed to find effectiveness and efficiency of the proposed DR algorithms.

The chronology of the CPP event is as follows:

1) An electric utility notifies a CPP event to the agent-based platform (developed in this work and discussed in Section 3.4) via the OpenADR agent through the HTTP webhook one day in advance prior to the CPP event on 06/19/2015 from 13:04 p.m. to 16:04 p.m.

2) The OpenADR agent, then, informs a demand response agent (DRA) of a CPP event.

3) A DRA implements the proposed DR algorithm with respect to the desired objectives on 06/19/2015. On the scheduled event, there are 15 people inside the Potomac conference room.

4) A DRA works with control agents: thermostat agent (TA), lighting load agent (LLA), and plugload agent (PLA) to execute decisions (e.g., thermostat agent to change temperature set point, lighting agent change brightness level of a light, or plug load agent to change status of a switch) based on the proposed DR algorithms in Section 3.5.

In order to verify and validate the efficiency and effectiveness of the proposed DR algorithm, the results of (i) the DR case study: where there is a CPP event on the observed day are compared with the results of (ii) the base case: where there is no CPP event on the day in which the outdoor weather conditions of that day are similar to the corresponding values on the observed day in the DR case study. In order to inspect and compare all stages both in the DR case study and the base case, the study period is six hours covering the normal stage prior to the pre-CPP stage, the pre-CPP stage, the CPP stage, the post-CPP stage, and the normal stage after the post-CPP stage.

Finally, in the last part of the this study, simulations to find effects on occupancy level to the energy consumption of the RTU are conducted to demonstrate the effectiveness of the proposed algorithm with variation in number of people in a space.

5.1.1 Description of the Test Site

The Potomac conference room 310, shown in Fig. 5-1, in the Virginia Tech Campus in Alexandria, VA is used to demonstrate the proposed platform and developed algorithms. This building is selected because it does not have an existing building automation system and relies on a facility manager to manually manage energy consumption in the building. It has been reported that energy consumption of the building is often wasted as students set the thermostat set point lower during their classes and left the setting on over nights/weekends, lightings, and other plug loads were also left on. There is no such a system that can tell the facility manager what has happened or there is something wrong in the operation of building equipment. There are mainly three kinds of electrical loads inside this conference room: HVAC, lighting and plug loads, as depicted in Fig. 5-2.

Fig. 5-1. Potomac conference room 310 at the Virginia Tech Campus in Alexandria, VA

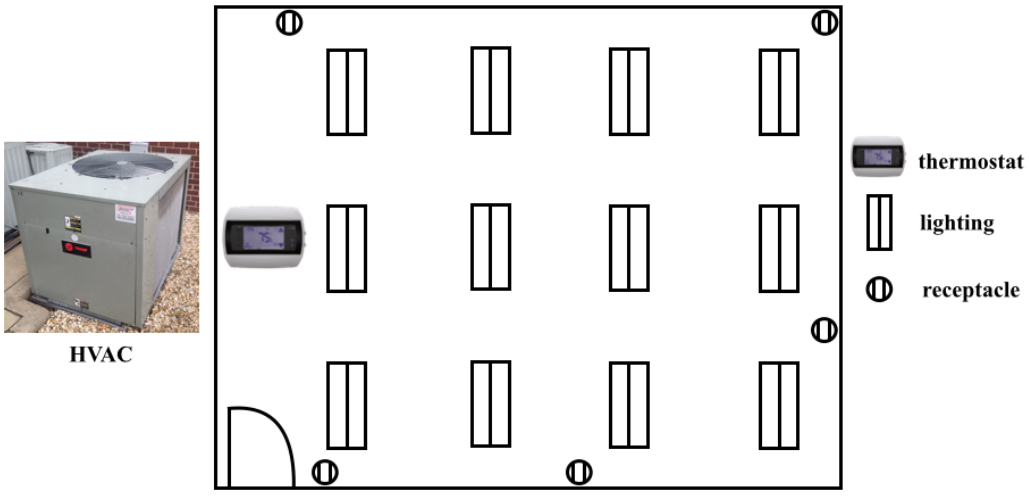

Fig. 5-2. Potomac conference room 310 floor plan

5.1.2 Set up of the proposed Agent-based Platform and Sensors/Controllers Installation

In order to test and validate the proposed DR algorithm presented in Section 3.5, selected sensors/controllers have been installed or replaced in the Potomac conference room 310 as listed in Table 5-1. These sensors/controllers are used with the proposed agent-based platform to provide required data and capabilities to change and configure settings in response to a CPP event. The agent-based platform serves as the control unit for these devices, and has been deployed in ODROID U3 [115]. It hosts a number of agents, including OpenADR, DR, TA, LLA, PLA#1, PLA#2, PLA#3, PMA, WSA, MTA and MSA.

Table 5-1. List of devices installed/replaced in the Potomac conference room

Category	Devices	Agent	Detail	Quantity
Thermostat	ICM Controls I2020 [116]	TA	Communication: Cloud, control the rooftop unit (RTU)	1
Lighting load controller	Philips Hue color ambiance starter kit [117]	LLA	Communication: LAN	1
Plug load controller	Belkin WeMo Insight Switch [118]	PLA#1, PLA#2, PLA#3	Communication: WLAN	3
Power meter	Wattnode WNC-3Y-208-MB [119]	PMA	Communication: Modbus TCP/IP, measure power consumption of the RTU	1
Hub/Coordinator	SmartThings Hub [120]	-	Communication: Cloud	1
Sensor	Netatmo weather station [121]	WSA	Communication: Cloud	1
Sensor	Aeon Labs multi sensor [122]	MTA	Communication: Z-Wave	1
Sensor	Proteus M5 WiFi motion sensor [123]	MSA	Communication: WLAN	1

Fig. 5-3 shows those devices mapped on the floor plan of the Potomac conference room and their corresponding control agents:

- the thermostat agent (TA) to monitor and control the ICM Controls I2020 thermostat that used to determine the operation of the Trane packaged rooftop unit;
- the lighting load agent (LLA) to monitor and control Philips Hue light bulbs;
- the plug load agent #1 (PLA#1) to monitor and control the desktop computer;
- the plug load agent #2 (PLA#2) to monitor and control the printer;
- the plug load agent #3 (PLA#3) to monitor and control the air purifier;
- the power meter agent (PMA) to monitor electrical data from the Wattnode power meter;
- the weather sensor agent (WSA) to monitor weather data from the Netatmo weather station;
- the multi sensor agent (MSA) to monitor illuminance level of the room from the Aeon Labs multi sensor that links to the SmartThings Hub;
- the motion sensor agent (MSA) to monitor motion inside the conference room from the Proteus M5 WiFi motion sensor.

In this figure, the demand response agent (DRA) receives the notification of the CPP event from the OpenADR agent.

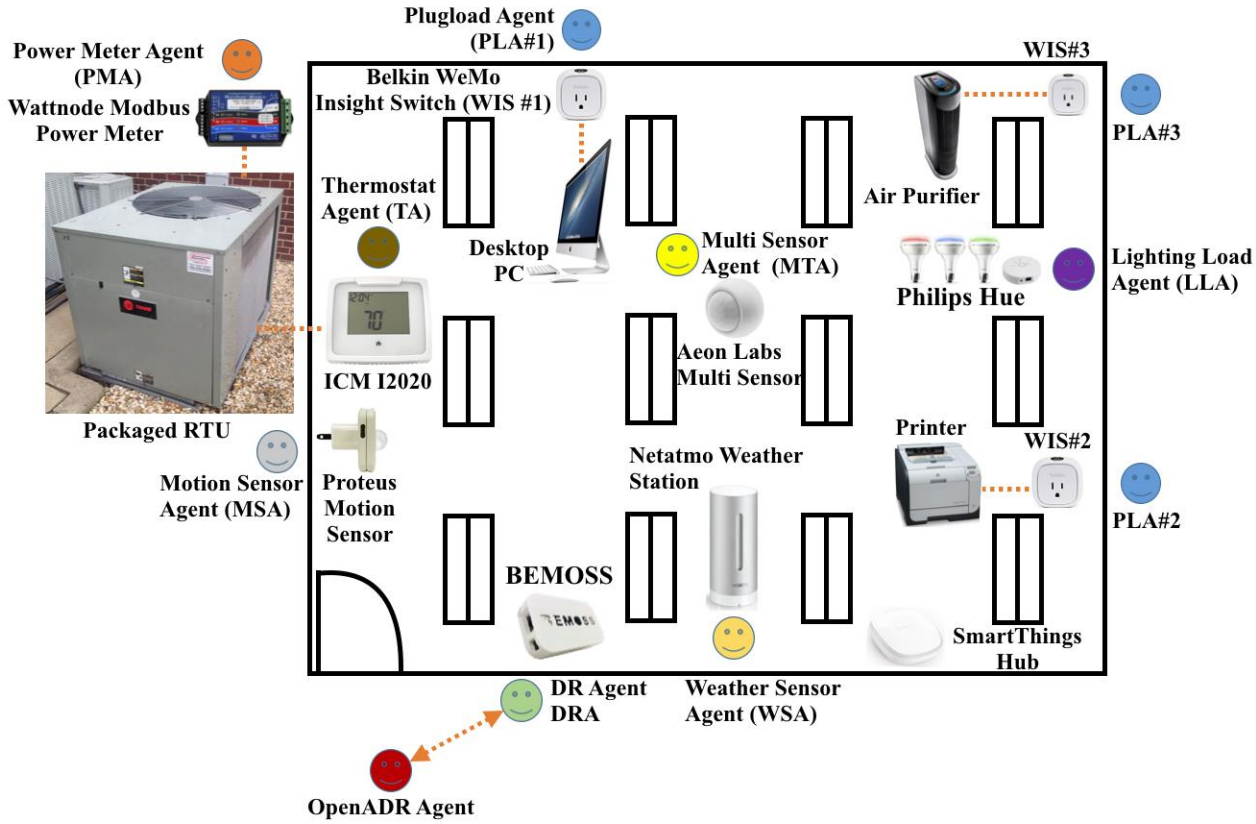

Fig. 5-3. Potomac conference room floor plan, indicating locations of sensors/controllers and corresponding agents

5.2 Case Study Results and Discussions

This section presents the results of the case study with and without the CPP event by comparing energy consumption and power demand of the conference room. Section 5.2.1 presents this results for all loads combined. Sections 5.2.2 and 5.2.3 look at HVAC load and lighting loads, respectively. Sections 5.2.3, 5.2.4 and 5.2.5 report individual plug load data of the desktop PC, the printer and the air purifier, respectively.

5.2.1 Comparison of the Total Energy Consumption and Total Power Demand of the Potomac Conference Room between the Base Case and the DR Case Study

Fig. 5-4 and Fig. 5-5 illustrates the total power demand (P_B) of the conference room 310 for the base case and the DR case study, respectively. The total power demand aggregates the power demand of the packaged RTU, the lighting load, the desktop PC, the printer, the air purifier in this room, presented over the 6-hour period. The power meter agent (PMA) measures the RTU power demand. The lighting load agent (LLA) measures the power demand of the lighting load. Three plugload agents (PLA#1-3) measure power demand of individual plug load in the room,

including the desktop PC, the printer, and the air purifier. The comparison of the total energy consumption (E_B), the maximum of the total power demand (max(P_B)), the minimum of the total power demand (min(P_B)), and the average total power demand (average(P_B)) of the conference room 310 for both the normal base case and the DR case study are summarized in Table 5-2.

Table 5-2. Comparison of the total power demand and the total energy consumption of the Potomac conference room 310 for both the base case and the DR case study

Parameter	Six-hour period (12:00 – 18:00 hrs)			CPP period (13:04 – 16:04 hrs)		
	Base case	DR case	% decrease	Base case	DR case	% decrease
max(P_B)	4.91 kW	4.70 kW	42.8%	4.91 kW	0.98 kW	80.0%
min(P_B)	1.41 kW	0.95 kW	32.6%	1.42 kW	0.95 kW	33.1%
average(P_B)	1.76 kW	1.67 kW	5.1%	1.81 kW	0.97 kW	46.4%
E_B	**10.54 kWh**	**10.02 kWh**	**4.9%**	**5.41 kWh**	**2.90 kWh**	**46.4%**

Table 5-2 shows that the peak demand is reduced by 80% during the CPP period. This is as a result of agents' control actions during the CPP event from max(P_B) = 4.91 kW in the base case to the max(P_B) = 0.98 kW in the DR case study). The total energy consumption is reduced by 46 % during the CPP period where the E_B = 2.90 kWh as compared to E_B = 5.41 kWh in the base case.

However, when considering the six-hour period from 12:00 to 18:00, the overall energy consumption is only reduced by 4.9%, i.e., the base case E_B is 10.54 kWh, while the DR case E_B is 10.02 kWh. This implies that there are compensation actions performed by the agents to pre-condition the space before the CPP event occurs, and restoration actions after the CPP event ends.

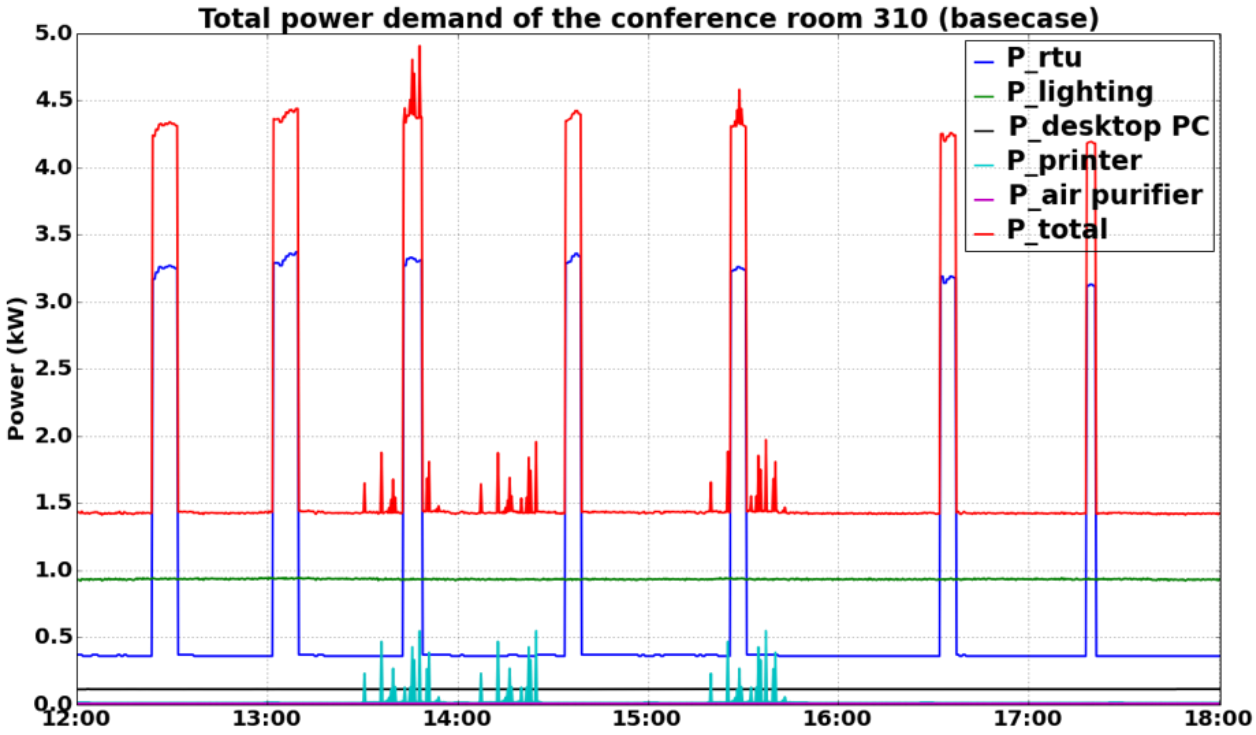

Fig. 5-4. Base Case: total power demand of the Potomac conference room 310

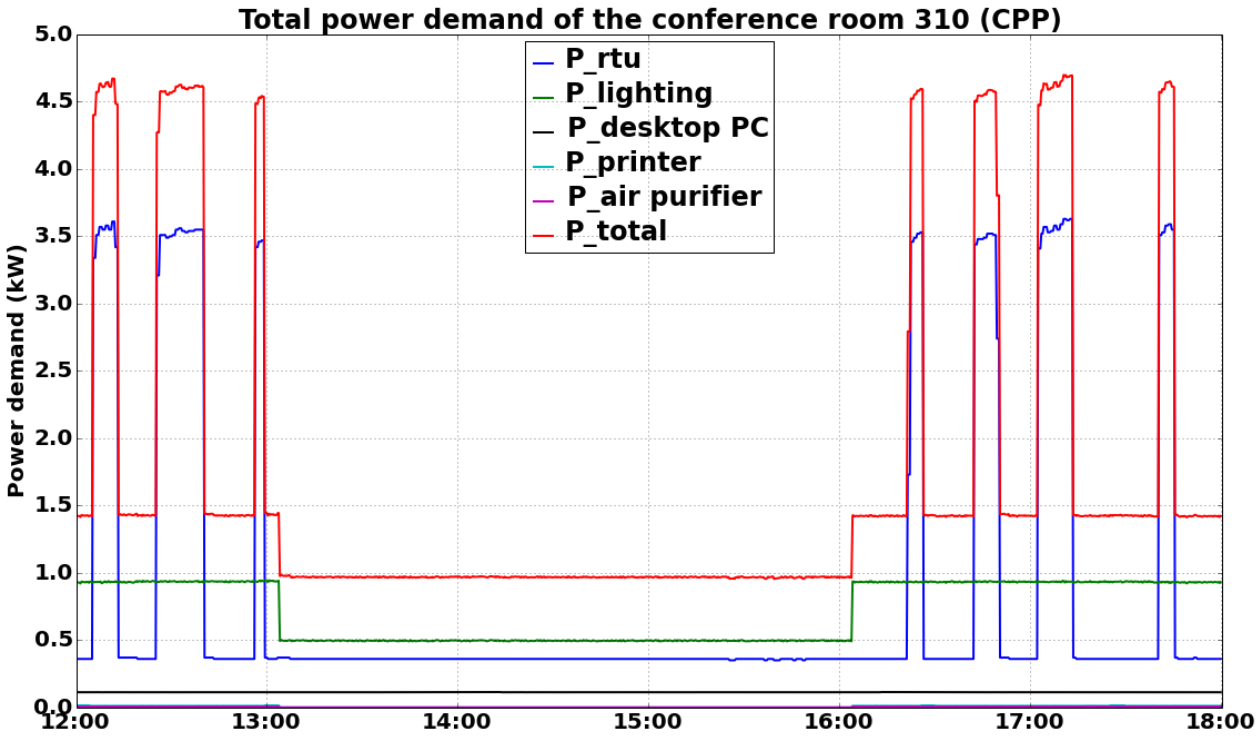

Fig. 5-5. DR Case Study: total power demand of the Potomac conference room 310

5.2.2 Comparison of the Energy Consumption, Power Demand, and Configuration of the Packaged RTU between the Base Case and the DR Case Study

Fig. 5-6 and Fig. 5-7 illustrate the plots of RTU power demand versus the thermostat cooling set point and the room temperature during the study period of six-hour from 12:00 to 18:00 hrs for the base case and the DR case study, respectively. It should be noted that the power demand of the RTU is monitored by the PMA; the TA monitors the thermostat cooling set point and the room temperature.

Table 5-3. Summary of energy and power demand of the RTU for both the base case and the DR case study compares the energy usage, maximum power demand, minimum power demand, and average power demand of the packaged RTU during the six-hour period, the pre-CPP stage, the CPP stage, and the post-CPP stage of both the base case and the DR case study given the corresponding thermostat cooling set point configuration in Table 5-4.

Table 5-3. Summary of energy and power demand of the RTU for both the base case and the DR case study

Parameter	Six-hour period (12:00 – 18:00 hrs)		Pre-CPP (12:24 – 13:04 hrs)		CPP (13:04 – 16:04 hrs)		Post-CPP (16:04 – 17:14 hrs)	
	Base case	DR case	Base case	DR case	Base case	DR case	Base case	DR case
max(P_{RTU})	**3.29 kW**	**3.63 kW**	3.29 kW	3.56 kW	**3.37 kW**	**0.37 kW**	3.19 kW	3.63 kW
min(P_{RTU})	0.36 kW	0.35 kW	0.36 kW	0.36 kW	0.36 kW	0.35 kW	0.36 kW	0.36 kW
average(P_{RTU})	0.69 kW	0.84 kW	1.08 kW	1.77 kW	0.72 kW	0.36 kW	0.56 kW	1.41 kW
E_{RTU}	**4.10 kWh**	**5.01 kWh**	0.70 kWh	1.18 kWh	**2.16 kWh**	**1.08 kWh**	0.65 kWh	1.64 kWh

Table 5-4. Settings of the ICM Controls I2020 thermostat for both the base case and the DR case study

Parameter	Pre-CPP (12:24 – 13:04 hrs)		CPP (13:04 – 16:04 hrs)		Post-CPP (16:04 – 17:14 hrs)	
	Base case	DR case	Base case	DR case	Base case	DR case
max($T_{cooling}$)	74°F	74°F	74°F	78°F	74°F	78°F
min($T_{cooling}$)	74°F	71°F	74°F	78°F	74°F	74°F
average($T_{cooling}$)	74°F	72.05°F	74°F	78°F	74°F	76°F
$status_{FAN}$	"ON"	"ON"	"ON"	"ON"	"ON"	"ON"

Table 5-3 shows the energy consumption of the RTU during the CPP period in the DR case study ($E_{RTU,CPP,DR\ case}$ = 1.08 kWh) is reduced by 50% as compared to the corresponding value in the base case ($E_{RTU,CPP,base}$ = 2.16 kWh). The maximum power demand of the RTU during the CPP period in the DR case study, max($P_{RTU,CPP,DR\ case}$) = 0.37 kW, is almost 90% lower than the corresponding value in the base case where max($P_{RTU,CPP,base}$) = 3.37 kW. This is due to the RTU does not need to operate during the CPP to maintain the comfort condition of the conference room as a result of the pre-cooling process taken by the TA. However, the overall energy consumption over six hours of the RTU for the DR case study ($E_{RTU,6hr,DR\ case}$=4.46 kWh) is higher than its corresponding value of the base case ($E_{RTU,6hr,base}$=4.10 kWh). This is due to the heat loss during the pre-cooling process in the pre-CPP stage and the post-cooling process in the post-CPP stage of the RTU in the DR case study.

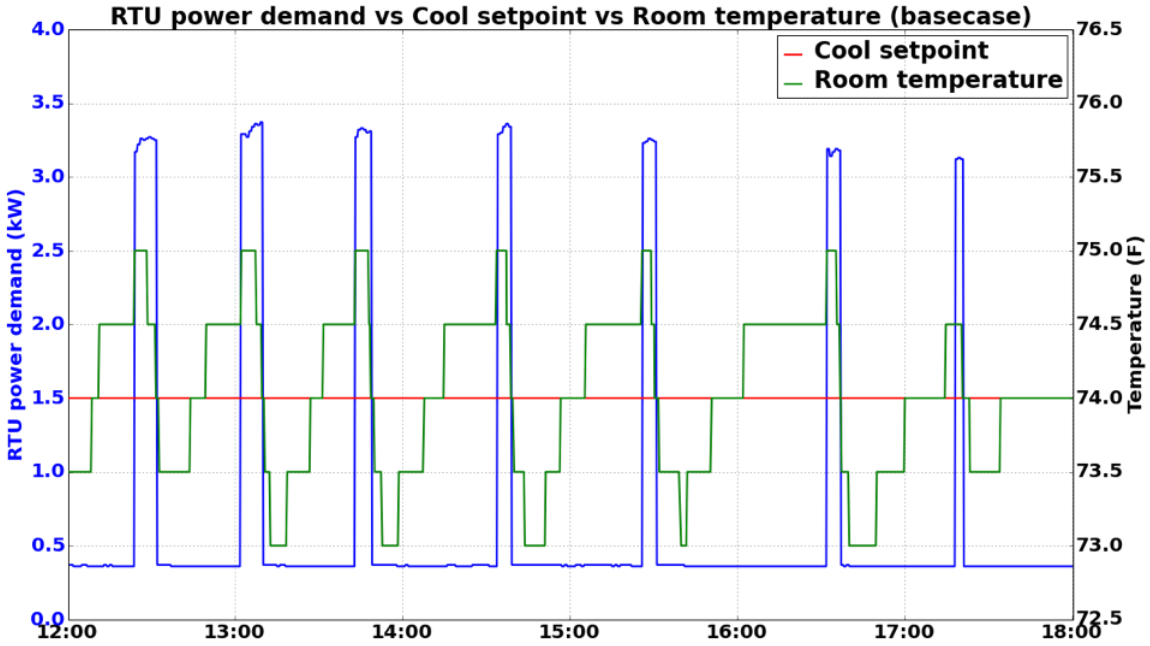

Fig. 5-6. Base Case: power demand of the packaged RTU

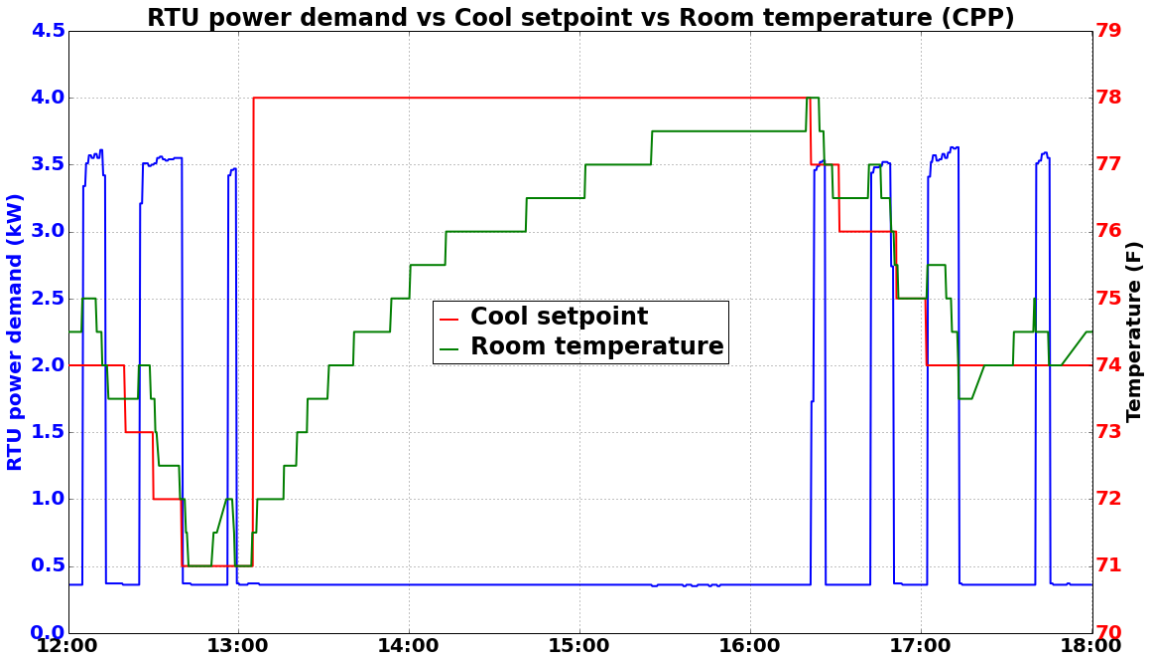

Fig. 5-7. DR Case Study: power demand of the packaged RTU

With the real-world experiment during a normal condition when there is no CPP event, the linear regression models that explain the thermal response of a building when the RTU does not operate (BT_{nop}) and the thermal response of a building when the RTU is in operation (BT_{op}) are given in Eq. 5-1 and Eq. 5-2 shown in Fig. 5-8 and Fig. 5-9, respectively. These regression models are obtained based on the algorithm proposed in Section 3.5.B subtask 2. The estimated

parameters of these linear regression models are learned by the thermostat agent (TA) during a normal condition and being used during in the DR case study to perform per-cooling, hold temperature during a CPP period, and perform post-cooling process.

The thermal response of a building when an RTU does not operate (BT_{nop}) is estimated by keeping the thermostat cooling setpoint higher than the room temperature. Therefore, the room temperature rises over time depending upon heat gain and heat loss through building envelope, lighting equipment, building equipment, and building occupants, etc. due to the change in outdoor weather condition ($T_{outdoor}$). The amount of power demand reduction, the duration for a room temperature to increase to a new cooling setpoint, and the duration for the power demand of an RTU to descend to a new steady-state are predicted based on the estimated building thermal response when an RTU does not operate.

The thermal response of a building when an RTU is in operation (BT_{op}) is estimated by keeping the cooling setpoint lower than the room temperature. Thereby, the room temperature descends over time depending upon heat gain and heat loss through building envelope, lighting equipment, building equipment, and building occupants, etc. due to the change in outdoor weather condition ($T_{outdoor}$). The amount of power demand increment, the duration for a room temperature to decrease to a new cooling setpoint, and the duration for the power demand of an RTU to ascend to a new steady-state are predicted based on the estimated building thermal response when an RTU is in operation.

$$BT_{nop} = 0.06 \cdot T_{outdoor,avg} - 3.12 \qquad \text{(Eq. 5-1)}$$

$$BT_{op} = -0.15 \cdot T_{outdoor,avg} + 20.89 \qquad \text{(Eq. 5-2)}$$

Where,

$T_{outdoor,avg}$: average outdoor temperature during 12:00 pm to 6:00 pm (°F)

BT : building thermal response (BT_{nop} or BT_{op})

$\theta_{0bto}, \theta_{1bto}$: learning parameters of the linear regression model between building thermal response and an average outdoor temperature

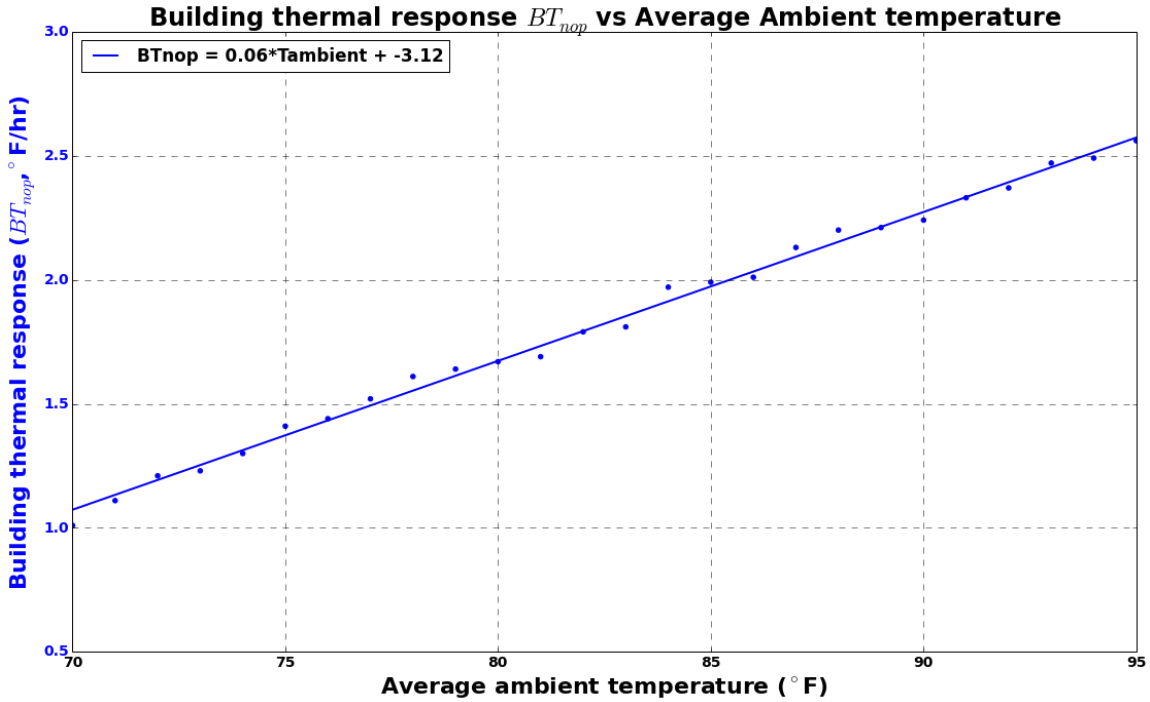

Fig. 5-8. Base Case: relationship between relative humidity and room temperature of the Potomac conference room 310 over six-hour period from 12:00 – 18:00 hrs

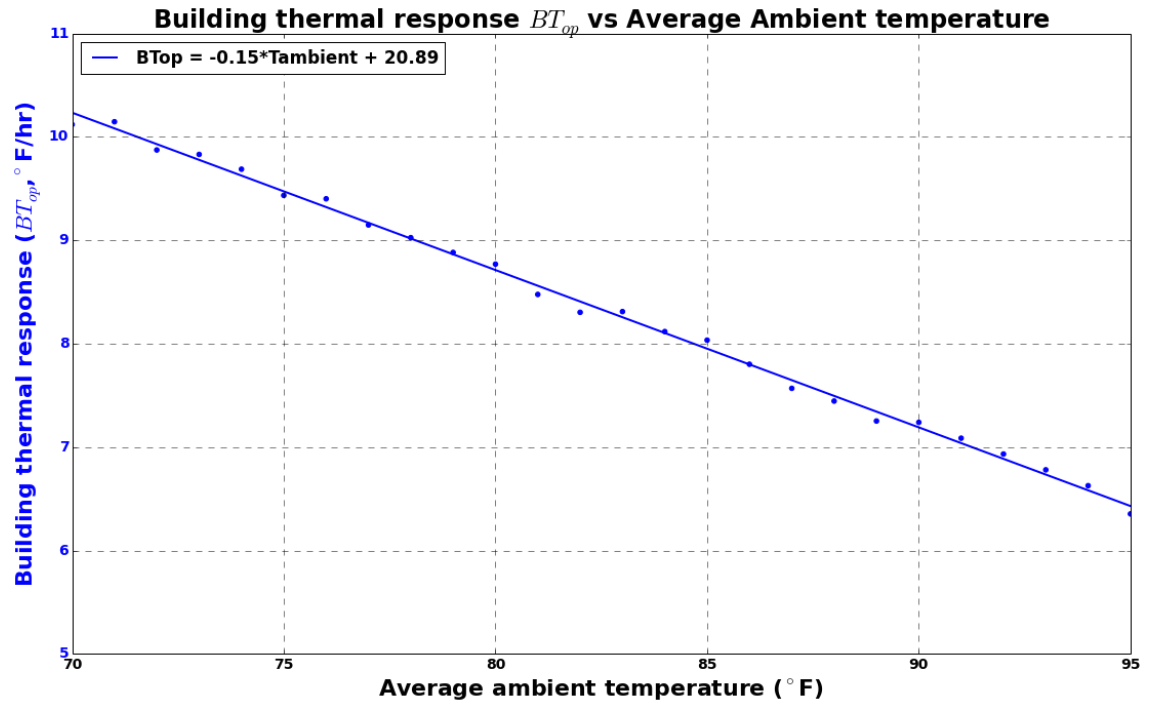

Fig. 5-9. DR Case Study: relationship between relative humidity and room temperature of the Potomac conference room 310 over six-hour period from 12:00 – 18:00 hrs

Fig. 5-10 and Fig. 5-11 illustrates the relationship between the relative humidity (%) and the temperature of the Potomac conference room 310 over 6 hours period for the base case and the DR case study, respectively. Table 5-5 compares relative humidity, room temperature, predicted mean vote (PMV) value, percentage of people dissatisfied value, and comfort violation index value between the base case and the DR case study. It should be noted that the relative humidity ($humidity_{room}$,%) and the room temperature (T_{room}) are monitored by the weather sensor agent (WSA) and the thermostat agent (TA), respectively.

Table 5-5. Summary of the temperature – relative humidity of the Potomac conference room 310 for both base case and the DR case study

Parameter	Six-hour period (12:00 – 18:00 hrs)		Pre-CPP (12:24 – 13:04 hrs)		CPP (13:04 – 16:04 hrs)		Post-CPP (16:04 – 17:14 hrs)	
	Base case	DR case	Base case	DR case	Base case	DR case	Base case	DR case
max(T_{room})	75 °F	78 °F	75 °F	74 °F	75 °F	77.5 °F	75 °F	78 °F
min(T_{room})	73 °F	71 °F	73.5 °F	71 °F	73 °F	72 °F	73 °F	73.5 °F
average(T_{room})	74.04 °F	74.54 °F	74.22 °F	72.06 °F	74 °F	75.9 °F	74 °F	75.67 °F
std(T_{room})	0.55 °F	1.90 °F	0.52 °F	0.99 °F	0.58 °F	1.57 °F	0.49 °F	1.34 °F
max($humidity_{room}$)	66%	71%	65%	68%	66%	71%	66%	68%
min($humidity_{room}$)	62%	62%	62%	63%	63%	63%	64%	62%
average($humidity_{room}$)	64.77%	65.84%	64%	66.50%	64.7%	66.18%	65.43%	64.85%
std($humidity_{room}$)	0.93%	2.56%	1.22 %	1.99%	0.64%	2.35%	0.68%	2.16%
max($\|PMV\|$)	0.18	**0.42**	0.05	0.42	0.18	0.25	0.18	0.34
max(PPD)	6%	**9%**	5%	9%	6%	7%	6%	7%
$T_{max,PMV}$	73 °F	71 °F	73.5 °F	71 °F	73 °F	77.5 °F	73 °F	78 °F
$humidity_{max,PMV}$	64%	63%	62%	63%	64%	63%	64%	64%
min($\|PMV\|$)	0.00	0.02	0.00	0.05	0.00	0.02	0.00	0.05
min(PPD)	5%	5%	5%	5%	5%	5%	5%	5%
$T_{min,PMV}$	74.5 °F	74.5 °F	74.5 °F	74 °F	74.5 °F	74.5 °F	74.5 °F	74 °F
$humidity_{min,PMV}$	65%	68%	65%	67%	65%	68%	65%	67%
CVI	0	0	0	0	0	0	0	0

The temperature – relative humidity charts for both cases are also plotted and compared with the ASHRAE standard 55-2013 as shown in Fig. 5-12 - Fig. 5-19 for the six-hour period, the pre-CPP stage, the CPP stage, and the post-CPP stage.

It can be seen in Fig. 5-12 and Fig. 5-13 that the TA acts to keep the room temperature and humidity within the limits specified by ASHRAE Standard 55-2013 [106] at all time in both the DR case study and the base case.

From Table 5-5, the maximum PMV of the DR case study is 0.42 (PPD is 9%), which is lower than the standard PMV at 0.5 and PPD at 10%. The corresponding room temperature and humidity for this PMV are 71 °F and 63%, respectively. This condition happens during the pre-cooling process of the TA.

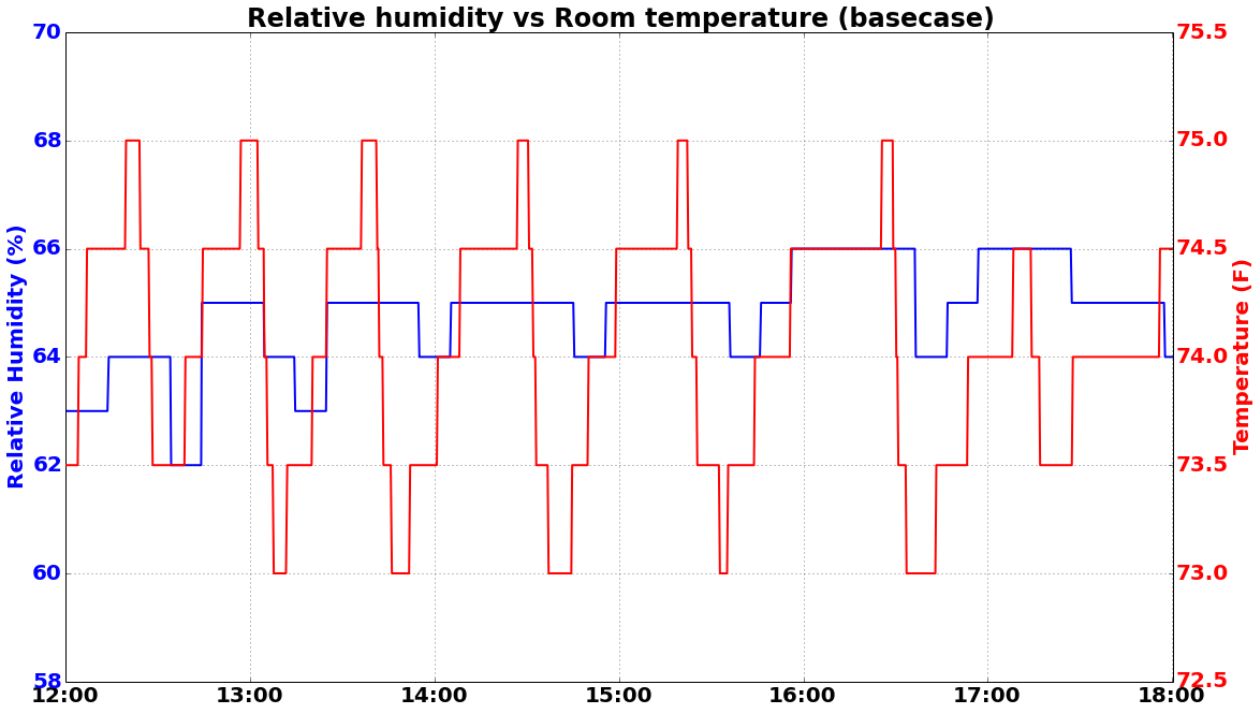

Fig. 5-10. Base Case: relationship between relative humidity and room temperature of the Potomac conference room 310 over six-hour period from 12:00 – 18:00 hrs

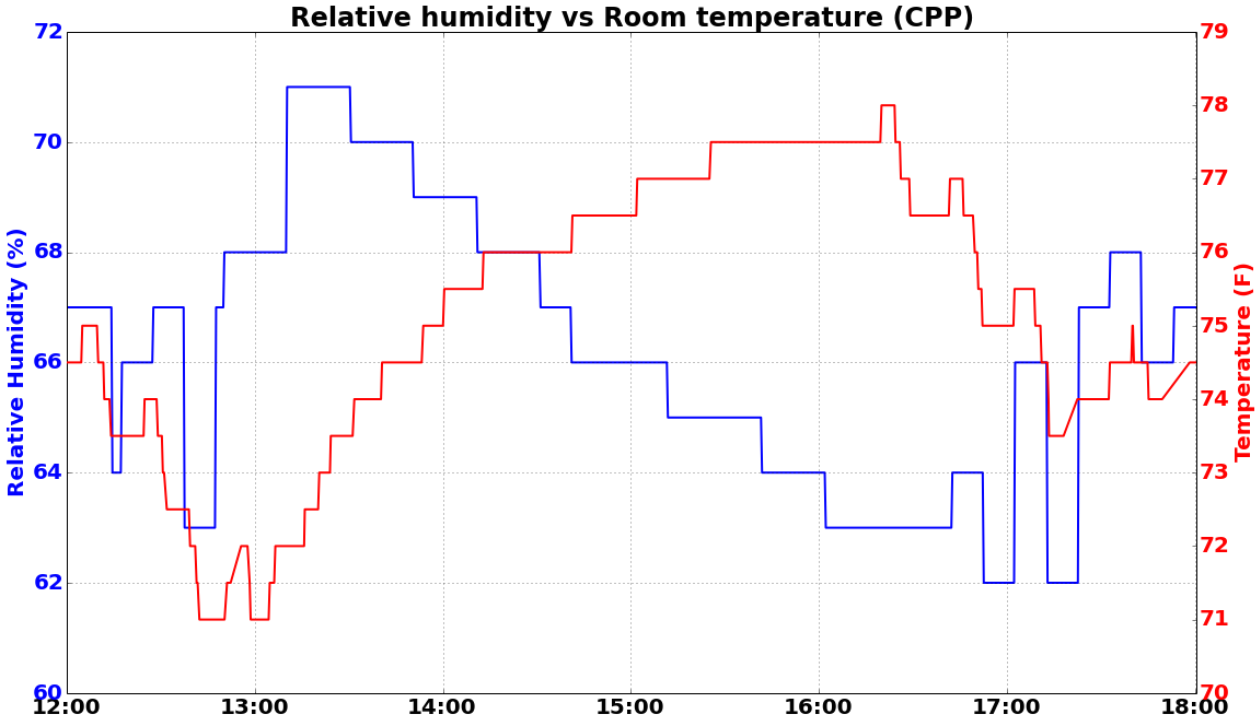

Fig. 5-11. DR Case Study: relationship between relative humidity and room temperature of the Potomac conference room 310 over six-hour period from 12:00 – 18:00 hrs

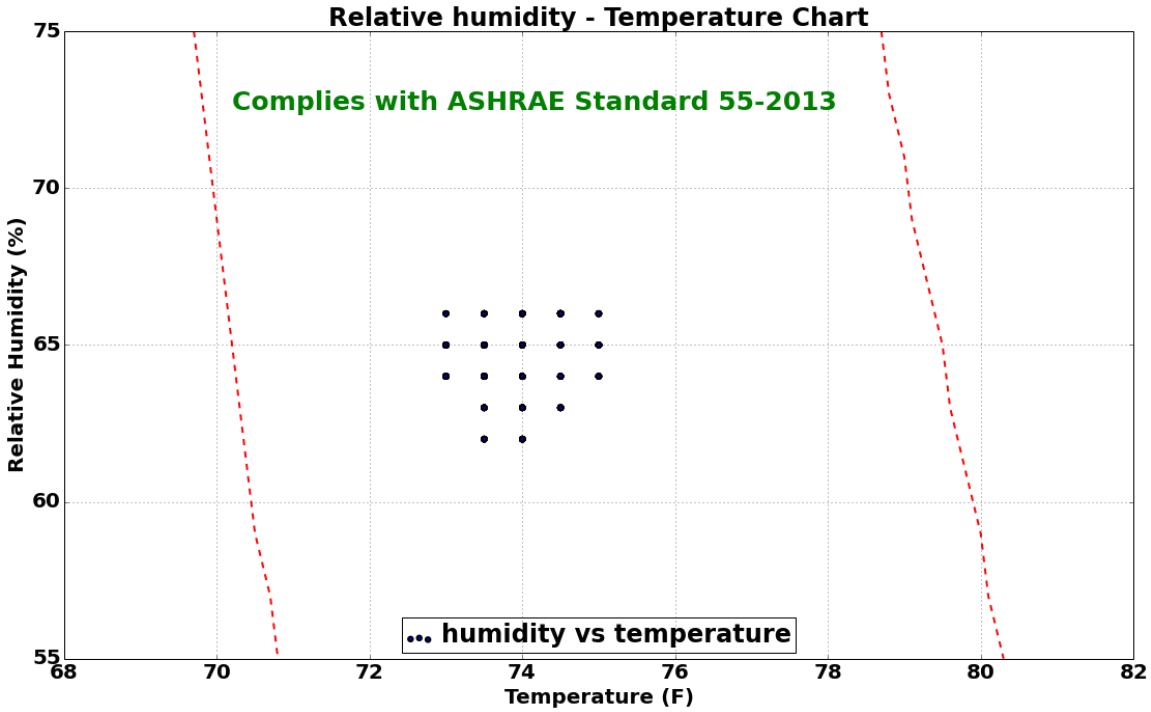

Fig. 5-12. Base Case: relationship between relative humidity and room temperature of the Potomac conference room 310 over the six-hour period

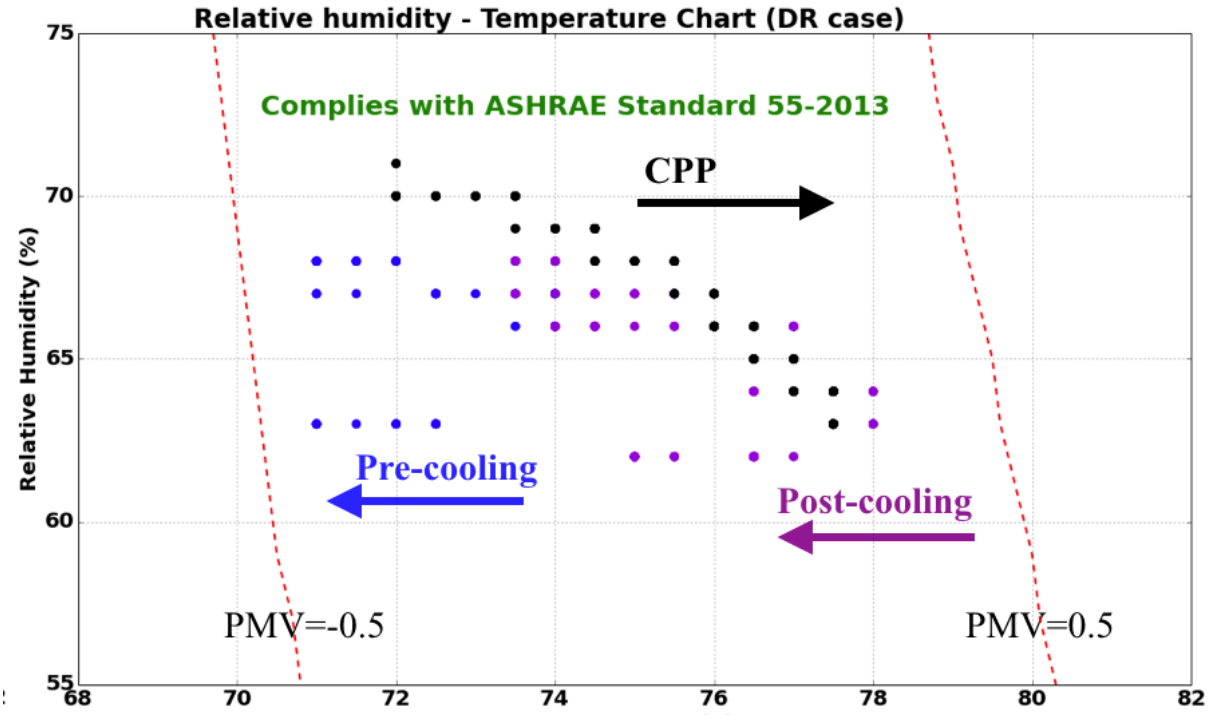

Fig. 5-13. DR Case Study: relationship between relative humidity and room temperature of the Potomac conference room 310 over the six-hour period

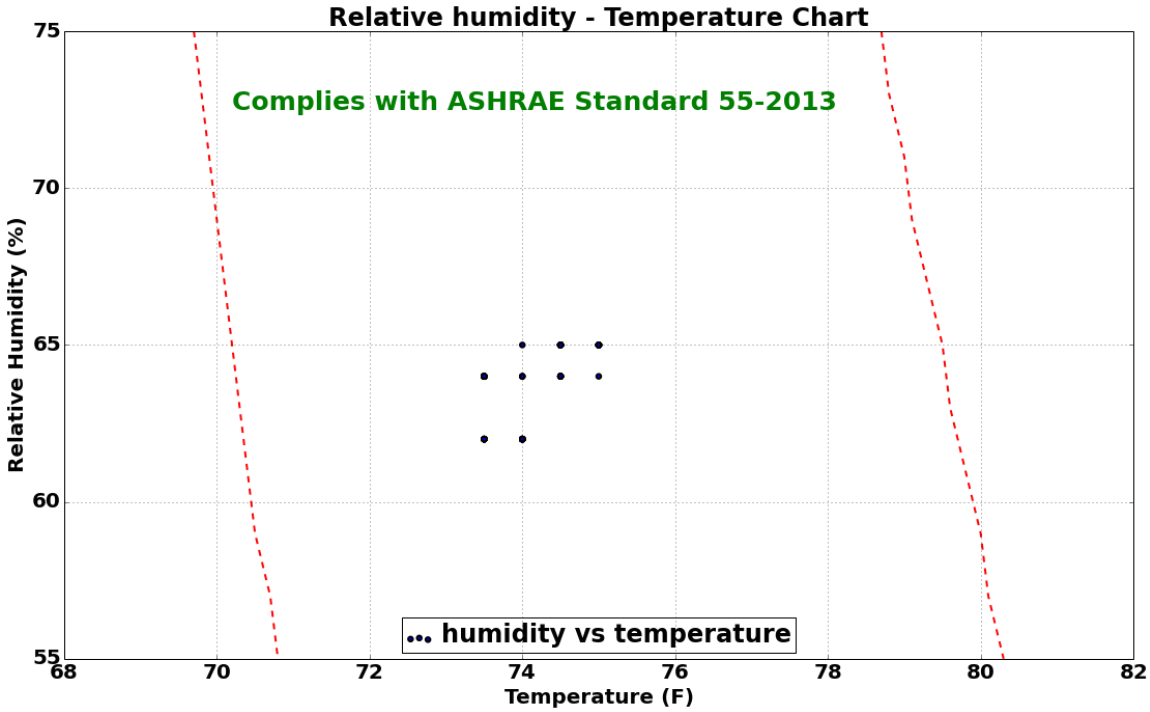

Fig. 5-14. Base Case: relationship between relative humidity and room temperature of the Potomac conference room 310 during the pre-CPP stage

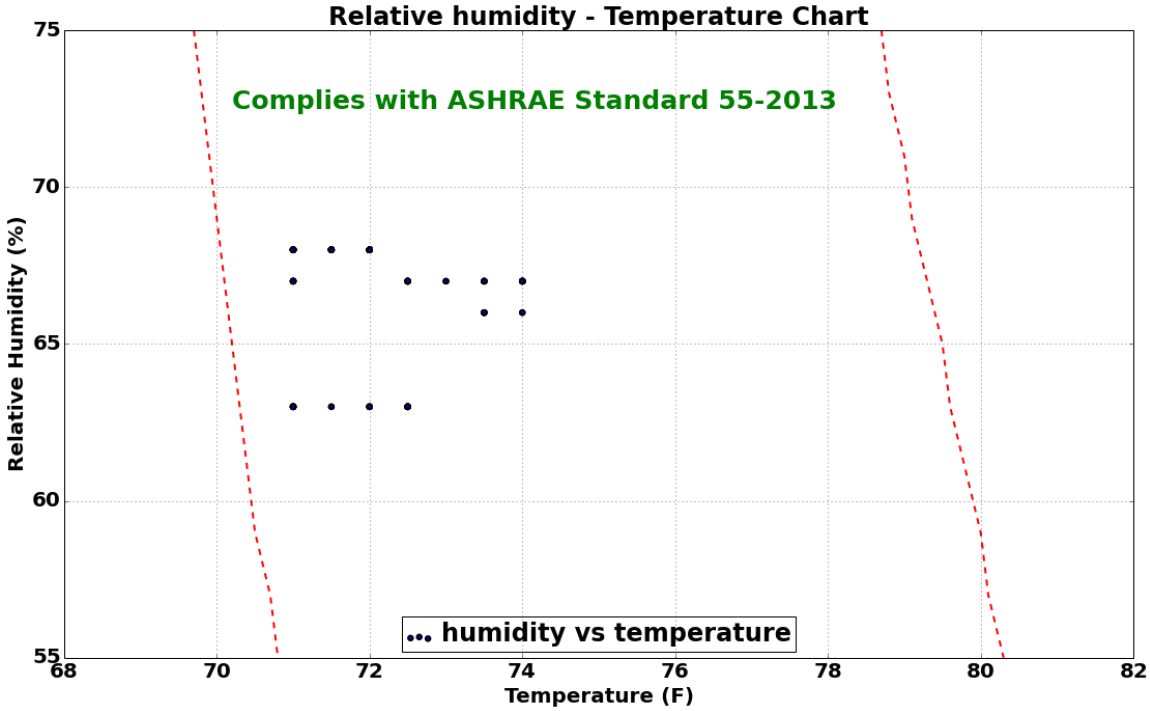

Fig. 5-15. DR Case: relationship between relative humidity and room temperature of the Potomac conference room 310 during the pre-CPP stage

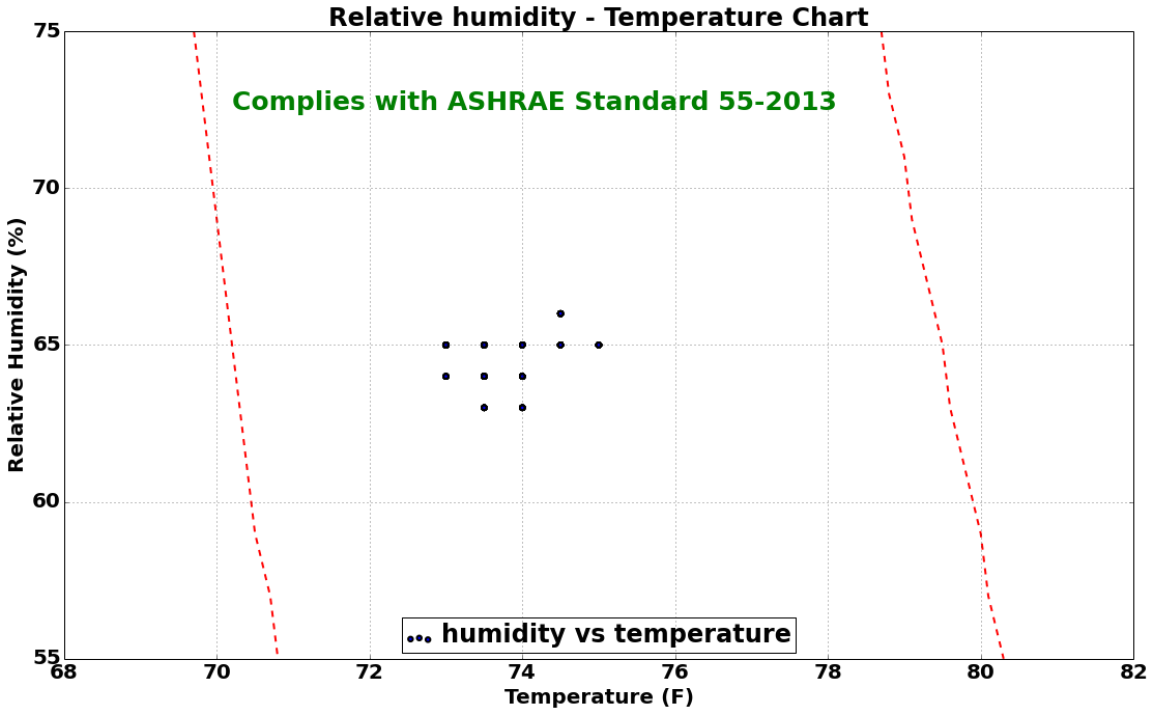

Fig. 5-16. Base Case: relationship between relative humidity and room temperature of the Potomac conference room 310 during the CPP stage

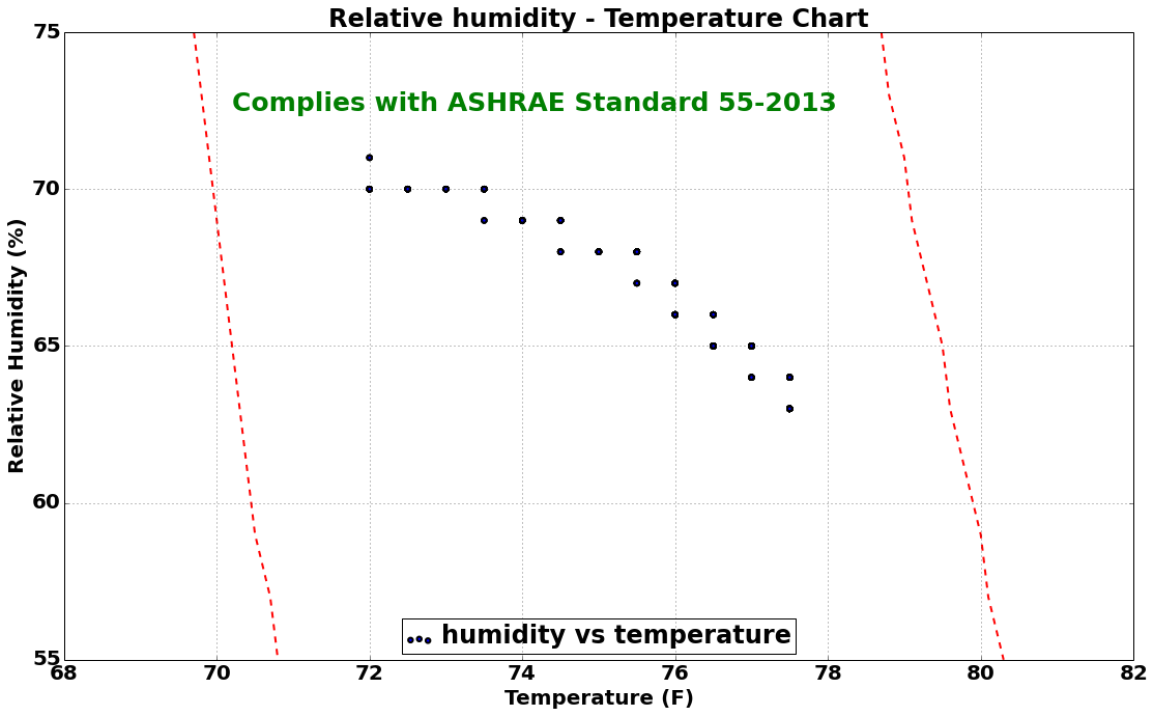

Fig. 5-17. DR Case: relationship between relative humidity and room temperature of the Potomac conference room 310 during the CPP stage

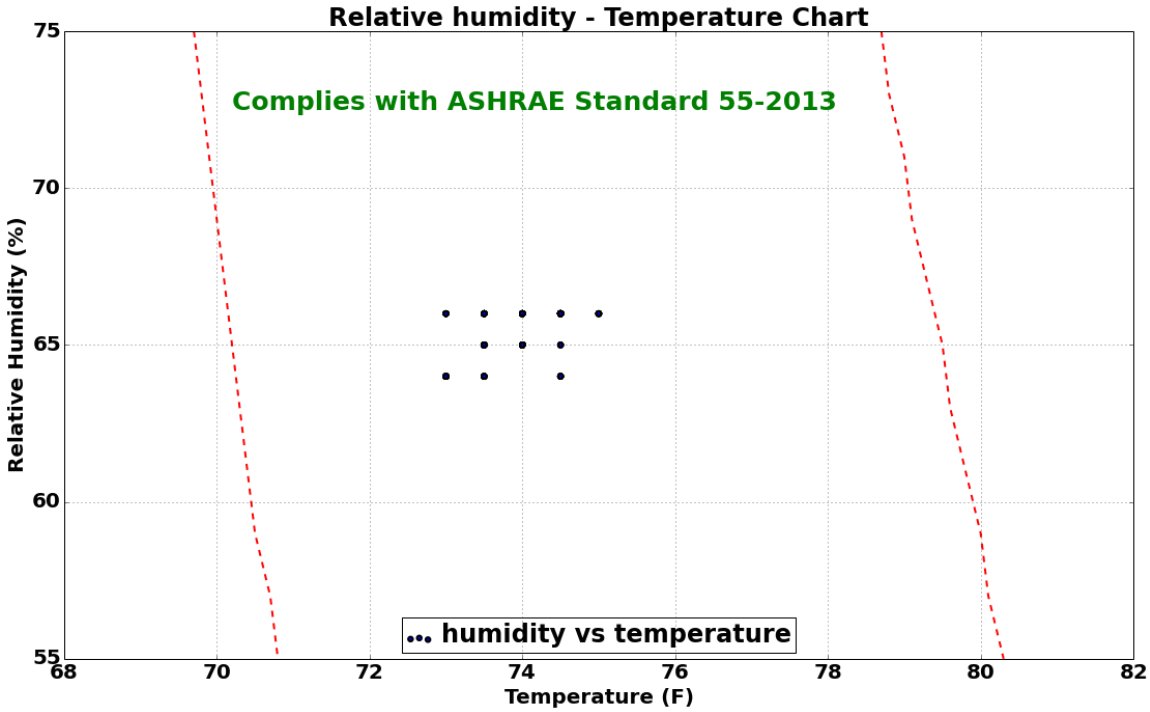

Fig. 5-18. Base Case: relationship between relative humidity and room temperature of the Potomac conference room 310 during the post-CPP stage

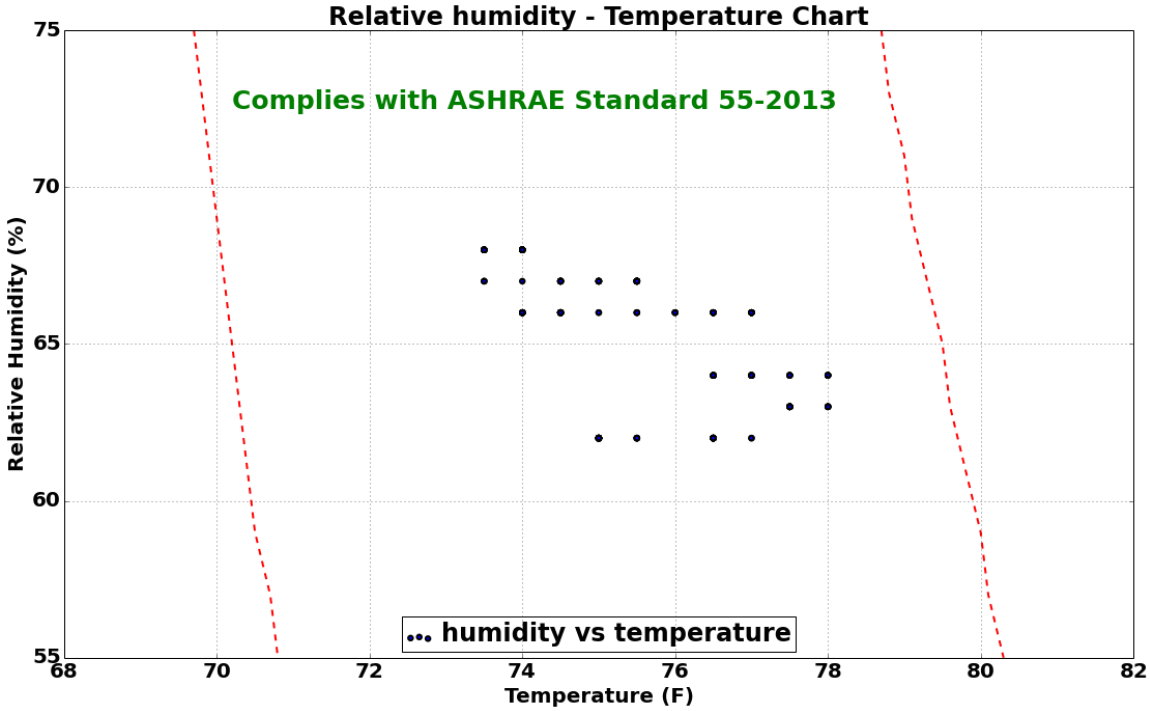

Fig. 5-19. DR Case: relationship between relative humidity and room temperature of the Potomac conference room 310 during the post-CPP stag

Fig. 5-20 and Fig. 5-21 depict the relationships between power demand of the RTU (monitored by the power meter agent, PMA) and the CO_2 level (monitored by the weather sensor agent, WSA) of the Potomac conference room 310 for the base case and the DR case study, respectively.

Table 5-6 compares the power demand and the CO_2 level inside the Potomac conference room 310 for both the base case and the DR case study over the six-hour period, the pre-CPP stage, the CPP stage, and the post-CPP stage. From Table 5-6, it shows that the TA is keeps the CO_2 level to be under the 1,000 ppm limit at all time where the maximum CO_2 level is 313 ppm happens during the CPP event when the RTU does not operate.

Table 5-6. Summary of the power demand of the RTU and the CO_2 level of the Potomac conference room 310 for both base case and the DR case study

Parameter	Six-hour period (12:00 – 18:00 hrs)		Pre-CPP (12:24 – 13:04 hrs)		CPP (13:04 – 16:04 hrs)		Post-CPP (16:04 – 17:14 hrs)	
	Base case	DR case	Base case	DR case	Base case	DR case	Base case	DR case
max(P_{RTU})	3.29 kW	3.63 kW	3.29 kW	3.56 kW	3.37 kW	0.37 kW	3.19 kW	3.63 kW
min(P_{RTU})	0.36 kW	0.35 kW	0.36 kW	0.36 kW	0.36 kW	0.35 kW	0.36 kW	0.36 kW
average(P_{RTU})	0.69 kW	0.84 kW	1.08 kW	1.77 kW	0.72 kW	0.36 kW	0.56 kW	1.41 kW
E_{RTU}	4.10 kWh	4.46 kWh	0.70 kWh	1.18 kWh	2.16 kWh	1.08 kWh	0.65 kWh	1.64 kWh
max(CO_2)	266 ppm	313 ppm	249 ppm	271 ppm	266 ppm	311 ppm	238 ppm	313 ppm
min(CO_2)	215 ppm	231 ppm	234 ppm	254 ppm	215 ppm	231 ppm	225 ppm	269 ppm
average(CO_2)	238.52 ppm	275.8 ppm	247.45 ppm	261.02 ppm	238.69 ppm	268.45 ppm	233.03 ppm	298.13 ppm

5.2.3 Comparison of Total Energy Consumption, Power Demand, and Configuration of the Lighting Load between the Base Case and the DR Case Study

Fig. 5-22 and Fig. 5-23 illustrate the plots of the lighting load power demand versus the brightness level and illuminance level of the Potomac conference room 310 over the six-hour period for the base case and the DR case study, respectively. The power demand and the brightness level of the lighting load are monitored by the lighting load agent (LLA); the illuminance level is monitored by the multi sensor agent (MTA).

Table 5-7 summarizes the energy usage, power demand, brightness level, and illuminance level of the lighting load for both the base case and the DR case study over the six-hour period, the CPP stage, and the post-CPP stage.

Table 5-7 shows that the energy consumption of the lighting load during the CPP period in the DR case study ($E_{lighting\ load,CPP,DR\ case}$ = 1.49 kWh) is reduced by 47% as compared to the corresponding value in the base case ($E_{lighting\ load,CPP,base}$ = 2.79 kWh). The maximum power demand of the lighting load during the CPP period in the DR case study, max($P_{lighting\ load,CPP,DR\ case}$) = 0.50 kW, is 47% lower than the corresponding value in the base case where max($P_{lighting\ load,CPP,base}$) = 0.945 kW. This is due to the brightness of the lighting is reduced from 100% to 62% during the CPP period in the DR case study.

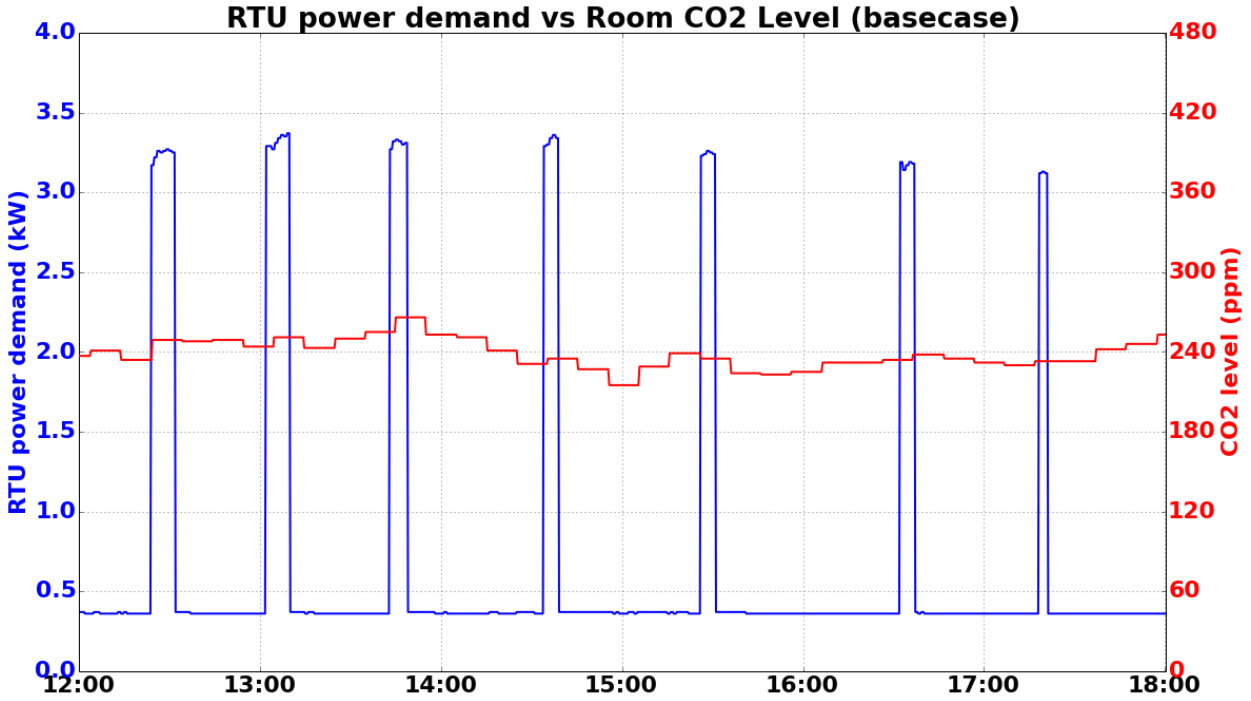

Fig. 5-20. Base Case: relationship between power demand of the RTU and the CO_2 level of the Potomac conference room 310 over the six-hour period

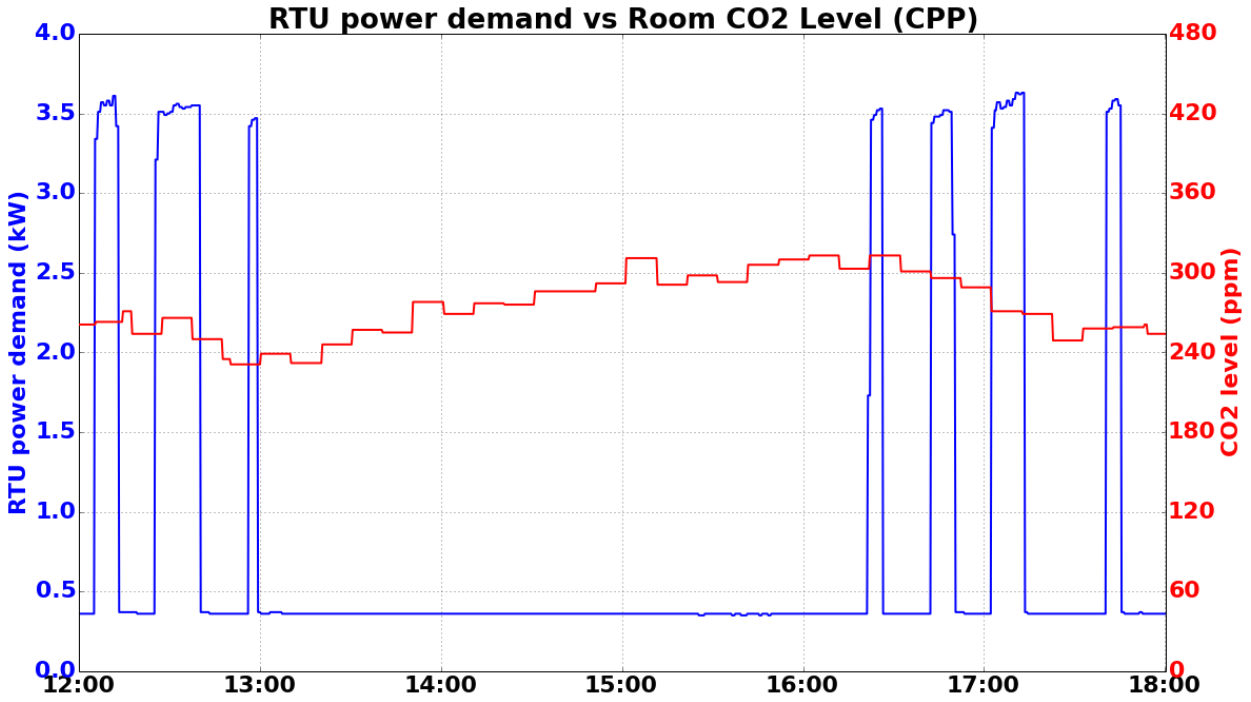

Fig. 5-21. DR Case Study: relationship between power demand of the RTU and the CO_2 level of the Potomac conference room 310 over the six-hour period

Table 5-7. Summary of the power demand, brightness level, and illuminance level of the lighting load for both base case and the DR case study

Parameter	Six-hour period (12:00 – 18:00 hrs)		CPP (13:04 – 16:04 hrs)		Post-CPP (16:05 – 16:12 hrs)	
	Base case	DR case	Base case	DR case	Base case	DR case
max($P_{lighting\_load}$)	0.945 kW	0.947 W	0.945 W	0.5 kW	0.938 kW	0.938 kW
min($P_{lighting\_load}$)	0.927 kW	0.491 W	0.927 W	0.491 kW	0.928 kW	0.490 kW
average($P_{lighting\_load}$)	0.936 kW	0.714 W	0.936 W	0.496 kW	0.932 kW	0.888 kW
$E_{lighting\_load}$	**5.59 kWh**	**4.28 kWh**	**2.79 kWh**	**1.49 kWh**	-	-
max($Brightness$)	100 %	100%	100%	62%	100%	100%
min($Brightness$)	100 %	62%	100%	62%	100%	100%
average($Brightness$)	100 %	81%	100%	62%	100%	100%
max($Illuminance$)	558 lux	555 lux	558 lux	356 lux	531 lux	536 lux
min($Illuminance$)	475 lux	**303 lux**	475 lux	**303 lux**	490 lux	307 lux
average($Illuminance$)	515 lux	422 lux	511 lux	326 lux	510 lux	365 lux

The energy consumption over 6-hour period of the lighting load in the DR case study ($E_{lighting\ load,6hr,DR\ case}$ = 4.28 kWh) is lower than the corresponding value in the base case ($E_{lighting\ load,6hr,base}$ = 5.59 kWh). Table 5-7 shows that while the LLA reducing the brightness of the lighting load during the CPP period in the DR case study, the minimum illuminance of the conference room (303 lux) is still higher than the recommended illumination level (300 lux) by the IESNA standard 90.1-2007 [109]. This illuminance reduces from 475 lux in the base case where the LLA keeps the lighting load brightness at 100%.

With the real-world experiment during a normal condition when there is no CPP event, the linear regression model that explains the relationship between the power demand and brightness level; and the relationship between the illuminance level and the brightness level, shown in Fig. 5-24, can be obtained using the algorithm presented in Section 3.5.B subtask 3.

The estimated parameters of these linear regression models are learned by the lighting load agent (LLA) during a normal condition by performing automatic brightness adjustment to observe the relationships between brightness level, power demand, and illuminance level. The linear regression model of the power demand and brightness level is given in Eq. 5-3. The linear regression model of the illuminance and brightness level is given in Eq. 5-4.

$$P_{Lighting\ load} = 9.12 \cdot Bri_{\%} - 74.95 \qquad \text{(Eq. 5-3)}$$

$$Illumiance = 4.97 \cdot Bri_{\%} + 18.3 \qquad \text{(Eq. 5-4)}$$

Where,

$P_{Lighting\ load}$: instantaneous power demand of a lighting load (W)
$Illuminance$: illuminance measured at 0.8 meter from the height off the floor (lux)
$Bri_{\%}$: brightness level in % of the lighting load controller (range from 0% - 100%)

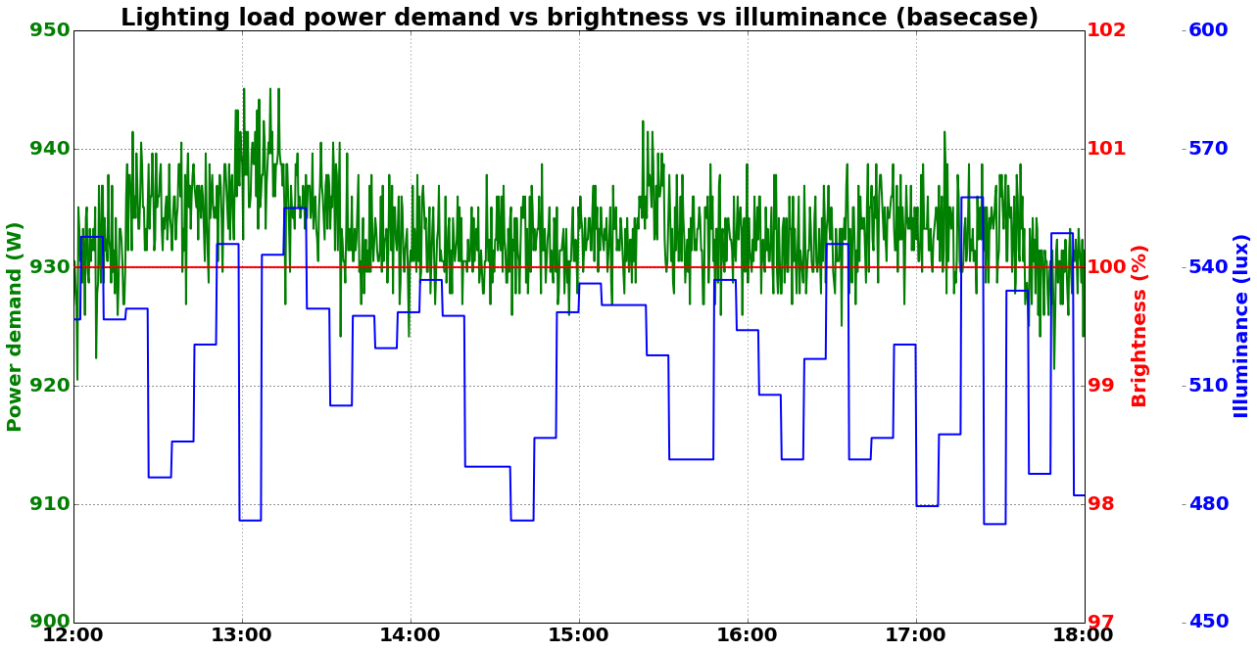

Fig. 5-22. Base Case: Lighting load power demand, brightness level, and illuminance level

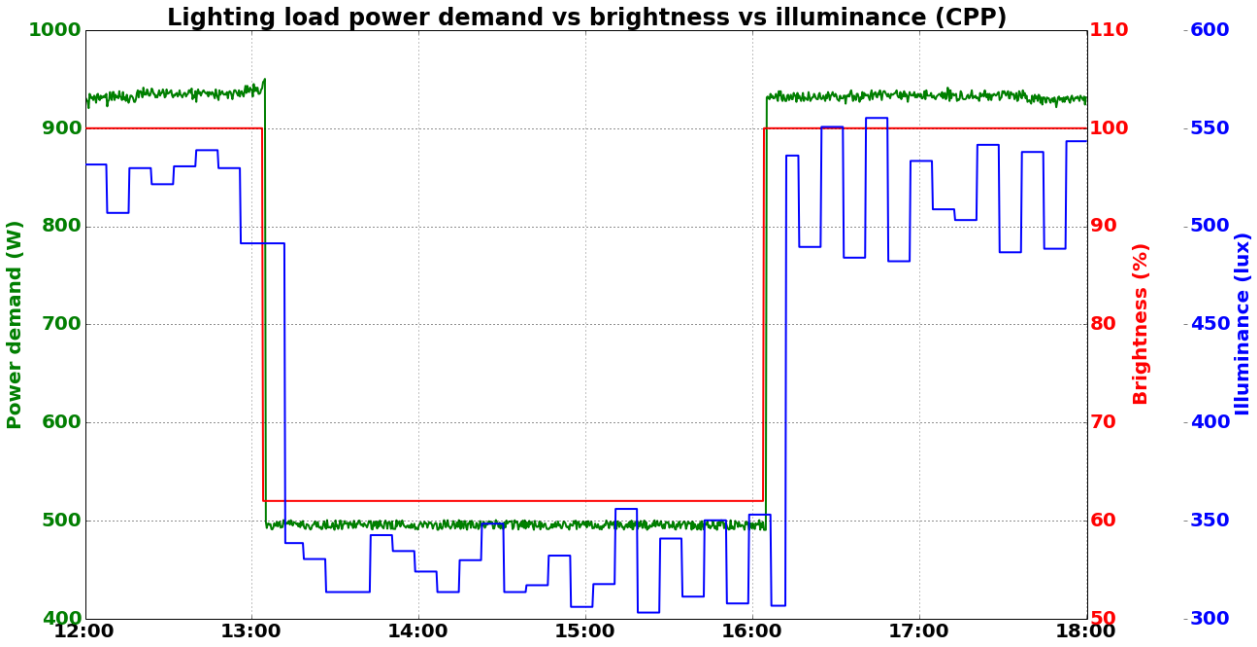

Fig. 5-23. DR Case Study: Lighting load power demand, brightness level, and illuminance level

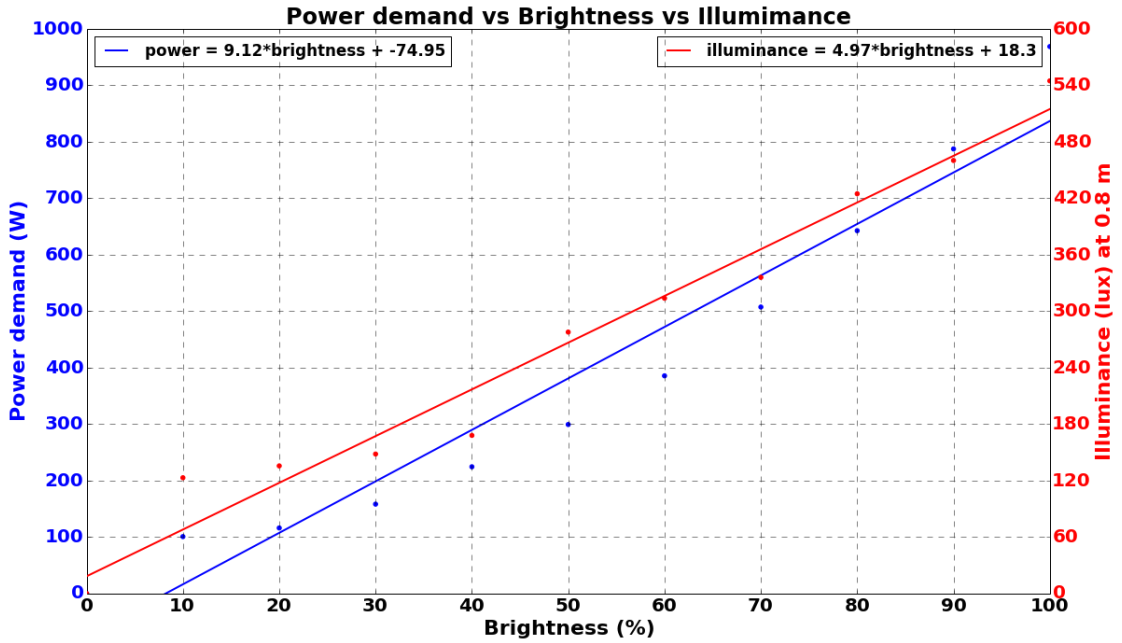

Fig. 5-24. Linear regression models of the load power demand ($P_{Lighting\ load}$) versus brightness level ($Bri_{\%}$), and illuminance level ($Illumiance$) versus brightness level ($Bri_{\%}$) learned by the LLA during a normal condition

5.2.4 Comparison of Total Energy Consumption, Power Demand, and Configuration of the Desktop PC between the Base Case and the DR Case Study

Fig. 5-25 and Fig. 5-26 illustrate power demand of the desktop PC and the corresponding plug load controller status monitored by the PLA#1 over the six-hour period for the base case and the DR case study, respectively.

Table 5-8 summarizes the power demand and the energy usage the desktop PC over the six-hour period and the CPP-period for both the base case and the DR case study. Table 5-8 shows that there is indifferent between the energy consumption of the desktop PC during the CPP period either in the DR case study ($E_{desktop\ PC,6hr,DR\ case}$ = 0.338 kWh) and the base case ($E_{desktop\ PC,6hr,base}$ = 0.338 kWh). This is because the desktop PC is the critical load; thus the PLA#1 does not need to take any action, but keeps status of a plug load $status_{desktop\_PC}$ to be the same as the normal stage prior to the CPP period as "ON".

Table 5-8. Summary of the desktop PC power demand energy consumption for both base case and DR case study

Parameter	Six-hour period (12:00 – 18:00 hrs)		CPP (13:04 – 16:04 hrs)	
	Base case	DR case	Base case	DR case
max($P_{desktop\_PC}$)	113.97 W	113.97 W	113.97 W	113.97 W
min($P_{desktop\_PC}$)	112.35 W	112.35 W	112.36 W	112.36 W
average($P_{desktop\_PC}$)	112.77 W	112.77 W	112.76 W	112.75 W
$E_{desktop\_PC}$	0.676 kWh	0.676 kWh	0.338 kWh	0.338 kWh
$Status_{desktop\_PC}$	"ON"	"ON"	"ON"	"ON"

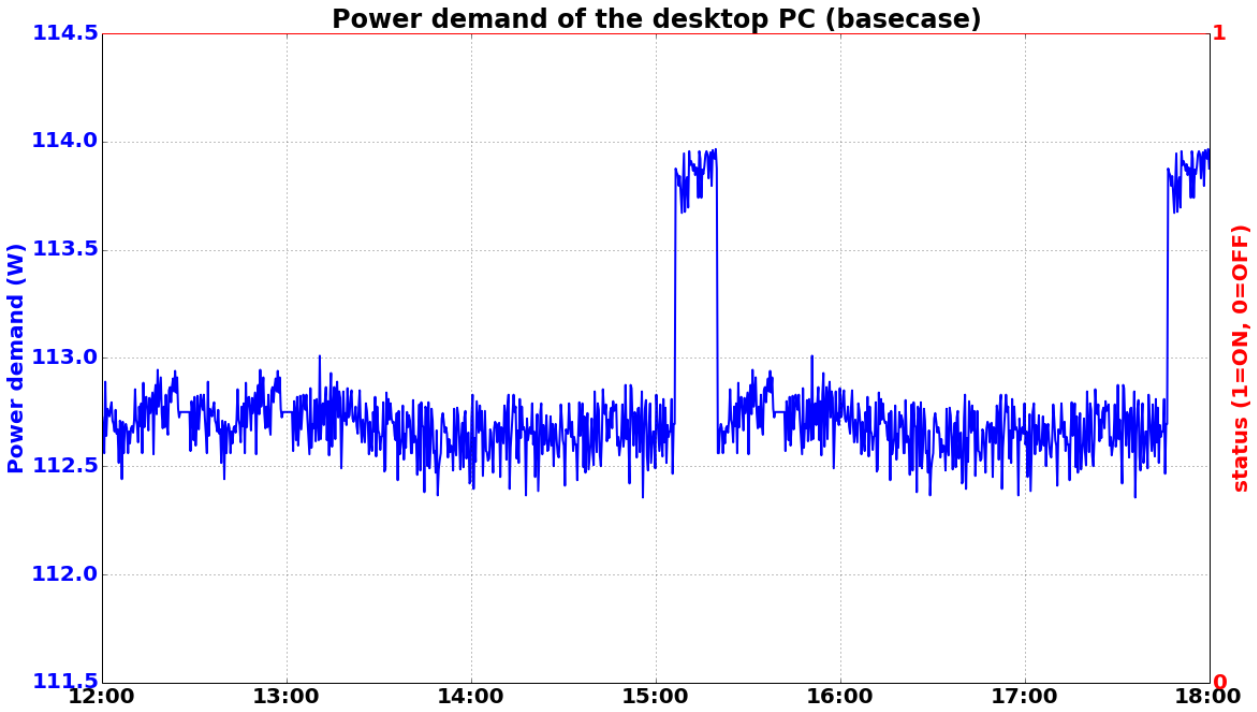

Fig. 5-25. Base Case: Desktop PC power demand and its status

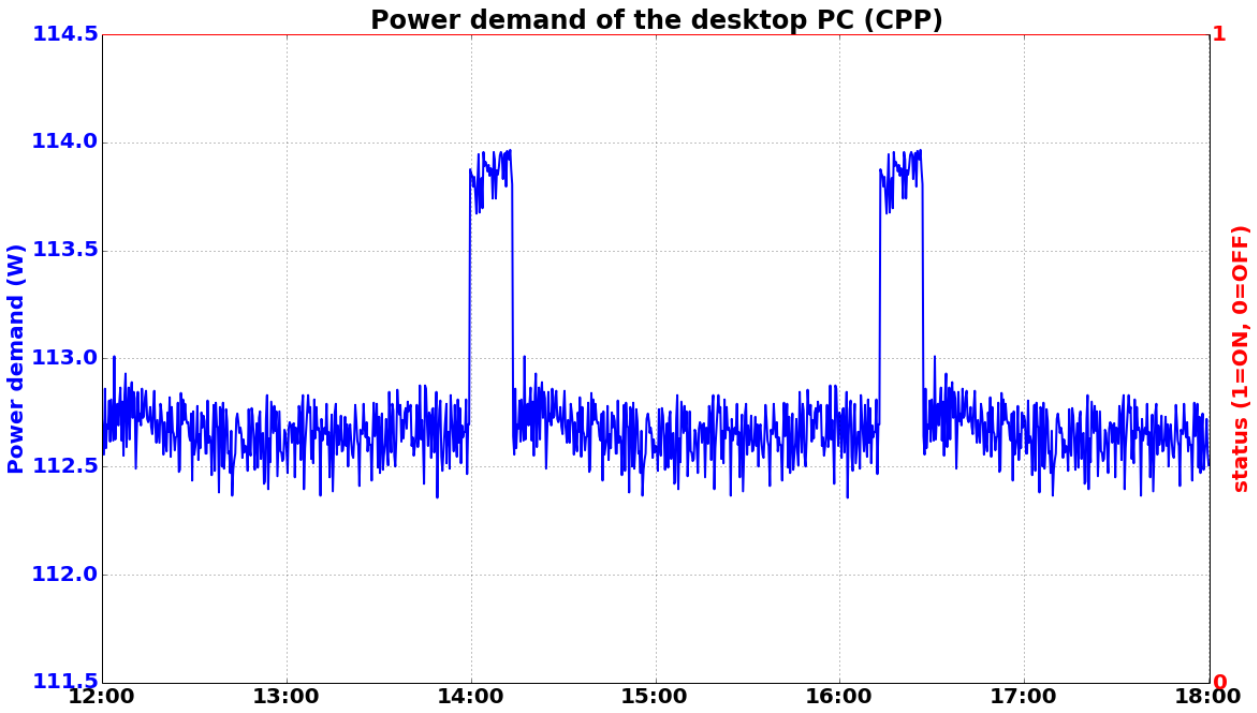

Fig. 5-26. DR Case Study: Desktop PC power demand and its status

5.2.5 Comparison of Total Energy Consumption, Power Demand, and Configuration of the Printer between the Base Case and the DR Case Study

Fig. 5-27 and Fig. 5-28 illustrate power demand of the printer and the corresponding plug load controller status monitored by the PLA#2 over the six-hour period for the base case and the DR case study, respectively.

Table 5-9 summarizes the power demand and the energy usage the desktop PC over the six-hour period and the CPP-period for both the base case and the DR case study.

Table 5-9 Summary of the printer power demand and its status for both base case and the DR case study

Parameter	Six-hour period (12:00 – 18:00 hrs)		Pre-CPP (13:03 hrs)		CPP (13:04 – 16:04 hrs)		Post-CPP (16:05 hrs)	
	Base case	DR case	Base case	DR case	Base case	DR case	Base case	DR case
max($P_{printer}$)	547.35 W	14.66 W	14.66 W	14.66 W	547.35 W	0 W	11.19 W	11.51 W
min($P_{printer}$)	11.19 W	0 W	14.66 W	14.66 W	11.19 W	0 W	11.19 W	11.51 W
average($P_{printer}$)	21.19 W	5.79 W	14.66 W	14.66 W	30.80 W	0 W	11.19 W	11.51 W
$E_{printer}$	0.127 kWh	0.035 kWh	-	-	0.092 kWh	0 kWh	-	-
$Status_{printer}$	"ON"	"ON/OFF/ ON"	"ON"	"ON"	"ON"	"OFF"	"ON"	"ON"

Table 5-9 shows that the energy consumption of the printer during the CPP period in the DR case study ($E_{printer,CPP,DR\ case}$ = 0 kWh) is reduced by 100% as compared to the corresponding value in the base case ($E_{printer,CPP,base}$ = 0.092 kWh). The maximum power demand of the printer during the CPP period in the DR case study, max($P_{printer,CPP,DR\ case}$) = 0 kW, is 100% lower than the corresponding value in the base case where max($P_{printer,CPP,base}$) = 0.547 kW. This is due to PLA#2 turn off the printer's smart plug the during the CPP period in the DR case study. The energy consumption over 6-hour period of the printer in the DR case study ($E_{printer,6hr,DR\ case}$ = 0.035 kWh) is 72% lower than the corresponding value in the base case ($E_{printer,6hr,base}$ = 0.127 kWh). This is because the printer is not turned on during the CPP period in the DR case study.

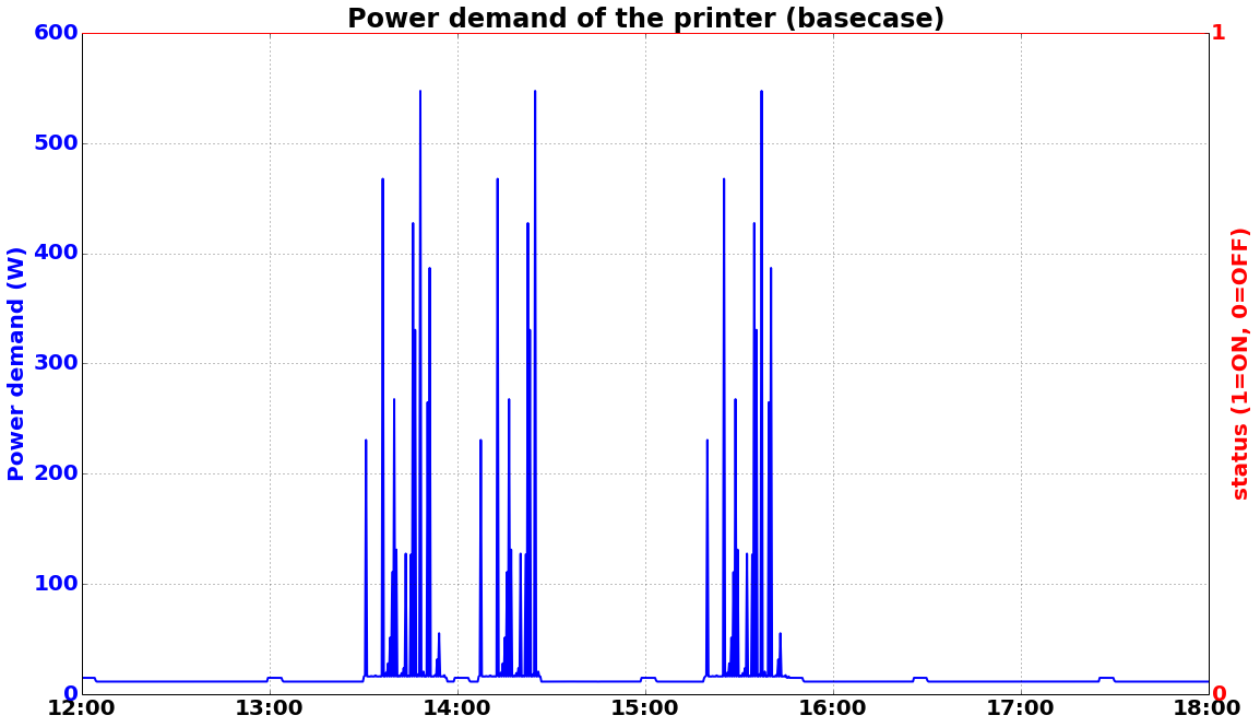

Fig. 5-27. Base Case: printer power demand and its status

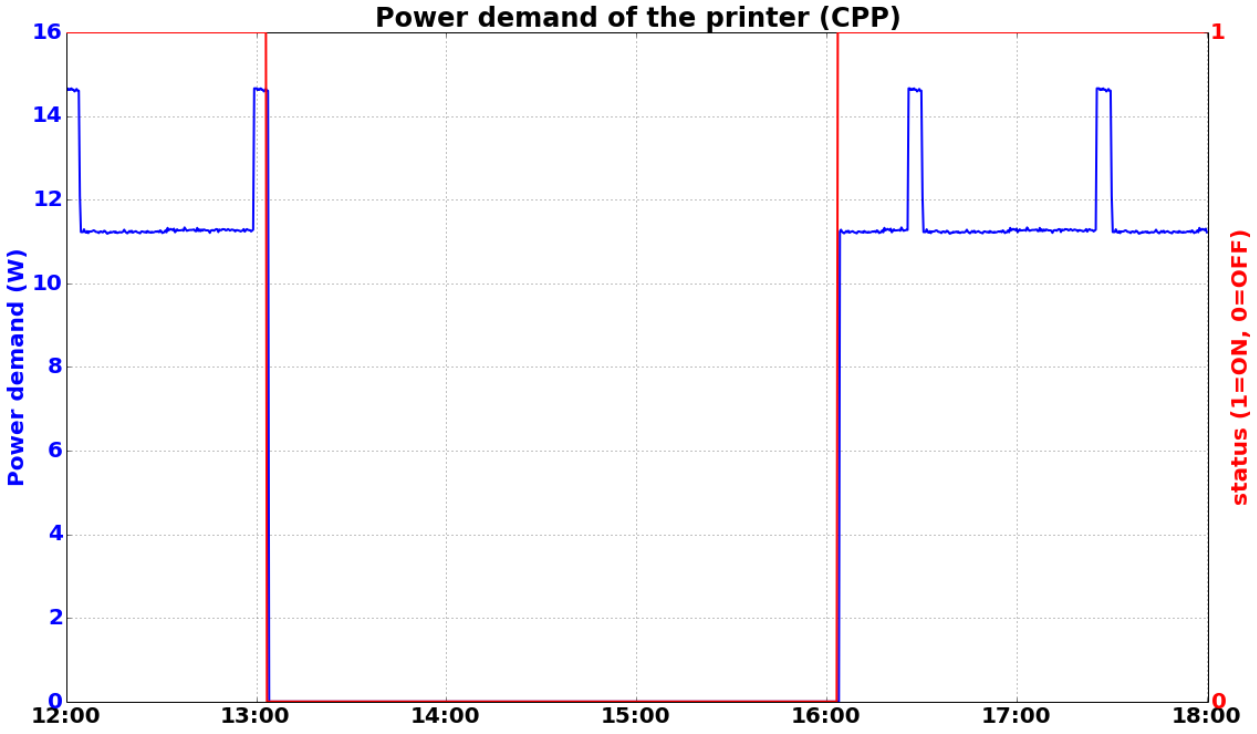

Fig. 5-28. DR Case Study: printer power demand and its status

5.2.6 Comparison of Total Energy Consumption, Power Demand, and Configuration of the Air Purifier between the Base Case and the DR Case Study

Fig. 5-29 and Fig. 5-30 illustrate power demand of the air purifier and the corresponding plug load controller status monitored by the PLA#3 over the six-hour period for the base case and the DR case study, respectively.

Table 5-10 summarizes the power demand and the energy usage the desktop PC over the six-hour period and the CPP-period for both the base case and the DR case study.

Table 5-10 Summary of the air purifier power demand and its status for both base case and DR case study

Parameter	Six-hour period (12:00 – 18:00 hrs)		Pre-CPP (13:03 hrs)		CPP (13:04 – 16:04 hrs)		Post-CPP (16:05 hrs)	
	Base case	DR case	Base case	DR case	Base case	DR case	Base case	DR case
max($P_{air\_purifier}$)	7.62 W	7.58 W	7.36 W	7.38 W	7.62 W	0 W	7.47 W	7.58 W
min($P_{air\_purifier}$)	5.81 W	0 W	7.36 W	7.38 W	5.81 W	0 W	7.47 W	7.58 W
average($P_{air\_purifier}$)	6.74 W	3.36 W	7.36 W	7.38 W	6.77 W	0 W	7.47 W	7.58 W
$E_{air\_purifier}$	0.040 kWh	0.020 kWh	-	-	0.020 kWh	0 kWh	-	-
$Status_{air\_purifier}$	"ON"	"ON/OFF/ON"	"ON"	"ON"	"ON"	"OFF"	"ON"	"ON"

Table 5-10 shows that the energy consumption of the air purifier during the CPP period in the DR case study ($E_{air\ purifier,CPP,DR\ case}$ = 0 kWh) is reduced by 100% as compared to the corresponding value in the base case ($E_{air\ purifier,CPP,base}$ = 0.020 kWh). The maximum power demand of the printer during the CPP period in the DR case study, max($P_{air\ purifier,CPP,DR\ case}$) = 0 kW, is 100% lower than the corresponding value in the base case where max($P_{air\ purifier,CPP,base}$) = 7.62 W. This is due to PLA#3 turn off the air purifier's smart plug the during the CPP period in the DR case study. The energy consumption over 6-hour period of the air purifier in the DR case study ($E_{air\ purifier,6hr,DR\ case}$ = 0.020 kWh) is 50% lower than the corresponding value in the base case ($E_{air\ purifier,6hr,base}$ = 0.040 kWh). This is because the air purifier does not turned on during the CPP period in the DR case study.

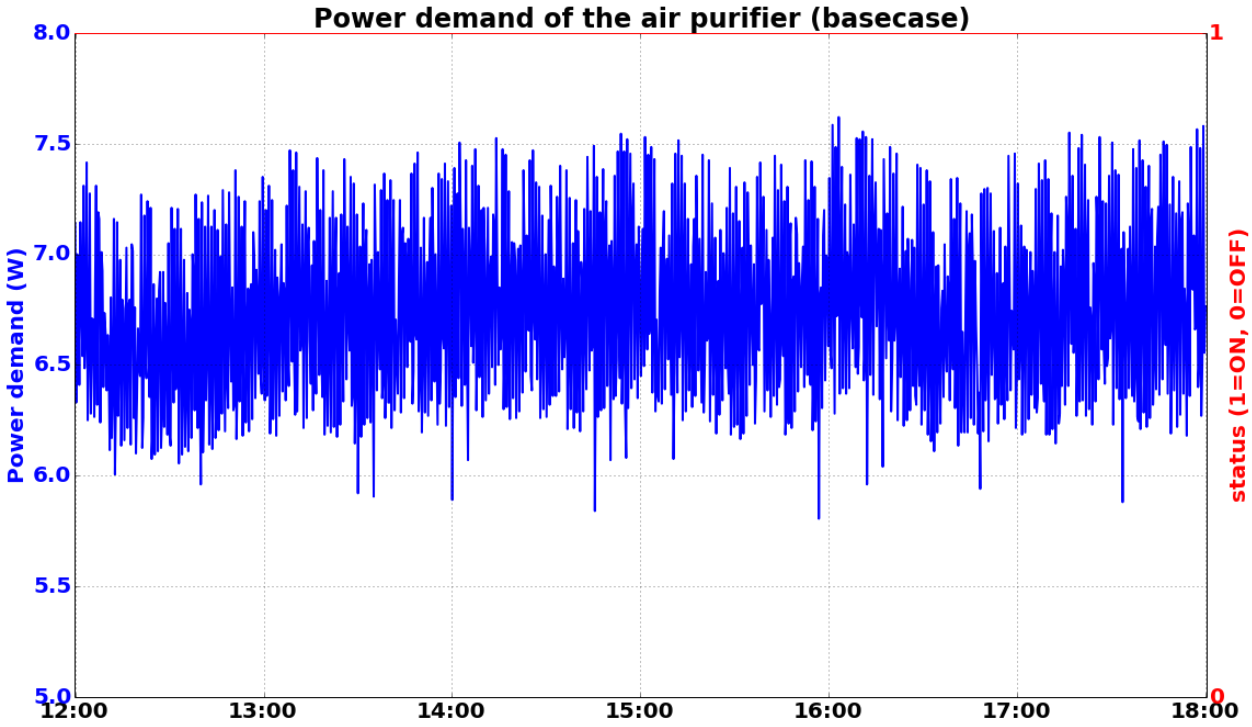

Fig. 5-29. Base Case: air purifier power demand and its status

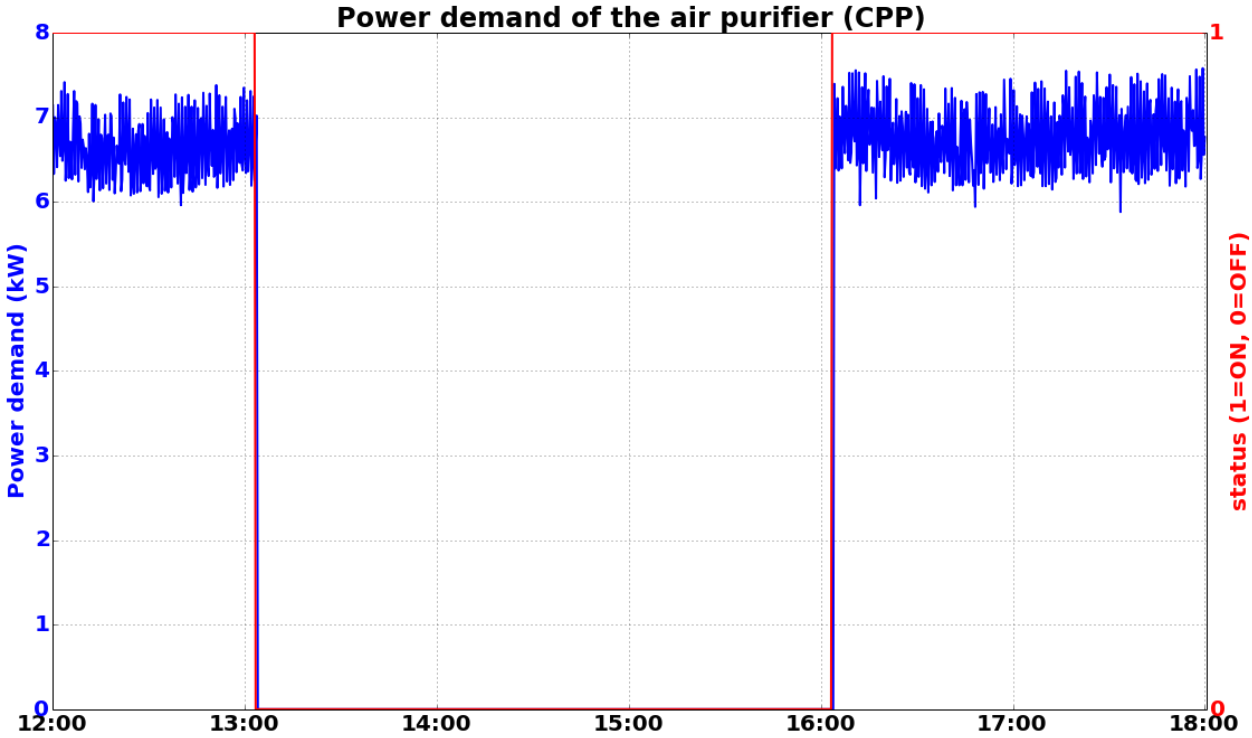

Fig. 5-30. DR Case: air purifier power demand and its status

5.3 DR Case Study Results Discussions based on Chronology of Events

5.3.1 Results of Implementing the Proposed DR algorithm during the pre-CPP Stage

Based on its own goals, a DRA coordinates with the other control agents to determine the optimal start time of the pre-CPP stage for the TA, LLA, and the PLA to take necessary actions before the CPP event.

The chronology of the events during the pre-CPP stage is discussed in detail below:

At 12:24 hrs, the TA shifts cooling load to the pre-CPP stage by performing pre-cooling action as shown in Fig. 5-7. Based on the DR algorithm proposed in Section 3.5, at this time the TA starts to gradually reduce the thermostat temperature setpoint from 74 °F ($T_{cooling,norm}$) to 71 °F ($T_{pre-cooling}$) with the time step to change the setpoint (Δt_{step}) at every 10 minutes. Thus it takes 30 minutes for the TA to lower the temperature by 3 °F.

In order to make sure that the occupants inside the conference room do not notice the change, the TA keeps the thermostat fan status "ON" during the pre-CPP stage. The summary of the TA settings and agent's actions during the TA's pre-CPP stage is given in Table 5-11.

Furthermore, from Table 5-3, it can be seen that the E_{RTU} of the DR case study during the pre-CPP stage (1.18 kWh) is 41% higher than the E_{RTU} of the base case in the same stage (0.70 kWh). This signifies that the cooling load which is expected during the CPP event period in the base case has been shifted to the pre-CPP stage prior to the CPP event in the DR case study.

According to the relationship between relative humidity and room temperature given in Table 5-5, the average(T_{room}) of the DR case study (72.06 °F) is lower than the average(T_{room}) of the base case (74 °F) due to the TA pre-cooling process. In addition, both the std(T_{room}) and the std($Humidity_{room}$) in the DR case study (0.99 °F, 1.99%) are also higher than their corresponding values in the base case (0.52 °F, 1.22%).

As a result, the max($|PMV|$) of the DR case study (0.42) is higher than the max($|PMV|$) of the base case (0.05); these $|PMV|$ correspond to 5% and 9% PPD, accordingly. Table 5-6 shows that the CO_2 level of the room of both cases are under the limit. Therefore, these values are comply with the ASHRAE Standard 55-2013 [106].

Table 5-11. TA settings and agent's actions during the pre-CPP stage

Parameter	Pre-CPP (12:24 – 13:04 hrs)	
	Base case	DR case
max($T_{cooling}$)	74 °F	74 °F
min($T_{cooling}$)	74 °F	71 °F
average($T_{cooling}$)	74 °F	72.05 °F
$status_{FAN}$	"ON"	"ON"
$T_{PMV=0}$	74.5 °F	74.5 °F
BT_{nop}	2.33 °F/hr	
BT_{op}	7 °F/hr	
$t_{CPP,duration}$	3 hours	
$T_{PMV=-0.5}$	70.5 F	
$T_{cooling,pre-CPP}$	-	71 °F
$T_{cooling,norm}$	74 °F	74 °F
ΔT	-	3 °F
Δt_{step}	-	10 mins
$steps_{T_{cooling,norm} \rightarrow T_{cooling,pre-CPP}}$	-	3
ΔT_{step}	-	1 °F
$t_{pre-cooling,duration}$	-	40 mins
$T_{cooling,post-CPP}$	-	74 °F
$t_{pre-cooling,start}$	-	12:24 hrs

At 12:54 hrs, the TA keeps the thermostat cooling set point at $T_{cooling,startup}$ = 74 °F to maintain the room temperature prior to the CPP event at 13:04 hrs.

At 13:04 hrs, the pre-CPP stage of the TA has ended. In Fig. 5-23, it can be seen that the LLA does not need to take any action during the pre-CPP stage as reducing the brightness does not contribute to a reduction in an energy consumption during CPP, occupant comfort violation, demand restrike, and the time to change its setting back to normal after the CPP event. However, $status_{lighting\ load,norm} = 1$ and $P_{lighting\ load,max}$= 0.945 kW is saved by a LLA to make an informed decision during the CPP event.

In Fig. 5-26, the PLA#1 of the desktop PC does not need to take any action during the pre-CPP stage. However, $status_{desktop_{PC},pre-CPP} = 1$ and $P_{desktop_{PC},pre-CPP}$ = 113.97 W is saved by the PLA#1 to make an informed decision during the CPP event.

In Fig. 5-28, the PLA#2 of the printer does not need to take any action during the pre-CPP stage. However, $status_{printer,pre-CPP} = 1$ and $P_{printer,pre-CPP}$ = 547.35 W is saved by the PLA#2 to make an informed decision during the CPP event.

In Fig. 5-30, the PLA#3 of the air purifier does not need to take any action during the pre-CPP stage. However, $status_{air_{purifier},pre-CPP} = 1$ and $P_{air_{purifier},pre-CPP}$ = 7.62 W is saved by the PLA#3 to make an informed decision during the CPP event.

5.3.2 Results of Implementing the Proposed DR algorithm during the CPP Event Stage

The chronology of the events during the CPP period is discussed in detail below:

At 13:04 hrs, the following are the control agents' actions at the beginning of the CPP event stage:

TA action: with respect to Fig. 5-7, in order to minimize the energy consumption of the RTU during the CPP event, the TA changes the thermostat cooling temperature set point ($T_{cooling,CPP}$) to 78 °F. This is the setpoint level that the TA believes that the RTU is not likely to operate and occupant comfort level is not violated during the CPP event according to the DR algorithms proposed in Section 3.5. This is based on the BT_{nop} (2.33 °F/hr) parameter that the TA has learned over time during the normal condition by observing the increase in room temperature when the RTU does not operate. At the same time, the TA keeps the status of the RTU's fan as "ON" to make sure that occupants do not notice that the CPP event as well as to help removing heat gain inside the conference room.

Thus, from Table 5-3, it can be seen that the RTU's energy consumption have substantially reduced by 50% from 2.16 kWh in the base case to 1.08 kWh in the DR case study during the CPP event stage. The maximum, minimum, and average power demand of the RTU in the DR case study (0.37 kW, 0.35kW, 0.36 kW) are also lower than their corresponding values in the base case (3.37 kW, 0.36 kW, 0.72 kW). This signifies that with the thermostat settings by the TA during the CPP event, the RTU does not need to operate to maintain occupant comfort except its fan.

According to the relationship between relative humidity and room temperature given in Table 5-5, the average(T_{room}) of the DR case study (75.9 °F) is higher than the average(T_{room}) of the base case (74 °F) since the RTU does not operate during the CPP event stage. As shown in Fig. 5-7, both the std(T_{room}) and the std($Humidity_{room}$) in the DR case study (1.57 °F, 2.35%) are also higher than their corresponding values in the base case (0.58 °F, 0.64%). This implies the room temperature has higher variation during the CPP period than the base case.

However, the max($|PMV|$) of the DR case study (0.25) is quite close to the max($|PMV|$) of the base case (0.18). Both $|PMV|$ correspond to 5% which is theoretically the lowest PPD of the room comfort condition. Table 5-6 shows that the average(CO_2) levels of the room of both cases are under the limit (268.5 ppm for the DR case study, 238.7 ppm for the base case). Therefore, these values are comply with the ASHRAE Standard 55-2013 [106].

The summary of the TA settings and actions is shown in Table 5-12.

Table 5-12. TA settings and actions during the CPP period for both the base case and the DR case study

Parameter	CPP (13:04 – 16:04 hrs)	
	Base case	DR case
max($T_{cooling}$)	74 °F	78 °F
min($T_{cooling}$)	74 °F	78 °F
average($T_{cooling}$)	74 °F	78 °F
$Status_{FAN}$	"ON"	"ON"
BT_{nop}	2.33 °F/hr	
BT_{op}	7 °F/hr	
$t_{CPP,duration}$	3 hours	
$T_{PMV=0.5}$	79.5 °F/hr	
$T_{cooling,norm}$	74 °F	74 °F
$T_{cooling,pre-CPP}$	-	71 °F
$T_{cooling,CPP}$	-	78 °F
ΔT	-	7 °F
Δt_{step}	-	10 mins
$steps_{T_{cooling,pre-CPP} \rightarrow T_{cooling,CPP}}$	-	1
ΔT_{step}	-	7 °F
$t_{T_{cooling,pre-CPP} \rightarrow T_{cooling,CPP}}$	-	13:04 hrs.

LLA action: According to Fig. 5-23, in order to minimize the energy consumption of the lighting load and ensure that occupant comfort level is not violated during the CPP event, the LLA changes the brightness of the lighting load to 62% based on the DR algorithm proposed in Section 3.5.

With respect to the results shown in Table 5-7, the maximum, minimum, and average power demand of the DR case study (500W, 491W, and 496W) when the brightness level is reduced to 62% are lower than their corresponding values in the base case (945W, 927W, and 936W). The energy consumption of the lighting load is 47% lower for the DR case study (1.49 kWh compared to 2.79 kWh). The minimum illuminance of the DR case study is 303 lux, which is still higher than the recommended 300-lux level of the maintained average illuminance at working level (0.8 m) for the conference room in an office building.

PLA#1 action: given in Table 5-1 the desktop PC is the critical load, thus the PLA#1 does not take any action during the CPP event as can be seen in Fig. 5-26. During this time, the PLA#1 ensures that the load is served at all time since building tenants can use the desktop PC in the conference room at any time. According to Table 5-8, the energy consumption of the desktop PC both in the DR case study and the base case are indifferent.

PLA#2 action: since the printer is the non-critical load, the PLA#2 change status of the plug load to "OFF" at this time in order to minimize the energy consumption during the CPP. The result summary in Table 5-9 shows that the power demand and energy consumption of the printer during the CPP event stage in the DR case study are 0. This is because the PLA#2 turn off the smart plug of the printer. Whereas, in the base case the maximum, minimum, average, and

energy consumption of the printer during the same period as the CPP event are 547.35 W, 11.19 W, 30.80 W, and 0.092 kWh respectively.

PLA#3 action: since the air purifier is non-critical load, the PLA#3 change status of the plug load to "OFF" at this time in order to minimize the energy consumption during the CPP. The result summary in Table 5-10 shows that the power and energy consumption of the air purifier during the CPP event stage in the DR case study are 0 since the PLA#3 turns off the smart plug of the air purifier. Whereas, in the base case the maximum, minimum, average, and energy consumption of the printer during the same period as the CPP event are 7.62 W, 5.81 W, 6.77 W, and 0.020 kWh respectively

5.3.3 Results of Implementing the Proposed DR algorithm during the post-CPP Stage

The chronology of the events after the CPP period is discussed in detail below:

At 16:04 hrs, After the CPP event ends, the DRA minimize impacts of demand restrike by coordinating with thermostat agents (TAs), lighting load agents (LLAs), and plug load agents (PLAs) with their own goals to minimize occupant comfort violation as well as to restore their settings as quickly as possible. At the same time, the DRA tries to slowly increase electricity consumption to avoid the rebound effect (so called demand restrike). The control agents gradually change all set points back to normal settings.

The calculated demand restrike of a building (DRK_B) at the end of the CPP is 5.37 kW which is higher than the maximum of the historical maximum power demand of the building, max($P_{B,hist}$) = 4.91 kW given in Table 5-3. Thus, the DRA cannot allow all control agents to restore their status at this time. It evaluates the operational tolerance of the TA, LLA, PLA#2, and PLA#3 based on their comfort violation index. For the TA, the PMV index at this time is evaluated as 0.28 with PPD at 7% ($T_{room} = 77.5$ °F, $Humidity_{room} = 63\%$). The operational tolerance of this PMV is 44% apart from the maximum PMV at 0.50 that complies with the ASHRAE Standard 55-2013 [106]. The time taken from PMV = 0.28 to PMV = 0.50 is one hour and twelve minutes approximately with the $BT_{nop} = 1.67$ °F$/hr$. For the LLA, the operational tolerance is calculated from the current illuminance level (352 lux) which is 17% higher than the lower limit of illuminance (300 lux) for this type of building according to the IESNA standard 90.1-2007 [109]. For the PLA#2 and PLA#3, the operational tolerance is 0% since their current status is "OFF" but the status prior to the CPP event is "ON" as shown in Fig. 5-28 and Fig. 5-29, respectively. After finishing operational tolerance evaluation, control agents inform their respective values to the DRA to use as the criteria to select next actions to perform.

The DRA, then, gives higher priority to the PLA#2, PLA#3, and the LLA to be able to restore their status at this time since their operational tolerances are lower than the corresponding value of the TA and the sum of $DRK_{Lighting\ load} = 0.217\ kW$, $DRK_{printer} = 0.547\ kW$, $DRK_{air\ purifier} = 0.0762\ kW$, and the max($P_{total,CPP}$) $= 0.98\ kW$ are lower than the historical maximum of power demand of the building max($P_{B,hist}$) = 4. 91 kW. The DRA delays the post-CPP stage of the TA until the room temperature reaches another temperature step of 0.5 °F, so that the TA can make another request to the DRA to restore thermostat temperature setpoint.

At 16.05 hrs, the following are the LLA, PLA#2, and PLA#3 control actions at the beginning of their post-CPP stage.

LLA: after receive the message with "agree" performative from the DRA to restore its setting, the LLA changes the brightness of the lighting load to 100% to the previous level before the CPP event as can be seen in Fig. 5-23. It can also be seen that it takes approximately 7 minutes after 16:05 hrs for the illuminance level of the room to reflect the changed brightness level. This is due to the limitation of the multi-sensor that reports illuminance it senses at every 8-minute time interval after the previous report. Thus, the restoration time of the LLA accounts for the time from the moment that the brightness is changed until the time that the illuminance level is also changed to reflect its corresponding brightness level. With respect to the results shown in Table 5-7, the lighting load power demand changes from 496 W to 938 W when the brightness is changed from 62% to 100% during the post-CPP stage.

PLA#2: after receiving the message with the "agree" performative from the DRA to restore its setting, the PLA#2 changes the status of the printer's smart plug to its previous state before the CPP event as "on" showing in Fig. 5-28. DR Case Study: printer power demand and its status. The result summary in Table 5-9 shows that the printer power demand increases from 0 W to 11.51 W after the PLA#2 post-CPP stage.

PLA#3: after receiving the message with the "agree" performative from the DRA to restore its setting, the PLA#3 changes the status of the air purifier's smart plug to its previous state before the CPP event as "on" showing in Fig. 5-30. DR Case: air purifier power demand and its status. The result summary in Table 5-10 shows that the printer power demand increases from 0 W to 7.58 W after the PLA#3 post-CPP stage.

At 16:25 hrs, the TA triggers that the room temperature (T_{room}) reaches 78 °F which is 0.5 °F higher than the previous value it senses at the end of the CPP event. To minimize the restoration time of the RTU, the TA sends another message with the "request" performative to the DRA to start its post-CPP stage. The DRA evaluates the demand restrike of the RTU (DRK_{RTU}) which is 3.20 kW with the total power demand (P_{total}) at the moment that the TA requests for its restoration which is 1.43 kW. Since the sum of these values (4.63 kW) is less than the maximum power demand of the building($\max(P_{B,hist})$ = 4.91 kW) in the base case, the DRA sends back the message with the "agree" performative to the TA.

After receiving the message, the TA gradually reduces the thermostat temperature set point during the CPP event ($T_{cooling,CPP}$) from 78 °F to the normal thermostat cooling temperature set point ($T_{cooling,norm}$) before the pre-CPP stage which is 74 °F as shown in Fig. 5-7. This is based on the DR algorithms proposed in Section 3.5. The TA control settings and actions during the post-CPP stage are summarized in Table 5-13. At each step, the TA reduces cooling temperature setpoint with ΔT_{step} = 1 °F and Δt_{step} = 10 minutes. Thus, the TA takes 4 steps to reduce temperature from 78 °F to the target temperature at 74 °F and another step to ensure that the room temperature is maintained at 74 °F. The total time that the TA takes to restore its settings and room temperature back to the normal condition ($t_{T_{cooling,CPP} \rightarrow T_{cooling,norm}}$) is 50 minutes. The thermostat fan status is also kept as "ON" during the post-CPP stage.

From Table 5-3, it can be seen that the E_{RTU} of the DR case study during the post-CPP stage (1.64 kWh) is 60% higher than the E_{RTU} of the base case (0.65 kWh). This signifies that the accumulated heat gain during the CPP event that is removed during the post-CPP stage in the DR case study is more than the heat removed in the base case.

According to the relationship between relative humidity and room temperature given in Table 5-5, the average(T_{room}) of the DR case study (75.67 °F) is higher than the average(T_{room}) of the base case (74 °F) due to the TA tries to restore the room temperature back to its normal condition in this stage. In addition, both the std(T_{room}) and the std($Humidity_{room}$) in the DR case study (1.34 °F, 2.16%) are also higher than their corresponding values in the base case (0.49 °F, 0.68%). As a result, the max(|PMV|) of the DR case study (0.34) is higher than the max(|PMV|) of the base case (0.18); these |PMV| correspond to 7% and 6% PPD accordingly.

Table 5-13. TA settings and agent's actions during the post-CPP stage both in the base case and the DR case study

Parameter	Post-CPP (16:04 – 17:14 hrs)	
	Base case	DR case
max($T_{cooling}$)	74 °F	78 °F
min($T_{cooling}$)	74 °F	74 °F
average($T_{cooling}$)	74 °F	76 °F
$status_{FAN}$	"ON"	"ON"
BT_{nop}	2.33 °F/hr	
BT_{op}	7 °F/hr	
$T_{cooling,norm}$	74 °F	74 °F
$T_{cooling,CPP}$	-	78 °F
$T_{cooling,post-CPP}$	-	74 °F
ΔT	-	4 °F
Δt_{step}	-	10 mins
$steps_{T_{cooling,CPP} \rightarrow T_{cooling,post-CPP}}$	-	4
ΔT_{step}	-	1 °F
$t_{T_{cooling,CPP} \rightarrow T_{cooling,norm}}$	-	50 mins
$t_{post-cooling,start}$	-	16:25 hrs

5.4 Base Case and DR Case Study Results Summary

Considering the performance measures of the proposed DR algorithm, the DRA effectively coordinates with the control agents (TA, LLA, PLA#1, PLA#2, and PLA#3) to achieve the overall system goals after receiving the notification of CPP event from a local electric utility via the OpenADR agent one day in advance.

With respect to the DRA's first objective to minimize the total energy consumption (E_B) during the CPP period, the following is the summary of the building energy consumption comparing both the DR case study and the base case.

Table 5-2 shows that 46 % energy consumption reduction is achieved during the CPP period in the DR case study where the E_B = 2.90 kWh as compared to E_B = 5.41 kWh in the base case. The maximum total power demand of the Potomac conference room also reduces by 80% as a result of agents' control actions during the CPP event from max(P_B) = 4.91 kW in the base case to the max(P_B) = 0.98 kW in the DR case study. However, for the overall energy consumption over the 6 hours period, E_B = 10.54 kWh of the base case is only 5% more than the E_B = 10.02 kWh of the DR case study.

This energy consumption reduction mainly comes from the RTU, the lighting load, the printer, and the air purifier as follows.

Table 5-3 shows that the energy consumption of the RTU during the CPP period in the DR case study ($E_{RTU,CPP,DR\ case}$ = 1.08 kWh) is reduced by 50% as compared to the corresponding value in the base case ($E_{RTU,CPP,base}$ = 2.16 kWh). The maximum power demand of the RTU during the CPP period in the DR case study, max($P_{RTU,CPP,DR\ case}$) = 0.37 kW, is almost 90% lower than the corresponding value in the base case where max($P_{RTU,CPP,base}$) = 3.37 kW. This is due to the RTU does not need to operate during the CPP to maintain the comfort condition of the conference room as a result of the pre-cooling process taken by the TA. However, the overall energy consumption of the RTU over six hours for the DR case study ($E_{RTU,6hr,DR\ case}$=4.46 kWh) is higher than its corresponding value for the base case ($E_{RTU,6hr,base}$=4.10 kWh). This is due to the heat loss during the pre-cooling process and the post-CPP stage of the RTU in the DR case study. In addition, there are more energy consumption needed during the pre-CPP stage ($E_{RTU,pre-CPP,DR\ case}$ = 1.18 kWh, $E_{RTU,pre-CPP,base}$ = 0.70 kWh) and the post-CPP stage ($E_{RTU,post-CPP,DR\ case}$ = 1.64 kWh, $E_{RTU,post-CPP,base}$ = 0.65 kWh) of the DR case study.

Table 5-7 shows that the energy consumption of the lighting load during the CPP period in the DR case study ($E_{lighting\ load,CPP,DR\ case}$ = 1.49 kWh) is reduced by 47% as compared to the corresponding value in the base case ($E_{lighting\ load,CPP,base}$ = 2.79 kWh). The maximum power demand of the lighting load during the CPP period in the DR case study, max($P_{lighting\ load,CPP,DR\ case}$) = 0.50 kW, is 47% lower than the corresponding value in the base case where max($P_{lighting\ load,CPP,base}$) = 0.945 kW. This is due to the brightness of the lighting is reduced from 100% to 62% during the CPP period in the DR case study. Unlike the RTU, the energy consumption over 6-hour period of the lighting load in the DR case study ($E_{lighting\ load,6hr,DR\ case}$ = 4.28 kWh) is lower than the corresponding value in the base case

($E_{lighting\ load,6hr,base}$ = 5.59 kWh). This is because the lighting load does not have thermal characteristics as with the RTU.

Table 5-8 shows there is indifferent between the energy consumption of the desktop PC during the CPP period either in the DR case study ($E_{desktop\ PC,6hr,DR\ case}$ = 0.338 kWh) and the base case ($E_{desktop\ PC,6hr,base}$ = 0.338 kWh). This is because the desktop PC is the critical load; thus the PLA#1 does not take the action to turn it "off" during the CPP period.

Table 5-9 shows that the energy consumption of the printer during the CPP period in the DR case study ($E_{printer,CPP,DR\ case}$ = 0 kWh) is reduced by 100% as compared to the corresponding value in the base case ($E_{printer,CPP,base}$ = 0.092 kWh). The maximum power demand of the printer during the CPP period in the DR case study, $\max(P_{printer,CPP,DR\ case})$ = 0 kW, is 100% lower than the corresponding value in the base case where $\max(P_{printer,CPP,base})$ = 0.547 kW. This is because PLA#2 turns off the printer's smart plug the during the CPP period in the DR case study. The energy consumption over the 6-hour period of the printer in the DR case study ($E_{printer,6hr,DR\ case}$ = 0.035 kWh) is 72% lower than the corresponding value in the base case ($E_{printer,6hr,base}$ = 0.127 kWh). This is because the printer does not turned on during the CPP period in the DR case study.

Table 5-10 shows that the energy consumption of the air purifier during the CPP period in the DR case study ($E_{air\ purifier,CPP,DR\ case}$ = 0 kWh) is reduced by 100% as compared to the corresponding value in the base case ($E_{air\ purifier,CPP,base}$ = 0.020 kWh). The maximum power demand of the printer during the CPP period in the DR case study, $\max(P_{air\ purifier,CPP,DR\ case})$ = 0 kW, is 100% lower than the corresponding value in the base case where $\max(P_{air\ purifier,CPP,base})$ = 7.62 W. This is because PLA#3 turns off the air purifier's smart plug the during the CPP period in the DR case study. The energy consumption over 6-hour period of the air purifier in the DR case study ($E_{air\ purifier,6hr,DR\ case}$ = 0.020 kWh) is 50% lower than the corresponding value in the base case ($E_{air\ purifier,6hr,base}$ = 0.040 kWh). This is because the air purifier is not turned on during the CPP period in the DR case study.

For the second objective of the DRA to minimize comfort violation index (CVI), it can be seen in Table 5-5 that the calculated CVI over the 6 hour period, pre-CPP stage, CPP stage, and post-CPP stage either in the DR case study and the base case are 0. This shows that all of the control agents: TA, LLA, PLA#1, PLA#2, PLA#3 effectively work with the DRA to minimize the CVI. For all of the observed periods, there is no violation of the PMV, the CO_2 level, the illuminance level, and the status of the critical load. Based on the control agents' responsibilities, their actions help to minimize the CVI as follows.

It can be seen in Fig. 5-13 that the TA acts to keep the room temperature and humidity to be within the limits specified by ASHRAE Standard 55-2013 [106] at all time in both the DR case study and the base case. The maximum PMV of the DR case study is 0.42 (PPD is 9%) which is lower than the standard PMV at 0.5 and PPD at 10%. The corresponding room temperature and humidity for this PMV are 71 °F and 63% respectively. This condition happens during the pre-cooling process of the TA. Fig. 5-21 also shows that the TA is able to keep the CO_2 level to be

under the 1,000 ppm limit at all time where the maximum CO_2 level = 331 ppm happens during the CPP event when the RTU does not operate.

Table 5-7. Summary of the power demand, brightness level, and illuminance level of the lighting load for both base case and the DR case studyshows that while the LLA reducing the brightness of the lighting load during the CPP period in the DR case study, the minimum illuminance of the conference room (303 lux) is still higher than the recommended illumination level (300 lux) based on the IESNA standard 90.1-2007 [109]. This illuminance reduces from 475 lux in the base case where the LLA keeps the lighting load brightness at 100%

Fig. 5-26 shows that the PLA#1 does not take action to turn off the desktop PC which is the critical load throughout the events in the DR case study. Therefore there is no comfort violation from the critical plug load.

With the DRA's third objective to minimize demand restrike after the CPP event ends, it can be seen that the DRA cooperates with other agents to queue them not to return to the normal settings at the same time. This is based on the estimated magnitude of the demand restrike of each load believed by its corresponding agent. The calculated demand restrike of a conference room (DRK_B) at the end of the CPP that the DRA perceives at 16:04 pm is 5.37 kW which is higher than the maximum of the historical maximum power demand of the building, $\max(P_{B,hist})$ = 4.91 kW. Thus, the DRA allows only the LLA, PLA#2, and PLA#3 to restore their status since their demand restrike combined with the current base load of the conference room is less than 4.91 kW. The TA restore action is deferred by the DRA because the PMV index of the conference room is 0.28 with the estimated time at 1 hour and 12 minutes to reach the PMV limit at 0.5. Therefore, it can be seen that the TA and the DRA effectively work together to defer the TA action to start restoring process at 16:25 hrs to avoid impacts of demand restrike.

According to the fourth objective of the DRA to minimize time to restore all settings back to normal condition, it can be seen that the DRA works with the TA, LLA, PLA#2, PLA#3 so that they are able to restore their setting as quickly as they can. The time taken by the TA to start restoring the thermostat cooling temperature setpoint: $t_{restore,HVAC}$ = 21 minutes, the LLA to start restoring the brightness of the lighting load: $t_{restore,lighting\ load}$ = 1 minute, the PLA#2 to start changing the status of the printer's smart plug to "on" : $t_{restore,PLA\#2}$ = 1 minute, and the PLA#3 to start to change the status of the air purifier's smart plug to "on" : $t_{restore,PLA\#3}$ = 1 minute. The time taken by the TA to finish restoring the thermostat cooling temperature setpoint and the room temperature: $T_{restore,HVAC}$ = 49 minutes, the LLA to finish restoring the brightness of the lighting load and the illuminance level of the conference room: $T_{restore,lighting\ load}$ = 7 minute, the PLA#2 to finish changing the status of the printer's smart plug to "on" : $T_{restore,PLA\#2}$ = 1 minute, and the PLA#3 to finish changing the status of the air purifier's smart plug to "on" : $T_{restore,PLA\#3}$ = 1 minute.

5.5 A Study of the Impacts of Occupancy Level to Energy Consumption of the RTU

In this section, the sensitivity analysis of the occupancy level that has direct impacts on building thermal response (both BT_{nop} and BT_{op}) is carried out based on the algorithm proposed in Section 3.5.B Subtask 2. The main objective is to find heat gain and heat loss due to the variation in the number of people in a given space. This is the Potomac conference room in this case study.

There are four factors that need to be taken into account: zone type designation, occupancy activity level, occupancy density, and cooling load factor adjustment. Based on the structure, room location, and furnishing of this room, the zone type designation is "D" as the room is in the middle floor, has a concrete floor, and carpet floor covering. The occupancy activity level is "seated, very light work". Therefore, the sensible heat generation (SHG_p) of each person is 245 Btu/hr; the latent heat (LHG_p) generation of each person is 155 Btu/hr. The approximated area of the Potomac conference room is 1,024 ft^2 (32ft x 32ft). With occupancy density range of 25 ft^2 per person, the maximum occupancy is approximately 40 people. With the given building zone type designation as "D", assuming that the total number of hours that the space is occupied is eight hours, starting from 12 noon and the class starts at 13:00 hrs. Therefore, the cooling load factor adjustment for the sensible heat (CLF_p) is 0.62.

This study compares the following cases with different occupant levels: 5 people, 10 people, 15 people, 20 people, 25 people, 30 people, 35 people and 40 people.

The sensible heat gain (q_{p-sen}), latent heat gain (q_{p-lat}) , and total heat gain ($q_{p,total}$) based on the occupant level (calculated from Eq. 3-56 and Eq. 3-57) with the adjusted building thermal response (when the RTU does not operate $BT_{nop,p}$; and the adjusted building thermal response when the RTU is in operation $BT_{op,p}$ calculated from Eq. 3-58 and Eq. 3-59, respectively) are shown in Table 5-14. Based on these values, the energy consumption of the RTU with the same conditions as the DR case study of all cases, as shown in Table 5- 15, has been estimated using the adjusted $BT_{nop,p}$ and $BT_{op,p}$.

From Table 5-14, it can be seen that the building gains more heat when there is more people inside the conference room as $q_{p,total}$ keeps increasing linearly with number of people. Thus, the adjusted building thermal response when the RTU does not operate ($BT_{nop,p}$) also increases as there is more heat gain from people inside the room; while the adjusted building thermal response when the RTU is in operation ($BT_{op,p}$) decreases with occupancy level since the RTU needs to handle more heat load due to the heat gain from people. From 5 people to 40 people, the $BT_{nop,p}$ increases by 25% from 2.18 °F/hr with 5 people in the room to 2.70 °F/hr with 40 people in the room; the $BT_{op,p}$ decreases by 26% from 7.56 °F/hr with 5 people to 5.59 °F/hr with 40 people in the conference room.

Table 5-15 shows the variation of the energy consumption of the RTU based on different occupancy levels and different stages of the CPP event: pre-CPP, CPP, and post-CPP. It can be seen that the energy consumption of the RTU increases with the increase in occupancy level. For

the energy consumption of the RTU over the six-hour observed period from 12:00 to 18:00, the energy consumption increases by 55% from 4.47 kWh with 5 people in the room to 6.94 kWh with 40 people in the room. Likewise, when consider only the periods from pre-CPP to post-CPP, the energy consumption of the RTU increases by 66% from 3.91 kWh with 5 people in the room to 6.38 kWh with 40 people in the room.

It should be noted that with the proposed DR algorithm, the thermostat (TA) is able to maintain occupant comfort from 5 people to 40 people without the need to run the RTU during the CPP period from 13:04 to 16:04 hrs. This can be seen from the energy consumption of the RTU during the CPP period ($E_{RTU,CPP}$) of all cases that are the same. This signifies the effectiveness of the proposed DR algorithm that performs pre-cooling and post-cooling of the conference room before and after the CPP period, respectively. The energy consumption of the RTU during the pre-CPP period and the post-CPP keeps increasing with number of people inside the conference room. This means that with more heat gain from people, thermostat agent (TA) has to reduce pre-cooling temperature to ensure that occupant comfort is not violated during the CPP event. Furthermore, the thermostat has to use more energy during the post-CPP stage to cool down the room after the CPP event to remove heat gain from people during the CPP event.

Table 5-16 shows that when there is more people inside the conference room, the TA has to reduce the pre-cooling temperature ($T_{cooling,pre-CPP}$) from 71.5 °F (5 people) to 70.5 °F (40 people). This is why the energy consumption of the RTU to pre-cool the conference room for 40 people is 89% higher than when there is only 5 people. In addition, the time use to pre-cool the conference room is longer when there is more people. This reflects in the CPP start time, which happens earlier in the case with higher occupancy level.

Table 5-17 shows that with an increase in the occupancy level, the TA has to increase the thermostat cooling temperature set point during the CPP period ($T_{cooling,CPP}$) in order to avoid a chance that the RTU operates when the room temperature exceeds the cooling set point. However, the TA also ensures that the cooling temperature set point during CPP period still provides comfort to occupants. It can be seen that with the increase in the occupancy level, the difference between $T_{cooling,pre-CPP}$ and $T_{cooling,CPP}$ increases.

Table 5-18 shows that with an increase in the occupancy level, the difference between the $T_{cooling,CPP}$ and the normal thermostat cooling set point ($T_{cooling,norm}$) increases. Therefore the energy consumption of the RTU is 86% higher in the case of 40 people as compared to that in the case of 5 people. In addition, the time it takes to restore the room temperature back to the normal condition is also longer.

Fig. 5-31 summarizes the impact of occupancy level on the RTU's energy consumption.

Table 5-14. Heat gain and adjusted building thermal response at different occupancy levels

Parameter	Occupancy level							
	5 people	10 people	15 people	20 people	25 people	30 people	35 people	40 people
q_{p-sen} (Btu/hr)	837	1,674	2,511	3,348	4,185	5,022	5,860	6,697
q_{p-lat} (Btu/hr)	775	1,150	2,325	3,100	3,875	4,650	5,425	6,200
$q_{p,total}$ (Btu/hr)	1,612	3,224	4,836	6,448	8.060	9,672	11,285	12,897
$BT_{nop,p}$(°F/hr)	2.18 °F/hr	2.25 °F/hr	2.33 °F/hr	2.4 °F/hr	2.48 °F/hr	2.55 °F/hr	2.63 °F/hr	2.70 °F/hr
$BT_{op,p}$ (°F/hr)	7.56 °F/hr	7.28 °F/hr	7 °F/hr	6.72 °F/hr	6.44 °F/hr	6.15 °F/hr	5.87 °F/hr	5.59 °F/hr

Table 5- 15. Energy consumption of the RTU at different occupancy levels

Parameter	Occupancy level							
	5 people	10 people	15 people	20 people	25 people	30 people	35 people	40 people
$E_{RTU,pre-CPP}$ (kWh)	1.09 kWh	1.36 kWh	1.41 kWh	1.47 kWh	1.53 kWh	1.87 kWh	1.96 kWh	2.06 kWh
$E_{RTU,CPP}$ (kWh)	1.08 kWh	1.08 kWh	1.08 kWh	1.08 kWh	1.08 kWh	1.08 kWh	1.08 kWh	1.08 kWh
$E_{RTU,post-CPP}$ (kWh)	1.74 kWh	1.81 kWh	1.88 kWh	2.20 kWh	2.30 kWh	2.41 kWh	2.80 kWh	3.24 kWh
$E_{RTU,pre-CPP\rightarrow post-CPP}$ (kWh)	3.91 kWh	4.25 kWh	4.37 kWh	4.75 kWh	4.91 kWh	5.36 kWh	5.84 kWh	6.38 kWh
$E_{RTU,six-hour}$ (kWh)	4.47 kWh	4.81 kWh	4.93 kWh	5.31 kWh	5.47 kWh	5.92 kWh	6.40 kWh	6.94 kWh
%$E_{RTU,pre-CPP\rightarrow post-CPP}$ (base 5 people)	100%	109%	111%	121%	126%	137%	149%	166%
%$E_{RTU,six-hour}$ (base 5 people)	100%	108%	110%	119%	122%	132%	143%	155%

Note:

$E_{RTU,pre-CPP}$: energy consumption of the RTU during the pre-CPP stage (kWh)

$E_{RTU,CPP}$: energy consumption of the RTU during the CPP stage (kWh)

$E_{RTU,post-CPP}$: energy consumption of the RTU during the post-CPP stage (kWh)

$E_{RTU,pre-CPP\rightarrow post-CPP}$: energy consumption of the RTU from the pre-CPP stage to the post-CPP stage (kWh)

$E_{RTU,six-hour}$: energy consumption of the RTU during the six-hour period from 12:00 to 18:00 hrs (kWh)

%$E_{RTU,pre-CPP\rightarrow post-CPP}$: % of RTU energy consumption with the base of 5 people from the pre-CPP to post-CPP stage

%$E_{RTU,six-hour}$: % of RTU energy consumption with the base of 5 people during the six-hour period from 12:00 to 18:00 hrs

Table 5-16. Thermostat setting for the thermostat agent (TA) during the pre-CPP event

Parameter	Base case	DR case							
		5 people	10 people	15 people	20 people	25 people	30 people	35 people	40 people
max($T_{cooling}$)	74 °F	74 °F	74 °F	74 °F	74 °F	74 °F	74 °F	74 °F	74 °F
min($T_{cooling}$)	74 °F	71.5 °F	71 °F	71 °F	71 °F	71 °F	70.5 °F	70.5 °F	70.5 °F
average($T_{cooling}$)	74 °F	72.75 °F	72.5 °F	72.5 °F	72.5 °F	72.5 °F	72.25 °F	72.25 °F	72.25 °F
$status_{FAN}$	"ON"	"ON"	"ON"	"ON"	"ON"	"ON"	"ON"	"ON"	"ON"
$T_{PMV=0}$	74.5 °F	74.5 °F	74.5 °F	74.5 °F	74.5 °F	74.5 °F	74.5 °F	74.5 °F	74.5 °F
BT_{nop}	-	2.18 °F/hr	2.25 °F/hr	2.33 °F/hr	2.4 °F/hr	2.48 °F/hr	2.55 °F/hr	2.63 °F/hr	2.70 °F/hr
BT_{op}	-	7.56 °F/hr	7.28 °F/hr	7 °F/hr	6.72 °F/hr	6.44 °F/hr	6.15 °F/hr	5.87 °F/hr	5.59 °F/hr
$t_{CPP,duration}$	-	3 hours	3 hours	3 hours	3 hours	3 hours	3 hours	3 hours	3 hours
$T_{PMV=-0.5}$	-	70.5 °F	70.5 F	70.5 F	70.5 F	70.5 F	70.5 F	70.5 F	70.5 F
$T_{cooling,pre-CPP}$	-	71.5 °F	71 °F	71 °F	71 °F	71 °F	70.5 °F	70.5 °F	70.5 °F
$T_{cooling,norm}$	74 °F	74 °F	74 °F	74 °F	74 °F	74 °F	74 °F	74 °F	74 °F
ΔT	-	2.5 °F	3 °F	3 °F	3 °F	3 °F	3.5 °F	3.5 °F	3.5 °F
Δt_{step}	-	10 mins	10 mins	10 mins	10 mins	10 mins	10 mins	10 mins	10 mins
$steps_{T_{cooling,norm} \rightarrow T_{cooling,start}}$	-	3	3	3	3	3	4	4	4
ΔT_{step}	-	1,0.5 °F	1 °F	1 °F	1 °F	1 °F	1,0.5 °F	1,0.5 °F	1,0.5 °F
$t_{pre-cooling,duration}$	-	40 mins	40 mins	40 mins	40 mins	40 mins	50 mins	50 mins	50 mins
$T_{cooling,post-CPP}$	-	74 °F	74 °F	74 °F	74 °F	74 °F	74 °F	74 °F	74 °F
$t_{pre-cooling,start}$	-	12:24 hrs	12:24 hrs	12:24 hrs	12:24 hrs	12:24 hrs	12:14 hrs	12:14 hrs	12:14 hrs
$E_{pre-CPP}$	-	1.09 kWh	1.36 kWh	1.41 kWh	1.47 kWh	1.53 kWh	1.87 kWh	1.96 kWh	2.06 kWh
%$E_{pre-CPP}$(base 5 people)	-	100%	125%	129%	135%	140%	172%	180%	189%

Table 5-17. Thermostat setting for the thermostat agent (TA) during the CPP event

Parameter	Base case	DR case							
		5 people	10 people	15 people	20 people	25 people	30 people	35 people	40 people
max($T_{cooling}$)	74 °F	78 °F	78 °F	78 °F	78.5 °F	78.5 °F	78.5 °F	79 °F	79.5 °F
min($T_{cooling}$)	74 °F	78 °F	78 °F	78 °F	78.5 °F	78.5 °F	78.5 °F	79 °F	79.5 °F
average($T_{cooling}$)	74 °F	78 °F	78 °F	78 °F	78.5 °F	78.5 °F	78.5 °F	79 °F	79.5 °F
$Status_{FAN}$	"ON"	"ON"	"ON"	"ON"	"ON"	"ON"	"ON"	"ON"	"ON"
BT_{nop}	-	2.18 °F/hr	2.25 °F/hr	2.33 °F/hr	2.4 °F/hr	2.48 °F/hr	2.55 °F/hr	2.63 °F/hr	2.70 °F/hr
BT_{op}	-	7.56 °F/hr	7.28 °F/hr	7 °F/hr	6.72 °F/hr	6.44 °F/hr	6.15 °F/hr	5.87 °F/hr	5.59 °F/hr
$t_{CPP,duration}$	-	3 hours	3 hours	3 hours	3 hours	3 hours	3 hours	3 hours	3 hours
$T_{PMV=0.5}$	-	79.5 °F/hr	79.5 °F/hr	79.5 °F/hr	79.5 °F/hr	79.5 °F/hr	79.5 °F/hr	79.5 °F/hr	79.5 °F/hr
$T_{cooling,norm}$	74 °F	74 °F	74 °F	74 °F	74 °F	74 °F	74 °F	74 °F	74 °F
$T_{cooling,pre-CPP}$	-	71.5 °F	71 °F	71 °F	71 °F	71 °F	70.5 °F	70.5 °F	70.5 °F
$T_{cooling,CPP}$	-	78 °F	78 °F	78 °F	78.5 °F	78.5 °F	78.5 °F	79 °F	79.5 °F
ΔT	-	6.5 °F	7 °F	7 °F	7.5 °F	7.5 °F	8 °F	8.5 °F	9 °F
Δt_{step}	-	10 mins	10 mins	10 mins	10 mins	10 mins	10 mins	10 mins	10 mins
$steps_{T_{cooling,pre-CPP} \rightarrow T_{cooling,CI}}$	-	1	1	1	1	1	1	1	1
ΔT_{step}	-	6.5 °F	7 °F	7 °F	7.5 °F	7.5 °F	8 °F	8.5 °F	9 °F
$t_{T_{cooling,pre-CPP} \rightarrow T_{cooling,CPP}}$	-	13:04 hrs.	13:04 hrs.	13:04 hrs.	13:04 hrs.	13:04 hrs.	13:04 hrs.	13:04 hrs.	13:04 hrs.
$t_{RTU,start,CPP}$	-	16:05 hrs	16:11 hrs	16:25 hrs	16:12 hrs	16:06 hrs	16:12 hrs	16:28 hrs	16:24 hrs
$E_{pre-CPP}$	-	1.08 kWh	1.08 kWh	1.08 kWh	1.08 kWh	1.08 kWh	1.08 kWh	1.08 kWh	1.08 kWh
%$E_{pre-CPP}$(base 5 people)	-	100%	100%	100%	100%	100%	100%	100%	100%

Table 5-18. Thermostat setting for the thermostat agent (TA) during the post-CPP event

Parameter	Base case	DR case							
		5 people	10 people	15 people	20 people	25 people	30 people	35 people	40 people
max($T_{cooling}$)	74 °F	78 °F	78 °F	78 °F	78.5 °F	78.5 °F	78.5 °F	79 °F	79.5 °F
min($T_{cooling}$)	74 °F	74 °F	74 °F	74 °F	74 °F	74 °F	74 °F	74 °F	74 °F
average($T_{cooling}$)	74 °F	76 °F	76 °F	76 °F	76.25 °F	76.25 °F	76.25 °F	76.5 °F	76.75 °F
$Status_{FAN}$	"ON"	"ON"	"ON"	"ON"	"ON"	"ON"	"ON"	"ON"	"ON"
BT_{nop}	-	2.18 °F/hr	2.25 °F/hr	2.33 °F/hr	2.4 °F/hr	2.48 °F/hr	2.55 °F/hr	2.63 °F/hr	2.70 °F/hr
BT_{op}	-	7.56 °F/hr	7.28 °F/hr	7 °F/hr	6.72 °F/hr	6.44 °F/hr	6.15 °F/hr	5.87 °F/hr	5.59 °F/hr
$T_{cooling,norm}$	74 °F	74 °F	74 °F	74 °F	74 °F	74 °F	74 °F	74 °F	74 °F
$T_{cooling,CPP}$	-	78 °F	78 °F	78 °F	78.5 °F	78.5 °F	78.5 °F	79 °F	79.5 °F
$T_{cooling,post-CPP}$	-	74 °F	74 °F	74 °F	74 °F	74 °F	74 °F	74 °F	74 °F
ΔT	-	4 °F	4 °F	4 °F	4.5 °F	4.5 °F	4.5 °F	5 °F	5.5 °F
Δt_{step}	-	10 mins	10 mins	10 mins	10 mins	10 mins	10 mins	10 mins	10 mins
$steps_{T_{cooling,CPP}\rightarrow T_{cooling,post-C}}$	-	4	4	4	5	5	5	5	6
ΔT_{step}	-	1 °F	1 °F	1 °F	1,0.5 °F	1,0.5 °F	1,0.5 °F	1 °F	1,0.5 °F
$t_{T_{cooling,CPP}\rightarrow T_{cooling,norm}}$	-	50 mins	50 mins	50 mins	60 mins	60 mins	60 mins	60 mins	70 mins
$t_{post-cooling,start}$	-	16:05 hrs	16:11 hrs	16:25 hrs	16:12 hrs	16:06 hrs	16:12 hrs	16:28 hrs	16:24 hrs
$E_{pre-CPP}$	-	1.74 kWh	1.81 kWh	1.88 kWh	2.20 kWh	2.30 kWh	2.41 kWh	2.80 kWh	3.24 kWh
$\%E_{pre-CPP}$(base 5 people)	-	100%	104%	108%	126%	132%	139%	167%	186%

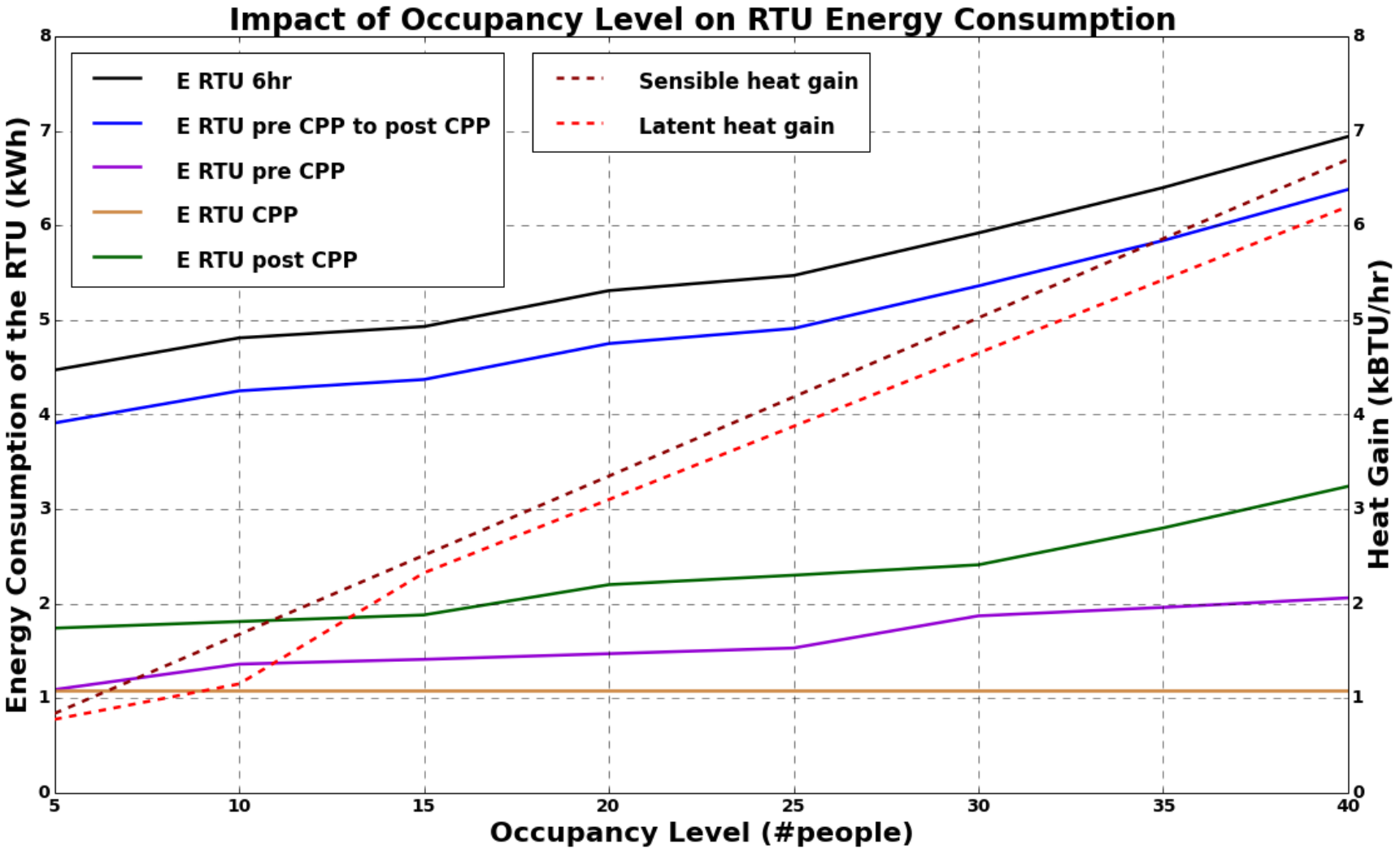

Fig. 5-31. Impacts of occupancy level on the energy consumption of the RTU

6. CONCLUSION AND RECOMMENDATIONS FOR FUTURE WORK

6.1 Conclusion

The objective of this research is to design, develop, and deploy the Multi-Agent Systems (MAS) that enable demand response (DR) implementation at the end-user side of a power distribution system. The developed MAS are validated in a simulated environment for a case of residential homes; and in a real-world environment for the case of a commercial building. The DR algorithm for residential homes is proposed to alleviate power system stress condition during a callout of an emergency demand response event (EDRE). The DR algorithm for commercial buildings is proposed to help improve efficiency of a power grid operation by participating in a Critical Peak Pricing (CPP) event.

At the transformer and the home levels:

The case study demonstrates the approach for smart distribution transformer management (SDTM) in response to the emergency demand response event (EDRE) at a transformer and a home levels. It can be concluded that the proposed algorithm can effectively perform DR implementation to achieve transformer agent's and home agent's goals during the DR event. At the distribution transformer level, the proposed approach ensures that an instantaneous power demand at the distribution transformer does not exceed a given DL while simultaneously minimizing impacts of demand restrike. At the home level, the proposed approach ensures that all critical loads are served and homeowner's comfort level is maintained during the DR event. At the appliance level, additional operating times of appliances due to load shifting and re-scheduling during the DR event are minimized. Simulation results show that the proposed DR algorithm outperforms the simple DR algorithm as the resulting demand restrike potential is reduced by 56%.

At the commercial building level:

The case study demonstrates the approach to improve efficiency of a power grid operation in response to the critical peak pricing (CPP) signal at a building level. The electric utility notifies participating buildings one day in advance with the main goal to encourage them to reduce power and energy consumption by charging significantly high electricity price during the CPP period. The practical implementation of the proposed DR algorithm has been implemented as a multi-agent system (MAS) on the BEMOSS platform to control hardware devices in the Virginia Tech building in Alexandria, VA. The Potomac conference room in the Virginia Tech building is chosen as the demonstration site and to deploy the proposed DR algorithm. Hardware devices being monitored and controlled include thermostat, packaged RTU, power meter, lighting system, desktop PC, printer, air purifier, smart plugs, multi sensor, weather sensor, embedded computer, etc. The results of the case study show that the proposed DR algorithm can effectively perform DR implementation given a day-ahead CPP event notification from an electric utility.

The first objective of the DRA to minimize the total energy consumption during the CPP period is achieved as the result shows that there is 46% energy consumption reduction during the CPP period in the DR case study as compared to the base case. In addition, the maximum total power demand is also reduced by 80% throughout the CPP period in the DR case study.

For the second objective of the DRA to minimize occupant comfort violation index (CVI), results show that occupant comfort is met throughout the CPP event. All control agents effectively act to maintain occupant comfort within the limits. The calculated CVI is 0 for both the DR case study and the base case.

Results also show that the DRA also achieves its third objective, i.e., to minimize demand restrike imposed on a building power demand after a CPP event ends. By working with the other control agents, the calculated demand restrike of a building (DRK_B) is also 0. This is because the DRA can effectively schedule with the control agents to gradually restore their settings so that the total power demand of the conference room after the CPP period ends does not exceed the maximum level of the historical power demand during its normal condition.

Taken into account all constraints and other objectives, results show that the DRA also achieves its fourth objective, i.e., to minimize the time to restore all device settings back to normal after the CPP period. The total time taken by all control agents to start to restore all settings back to their original operating conditions is 24 minutes after the CPP event. The total time taken by the control agents to finish restoring their states is 59 minutes after the CPP event.

Lastly, the sensitivity analysis is performed to study impacts of occupancy level to the change in energy consumption of the RTU with a CPP event. From simulation results, it is discovered that the proposed DR algorithm can effectively maintain occupant comfort while minimizing energy consumption during the CPP period even when the occupancy level inside the room changes from as less as 5 people to as many as 40 people (the room capacity). The study concludes that the total energy consumption over the six-hour observed period is higher when there are more people in the room as a result of pre-cooling and post-cooling process of the RTU. The energy consumption of the RTU during the CPP period remains the same for all cases regardless of number of people since the thermostat agent (TA) can optimally select temperature setpoints at the pre-CPP stage, CPP stage, and at the post-CPP stage while the occupant comfort during the CPP period is not violated.

6.2 Recommendations for Future Work

At the transformer and the home levels:

For the recommended future work of DR implementation at the distribution transformer and the home levels, the proposed approach can be improved by considering factors such as implementation costs, transformer's loss of life, or economic aspect of electricity market. Some of the load forecasting algorithms, such as nonlinear regression or neural network techniques, can be used to forecast load profiles of a distribution transformer based day type (weekday/weekend), weather, season, etc. Future work can also include scaling up the proposed MAS to handle DR for a distribution network with multiple distribution transformers that have a

number of homes and controllable appliances. In addition, the proposed MAS can be deployed on a small single-board computer with limited computation capability to work in a real-world environment.

At the commercial buildings level:

For the recommended future work of DR implementation at commercial buildings level, the proposed approach can be improved by implementing feature such as real-time tracking of space occupancy by having a device that can count or predict number of people inside a room or a building at a given time. This can help improving the heat loss and heat gain model due to variation on number of people in the space resulting in a more effective and efficient DR algorithm for the CPP event. There are several approaches to implement such feature. For example, use the embedded system such as Raspberry Pi with the camera module to capture an image of the room prior and during the CPP event, and then use machine learning technique for image processing to count number of people inside the room. Another approach is to use beacon device such as the Estimote iBeacon and have every tenants install an app that is able to communicate with the beacon to do a headcount. Another possibility is to detect space occupancy by looking into a router tables for devices and their signal strength (rssi).

In addition, some of the load forecasting algorithms, such as nonlinear regression or neural network techniques, can be used to forecast load profiles of a building based on multiple factors such as time of the day, weather, season, or activity level to improve the effectiveness of the DR algorithm. Future work can also include scaling up the proposed DR algorithm to be able to deploy in a wider area such as multiple rooms, the whole floor, the whole building, or even use with multiple buildings.

7. REFERENCES

[1] National Energy Technology Laboratory (NETL) Modern grid initiative [Online]. Available: http://www.netl.doe.gov/research/energy-efficiency/energy-delivery/smart-grid. Retrieved: February 2016.

[2] U.S. Department of Energy, Office of Electricity Delivery and Energy Reliability "Smart Grid" [Online]. Available: http://energy.gov/oe/services/technology-development/smart-grid. Retrieved: February 2016.

[3] U. S. Department of Energy, "Benefits of demand response in electricity markets and recommendations for achieving them, a report to the United States congress pursuant to Section 1252 of the Energy Policy Act of 2005," Feb. 2006.

[4] FERC, "Federal Energy Regulatory Commission Staff Report: Assessment of Demand Response and Advanced Metering", 2012 [Online]. Available: http://www.ferc.gov/legal/staff-reports/12-20-12-demand-response.pdf. Retrieved: February 2016.

[5] Pacific Gas and Electric Company (PG&E) Demand Response Programs [Online]. Available: www.pge.com/mybusiness/energysavingsrebates/demandresponse. Retrieved: February 2016.

[6] Southern California Edison (SCE) Demand Response Programs [Online]. Available: www.sce.com/b-rs/demand-response.../demand-response-programs.htm. Retrieved: February 2016.

[7] P.L, Langbein, "Demand response participation in PJM wholesale markets," *In Proc. 2012 IEEE Innovative Smart Grid Technologies (ISGT),* Washington D.C., 16-20 Jan. 2012.

[8] R. Mukerji, "Demand response in the NYISO markets," *In Proc. 2011 IEEE PES Power Systems Conference and Exposition,* Mar. 2011.

[9] H. Zerriffi, H. Dowlatabadi and A. Farrell, "Incorporating stress in electric power systems reliability models", *Energy Policy,* vol. 35 pp. 61–75, Nov. 2005.

[10] P. Khajavi, H. Abniki and A. B. Arani, "The role of incentive based demand response programs in smart grid," *In Proc. 2011 10th Int'l Conf. on Environment and Electrical Engineering (EEEIC),* May 2011.

[11] K. Schisler, T. Sick and K. Brief, "The role of demand response in ancillary services markets," *In Proc. 2008 IEEE T&D Conference and Exposition,* 21-24 April 2008.

[12] Baltimore Gas and Electric (BGE), "Comments of the public service commission staff direct load control program activation", Sept. 2011.

[13] Y. Peizhong, D. Xihua, A. Iwayemi, Z. Chi and L. Shufang, "Real-time opportunistic scheduling for residential demand response," *IEEE Trans on Smart Grid,* vol.4, no.1, pp.227,234, March 2013.

[14] Demand Response Program Categories, North America Electric Reliability Corporation (NERC) [Online]. Available: http://www.nerc.com/docs/pc/dadswg/2011%20DADS%20Report.pdf. Retrieved: February 2016.

[15] Y. Peizhong, X. Dong, A. Iwayemi, C. Zhou and S. Li, "Real-time opportunistic scheduling for residential demand response," IEEE Trans on Smart Grid, vol.4, no.1, pp.227-234, March 2013.

[16] H. Qinran, L. Fangxing, "Hardware Design of Smart Home Energy Management System With Dynamic Price Response," IEEE Transactions on Smart Grid, vol.4, no.4, pp.1878-1887, Dec. 2013.

[17] B. Chai, J. Chen, Z. Yang, Y. Zhang, "Demand Response Management With Multiple Utility Companies: A Two-Level Game Approach," IEEE Transactions on Smart Grid, vol.5, no.2, pp.722-731, March 2014.

[18] J.C. Fuller, K.P. Schneider and D. Chassin, "Analysis of residential demand response and double-auction markets," IEEE Power and Energy Society General Meeting, 2011, vol., no., pp.1-7, 24-29 July 2011.

[19] L. Ying, B.L. Ng, M. Trayer and L. Liu, "Automated residential DR: algorithmic implications of pricing models," IEEE Trans on Smart Grid, vol.3, pp.1712-1721, Dec. 2012.

[20] Z. Chen, L. Wu and Y. Fu, "Real-time price-based DR management for residential appliances via stochastic and robust optimization," IEEE Trans on Smart Grid, vol.3, no.4, pp.1822-1831, Dec. 2012.

[21] Y. Ozturk, D. Senthilkumar, S. Kumar and G. Lee, "An intelligent home energy management system to improve demand response," IEEE Transactions on Smart Grid, vol.4, no.2, pp.694-701, June 2013.

[22] Y. Wang, I.R. Pordanjani and X. Wilsun, "An event-driven demand response scheme for power system security enhancement," IEEE Trans on Smart Grid, vol.2, no. 1, pp. 23-29, March 2011.

[23] K. Dong-Min and K. Jin-O, "Design of emergency demand response program using analytic hierarchy process," IEEE Trans on Smart Grid, vol.3, no.2, pp.635-644, June 2012.

[24] M.M. Sahebi, E.A. Duki, M. Kia and A. Soroudi, Ehsan, "Simultanous emergency demand response programming and unit commitment programming in comparison with interruptible load contracts," IET Gen, Tran & Dist, vol.6, no.7, pp.605-611, July 2012.

[25] Heffner, C. Grayson, C.A. Goldman and M.M. Moezzi, "Innovative approaches to verifying demand response of water heater load control," IEEE Trans on Power Delivery, vol.21, pp.388-397, Jan. 2006.

[26] M. Sullivan, J. Bode, B. Kellow, S. Woehleke and J. Eto, "Using residential AC load control in grid operations: PG&E's Ancillary Service Pilot," IEEE Trans on Smart Grid, vol.4, no.2, pp.1162-1170, Jun 2013.

[27] Siemens Demand Response Management System (DRMS) Version 2.0 [Online]. Available: http://www.siemens.com/DRMS. Retrieved: February 2016.

[28] OpenADR Specification Version 1.0. [Online]. Available: http://openadr.lbl.gov Retrieved: February 2016.

[29] Demand Response Research Center, Berkeley Lab, Department of Energy [Online]. Available: http://drrc.lbl.gov/. Retrieved: February 2016.

[30] Extensible Markup Language (XML) [Online]. Available: http://en.wikipedia.org/wiki/XML Retrieved: February 2016.

[31] EnerNOC [Online]. Available: http://www.enernoc.com/. Retrieved: February 2016.

[32] SmartThings - Home Automation [Online]. Available: www.smartthings.com/ Retrieved: February 2016.

[33] Staples Connect powered by Linksys [Online]. Available: www.staples.com/sbd/cre/marketing/staples-connect/ Retrieved: February 2016.

[34] GE Brillion Connected Appliances [Online]. Available: www.geappliances.com/connected-home-smart-appliances/ Retrieved: February 2016.

[35] Iris Smart Home Management System [Online]. Available: www.lowes.com/cd_Iris_239939199 Retrieved: February 2016.

[36] Revolv: Life & Smart Home Awesomation [Online]. Available: http://revolv.com/ Retrieved: February 2016.

[37] Buildings Energy Data Book, Buildings Sector, [Online]. Available: http://buildingsdatabook.eren.doe.gov/ChapterIntro1.aspx?1#4, November 1, 2011. Retrieved: February 2016.

[38] Building Technologies Office, Office of Energy Efficiency & Renewable Technology, Department of Energy [Online]. Available: http://energy.gov/eere/efficiency/buildings Retrieved: February 2016.

[39] "Small- and Medium-Sized Commercial Building Monitoring and Controls Needs: A Scoping Study," October 2012, http://www.pnnl.gov/main/publications/external/technical_reports/PNNL-22169.pdf Retrieved: February 2016.

[40] Buildings Energy Data Book, Commercial Sector, [Online]. Available: http://buildingsdatabook.eren.doe.gov/ChapterIntro3.aspx Retrieved: February 2016.

[41] "Small- and Medium-Sized Commercial Building Monitoring and Controls Needs: A Scoping Study," October 2012, http://www.pnnl.gov/main/publications/external/technical_reports/PNNL-22169.pdf Retrieved: February 2016.

[42] Building Management System [Online]. Available: http://en.wikipedia.org/wiki/Building_management_system. Retrieved: Jan. 2015.

[43] Freedomotic Open Source Building Automation [Online]. Available: http://freedomotic.com/ Retrieved: February 2016.

[44] OpenRemote Open Source Automation Platform [Online]. Available: http://www.openremote.org/ Retrieved: February 2016.

[45] OpenHAB empowering the smart home [Online]. Available: http://www.openhab.org/ Retrieved: February 2016.

[46] F. Bellifemine, A. Poggi, and G. Rimassa, "JADE: A FIPA2000 compliant agent development environment," Proceedings of the Fifth International Conference on Autonomous Agents. ACM, New York, 2001.

[47] Spade2 - Smart Python Agent Development Environment [Online]. Available: https://code.google.com/p/spade2/. Retrieved: February 2016.

[48] AgentScape - Distributed Agent Middleware [Online]. Available: http://www.agentscape.org/about. Retrieved: February 2016.

[49] F. Bellifemine, G. Caire, D. Greenwood, *Developing Multi-Agents system with JADE*, John Wiley & Sons, Ltd., 2007

[50] D. Camacho, R. Aler, D. Borrajo and J. Molina, "Agent architecture for intelligent gathering system", AI Communications, Vol. 18, Iss. 1, pp. 15-32, January 2005.

[51] Foundation of Intelligent Physical Agent [Online]. Available: http://sourceforge.net/projects/fipa-os/. Retrieved: February 2016.

[52] V. Krishna and V. C. Ramesh, "Intelligent agent for negotiation in market games, part I: Model," in *IEEE Transactions on Power Systems*, vol. 13, pp. 1103–1108, 1998.

[53] V. Krishna and V. C. Ramesh, "Intelligent agents for negotiations in market games. 2. Application," in *IEEE Transactions on Power Systems*, vol. 13, no. 3, pp. 1109-1114, Aug 1998.

[54] R. Fenghui, Z. Minjie, D. Soetanto and S. XiaoDong, "Conceptual design of a multi-agent system for interconnected power systems restoration", *IEEE Trans on Power Systems*, vol.27, May 2012.

[55] L. Haoming, C. Xingying, Y. Kun Yu, and H. Yunhe, "The control and analysis of self-healing urban power grid", *IEEE Trans on Smart Grid*, vol.3, no.3, pp.1119-1129, Sept. 2012.

[56] N. Kumar Nunna, H.S.V.S. and S. Doolla, "Multiagent-based distributed-energy-resource management for intelligent microgrids", *IEEE Trans on Industrial Electronics*, vol.60, pp.1678-1687, April 2013.

[57] C.P. Nguyen, and A.J. Flueck, "Agent based restoration with distributed energy storage support in smart grids", *IEEE Trans on Smart Grid*, vol.3, no.2, pp.1029-1038, June 2012.

[58] J. Q. Feng, C. Ma, W. H. Tang, J.S. Smith, and Q.H. Wu, "A Transformer Predictive Maintenance System Based On Agent-Oriented Programming," *In Proc. 2005 IEEE/PES Transmission and Distribution Conference and Exhibition: Asia and Pacific*, Aug. 2005.

[59] S. D J McArthur, S.M. Strachan, and G. Jahn, "The design of a multi-agent transformer condition monitoring system," *IEEE Trans on Power Systems*, vol.19, no.4, pp.1845-1852, Nov. 2004.

[60] Multi-Agent Systems Working Group, IEEE Power and Energy Society [Online]. Available: http://sites.ieee.org/pes-mas/. Retrieved: February 2016.

[61] Y. Peizhong, D. Xihua, A. Iwayemi, Z. Chi and L. Shufang, "Real-time opportunistic scheduling for residential demand response," *IEEE Trans on Smart Grid*, vol.4, no.1, pp.227,234, March 2013.

[62] T. Hubert and S. Grijalva, "Modeling for residential electricity optimization in dynamic pricing environments," *IEEE Trans on Smart Grid*, vol.3, no.4, pp.2224-2231, Dec. 2012.

[63] L. Ying, Boon Loong Ng, M. Trayer and L. Lingjia, "Automated residential demand response: algorithmic implications of pricing models," *IEEE Trans on Smart Grid*, vol.3, pp.1712-21, Dec. 2012

[64] C. Gouveia, J. Moreira, C.L. Moreira, J.A. Pecas Lopes, "Coordinating Storage and Demand Response for Microgrid Emergency Operation," IEEE Trans on Smart Grid, vol.4, pp.1898-1908, Dec. 2013.

[65] S. Shao, M. Pipattanasomporn and S. Rahman, "An approach for demand response to alleviate power system stress conditions," IEEE PES General Meeting, vol., no., pp.1-7, 24-29 July 2011.

[66] L. Ying, B.L. Ng, M. Trayer and L. Liu, "Automated residential DR: algorithmic implications of pricing models," IEEE Trans on Smart Grid, vol.3, pp.1712-1721, Dec. 2012.

[67] J. H. Yoon, R. Baldick, and A. Novoselac, "Dynamic Demand Response Controller Based on Real-Time Retail Price for Residential Buildings," IEEE Trans on Smart Grid, vol.5, pp.121-129, Jan. 2014.

[68] S. Wencong, H. Eichi, Z. Wente, and C. Mo-Yuen, "A Survey on the Electrification of Transportation in a Smart Grid Environment," IEEE Trans on Industrial Informatics, vol.8, no.1, pp.1,10, Feb. 2012.

[69] K. Clement-Nyns, E. Haesen, and J. Driesen, "The impact of charging plug-in hybrid electric vehicles on a residential distribution grid," IEEE Trans on Power Systems, vol. 25, no. 1, pp. 371-380, 2010.

[70] K. Dyke, N. Schofield, M. Barnes, "The Impact of Transport Electrification on Electrical Networks," IEEE Trans. Industrial Electronics, vol. 57, no. 12, pp. 3917 – 3926, 2010.

[71] L. Pieltain Fernandez, T. Gomez San Roman, R. Cossent, C. Mateo Domingo, and P. Frias, "Assessment of the Impact of Plug-in Electric Vehicles on Distribution Networks," IEEE Trans on Power Systems, vol. 26, no. 1, pp. 206 – 213, 2011.

[72] J. A. P. Lopes, F. J. Soares, and P. M. R. Almeida, "Integration of Electric Vehicles in the Electric Power System," Proceedings of the IEEE, vol. 99, no. 1, pp. 168-183, 2011.

[73] E. Sortomme, M. Hindi, S. D. J. MacPherson, and S. S. Venkata, "Coordinated Charging of Plug-In Hybrid Electric Vehicles to Minimize Distribution System Losses," IEEE Trans on Smart Grid, vol. 2, no. 1, pp. 198 – 206, 2011.

[74] E.L. Karfopoulos, E.L, and N.D. Hatziargyriou, "A Multi-Agent System for Controlled Charging of a Large Population of Electric Vehicles," IEEE Trans on Power Systems, vol.28, no.2, pp.1196-1204, May 2013.

[75] P. Papadopoulos, N. Jenkins, L.M. Cipcigan, I. Grau, and E. Zabala, "Coordination of the Charging of Electric Vehicles Using a Multi-Agent System," IEEE Trans on Smart Grid, vol.4, pp.1802-1809, Dec. 2013.

[76] S. Vandael, N. Bouck´e, T. Holvoet, and G. Deconinck, "Decentralized Demand Side Management of Plug-in Hybrid Vehicles in a Smart Grid", In Proceedings of the 1st International Workshop on Agent Technologies for Energy Systems (Toronto, Canada, May, 11 2010).

[77] M. Biabani, M.A. Golkar and A. Sajadi, "Operation of a multi-agent system for load management in smart power distribution system," *In Proc. 2012 Int'l Conf. on Environment and Electrical Engineering (EEEIC)*, pp.525-530, 18-25 May 2012.

[78] R. Fazal, J. Solanki and S.K. Solanki, "Demand response using multi-agent system," *In Proc. 2012 North American Power Symposium (NAPS)*, 9-11 Sept. 2012.

[79] M. Pipattanasomporn, M. Kuzlu and S. Rahman, "An algorithm for Intelligent home energy management and demand response analysis," *IEEE Trans on Smart Grid*, vol.3, no.4, pp.2166-73.

[80] L. Ying, Boon Loong Ng, M. Trayer and L. Lingjia, "Automated residential demand response: algorithmic implications of pricing models," *IEEE Trans on Smart Grid*, vol.3, pp.1712-21, Dec. 2012

[81] K. Schisler, T. Sick, and K. Brief, "The role of demand response in ancillary services markets," Transmission and Distribution Conference and Exposition, 2008. T&D. IEEE/PES , vol., no., pp.1,3, 21-24 April 2008.

[82] N. Lu, and Katipamula, "Control strategies of thermostatically controlled appliances in a competitive electricity market," *IEEE Power Engineering Society General Meeting, 2005*, vol., no., pp.202,207 Vol. 1, 12-16 June 2005.

[83] L. Wang, Z. Wang, and R. Yang, "Intelligent Multiagent Control System for Energy and Comfort Management in Smart and Sustainable Buildings," *IEEE Transactions on Smart Grid*, vol.3, no.2, pp.605, 617, June 2012

[84] S.D. Smitha, J.S. Savier, and F.M. Chacko, "Intelligent control system for efficient energy management in commercial buildings," Emerging Research Areas and 2013 International Conference on Microelectronics, Communications and Renewable Energy (AICERA/ICMiCR), 2013 Annual International Conference on , vol., no., pp.1,6, 4-6 June 2013

[85] P. Zhao, S. Suryanarayanan, and M.G. Simoes, "An Energy Management System for Building Structures Using a Multi-Agent Decision-Making Control Methodology," Industry Applications, IEEE Transactions on , vol.49, no.1, pp.322,330, Jan.-Feb. 2013

[86] EnergyPlus Energy Simulation Software, U.S. Department of Energy [Online]. Available: http://apps1.eere.energy.gov/buildings/energyplus/. Retrieved: February 2016.

[87] AMPL, Streamlined Modeling for Real Optimization [Online]. Available: http://ampl.com/. Retrieved: February 2016.

[88] IBM CPEX Optimizer, High-performance mathematical solver for linear programming, mixed integer programming, and quadratic programming [Online]. Available: http://www-01.ibm.com/software/commerce/optimization/cplex-optimizer/. Retrieved: February 2016.

[89] Y. Guo, J. Wu, and C. Long, "Agent-based multi-time-scale plug load energy management in commercial building," 10th IEEE International Conference on Control and Automation (ICCA), vol., no., pp.1884-1889, 12-14 June 2013

[90] M. Pipattanasomporn, M. Kuzlu and S. Rahman, "An algorithm for Intelligent home energy management and demand response analysis," *IEEE Trans on Smart Grid*, vol.3, no.4, pp.2166-2173, Dec. 2012.

[91] S. Shao, "An Approach to Demand Response for Alleviating Power System Stress Conditions due to Electric Vehicle Penetration," Ph.D. dissertation, Dept. Elec. Eng., Virginia Tech, Blacksburg, VA, 2011.

[92] National Climate Data Center, National Oceanic and Atmospheric Administration [Online]. Available: http://www.ncdc.noaa.gov/. Retrieved: February 2016.

[93] The Standards for Ventilation and Indoor Air Quality, ANSI/ASHRAE Standard 62.1-2013, American Society of Heating, Refrigerating, and Air-Conditioning Engineers (ASHRAE) [Online]. Available: https://www.ashrae.org/resources--publications/bookstore/standards-62-1--62-2. Retrieved: February 2016.

[94] American Housing Survey (AHS), United States Census Bureau [Online]. Available: http://www.census.gov/programs-surveys/ahs.html. Retrieved: February 2016.

[95] Soil Climate Analysis Network (SCAN) Data & Products, Natural Resources Conservation Service [Online]. Available: http://www.wcc.nrcs.usda.gov/scan/. Retrieved: February 2016.

[96] RELOAD Database Documentation and Evaluation and Use in NEMS [On-line]. Available: www.onlocationinc.com/LoadShapesAlternative2001.pdf. Retrieved: February 2016.

[97] M. Biabani, M.A. Golkar and A. Sajadi, "Operation of a multi-agent system for load management in smart power distribution system," *In Proc. 2012 Int'l Conf. on Environment and Electrical Engineering (EEEIC)*, pp.525-530, 18-25 May 2012.

[98] The Foundation for Intelligent Physical Agents [Online]. Available: http://www.fipa.org/. Retrieved: February 2016.

[99] American National Standard for Electrical Power Systems and Equipment - Voltage Ratings (60 Hertz), ANSI C84.1-2006.

[100] B. Akyol, J. Haack, C. Tews, B. Carpenter, A. Kulkarni, and P. Craig "An Intelligent Sensor Framework for the Power Grid." In ASME Conf. Proc. 2011, 1485 (2011), DOI=10.1115/ES2011-54619

[101] B. Akyol, J. Haack, S. Ciraci, B. Carpenter, M. Vlachopoulou and C. Tews "VOLTTRON: an agent execution platform for the electric power system." In Proceedings of the 3rd International Workshop on Agent Technologies for Energy Systems (Valencia, Spain, June 5, 2012).

[102] J. Haack, B. Akyol, B. Carpenter, C. Tews, and L. Foglesong "VOLTTRON: An agent platform for smart grid." In Proceedings of the 4th International Workshop on Agent Technologies for Energy Systems (Minnesota, USA, May 10, 2014).

[103] ZeroMQ Python Binding [Online]. Available: http://zeromq.org/bindings:python Retrieved: February 2016.

[104] If This Then That (IFTTT) [Online]. Available: https://ifttt.com/. Retrieved: February 2016.

[105] The Standards for Ventilation and Indoor Air Quality, ANSI/ASHRAE Standard 62.1-2013, American Society of Heating, Refrigerating, and Air-Conditioning Engineers (ASHRAE) [Online]. Available: https://www.ashrae.org/resources--publications/bookstore/standards-62-1--62-2. Retrieved: February 2016.

[106] P. Ple Fanger (1970). Thermal Comfort: Analysis and applications in environmental engineering. McGraw-Hill.

[107] T. Hoyt, S. Schiavon, A. Piccioli, D. Moon, and K. Steinfeld, CBE Thermal Comfort Tool. Center for the Built Environment, University of California Berkeley [Online]. Available: http://cbe.berkeley.edu/comforttool/. Retrieved: February 2016.

[108] The Lighting Handbook, 10th Edition, Illuminating Engineering Society of North America (IESNA) [Online]. Available: http://www.ies.org/handbook/. Retrieved: Jan. 2016.

[109] W. Bobenhausen, "Simplified Design of HVAC Systems," John Wiley & Son Inc. 1994

[110] M. Pipattanasomporn, M. Kuzlu and S. Rahman, "An algorithm for Intelligent home energy management and demand response analysis," *IEEE Trans on Smart Grid*, vol.3, no.4, pp.2166-2173, Dec. 2012.

[111] JADE agent development toolkit [Online]. Available: http://jade.tilab.com. Retrieved: February 2016.

[112] C. R. Robinson, P. Mendham and T. Clarke, "MACSimJX : A tool for enabling agent modelling with Simulink using JADE," *Journal of Physical Agents*, vol. 4, no. 3, pp. 1–7, 2010.

[113] H. Liu. "SCE SmartGrid communications architecture, strategy, and roadmap." *In Proc. IEEE PES General Meeting*, July 2012.

[114] S. Shao, M. Pipattanasomporn and S. Rahman, "An approach for demand response to alleviate power system stress conditions," *IEEE PES General Meeting*, vol., no., pp.1-7, 24-29 July 2011.

[115] ODROID-U3 [Online]. Available: http://www.hardkernel.com/main/products/prdt_info.php?g_code=g138745696275

[116] ICM Controls [Online]. Available: http://www.icmcontrols.com/i3-Series-of-Programmable-Touch-Screen-Thermostats-Prodview.html. Retrieved: Jan 2016.

[117] Philips Hue color ambiance starter kit [Online]. Available: http://www2.meethue.com/en-us/productdetail/philips-hue-white-and-color-ambiance-starter-kit-a19. Retrieved: Jan 2016.

[118] Belkin WeMo Insight Switch [Online]. Available: http://www.belkin.com/us/p/P-F7C029/. Retrieved: Jan 2016.

[119] Continental Control System Wattnode Modbus Power and Energy Meter model WNC-3Y-208-MB [Online]. Available: http://www.ccontrolsys.com/w/WattNode_Modbus. Retrieved: Jan 2016.

[120] SmartThings hub [Online]. Available: https://shop.smartthings.com/#!/products/smartthings-hub. Retrieved: Jan 2016.

[121] Netatmo weather station [Online]. Available: https://www.netatmo.com/en-US/product/weather-station. Retrieved: Jan 2016.

[122] Aeotec by Aeon Labs MultiSensor [Online]. Available: http://aeotec.com/z-wave-sensor. Retrieved: Jan 2016.

[123] Proteus M5 WiFi motion sensor [Online]. Available: https://proteussensor.com/wi-fi-motion-sensor.html. Retrieved: Jan 2016.